



E-29369

April 30, 2010

U.S. Department of Transportation
 Attn: Mr. Richard W. Boyle, Chief
 Radioactive Materials Branch
 1200 New Jersey Avenue, S.E.
 East Building, PHH-23
 Washington, DC 20590

Subject: Affidavit and Non-proprietary SAR for Validation of Japanese Competent Authority Certificate J/105/AF-96, Revision 2 (issued December 1, 2009) for the Model No. MFC-1 PWR Fuel Assembly Package

Reference: Letter from Jayant Bondre (TN) to U.S. Department of Transportation, "Validation of Japanese Competent Authority Certificate J/105/AF-96, Revision 2 (issued December 1, 2009) for the Model No. MFC-1 PWR Fuel Assembly Package," February 24, 2010 (TN Letter E-29032)

Dear Mr. Boyle:

In the submittal referenced above, Transnuclear, Inc. (TN) requested validation of Japanese Certificate of Approval of Package Design for the Transport of Radioactive Material J/105/AF-96, Revision 2 (issued December 1, 2009) for the Model MFC-1 PWR fuel assembly package.

To facilitate the validation, please find enclosed an affidavit for withholding proprietary information contained in the safety analysis report (SAR) for the Model MFC-1 Package, and a non-proprietary version of that SAR, as Enclosures 1 and 2, respectively.

If you have questions or require further information, please call Don Shaw at (410) 910-6878 or me at (410) 910-6881.

Very truly yours,

Jayant Bondre, PhD
 Vice President - Engineering

Enclosures:

1. Affidavit Pursuant to 10 CFR 2.390
2. Safety Analysis Report for Model MFC-1 Package, October, 2009 (Non-proprietary version)

AFFIDAVIT PURSUANT
TO 10 CFR 2.390

Transnuclear, Inc.)
State of Maryland) SS.
County of Howard)

I, Jayant Bondre, depose and say that I am a Vice President of Transnuclear, Inc., duly authorized to execute this affidavit, and have reviewed or caused to have reviewed the information which is identified as proprietary and referenced in the paragraph immediately below. I am submitting this affidavit in conformance with the provisions of 10 CFR 2.390 of the Commission's regulations for withholding this information.

The information for which proprietary treatment is sought is contained in Enclosure 3 of the reference listed in the cover letter (TN letter E-29032) and as listed below:

1. The following pages of the Safety Analysis Report for Model MFC-1 Package:

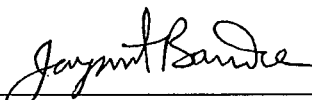
I-A-2
I-C-1, 2, 3
I-C-8 to 28
I-D-1 to 37
II-A-18 to 20, 23
II-A-48
II-A-58 to 60
II-A-65 to 69, 71 to 80, 82 to 86
II-A-122 to 133
II-A-138
II-A-139 to 146
II-A-149, 150
II-B-1
II-B-4 to 10
II-B-13 to 16
II-B-22
II-B-24, 25
II-B-31 to 40
II-B-42, 43
II-C-5, 6
II-D-4 to 7
II-E-7
II-E-8
II-E-11 to 14
II-E-20
II-F-6 to 8
II-F-29
II-F-43
III-1 to 22
IV-A-6 to 13
IV-A-15
IV-B-1 to 3 (All Pages)
(Appendix III Manufacturing Procedures of Packaging) Pages 1 to 53

I have personal knowledge of the criteria and procedures utilized by Transnuclear, Inc. in designating information as a trade secret, privileged or as confidential commercial or financial information.


Pursuant to the provisions of paragraph (b) (4) of Section 2.390 of the Commission's regulations, the following is furnished for consideration by the Commission in determining whether the information sought to be withheld from public disclosure, included in the above referenced document, should be withheld.

- 1) The information sought to be withheld from public disclosure are portions of radioactive material transportation cask design analyses which are owned by others and have been held in confidence by Transnuclear, Inc.
- 2) The information is of a type customarily held in confidence by Transnuclear, Inc. and not customarily disclosed to the public. Transnuclear, Inc. has a rational basis for determining the types of information customarily held in confidence by it.
- 3) Public disclosure of the information is likely to cause substantial harm to the competitive position of Transnuclear, Inc. and the owner of the information because the information consists of descriptions of the design and analysis of transportation package for fuel, the application of which provides a competitive economic advantage. The availability of such information to competitors would enable them to modify their product to better compete with Transnuclear, Inc. and the owner of the information, take marketing or other actions to improve their product's position or impair the position of Transnuclear, Inc.'s and the owner of the information's product, and avoid developing similar data and analyses in support of their processes, methods or apparatus.

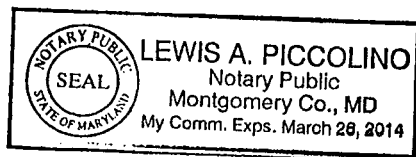
Further the deponent sayeth not.


 Jayant Bondre
 Vice President, Transnuclear, Inc.

Subscribed and sworn to me before this 30th day of April, 2010.


 Notary Public

My Commission Expires 03/26/14



Enclosure 2 to TN E-29369

**Safety Analysis Report for Model MFC-1 Package,
October, 2009 (Non-proprietary version)**

Non-Proprietary Version

ENCLOSURE

SAFETY ANALYSIS REPORT FOR
MODEL MFC-1 PACKAGE

Submitted by:

mitsubishi nuclear fuel company ltd.

October, 2009

Contents

Summary of Package

I	Package Description	I
I-A	Objective and Condition	I-A-1
I-B	Classification of Package	I-B-1
I-C	Packaging	I-C-1
I-C.1	Outline of Packaging	I-C-1
I-C.2	Structure of Packaging	I-C-1
I-C.2.1	Outer Shell	I-C-1
I-C.2.2	Cradle Assembly	I-C-2
I-C.2.3	Shock Mount	I-C-3
I-C.2.4	Auxiliary Devices	I-C-4
I-C.3	Materials and Dimensions of Main Parts of Packaging	I-C-4
I-C.4	Dimensions and Weight of Packaging	I-C-5
I-C.5	Containment Boundary	I-C-5
I-D	Contents of Packaging	I-D-1
I-D.1	Description of Contents	I-D-1
I-D.2	Type of Contents and Quantities of Main Parts	I-D-31
I-D.3	Structures of Contents and Dimensions of Main Parts	I-D-31
I-D.4	Material of Contents	I-D-32
I-D.5	Physical and Chemical Properties of Contents	I-D-34
I-D.5.1	Heat Resistance	I-D-34
I-D.5.2	Corrosion Resistance	I-D-34
I-D.5.3	Electrochemical Reaction	I-D-34
I-D.6	Containing Conditions of Contents	I-D-35
I-D.7	Enrichment of Contents	I-D-35
I-D.8	Weight of Contents	I-D-36
I-D.9	Densities of Main Materials of Contents	I-D-36
I-D.10	Moderating Ratio	I-D-36
I-D.11	Maximum Decay Heat Load	I-D-37
I-D.12	Maximum Pressure of Fuel Rods for Containment Boundary	I-D-37

Contents

II	Safety Analysis for Package	II
II-A	Structural Analysis	II-A-1
II-A.1	Structural Design	II-A-1
II-A.1.1	Outline	II-A-1
II-A.1.2	Design Criteria	II-A-2
II-A.2	Weight and Center of Gravity	II-A-16
II-A.3	Mechanical Properties of Materials	II-A-16
II-A.4	General Standards of Package	II-A-24
II-A.4.1	Chemical and Galvanic Reactions	II-A-24
II-A.4.2	Cold Strength	II-A-24
II-A.4.3	Containment System	II-A-28
II-A.4.4	Lifting Devices	II-A-28
II-A.4.4.1	Brackets for Lifting up Container	II-A-29
II-A.4.4.2	Tightening Bolts	II-A-47
II-A.4.5	Tie-Down Devices	II-A-51
II-A.4.6	Pressure	II-A-52
II-A.4.7	Vibration	II-A-52
II-A.5	Normal Conditions of Transport	II-A-55
II-A.5.1	Thermal Test	II-A-55
II-A.5.1.1	Summary of Pressure and Temperatures	II-A-55
II-A.5.1.2	Thermal Expansion	II-A-55
II-A.5.1.3	Stress Calculation	II-A-56
II-A.5.1.4	Comparison with Allowable Stresses	II-A-60
II-A.5.2	Water Spray Test	II-A-62
II-A.5.3	Free Drop Test	II-A-62
II-A.5.4	Stacking Test	II-A-91
II-A.5.5	Penetration Test	II-A-93
II-A.5.6	Corner or Edge Drop	II-A-95
II-A.5.7	Summary of Results and Evaluation	II-A-95
II-A.6	Hypothetical Accident Conditions of Transport	II-A-99
II-A.7	Reinforced Immersion Test	II-A-99
II-A.8	Radioactive Contents	II-A-99
II-A.9	Fissile Materials Package	II-A-100

Contents

II-A.9.1	Normal Conditions of Transport for Fissile Materials Package	II-A-100
II-A.9.1.1	Water Spray Test	II-A-100
II-A.9.1.2	Free Drop	II-A-100
II-A.9.1.3	Stacking Test	II-A-100
II-A.9.1.4	Penetration Test	II-A-100
II-A.9.2	Hypothetical Accident Conditions of Transport for Fissile Materials Package	II-A-101
II-A.9.2.1	Strength Test/Drop Test I (as drop is made from a height of 9m)	II-A-103
II-A.9.2.2	Strength Test/Drop Test II (drop from a height of 1m)	II-A-113
II-A.9.2.3	Thermal Test	II-A-116
II-A.9.2.4	Water Immersion Test	II-A-116
II-A.9.2.5	Summary of Results and their Evaluation	II-A-117
II-A.10	Annex	II-A-120
II-A.10.1	Reference	II-A-120
II-A.10.2	Dimensionless Curve to Cylindrical Shell	II-A-121
II-A.10.3	Searing Section Modulus of Tightening Bolts	II-A-134
II-A.10.4	Impact Response Analysis Code by Non-Linear Spring –Mass System Model “SHOCK”	II-A-135
II-A.10.5	Analysis of Free Drop from Heights of 1.2m and 9m of Model MFC-1 Package with “SHOCK” Code	II-A-138
II-A.10.6	Adequacy of Analysis of Free Drop of Model MFC-1 Package by “SHOCK” Code	II-A-148
II-A.10.7	Equivalent Section Modulus of Fuel Rod during Horizontal Drop	II-A-149
II-A.10.8	Presence of Interference by Deformation Amount to Packaging	II-A-151
II-B	Thermal Analysis	II-B-1
II-B.1	Outline	II-B-1
II-B.1.1	Thermal Design	II-B-1
II-B.1.2	Thermal Analysis	II-B-2
II-B.1.3	Conditions and Methods of Thermal Analysis	II-B-4
II-B.2	Thermal Properties of Materials	II-B-5
II-B.3	Specification of Components	II-B-7
II-B.4	Normal Conditions of Transport	II-B-8

Contents

II-B.4.1 Thermal Analysis Model	II-B-8
II-B.4.1.1 Analysis Model	II-B-8
II-B.4.1.2 Test Model	II-B-9
II-B.4.2 Maximum Temperatures	II-B-9
II-B.4.3 Minimum Temperatures	II-B-9
II-B.4.4 Maximum Internal Pressures	II-B-10
II-B.4.5 Maximum Thermal Stresses	II-B-10
II-B.4.6 Summary of Results and Evaluation	II-B-11
II-B.5 Hypothetical Accident Conditions of Transport	II-B-12
II-B.5.1 Thermal Analysis Code	II-B-12
II-B.5.1.1 Analysis Model	II-B-12
II-B.5.1.2 Test Model	II-B-17
II-B.5.2 Evaluation Conditions of Package	II-B-17
II-B.5.3 Temperatures of Package	II-B-17
II-B.5.4 Maximum Internal Pressures	II-B-18
II-B.5.5 Maximum Thermal Stresses	II-B-19
II-B.5.6 Summary of Results and Evaluation	II-B-19
II-B.6 Annex	II-B-23
II-B.6.1 Reference	II-B-23
II-B.6.2 Maximum Temperature of Package under Normal Conditions of Transport	II-B-24
II-B.6.3 Outline of Heat Transfer General-Purpose Program "TRUMP"	II-B-26
II-B.6.4 Modeling of Fuel Assembly (Homogenized Model of Fuel)	II-B-31
II-B.6.5 Thermal Properties of Homogenized Fuel Part	II-B-32
II-B.6.6 Boundary Conditions Used for Analysis	II-B-34
II-B.6.7 Solar Insolation	II-B-40
II-B.6.8 Influence of Drop Test II at Thermal Test on Thermal Analyses	II-B-40
II-B.6.9 Maximum Internal Pressure in Fuel Rod	II-B-42
II-C Containment Analysis	II-C-1
II-C.1 Outline	II-C-1
II-C.2 Containment System	II-C-1
II-C.2.1 Containment System	II-C-1

Contents

II-C.2.2	Penetration of Containment System	II-C-1
II-C.2.3	Gaskets and Welds of Containment System	II-C-2
II-C.2.4	Closure System	II-C-2
II-C.3	Normal Conditions of Transport	II-C-2
II-C.3.1	Leakage of Radioactive Materials	II-C-2
II-C.3.2	External Pressure on Containment System	II-C-3
II-C.3.3	Contamination of Coolant Materials	II-C-3
II-C.3.4	Loss of Coolant Materials	II-C-3
II-C.4	Hypothetical Accident Conditions of Transport	II-C-3
II-C.4.1	Nuclear Fission Gas	II-C-3
II-C.4.2	Leakage of Radioactive Materials	II-C-4
II-C.5	Summary of Results and Evaluation	II-C-4
II-C.6	Annex	II-C-7
II-C.6.1	Containment Boundary	II-C-7
II-D	Shielding Analysis	II-D-1
II-D.1	Outline	II-D-1
II-D.2	Specifications of Source Terms	II-D-1
II-D.2.1	Gamma Emission Rate	II-D-1
II-D.2.2	Neutrons Source	II-D-1
II-D.3	Specification of Model	II-D-4
II-D.3.1	Analysis Model	II-D-4
II-D.3.2	Atomic Number Densities in Each Region of Analysis Model	II-D-6
II-D.4	Shielding Analysis	II-D-8
II-D.4.1	Routine Transport Conditions	II-D-8
II-D.4.2	Normal Conditions of Transport	II-D-8
II-D.5	Summary of Results and Assessment	II-D-10
II-D.6	Annex	II-D-11
II-D.6.1	Description of ORIGEN-2 Code	II-D-11
II-D.6.2	Description of ANISN Code	II-D-13

Contents

II-E Criticality Analysis	II-E-1
II-E.1 Outline	II-E-1
II-E.2 Objects of Analysis	II-E-1
II-E.2.1 Contents	II-E-1
II-E.2.2 Packaging	II-E-1
II-E.2.3 Neutron Absorbers	II-E-2
II-E.3 Specification of Model	II-E-3
II-E.3.1 Analysis Model	II-E-3
II-E.3.2 Atomic Number Densities in Each Region of Analysis Model	II-E-4
II-E.4 Subcriticality Evaluation	II-E-4
II-E.4.1 Calculation Conditions	II-E-4
II-E.4.2 Assumption of Water Leakage into Package	II-E-5
II-E.4.3 Calculation Procedures	II-E-5
II-E.4.4 Results of Calculation	II-E-5
II-E.5 Summary of Results and Evaluation	II-E-9
II-E.6 Annex	II-E-16
II-E.6.1 Reference	II-E-16
II-E.6.2 Description of KENO-V.a Code	II-E-17
II-E.6.3 Bench Mark Test	II-E-17
II-E.6.3.1 Outline of Test	II-E-17
II-E.6.3.2 Details of Test	II-E-18
II-E.6.3.3 Results of Test and Evaluation	II-E-18
II-F Test Report of Prototype Packaging for Model MFC-1 Container	
ZEG-3222	II-F-1

Contents

III Quality Management Principles	III-1
A Quality Management System	III-1
A.1 Quality Manual	III-1
A.2 Document and Data Control	III-4
A.3 Control of Quality Records	III-4
B Responsibility of Applicants	III-6
C Education and Training	III-11
D Design Control	III-12
D.1 Design Control for Commission to Outside Company	III-12
D.2 Design Control for In-House Design	III-13
E Production Order of Packaging	III-15
E.1 Quality Control by the Packaging Manufacturer	III-15
E.2 Criteria of Selecting Packaging Supplier	III-17
E.3 Inspections	III-18
E.4 Schedule Control and Approval of Special Process	III-19
F Handling and Maintenance	III-21
F.1 Maintenance Control	III-21
F.2 Inspection before Shipment	III-21

Contents

IV Handling Procedures and Maintenance Conditions of Package	IV-A-1
IV-A Handling Procedures of Package	IV-A-1
IV-A.1 Loading Procedures	IV-A-1
IV-A.1.1 Preparation	IV-A-1
IV-A.1.2 Loading Procedures	IV-A-2
IV-A.2 Inspection before Shipment of Package	IV-A-14
IV-A.3 Unloading Procedures	IV-A-16
IV-A.4 Preparation of Empty Packaging	IV-A-18
IV-A-4.1 Visual Inspection	IV-A-18
IV-A-4.2 Operating Tests	IV-A-18
IV-B Maintenance Conditions	IV-B-1
IV-B.1 Visual Inspection and Pressure Proof Test	IV-B-1
IV-B.1.1 Visual Inspection	IV-B-1
IV-B.1.2 Pressure Proof Test	IV-B-1
IV-B.2 Air-Tight Test	IV-B-1
IV-B.3 Maintenance of Auxiliary Systems	IV-B-1
IV-B.4 Maintenance of Valves and Gaskets of Closed Packaging	IV-B-1
IV-B.5 Shielding Inspection	IV-B-2
IV-B.6 Subcriticality Test	IV-B-2
IV-B.7 Thermal Test	IV-B-2
IV-B.8 Others	IV-B-2
V Particular Items on Safety Design and Safe Transport	V-1
Appendix III Manufacturing Procedures of Packaging	III-1

Figure List (1)

SUMMARY OF PACKAGE

Summary-1	Illustration of Package (Bird's Eye View).....	Summary-3
-----------	--	-----------

I

Fig.I-C.1	Illustration of Package (Bird's Eye View).....	I-C-6
Fig.I-C.2	Cradle Assembly and Outer Shell	I-C-7
Fig.I-C.3	General Assembly Drawing (MFC-1Type (A)).....	I-C-8
Fig.I-C.4	General Assembly Drawing (MFC-1 Type (B)).....	I-C-9
Fig.I-C.5	Upper Cover.....	I-C-10
Fig.I-C.6	Lower Container.....	I-C-11
Fig.I-C.7	Shock Mount Frame.....	I-C-12
Fig.I-C.8	Cross Frame (MFC-1 Type (A)).....	I-C-13
Fig.I-C.9	Cross Frame (MFC-1Type (B))	I-C-14
Fig.I-C.10	Bottom Support	I-C-15
Fig.I-C.11	Top End of Cross Frame (MFC-1 Type (A))	I-C-16
Fig.I-C.12	Top End of Cross Frame (MFC-1Type (B))	I-C-17
Fig.I-C.13	Clamping Frame (MFC-1 Type (A)).....	I-C-18
Fig.I-C.14	Clamping Frame (MFC-1Type (B)).....	I-C-19
Fig.I-C.15	Shock Mount.....	I-C-20
Fig.I-C.16	Auxiliary Legs (MFC-1 Type (A)).....	I-C-21
Fig.I-C.17	Auxiliary Legs (MFC-1Type (B)).....	I-C-22
Fig.I-C.18	Relief Valve	I-C-23
Fig.I-C.19	Air Valve and Hygrometer (MFC-1 Type (A))	I-C-24
Fig.I-C.20	Air Valve and Hygrometer (MFC-1Type (B))	I-C-25
Fig.I-C.21	Containment Boundary	I-C-26

Figure List (2)

Fig.I-D.1	Fuel Assembly (Type 14×14, 10 feet).....	I-D-4
Fig.I-D.2	Fuel Assembly (Type 14×14, 12 feet).....	I-D-5
Fig.I-D.2.a	Fuel Assembly (Type 14×14, 12 feet) (High Burnup Fuel).....	I-D-6
Fig.I-D.3	Fuel Assembly (Type 15×15, 12 feet).....	I-D-7
Fig.I-D.3.a	Fuel Assembly (Type 15×15, 12 feet) (High Burnup Fuel).....	I-D-8
Fig.I-D.4	Fuel Assembly (Type 17×17, 12 feet).....	I-D-9
Fig.I-D.4.a	Fuel Assembly (Type 17×17, 12 feet) (High Burnup Fuel).....	I-D-10
Fig.I-D.4.b	Fuel Assembly (Type 17×17, 12 feet) (HTP type).....	I-D-11
Fig.I-D.5	Detail Drawing of Inserts and Mixing Vanes	I-D-12
Fig.I-D.6	Skeleton Assembly (Type 14×14, 10 feet).....	I-D-13
Fig.I-D.7	Skeleton Assembly (Type 14×14, 12 feet).....	I-D-14
Fig.I-D.8	Skeleton Assembly (Type 15×15, 12 feet).....	I-D-15
Fig.I-D.9	Skeleton Assembly (Type 17×17, 12 feet).....	I-D-16
Fig.I-D.10	Fuel Rod (Type 14×14, 10 feet).....	I-D-17
Fig.I-D.11	Fuel Rod (Type 14×14 & 15×15, 12 feet)	I-D-18
Fig.I-D.11. a	Fuel Rod (Type 14×14 & 15×15, 12 feet) (High Burnup Fuel)	I-D-19
Fig.I-D.12	Fuel Rod (Type 17×17, 12 feet).....	I-D-20
Fig.I-D.12.a	Fuel Rod (Type 17×17, 12 feet) (High Burnup Fuel).....	I-D-21
Fig.I-D.12. b	Fuel Rod (Type 17×17, 12 feet) (HTP type).....	I-D-22
Fig.I-D.13	Control Rod Assembly (Type 14×14, 10 feet).....	I-D-23
Fig.I-D.14	Control Rod Assembly (Type 14×14, 12 feet).....	I-D-24
Fig.I-D.15	Control Rod Assembly (Type 15×15, 12 feet).....	I-D-25
Fig.I-D.16	Control Rod Assembly (Type 17×17, 12 feet).....	I-D-26
Fig.I-D.17	Burnable Poison Assembly (Type 14×14, 10 feet).....	I-D-27
Fig.I-D.18	Burnable Poison Assembly (Type 14×14, 12 feet)	I-D-28
Fig.I-D.19	Burnable Poison Assembly (Type 15×15, 12 feet)	I-D-29
Fig.I-D.20	Burnable Poison Assembly (Type 17×17, 12 feet)	I-D-30

Figure List (3)

II

Fig.II-A.1	Center of Gravity of Package	II-A-17
Fig.II-A.2	Change of Mechanical Properties of SS400 for Temperatures	II-A-21
Fig.II-A.3	Change of Mechanical Properties of SCM435 for Temperatures	II-A-22
Fig.II-A.4	Change of Mechanical Properties of Zircaloy-4, MDA and ZIRLO for Temperatures	II-A-23
Fig.II-A.5	Mechanical Properties of Carbon Steel at Low Temperatures	II-A-27
Fig.II-A.6	Lifting Devices	II-A-31
Fig.II-A.7	Bracket Welds	II-A-32
Fig.II-A.8	Load Conditions	II-A-34
Fig.II-A.9	Stress Evaluation Position and Analysis Model	II-A-35
Fig.II-A.10	Relationship between M_x , M_ϕ , N_x , N_ϕ and α in Acting of Radial Load (considering $\alpha = 8$ as a criterion)	II-A-40
Fig.II-A.11	Tightening Bolt Assembly	II-A-48
Fig.II-A.12	Cross Pin Analysis Model	II-A-50
Fig.II-A.13	Primary Mode Coefficient	II-A-52
Fig.II-A.14	Tie-down State of Package and Natural Frequency Analysis Model ..	II-A-54
Fig.II-A.15	Fuel Rod Cladding Analysis Model	II-A-59
Fig.II-A.16	Evaluation Item during 1.2m Horizontal Drop	II-A-64
Fig.II-A.17	Deformation Amount Analysis Model of Outer Shell during 1.2m Horizontal Drop	II-A-64
Fig.II-A.18	Clamping Frame Analysis Model	II-A-65
Fig.II-A.19	Skin Analysis Model	II-A-67
Fig.II-A.20	Maximum Stress Factors, β_1 and β_1' of Rectangular Plate	II-A-67
Fig.II-A.21	Fuel Rod Cladding Analysis Model during 1.2m Horizontal Drop	II-A-67
Fig.II-A.22	Evaluation Item during 1.2m Top End Vertical Drop	II-A-69
Fig.II-A.23	Deformation Amount Analysis Model of Outer Shell during 1.2m Top End Vertical Drop	II-A-70
Fig.II-A.24	Jack Screw Analysis Model	II-A-71
Fig.II-A.25	Fixed Frame Analysis Model (1)	II-A-73
Fig.II-A.26	Fixed Frame Analysis Model (2)	II-A-74

Figure List (4)

II

Fig.II-A.27	Skin Analysis Model	II-A-76
Fig.II-A.28	Fuel Rod Cladding Buckling Analysis Model	II-A-79
Fig.II-A.29	Evaluation Item during 1.2m Bottom End Vertical Drop	II-A-80
Fig.II-A.30	Analysis Model of Deformation Amount of Outer Shell during 1.2m Bottom End Vertical Drop	II-A-81
Fig.II-A.31	Pivot Mount Attaching Bolt Analysis Model	II-A-82
Fig.II-A.32	Guide Thimble Analysis Model	II-A-84
Fig.II-A.33	Evaluation Item during 1.2m Corner Drop	II-A-87
Fig.II-A.34	Deformation Amount Analysis Model of Outer Shell during 1.2m Corner Drop	II-A-88
Fig.II-A.35	Bending Stress Analysis Model	II-A-91
Fig.II-A.36	Penetration Model	II-A-94
Fig.II-A.37	Shear Model	II-A-94
Fig.II-A.38	Test Procedures in Normal Conditions of Transport	II-A-100
Fig.II-A.39	Test Procedures in Hypothetical Accident Conditions of Transport	II-A-101
Fig.II-A.40	Deformation Amount Analysis Model of Outer Shell during 9m Vertical Drop (with the upper cover downward)	II-A-103
Fig.II-A.41	Deformation Amount Analysis Model of Outer Shell during 9m Vertical Drop (with the lower container downward)	II-A-104
Fig.II-A.42	Deformation Amount Analysis Model of Outer Shell during 9m Horizontal Drop (with the upper cover downward)	II-A-105
Fig.II-A.43	Deformation Amount Analysis Model of Outer Shell during 9m Corner Drop (with the upper cover downward)	II-A-107
Fig.II-A.44	Deformation Amount Analysis Model of Outer Shell during 9m Corner Drop (with the lower container downward)	II-A-109
Fig.II-A.45	Relationship between N_x and β with Load in Radial Direction	II-A-122
Fig.II-A.46	Relationship between M_x and β with Load in Radial Direction	II-A-123
Fig.II-A.47	Relationship between N_ϕ and β with Load in Radial Direction	II-A-124
Fig.II-A.48	Relationship between M_ϕ and β with Load in Radial Direction	II-A-125

Figure List (5)

II

Fig.II-A.49	Relationship between N_x and β with External Moment in Axial Direction	II-A-126
Fig.II-A.50	Relationship between M_x and β with External Moment in Axial Direction	II-A-127
Fig.II-A.51	Relationship between N_ϕ and β with External Moment in Axial Direction	II-A-128
Fig.II-A.52	Relationship between M_ϕ and β with External Moment in Axial Direction	II-A-129
Fig.II-A.53	Relationship between N_x and β with External Moment in Circumferential Direction	II-A-130
Fig.II-A.54	Relationship between M_x and β with External Moment in Circumferential Direction	II-A-131
Fig.II-A.55	Relationship between N_ϕ and β with External Moment in Circumferential Direction	II-A-132
Fig.II-A.56	Relationship between M_ϕ and β with External Moment in Circumferential Direction	II-A-133
Fig.II-A.57	Tightening Bolt Analysis Model	II-A-134
Fig.II-A.58	Analysis Evaluation Model for "SHOCK" Code	II-A-137
Fig.II-A.59	Package Analysis Model during Vertical and Corner Drop	II-A-138
Fig.II-A.60	Package Analysis Model during Horizontal Drop	II-A-138
Fig.II-A.61	Load-displacement Relationship in Analytical Model (1) (Vertical Drop with the Top and Bottom End of Container Downward (a))	II-A-142
Fig.II-A.62	Load-displacement Relationship in Analytical Model (2) (Corner drop (a))	II-A-142
Fig.II-A.63	Load-displacement Relationship in Analytical Model (3) (Vertical Drop with the Lower Container Downward (i))	II-A-143
Fig.II-A.64	Load-displacement Relationship in Analytical Model (4) (Vertical Drop with the Upper Cover Downward (i))	II-A-143
Fig.II-A.65	Load-displacement Relationship in Analytical Model (5) (Corner Drop with the Upper Cover Downward (i))	II-A-144

Figure List (6)

II

Fig.II-A.66	Load-displacement Relationship in Analytical Model (6) (Corner Drop with the Lower Container Downward (i))	II-A-144
Fig.II-A.67	Load-displacement Relationship in Analytical Model (7) (Horizontal Drop (a))	II-A-145
Fig.II-A.68	Load-displacement Relationship in Analytical Model (8) (Horizontal Drop with the Direction of 0° in the Lower Container Downward (b))	II-A-145
Fig.II-A.69	Load-displacement Relationship in Analytical Model (9) (Horizontal Drop with the Direction of 90° in the Lower Container Downward (b)).....	II-A-146
Fig.II-A.70	Load-displacement Relationship in Analytical Model (10) (Horizontal Drop with the Direction of 180° in the Lower Container Downward (b)).....	II-A-146
Fig.II-A.71	Analysis Model for Equivalent Section Modulus.....	II-A-149
Fig.II-A.72	Analysis Model of Deformation Amount in Outer Shell.....	II-A-151

Figure List (7)

II

Fig.II-B.1	Package Component Drawing	II-B-3
Fig.II-B.2	Thermal Analysis Model based on Deformation due to Drop Test I.....	II-B-13
Fig.II-B.3	Analysis Model and Regional Boundary Conditions under Hypothetical Accident Conditions of Transport.....	II-B-16
Fig.II-B.4	Temperature Histories at Each Part under Hypothetical Accident Conditions of Transport.....	II-B-22
Fig.II-B.5	TRUMP Flow Chart (1/3).....	II-B-28
Fig.II-B.5	TRUMP Flow Chart (2/3).....	II-B-29
Fig.II-B.5	TRUMP Flow Chart (3/3).....	II-B-30
Fig.II-B.6	Homogenized Model of Fuel Assembly.....	II-B-31
Fig.II-B.7	Cross Section of Fuel Rod	II-B-31
Fig.II-B.8	Diagonal Array of Fuel Rod	II-B-31
Fig.II-B.9	Calculation Results of B Values	II-B-37
Fig.II-B.10	Effect of Drop Test II at Fire Test at 800°C for 30 Minutes on Thermal Analyses.....	II-B-41

Figure List (8)

II

Fig.II-C.1	General Drawing of Fuel Rod (Containment Boundary).....	II-C-5
Fig.II-C.2	Fuel Rod Welding Positions	II-C-6

Figure List (9)

II

Fig.II-D.1	Minimum Distance between Fuel Assembly and Package Surface (under Routine Conditions of Transport)	II-D-4
Fig.II-D.2	Shielding Analysis Model under Routine Conditions of Transport (per Fuel Assembly, One-Dimensional Cylindrical Shape)	II-D-5
Fig.II-D.3	Minimum Distance between Fuel Assembly and Package Surface considering Maximum Displacement (under Normal Conditions of Transport)	II-D-6
Fig.II-D.4	Shielding Analysis Model under Normal Conditions of Transport (per Fuel Assembly, One-Dimensional Cylindrical Shape)	II-D-6
Fig.II-D.5	Mesh Division Drawing	II-D-14

Figure List (10)

II

Fig.II-E.1	Calculation Geometry under Hypothetical Accident Conditions of Transport.....	II-E-11
Fig.II-E.2	Sectional Drawing of Type 14 × 14 Fuel Assembly	II-E-12
Fig.II-E.3	Sectional Drawing of Type 15 × 15 Fuel Assembly	II-E-13
Fig.II-E.4	Sectional Drawing of Type 17 × 17 Fuel Assembly	II-E-14
Fig.II-E.5	Flow of Criticality Calculation	II-E-15
Fig.II-E.6	Specification of Fuel Rod used for Criticality Experiment	II-E-22
Fig.II-E.7	Criticality Experiment System	II-E-23

Figure List (11)

III

Fig.III-1	Quality System of Design, Fabrication, Procurement, Maintenance of Package	III-9
Fig.III-2	Organization of MNF Packaging Quality	III-10

Figure List (12)

IV

Fig.IV-A-1	Preparation of Empty Packaging.....	IV-A-2
Fig.IV-A-2	Fuel Assembly Loading Flow	IV-A-5
Fig.IV-A-3	Auxiliary Legs (MFC-1 Type (A)).....	IV-A-6
Fig.IV-A-4	Auxiliary Legs (MFC-1 Type (B)).....	IV-A-7
Fig.IV-A-5	Tightening Bolt Detail	IV-A-8
Fig.IV-A-6	Tightening Bolt Receptacle	IV-A-9
Fig.IV-A-7	Container Top End Detail (MFC-1 Type (A)).....	IV-A-10
Fig.IV-A-8	Container Top End Detail (MFC-1 Type (B)).....	IV-A-11
Fig.IV-A-9	Bottom End Detail	IV-A-12
Fig.IV-A-10	Assembling Drawing of Cradle Assembly.....	IV-A-13
Fig.IV-A-11	Fuel Assembly Unloading Flow	IV-A-17

Table List (1)

Table I-A. 1	Specification of Radioactive Contents	I-A-2
Table I-C. 1	List of Packaging Main Parts	I-C-27
Table I-D. 1	Types of Fuel Assemblies and Quantities of their Main Parts	I-D-31
Table I-D. 2	Dimensions of Fuel Assemblies with NFBC	I-D-31
Table I-D. 3	Dimensions of Main Parts of Fuel Rod	I-D-32
Table I-D. 4	Dimensions of Main Parts of Control Rod Guide Thimbles	I-D-32
Table I-D. 5	Materials of Main Parts of Fuel Assembly	I-D-33
Table I-D. 6	Specification of Enriched Uranium	I-D-35
Table I-D. 7	Radiation Source Intensity of Assemblies and Packaging	I-D-35
Table I-D. 8	Weights of Main Parts of Fuel Assemblies	I-D-36
Table I-D. 9	Internal Pressure of Fuel Rods and Filled Gas	I-D-37

Table List (2)

II

Table II-A.1	Stress Evaluation Criteria used for Structural Analysis	II-A-3
Table II-A.2	Design Loads and Combination of Loads	II-A-4
Table II-A.3	Load Conditions	II-A-5
Table II-A. 4(1)	Conditions of Packaging Structure Design and Analysis Method ·	II-A-6
Table II-A. 4(2)	Conditions of Packaging Structure Design and Analysis Method ·	II-A-7
Table II-A. 4(3)	Conditions of Packaging Structure Design and Analysis Method ·	II-A-8
Table II-A. 4 (4)	Conditions of Packaging Structure Design and Analysis Method ·	II-A-9
Table II-A. 4 (5)	Conditions of Packaging Structure Design and Analysis Method ·	II-A-10
Table II-A. 4 (6)	Conditions of Packaging Structure Design and Analysis Method ·	II-A-11
Table II-A. 4 (7)	Conditions of Packaging Structure Design and Analysis Method ·	II-A-12
Table II-A. 4 (8)	Conditions of Packaging Structure Design and Analysis Method ·	II-A-13
Table II-A. 4 (9)	Conditions of Packaging Structure Design and Analysis Method ·	II-A-14
Table II-A. 4 (10)	Conditions of Packaging Structure Design and Analysis Method ·	II-A-15
Table II-A.5	Maximum Weight of Each Part	II-A-16
Table II-A.6	Mechanical Properties of Materials	II-A-18
Table II-A.7	Mechanical Properties of Materials (Design Basis)	II-A-19
Table II-A.8	Compression Deformation Stress of Shock Absorber	II-A-19
Table II-A.9	Dynamic Spring Constants of Shock Mounts	II-A-20
Table II-A.10	List of Different Materials in Contact	II-A-24
Table II-A.11	Minimum Atmospheric Temperature at Each Area	II-A-25
Table II-A.12	Material of Main Component	II-A-25
Table II-A.13	K_1 and K_2 in Acting of Radial Load	II-A-37
Table II-A.14	C_c and K_c in Acting of Circumferential External Moment	II-A-38
Table II-A.15	C_L and K_L in Acting of Axial External Moment	II-A-39
Table II-A.16	Stress during Lifting	II-A-46
Table II-A.17	Temperature at Each Part	II-A-55
Table II-A.18	Analysis Specification of Fuel Assemblies	II-A-58
Table II-A.19	Stress Produced in Cladding due to Internal Pressure	II-A-59
Table II-A.20	Comparison with Allowable Stress	II-A-61
Table II-A.21	Stress Produced in Fuel Rod Cladding during 1.2m Horizontal Drop	II-A-69

Table List (3)

II

Table II-A.22	Stress Produced in Each Part	II-A-75
Table II-A.23	Compressive Stress Produced in Each Fuel Rod Cladding	II-A-78
Table II-A.24	Impact Load Produced in Fuel Rod Cladding	II-A-80
Table II-A.25	Compressive Stress Produced in Skeleton Assembly	II-A-85
Table II-A.26	Analysis Acceleration during Corner Drop	II-A-86
Table II-A.27(1)	Analysis Result of 1.2m Corner Drop	II-A-89
Table II-A.27(2)	Analysis Result of 1.2m Corner Drop	II-A-90
Table II-A.28(1)	Comparison with Allowable Stress	II-A-96
Table II-A.28(2)	Comparison with Allowable Stress	II-A-97
Table II-A.28(3)	Comparison with Allowable Stress	II-A-98
Table II-A.29	Analysis Acceleration during Corner Drop	II-A-108
Table II-A.30	Analysis Acceleration during Corner Drop	II-A-110
Table II-A.31	Results of Drop Test II of Prototype Test (1)	II-A-114
Table II-A.31	Results of Drop Test II of Prototype Test (2)	II-A-115
Table II-A.32(1)	Comparison with Allowable Stress	II-A-118
Table II-A.32(2)	Comparison with Allowable Stress	II-A-119
Table II-A.33	Comparison between Experiment Value and Analytical Value ..	II-A-137
Table II-A.34	Physical Values of Material (used in SHOCK)	II-A-139
Table II-A.35	Analysis Model, Weight of Each Material Point (Vertical, Corner Drop Model)	II-A-139
Table II-A.36	Analysis Model, Weight of Each Material Point (Horizontal Drop Model)	II-A-139
Table II-A.37	Spring Constant of Analytical Model (Vertical, Corner Drop Model)	II-A-140
Table II-A.38	Spring Constant of Analytical Model (Horizontal Drop Model)	II-A-140
Table II-A.39	Drop Analysis Result	II-A-147
Table II-A.40	Comparison between Analysis Value and Experiment Value for 9m Drop	II-A-148
Table II-A.41	Stress Produced in Fuel Rod during Horizontal Drop	II-A-149
Table II-A.42	Analysis Result of Deformation Width during Horizontal Drop ..	II-A-152

Table List (4)

II

Table II-B.1	Thermal Analysis Conditions	II-B-4
Table II-B.2	Method of Thermal Analysis	II-B-4
Table II-B.3	Thermal Properties of Carbon Steel	II-B-5
Table II-B.4	Thermal Properties of Wood	II-B-5
Table II-B.5	Thermal Properties of UO ₂ Pellets	II-B-6
Table II-B.6	Thermal Properties of Air	II-B-6
Table II-B.7	Thermal Properties of Fuel Rod Cladding Tube	II-B-6
Table II-B.8	Thermal Properties of Homogenized Model of Fuel	II-B-7
Table II-B.9	Thermal Conditions under Normal Conditions of Transport	II-B-9
Table II-B.10	Thermal Analysis Conditions under Hypothetical Accident Conditions of Transport	II-B-15
Table II-B.11	Maximum Temperature of Each Part of Package under Normal and Accident Conditions of Transport	II-B-20
Table II-B.12	Maximum Pressure in Fuel Rods and in Packaging under Normal and Accident Conditions of Transport	II-B-20
Table II-B.13	Integrity of Package under Hypothetical Accident Conditions of Transport	II-B-21
Table II-B.14	Area Ratio of Homogenized Fuel Part	II-B-32
Table II-B.15	Calculation Results of B Values	II-B-35
Table II-B.16	Radiation Factor of Each Part	II-B-38
Table II-B.17	Heat Transfer Coefficient of External Cylinder	II-B-39
Table II-B.18	Radiation Factor of Each Material	II-B-40
Table II-B.19	Configuration Factor	II-B-40
Table II-B.20	Initial Values of Fuel Rod	II-B-43
Table II-B.21	Void Volume and Internal Pressure of Fuel Rod at Maximum Temperature	II-B-43
Table II-B.22	Hoop Stress on Fuel Rod at Maximum Temperature	II-B-43

Table List (5)

II

Table II-C.1	Maximum Temperature of Containment Boundary (1/2).....	II-C-8
Table II-C.1	Maximum Pressure of Containment Boundary (2/2)	II-C-8

Table List (6)

II

Table II-D.1	Gamma Emission Rate	II-D-2
Table II-D.2	Radioactivity of Major Nuclides	II-D-3
Table II-D.3	Volume Ratio for Each Material in Each Region of Shielding Analysis Model	II-D-7
Table II-D.4	Atomic Number Density of Each Material.....	II-D-7
Table II-D.5	γ -ray Energy Group Structure and Conversion Coefficient of Dose-Equivalent Rate	II-D-9
Table II-D.6	Summary of Maximum Dose Rate	II-D-10

Table List (7)

II

Table II-E.1	Data for Various Types of Fuel Assemblies	II-E-7
Table II-E.2	Distance from Fuel Assembly to Packaging Surface	II-E-8
Table II-E.3	Atomic Number Density in Each Region	II-E-8
Table II-E.4	Criticality Analysis Conditions and Analysis Results	II-E-10
Table II-E.5	Criticality Dimensions in Criticality Experiment	II-E-19
Table II-E.6	Material Densities and Atomic Densities used for Criticality Experiment	II-E-20
Table II-E.7	Results of Criticality Experiment Analysis	II-E-21

Table List (8)

IV

Table IV-A.1	Test/Inspection Procedures before Shipment of Package	IV-A-15
Table IV-B.1	Periodical Test/Inspection Procedures	IV-B-3

SUMMARY OF PACKAGE

Summary of Package

- (1) Name of Package : MFC-1
- (2) Type of Package : Type A Package containing Fissile Material
- (3) For Package containing Fissile Material
- (i) Restriction Number "N" : No restriction
 - (ii) Array of Package : No restriction
 - (iii) Criticality Safety Index : 0
- (4) Transport Index : 0.6 or less
- (5) Total Weight of Package : 4,320kg or less (including two Assemblies)
- (6) Outer Dimensions of Packaging
- | | MFC-1 Type (A) | MFC-1Type (B) |
|----------------|-------------------|---------------|
| Length | : Approx. 5,400mm | Same as left |
| Outer Diameter | : Approx. 1,150mm | Same as left |
| Height | : Approx. 1,275mm | Same as left |
- (7) Total Weight of Packaging
- | | MFC-1 Type (A) | MFC-1Type (B) |
|--------|-------------------|---------------|
| Weight | : Approx. 2,804kg | Same as left |
- (8) Materials of Packaging
- Outer Shell : Carbon Steel (SPCC and SS400)
 - Shock Absorber : Wood
 - Cradle Assembly : Carbon Steel (SM490A and SS400)
and Boronated Stainless Steel
 - O-Ring : Synthetic Rubber (Neoprene)
 - Shock Mounts : Synthetic Rubber (Polybutadiene)

(9) Specification of Radioactive Contents

- (i) Type of Material : Fuel assembly for PWR (UO₂)
Fuel assembly for PWR(UO₂ Pellet and Gadolinia-UO₂ Pellet)
- (ii) Maximum Quantity of Material per Package : Two Fuel Assemblies

Type of Fuel Assembly	Maximum UO ₂ mass	
	Fuel Assembly for PWR (UO ₂ Pellet)	Fuel Assembly for PWR (UO ₂ Pellet and Gadolinia-UO ₂ Pellet)
Type 14×14, 10 feet	780kg-UO ₂ or less	778kg-UO ₂ or less
Type 14×14, 12 feet	940kg-UO ₂ or less	937kg-UO ₂ or less
Type 15×15, 12 feet	1,080kg-UO ₂ or less	1,077kg-UO ₂ or less
Type 17×17, 12 feet	1,080kg-UO ₂ or less	1,077kg-UO ₂ or less

(iii) Initial Enrichment

a. Initial Enrichment of Uranium Dioxide

: 5 wt% or less for Type 14×14, Type 15×15 and Type 17×17

b. Maximum Enrichment of Gadolinia - Uranium Dioxide

: 3.3 wt% or less (with Gadolinia of up to 10.2wt%)
for Type 14×14, Type 15×15 and Type 17×17

- (iv) Burn-up Rate : Not applicable
- (v) Cooling Time : Not applicable
- (vi) Total Activity : 1.54×10^{11} Bq (for two Assemblies)
(Uranium Dioxide and Gadolinia - Uranium Dioxide)
- (vii) Heat Generation Rate : Not applicable

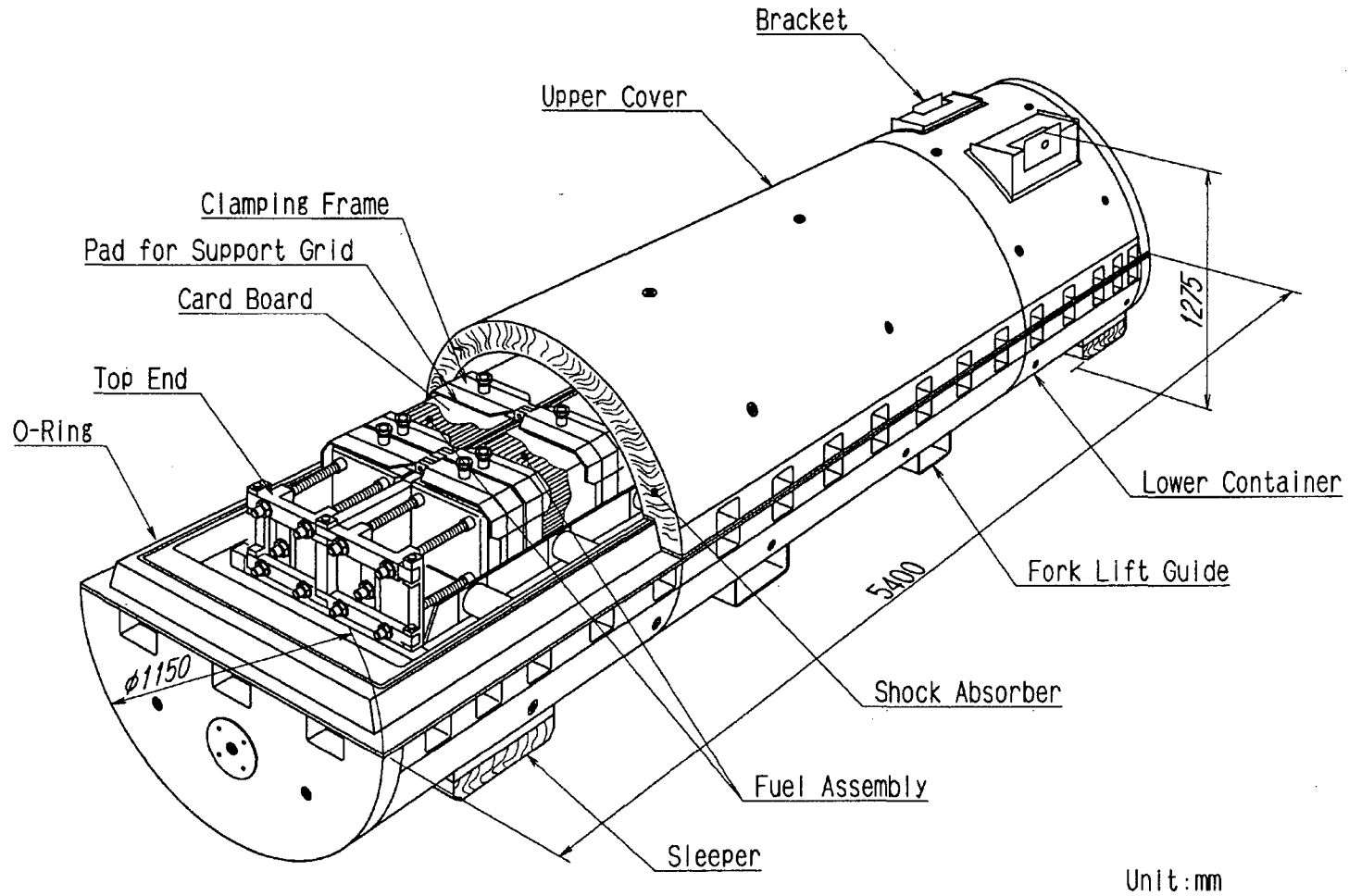


Fig. Summary- 1 Illustration of Package (Bird's Eye View)

I PACKAGE DESCRIPTION

I-A Objective and Condition

I Package Description

I-A Objective and Condition

(1) Purpose of Package

This packaging is used for the transport of the fresh fuel assemblies of type 14×14 (10 feet), type 14×14 (12 feet), type 15×15 (12 feet) and type 17×17 (12 feet) (also including the case where non-nuclear fuel core internals are built in for each type), which are fabricated in Mitsubishi Nuclear Fuel Co. Ltd. and charged in Pressurized Water type Light Water Reactors (PWR), from Mitsubishi Nuclear Fuel Co., Ltd. to Nuclear Power Plants. This packaging is used to transport the fresh fuel assemblies of type 17×17 (12 feet), which are fabricated overseas, to the Nuclear Power Plants in Japan.

There are MFC-1 type (A) and MFC-1 type (B) as for this packaging. MFC-1 Type (B) is a packaging produced by improving handling ability of MFC-1 Type (A). They consist of the same basic components and have the same main dimensions.

(2) Name of Package : MFC-1

(3) Type of Package : Type A Package containing Fissile Material

(4) For Package containing Fissile Material

(i) Restriction Number "N" : No restriction

(ii) Array of Package : No restriction

(iii) Criticality Safety Index : 0

(5) Transport Index : 0.6 or less

(6) Total Weight of Package : 4,320kg or less (including two Assemblies)

(7) Outer Dimensions of Packaging

	MFC-1 Type (A)	MFC-1Type (B)
Length	: Approx. 5,400mm	Same as left
Outer Diameter	: Approx. 1,150mm	Same as left
Height	: Approx. 1,275mm	Same as left

(8) Total Weight of Packaging

	MFC-1 Type (A)	MFC-1Type (B)
Weight:	: Approx. 2,804kg	Same as left

Proprietary Information Withheld Pursuant to 10 CFR 2.390

(11) Transport Mode

(a) Transport Method

Road vehicles are used in the case of land transport, and vessels are used in the case of sea transport.

(b) Loading Method

In the case of road vehicles, two packages are loaded on a track in parallel. In the case of ship transport, the maximum quantity of packages to be loaded in one division is obtained by dividing 50 by the transport index. These packages are loaded in parallel or stacked in two stages.

(12) Cooling Method

Natural Air Cooling

I-B CLASSIFICATION OF PACKAGE

I-B Classification of Package

This package is designed as a type A packaging containing fissile material.

- (1) Contents in this package are PWR new fuels, which are made of uranium 235 of natural uranium enriched below 5wt%. The A_2 value of the uranium 235 is unlimited.
- (2) This package contains 15g or more fissile material, uranium 235.

I-C PACKAGING

Proprietary Information on Pages I-C-1 through I-C-3
Withheld Pursuant to 10 CFR 2.390

C.2.4 Auxiliary Devices

Auxiliary legs are provided to prevent overturning of the packaging during loading and unloading of fuel assemblies. The auxiliary legs under housing and fixing conditions are shown in Fig.I-C.16 for type (A) and in Fig.I-C.17 for type (B)).

For a measurement, storage and control of the fuel assemblies and the packaging, there are shock indicators shown in Fig.I-C.3 and Fig.I-C.4, a relief valve shown in Fig.I-C.18, a hygrometer and an air valve shown in either Fig.I-C.19 (type (A)) or Fig.I-C.20 (type (B)).

The shock indicators shown in Fig.I-C.3 and Fig.I-C.4 are attached on the top and bottom ends of the cradle assembly in downward and axial direction, to monitor whether or not an impact on the fuel assembly exceeds a limit during the handling and transportation of the package.

In order to limit the rise of inner pressure, the relief valve shown in Fig.I-C.18 is provided on the packaging. This valve has configuration of check valve and is adjusted to open when the difference between inner and outer pressures reaches max. 0.049MPa·G.

The hygrometer is provided on the packaging, to indicate the humidity in the packaging. Also, air valve is provided to pressurize or depressurize the packaging. The construction of the hygrometer and the air valve is shown in Fig.I-C.19 (type A) or Fig.I-C.20 (type B). The air valve is covered by a cover and configured so that it cannot be easily removed. This valve cannot be opened or closed by rise of inner pressure, and can be actuated only in case it is pushed using the jig from the outside.

O-ring of neoprene is provided in the packaging to seal between the upper cover and the lower container (refer to Fig.I-C.6). The O-ring is inserted in a groove provided in the flange part of the lower container.

C.3 Materials and Dimensions of Main Parts of Packaging

The materials and the dimensions of main parts are shown in Table I-C. 1

C.4 Dimensions and Weight of Packaging

(I) Outer dimensions of packaging

	MFC-1 Type A	MFC-1Type B
Length	: Approx. 5,400mm	Same as left
Outer Diameter	: Approx. 1,150mm	Same as left
Height	: Approx. 1,275mm	Same as left

(II) Weight of Packaging

	MFC-1 Type A	MFC-1Type B
Weight:	: Approx. 2,804kg	Same as left

C.5 Containment Boundary

There are no components as the containment device in this packaging, and the containment boundary consists of cladding tube and end plugs of fuel rod. Fig.I-C.21 shows the containment boundary.

LC-6

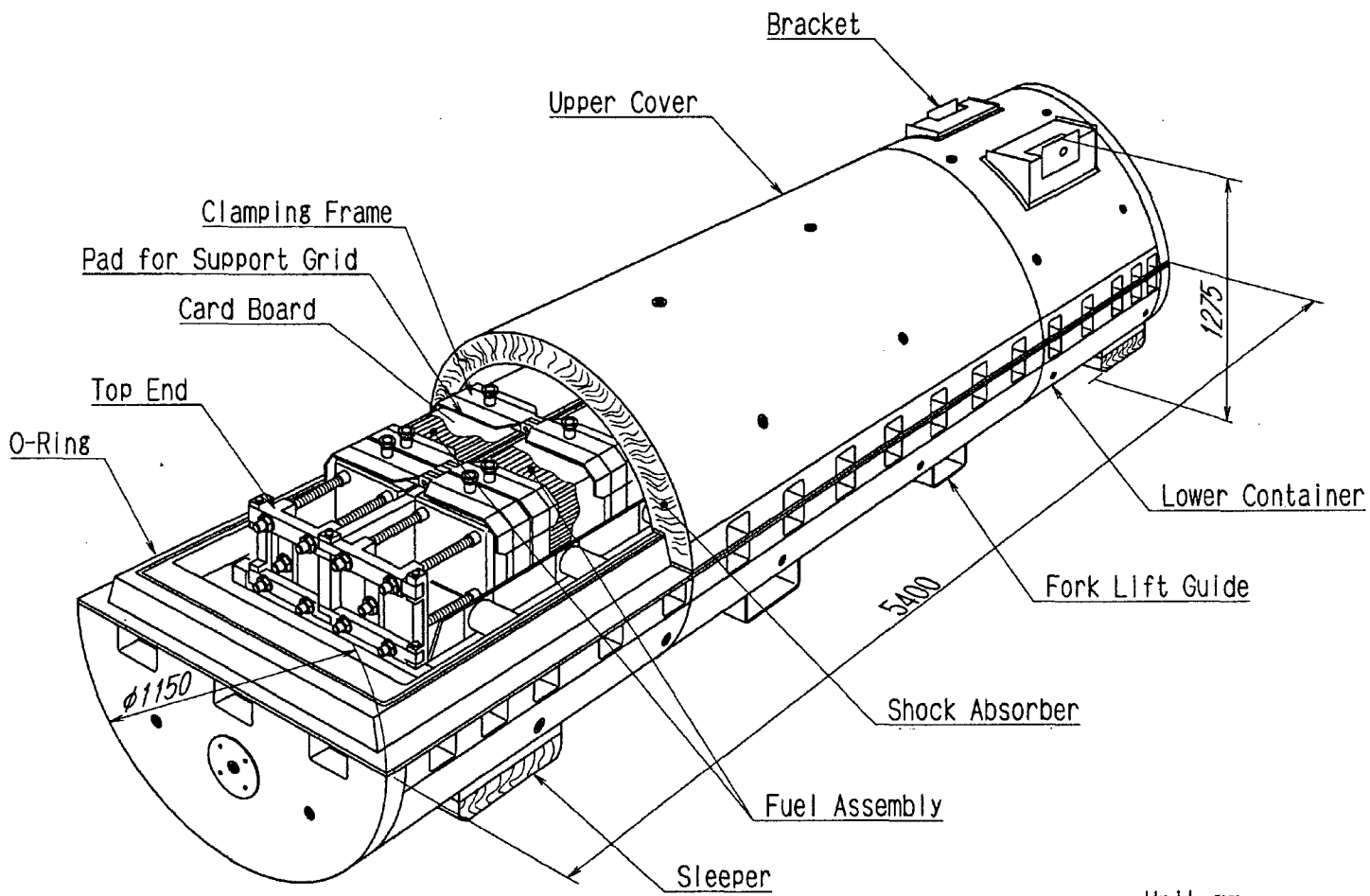


Fig.I-C.1 Illustration of Package (Bird's Eye View)

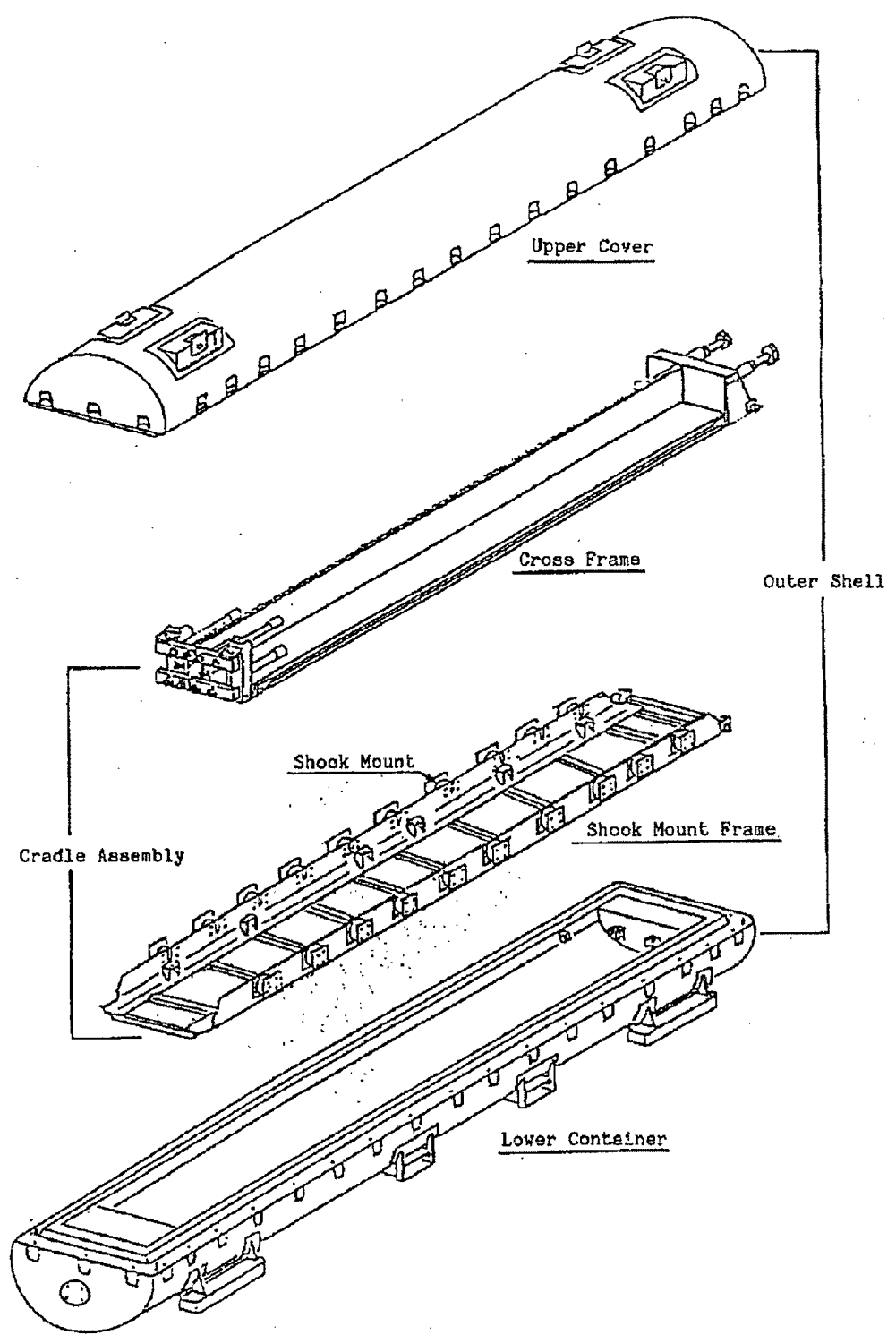


Fig.I-C.2 Cradle Assembly and Outer Shell

Proprietary Information on Pages I-C-8 through I-C-28 Withheld Pursuant to 10 CFR 2.390

I-D CONTENTS OF PACKAGING

Proprietary Information on Pages I-D-1 through I-D-37
Withheld Pursuant to 10 CFR 2.390

II SAFETY ANALYSIS FOR PACKAGE

II Safety Analysis for Package

It shall be verified analytically that this package meets the requirements for the Type A package containing fissile material specified in the 2005 Edition of the Regulations for the Safe Transport of Radioactive Materials (International Atomic Energy Agency, Safety Standards Series No. TS-R-1, hereinafter referred to as "2005 IAEA regulations"), and the Japanese rules based on the Act on the Regulation of Nuclear Source Materials, Nuclear Fuel Materials and Reactors (hereinafter referred to as "Japanese transport regulations").

(1) Standards relating to Type A Package containing Fissile Material

(A) Routine transport conditions for Type A Package containing fissile material

- (a) The package shall be able to be handled easily and safely.
(Ref: Paragraph 606 of 2005 IAEA regulations)
- (b) The package shall be capable of withstanding the effects of any acceleration, vibration or vibration resonance which may arise under routine conditions of transport without any deterioration. (Ref: Para. 612)
- (c) As far as practicable, the surface of the package shall be free from protruding features and can be easily decontaminated. (Ref: Para. 609)
- (d) The materials of the packaging and any components or structures shall be physically and chemically compatible with each other and with the radioactive contents. (Ref: Para. 613)
- (e) All valves through which the radioactive contents could otherwise escape shall be protected against unauthorized operation. (Ref: Para. 614)
- (f) The non-fixed contamination on the external surfaces of the packaging shall not exceed the following limits: (Ref: Para. 508)
4Bq/cm² for beta and gamma emitters and low toxicity alpha emitters
0.4 Bq/cm² for all other alpha emitters
- (g) The smallest overall external dimension of the package shall not be less than 10cm. (Ref: Para. 634)
- (h) The outside of the package shall incorporate a feature such as a seal, which is not readily breakable and which, when intact, will be evidence that it has not been opened. (Ref: Para. 635)
- (i) Unless the expected temperature limit during the transport can be identified, no cracking or damage shall occur on the component parts taking into account temperature ranging from -40 to 70°C. (Ref: Para. 637, the underlined requirement is in accordance with the Japanese transport regulations)
- (j) The containment system shall retain its radioactive contents under a reduction of ambient pressure to 60 kPa. (Ref: Para. 643)

- (k) The dose-equivalent rate on the surface shall not exceed 2mSv/h. (Ref: Para.531)
 - (l) The dose-equivalent rate at positions apart 1m from the surface shall not exceed 100μSv/h. (Ref: Para. 573(b), the underlined requirement is in accordance with the Japanese transport regulations.)
 - (m) Any materials other than the documents and objects required for use of nuclear fuel materials (limited to those which do not impair the safety of the package for nuclear fuel materials) shall not be contained. (This requirement is in accordance with the Japanese transport regulations.)
- (B) Normal conditions of transport of Type A Package containing fissile material
- Type A Package containing fissile material under the normal conditions of transport specified in item (b) below shall meet the requirements specified in item (a) below.
- (a) Requirements
 - (i) No leakage of radioactive material shall occur (Ref: Para: 646(a)).
 - (ii) The dose-equivalent rate on the surface shall not increase remarkably and shall not exceed 2mSv/h at the surface of the package (Ref: Para. 646 (b) and 531)
 - (b) Normal Conditions of transport
 - (i) Water spray test: The specimen shall be subjected to a water spray test that simulates exposure to rainfall of approximately 50mm per hour for one hour. (Ref: Para. 721)
 - (ii) After the package has been put under the condition of item (i) above, it shall be put under the conditions below.
 - Free drop: The specimen shall drop from a height of 1.2m so as to suffer maximum damage (Ref: Para. 722).
 - Stacking test: the specimen shall be subjected, for a period of 24 h, to a compressive load equal to 5 times the mass of the actual package or a compressive load equal to 13 kPa multiplied by the vertically projected area of the package. (Ref: Para. 723)
 - Penetration test: A steel bar of 6kg in weight and 3.2cm in diameter with a hemispherical end shall be dropped on the weakest part of the package from a height of 1m (Ref: Para. 724).

(2) Standards relating to Fissile Material Package

(A) Routine transport conditions for fissile material package

- (a) The individual package in isolation*¹ shall be subcritical.
- (b) Unless the expected temperature limit during the transport can be identified, no cracking or damage shall occur on the component parts taking into account temperature ranging from -40 to 70°C.

*¹ Water can leak into or out of all void space of the package with the conditions that result in the maximum neutron multiplication, and water reflector of 20cm thick is provided around the packaging (Ref: Para. 678).

(B) Normal conditions of transport of fissile material package

The fissile material package under the normal conditions of transport specified in item (b) below shall meet the requirements specified in item (a) below.

(a) Requirements

- (i) The packaging must prevent the entry of a 10 cm cube. (Ref: Para. 675)
- (ii) The individual package in isolation shall be subcritical under the normal conditions of transport. (Ref: Para. 679(b))
- (iii) Five times the allowable number "N" of the packages shall be subcritical for the arrangement*² and the package conditions that result in the maximum neutron multiplication between such fissile packages. (Ref: Para. 681)

*² The package is arranged in any position, and the package arrangement shall be reflected on all sides by at least 20 cm of water. (Ref: Para. 681 (a))

(b) Normal conditions of transport

- (i) Water spray test: The specimen shall be subjected to a water spray test that simulates exposure to rainfall of approximately 50mm per hour for one hour. (Ref: Para. 721)
- (ii) After the package has been put under the condition of item (i) above, it shall be put under the conditions below.
 - Free drop: The specimen shall drop from a height of 1.2m so as to suffer maximum damage. (Ref: Para. 722)
 - Stacking test: the specimen shall be subjected, for a period of 24 h, to a compressive load equal to 5 times the mass of the actual package or a compressive load equal to 13 kPa multiplied by the vertically projected area of the package. (Ref: Para. 723)
 - Penetration test: A steel bar of 6kg in weight and 3.2cm in diameter with a hemispherical end shall be dropped on the weakest part of the package from a height of 1m. (Ref: Para. 724)

(C) Hypothetical accident conditions of transport

The fissile material package under the hypothetical accident conditions of transport specified in item (b) below shall meet the requirements specified in item (a) below.

(a) Requirements

- (i) The individual package in isolation under the hypothetical accident conditions of transport shall be subcritical.**
- (ii) Twice the allowable number "N" of the packages shall be subcritical for the arrangement and the package conditions that result in the maximum neutron multiplication between such fissile packages. (Ref: Para. 682).**

(b) Hypothetical accident conditions of transport

- (i) After the normal conditions of transport of item (B) (b) above have been satisfied, the specimen shall drop onto the target from a height of 9m. (Ref: Para. 727(a))**
- (ii) The specimen shall drop from a height of 1m onto a mild steel bar of 15cm in diameter and 20cm in length. (Ref: Para. 727(b))**
- (iii) After (i) and (ii) above, the specimen shall be in thermal equilibrium under conditions of an ambient temperature of 38°C, subject to the solar insolation conditions. The specimen shall be exposed for a period of 30 minutes to a thermal environment which provides a heat flux in sufficiently quiescent ambient conditions to give an average temperature of 800°C, and be followed by exposure to an ambient temperature of 38°C, subject to the solar insolation conditions without any artificial cooling. (Ref: Para. 728)**
- (iv) After (iii) above, the specimen shall be immersed under a head of water of 0.9m for a period of eight hours. (Ref: Para. 733)**
- (v) After (B) (b) above, in addition to the test conditions of items (i) to (iv) above, the specimen shall be immersed under a head of a water of 15m for a period of eight hours. (Ref: Para. 729)**

II-A STRUCTURAL ANALYSIS

II-A Structural Analysis

A.1 Structural Design

A.1.1 Outline

This packaging has two models: MFC-1 Type (A) and Type (B). They differ in shape slightly due to improvement in handling, and their structures are all identical to each other.

The packaging consist of the cradle assembly on which fuel assemblies as package are loaded, upper cover, lower shell, and auxiliary devices.

As shown in Fig. I-C.2, the cradle assembly consists of a shock mount frame, a cross frame, and clamping frames.

The cross frame can carry two units of fuel assemblies, and rubber cushions are attached on the contact surface between the cross frame and fuel assemblies to increase the cushioning effect. Boron stainless steels (hereinafter called the skin) of 4.5mm thick minimum as neutron absorber are attached on the entire surface of the cross frame.

The clamping frames are used to fix the support grids of fuel assemblies and the top nozzle during the transport.

The shock mount frame fixes the cross frame during the transport.

The shock mount frame is mounted inside the packaging through the shock mounts.

The outer shell consists of the upper cover and the lower container, and balsa wood acting as heat insulator and shock absorber is filled into the hollow part between the external cylinder and internal cylinder of each packaging.

The outer shell is of the watertight structure formed in cylindrical shape, and its outer surface is so structured that rainfall is difficult to be accumulated. Also, a bracket is attached to the upper cover at four positions for lifting the packaging in transportation.

In addition, a sealing is attached to the upper cover tightening bolts so that, if the packaging is unsealed, it can be identified.

A.1.2 Design Criteria

(1) Analysis criteria

The stress evaluation criteria used for structural analysis are as shown in Table II-A. 1.

- (a) When a tensile stress and a compressive stress are evaluated under the routine transport conditions (these criteria are applied to lifting device and tie-down device) and normal conditions of transport, the analysis criteria for shear stress shall be 60% of the design yield strength (S_y) on use material design yield strength (S_y) basis.
- (b) For the strength evaluation under the hypothetical accident conditions of transport, the design tensile strength (S_u) shall be used as the analysis criteria.
- (c) For sealing boundary, see Table II-A. 1.
- (d) When a stress generated at a weld is evaluated, the welding efficiency shall be 0.6.
- (e) Those materials of which usable temperature range is identified shall be used within that range, and the mechanical properties which are satisfied under that temperature range shall be used as the analysis criteria.
- (f) The other special specifications, if any, shall be explained in the analysis of each specification.

(2) Combination of loads

The combination of loads shall be determined according to the design requirements and considering the materials, temperatures, and safety factors of structures as shown in Table II-A.2 and Table II-A.3 for each analysis item.

(3) Safety Margin

The results obtained quantitatively shall be evaluated with a safety margin (M_s) specified below.

$$\text{Safety Margin } (M_s) = \text{Analysis criteria/Analysis result} - 1$$

If a safety margin cannot be used, the criteria shall be put at the applicable position. In accordance with the design requirements as described above, the requirements for structural analysis, analysis items, and analysis methods are summarized, and shown in Table II-A. 4 (1) to Table-II-A.4 (10).

Table II-A. 1 Stress Evaluation Criteria used for Structural Analysis

Analysis Item	Condition	Load Condition	Evaluation Criteria
Lifting device	Routine transport conditions	Self-weight	$\sigma < S_y$
Bolt part	Normal conditions of transport	· Inner pressure · Impact load	$\sigma < S_y$
Cradle assembly	Hypothetical accident conditions of transport	· Thermal load	$\sigma < S_u$
Sealing boundary	Normal conditions of transport	· Inner pressure · Impact load	$P_m < S_m$ $P_L + P_b < 1.5 S_m$
	Hypothetical accident conditions of transport	· Thermal load	$P_m < S_y$ or $2/3 S_u$ $P_L + P_b < 1.5 S_y$ or S_u

NOTES:

σ : Analysis stress P_m : Primary general membrane stress P_l : Local membrane stress
 P_b : Bending stress S_y : Design yield strength S_u : Design tensile strength
 $S_m = \min(2/3 S_y, 1/3 S_u)$

Table II-A.2 Design Loads and Combination of Loads

○: Evaluation by combination of loads

△: Evaluation by single load

Requirement	Condition	Analysis Load	Evaluation Item Classification of loads	Gravity	Pressure	Others
Requirements for Type A package	Routine transport conditions	Lifting load	Lifting device and lifting device mounting part of main body	△	—	—
			Tightening bolt	○	○	—
		Pressure	Outer shell	—	△	—
		Vibration	Package	—	—	△
	Normal conditions of transport	Thermal test	Outer shell	—	△	—
			Fuel rod cladding	—	△	—
		Water spray	Package	—	—	△
		Free drop	Outer shell	△	—	—
			Cradle assembly	△	—	—
			Fuel rod cladding	○	○	—
	Stacking test	Outer shell	△	—	—	
	Penetration	Outer shell	—	—	△	
	Requirements for fissile material package	Normal conditions of transport	Water spray	Package	—	—
Free drop			Outer shell	△	—	—
			Cradle assembly	△	—	—
			Fuel rod cladding	○	○	—
Stacking test			Outer shell	△	—	—
Penetration		Outer shell	—	—	△	
Hypothetical accident conditions of transport		Drop test I	Outer shell	△	—	—
			Cradle assembly	△	—	—
			Fuel rod cladding	○	○	—
		Drop test II	Outer shell	△	—	—
		Thermal test	Fuel rod cladding	—	△	—
	Immersion	Fuel rod cladding	—	△	—	

Table II-A.3 Load Conditions

Requirement	Condition	Analysis Load	Evaluation Item				
			Classification of loads	Gravity	Pressure	Others	
Requirements for Type A package	Routine transport conditions	Lifting load	Lifting device and lifting device mounting part of main body	1.27 × 10 ⁵ N (Equal to three times of self weight)	—	—	
			Tightening bolt	1.27 × 10 ⁵ N (Equal to three times of self weight)	ΔP=* 50.0kPa·G	—	
		Pressure	Outer shell	—	ΔP=* 50.0kPa·G	—	
			Vibration	Package	—	—	—
	Normal conditions of transport	Thermal test	Outer shell	—	ΔP=* 50.0kPa·G	—	
			Fuel rod cladding	—	3.73MPa·G	—	
		Water spray	Package	—	—	Rainfall 50mm/h	
			Free drop	Outer shell	Multiplied by Acceleration Horizontal drop 199g Vertical drop 298g Corner drop 55g	—	—
				Cradle assembly	Multiplied by Acceleration Horizontal drop 72g	—	—
		Fuel rod cladding	Vertical drop 17g Corner drop 20g	3.73MPa·G	—		
		Stacking test	Outer shell	5 times + Self-weight	—	—	
	Penetration	Outer shell	—	—	Dropping of 6kg mild steel bar		
	Requirements for fissile material package	Normal conditions of transport	Water spray	Package	—	—	Rainfall 50mm/h
				Free drop	Outer shell	Multiplied by Acceleration Horizontal drop 189g Vertical drop 298g Corner drop 55g	—
Cradle assembly			Multiplied by Acceleration Horizontal drop 72g		—	—	
Fuel rod cladding			Vertical drop 17g Corner drop 20g		3.73MPa·G	—	
Stacking test			Outer shell	5 times + Self-weight	—	—	
Penetration			Outer shell	—	—	Dropping of 6kg mild steel bar	
Hypothetical accident conditions of transport		Drop test I	Outer shell	Multiplied by Acceleration Horizontal drop 652g Vertical drop 381g Corner drop 218g	—	—	
			Cradle assembly	Multiplied by Acceleration Horizontal drop 350g	—	—	
			Fuel rod cladding	Vertical drop 111g Corner drop 169g	3.73MPa·G	—	
		Drop test II	Outer shell	Evaluation based on the prototype test results	—	—	
		Thermal test	Fuel rod cladding	—	7.79MPa·G	—	
Immersion	Fuel rod cladding	—	0.009MPa·G	—			

*Relief valve maximum working pressure difference

Description of Symbols

σ : Principal stress
 σ_t : Tensile stress
 σ_c : Compressive stress
 τ : Shear stress
 τ_t : Torsional stress
F: Load
P: Pressure
A: Cross-sectional area

Table II-A. 4 (1) Conditions of Packaging Structure Design and Analysis Method

Requirement	Condition	Analysis Item	Design Requirements						Analysis Method		Remark
			Reference drawing	Material	Temperature	Design load			Applicable equation or factor	Analysis Criteria	
						Type	Safety factor	Factor			
Type A Package containing fissile material	Routine transport conditions	Chemical and electrical reactions	Table II-A. 10	-	-	Corrosion	-	Active	Presence or absence of activity	Activity: None	
		Chemical reaction Electrical reaction				Corrosion	-	Potential difference	Presence or absence of water content	Water content: None	
		Cold strength	Table II-A. 11	See Table II-A. 12	-20°C	Material	-	Cold brittleness	Presence or absence of cold brittleness	Presence or absence of cold brittleness and usable temperature range	
		Containment system Fuel rod	Fig. I-C.21	Zircaloy-4 MDA and ZIRLO	73°C	-	-	Sealing function	Presence or absence of sealing function	Sealing function: Present	A temperature of 73°C is the maximum temperature of the package obtained by the thermal analysis (See B.4.2). This is also applicable to the following.
	Lifting device 1. Lifting device (1) Bracket hole	Fig. II-A. 6	SS400	73°C	Maximum weight of package	3	Shear stress	$\tau = F/A$	0.6S _y	σ_b =Bending + Membrane stress M=Bending moment Z=Section modulus η =Weld efficiency 0.6	
(2) Bracket weld	Fig. II-A. 7	SS400	73°C	Maximum weight of package	3	Combined stress	$\sigma = 1/2(\sigma_b + \sqrt{\sigma_b^2 + 4\tau^2})$ $(\sigma_b = (M/Z + P/A))$ $(\tau = P/A)$	ηS_y			

Description of Symbols

σ : Principal stress
 σ_t : Tensile stress
 σ_c : Compressive stress
 τ : Shear stress
 τ_t : Torsional stress
F : Load
P : Pressure
A : Cross-sectional area

Table II-A. 4 (2) Conditions of Packaging Structure Design and Analysis Method

Requirement	Condition	Analysis Item	Design Requirements						Analysis Method		Remark
			Reference drawing	Material	Temperature	Design load			Applicable equation or factor	Analysis Criteria	
						Type	Safety factor	Factor			
Type A Package containing fissile material	Routine transport conditions	(3) External Cylinder	Fig. II-A. 8	SS400	73°C	Maximum weight of package	3	Combined stress	$\sigma = 1/2(\sigma_\phi + \sigma_x + \{(\sigma_\phi - \sigma_x)^2 + 4\tau^2\}^{1/2})$ $(\sigma_x = N_p/T \pm 6M_p/T^2)$ $(\sigma_\phi = N_p/T \pm 6M_p/T^2)$ $(\tau = V/4CT)$	S_y	V = Load σ_x = Axial stress σ_ϕ = Circumferential stress N = Membrane force T = External cylinder plate thickness + Seat plate thickness C = Length of load area
		2. Tightening bolt									
		(1) Tightening bolt	Fig. II-A. 11	SCM435	73°C	Maximum weight of package + Maximum inner pressure	3	Combined stress	$\sigma = 1/2(\sigma_t + \sqrt{\sigma_t^2 + 4\tau^2})$ $(\sigma_t = P_n/nA)$ $(\tau = T_t/Z_p)$	S_y	P_n = Tightening force n = Number of bolts T_t = Torque load Z_p = Torsional section modulus
	(2) Cross pin	Fig. II-A. 12	SCM435	73°C	Maximum weight of package + Maximum inner pressure	3	Combined stress	$\sigma = 1/2(\sigma_b + \sqrt{\sigma_b^2 + 4\tau^2})$ $(\sigma_b = M/Z)$ $(\tau = P_n/2nA)$	S_y		
	Fixing device			*			*				

II-A-7

Description of Symbols

σ : Principal stress
 σ_t : Tensile stress
 σ_c : Compressive stress
 τ : Shear stress
 τ_t : Torsional stress
F: Load
P: Pressure
A: Cross-sectional area

Table II-A. 4 (3) Conditions of Packaging Structure Design and Analysis Method

Requirement	Condition	Analysis Item	Design Requirements						Analysis Method		Remark	
			Reference drawing	Material	Temperature	Design load			Applicable equation or factor	Analysis Criteria		
						Type	Safety factor	Factor				
Type A Package containing fissile material	Routine transport conditions	Pressure External Cylinder	-	SS400	73°C	$\Delta P = 0.05 \text{ MPa}$	1	Tensile stress	$\sigma_a = PD/2t \eta$	S_y	D = Inner diameter t = Wall thickness	
		Vibration	Fig. II-A. 14	SS400	73°C	Vibration	1	sympathetic vibration	$f = a_1/2 \pi \sqrt{E \cdot I \cdot g/W \ell^4}$	10Hz and over	f = Natural frequency a ₁ = Primary mode coefficient E = Young's modulus 2.06 x 10 ⁵ (N/mm ²) ℓ = Overall length of packaging W = Weight per unit length I = Moment of inertia of area	
	Normal conditions of transport	Thermal test stress calculation										
		(1) External cylinder	Table II-A. 20	SS400	73°C	Inner pressure	1	Tensile stress	$\sigma_a = PD/2t \eta$	S_y		
		(2) Dome plate	Table II-A. 20	SS400	73°C	Inner pressure	1	Combined stress	Equation for flat plate deflection	S_y		
		(3) Fuel rod cladding	Fig. II-A. 15	Zircaloy-4 MDA and ZIRLO	73°C	Inner pressure	1	Combined stress	Equation for thin wall cylinder	S_m		
	(4) Fuel rod weld	Fig. II-A. 15	Zircaloy-4 MDA and ZIRLO	73°C	Inner pressure	1	Combined stress	Equation for thin wall cylinder	S_m	Weld efficiency 1.0 (because X-ray inspection is performed).		
Water spray	-	-	73°C	Water spray	1	Water absorbing Draining	Water absorptivity Draining capability	None Present				

Description of Symbols

σ : Principal stress

σ_t : Tensile stress

σ_c : Compressive stress

τ : Shear stress

τ_t : Torsional stress

F: Load

P: Pressure

A: Cross-sectional area

Table II-A. 4 (4) Conditions of Packaging Structure Design and Analysis Method

Requirement	Condition	Analysis Item	Design Requirements						Analysis Method		Remark
			Reference drawing	Material	Temperature	Design load			Applicable equation or factor	Analysis Criteria	
						Type	Safety factor	Factor			
Type A Package containing fissile material	Normal conditions of transport	Free drop									δ_o = Thickness before deformation δH_i = Amount of inside deformation δH_o = Amount of outside deformation
		(1) 1.2m horizontal drop									
		(a) Amount of deformation of outer shell	Fig. II-A. 17	-	-	1.2m horizontal drop	1	Amount of deformation	$\delta_o = \delta_o' - (\delta H_i + \delta H_o)$	125mm	
		(b) Stress calculation									
		(i) Clamping frame	Fig. II-A. 18	SS400	73°C	1.2m horizontal drop	1	Bending stress	$\sigma_b = M/Z$	S_y	
		(ii) Skin	Fig. II-A. 19	Boron stainless	73°C	1.2m horizontal drop	1	Bending stress	Circumferentially simple supported flat plate equation	S_y	
(iii) Fuel rod cladding	Fig. II-A. 21	Zircaloy-4 MDA and ZIRLO	73°C	1.2m horizontal drop	1	Combined stress	Both end supported beam equation	1.5S _m			
(2) 1.2m top end vertical drop											
(a) Amount of deformation of outer shell	Fig. II-A. 23	-	-	1.2m top end vertical drop	1	Amount of deformation	$\delta_o = \delta_o' - (\delta H_i + \delta H_o)$	250mm	δ_o = Thickness before deformation δH_i = Amount of inside deformation δH_o = Amount of outside deformation		
(b) Stress calculation											
(i) Jack screw	Fig. II-A. 24	SCM435	73°C	1.2m top end vertical drop	1	Shear stress	Thread shear fracture equation	0.6S _y			

Description of Symbols

σ : Principal stress
 σ_t : Tensile stress
 σ_c : Compressive stress
 τ : Shear stress
 τ : Torsional stress
F: Load
P: Pressure
A: Cross-sectional area

Table II-A. 4 (5) Conditions of Packaging Structure Design and Analysis Method

Requirement	Condition	Analysis Item	Design Requirements						Analysis Method		Remark
			Reference drawing	Material	Temperature	Design load			Applicable equation or factor	Analysis Criteria	
						Type	Safety factor	Factor			
Type A Package containing fissile material	Normal conditions of transport	(ii) Fixed frame	Fig. II-A. 25	SS400	73°C	1.2m top end vertical drop	1	Combined stress	$\sigma = 1/2 (\sigma_b + \sqrt{\sigma_b^2 + 4\tau^2})$ ($\sigma_b = M/Z$) ($\tau = W/A$)	S_y	m = Weight N = Acceleration m _t = Weight
		(iii) Fixed frame screw	Fig. II-A. 26	SS400	73°C	1.2m top end vertical drop	1	Shear stress	Thread shear fracture equation	0.6S _y	
		(iv) Skin	Fig. II-A. 27	Boron stainless	73°C	1.2m top end vertical drop	1	Compressive stress	$\sigma_c = m/A \cdot N$	S _y	
		(v) Fuel rod cladding	Fig. II-A. 28	Zircaloy-4 MDA and ZIRLO	73°C	1.2m top end vertical drop	1	Compressive stress Buckling	$\sigma_c = -P/A$ $P = m_t \times N$	S _m P _k	
		(3) 1.2m bottom end vertical drop									
		(a) Amount of deformation of outer shell	Fig. II-A. 30	-	-	1.2m bottom end vertical drop	1	Amount of deformation	$\delta_o = \delta_o' - (\delta H_i + \delta H_o)$	250mm	δ_o' = Thickness before deformation δH_i = Amount of inside deformation δH_o = Amount of outside deformation

Description of Symbols

σ : Principal stress
 σ_t : Tensile stress
 σ_c : Compressive stress
 τ : Shear stress
 τ_c : Torsional stress
F: Load
P: Pressure
A: Cross-sectional area

Table II-A. 4 (6) Conditions of Packaging Structure Design and Analysis Method

Requirement	Condition	Analysis Item	Design Requirements						Analysis Method		Remark	
			Reference drawing	Material	Temperature	Design load			Applicable equation or factor	Analysis Criteria		
						Type	Safety factor	Factor				
Type A Package containing fissile material	Normal conditions of transport	(b) Stress calculation (i) Pivot mount fixing bolt	Fig. II-A. 31	SS400	73°C	1.2m bottom end vertical drop	1	Combined stress	$\sigma = 1/2 (\sigma_t + \sqrt{\sigma_t^2 + 4\tau^2})$ $(\sigma_t = F/A)$ $(\tau = P/nA \times N)$	S _y	δ_o' = Thickness before deformation δH_i = Amount of inside deformation δH_o = Amount of outside deformation	
		(ii) Skeleton assembly	Fig. II-A. 32	Zircaloy-4	73°C	1.2m bottom end vertical drop	1	Compressive stress		$\sigma_c = \sum n/nA \times N$		S _y
		(4) 1.2m top end corner drop	Fig. II-A. 34	-	-	1.2m top end vertical drop	1	Amount of deformation	$\delta_o = \delta_o' (\delta H_i + \delta H_o)$ Evaluate stress calculation based on the results of A.5.3.	375mm		
		(5) 1.2m bottom end corner drop	Fig. II-A. 34	-	-	1.2m bottom end vertical drop	1	Amount of deformation		375mm		
		Stacking test Compression of external cylinder	Fig. II-A. 35	SS400	73°C	Load of 5 times the load of package	1	Bending stress	$\sigma_b = M/Z$	S _y		
		Penetration External cylinder	Fig. II-A. 36	SS400	73°C	Drop impact of mild steel bar	1	Absorbing energy	$E_2 = \tau_{cr} \cdot \pi d \cdot 1/2 \cdot t^2$	5.89 x 10 ⁴ (N·mm)		τ_{cr} = Shear strength of external cylinder
		Corner or edge drop					*			*		

Description of Symbols

σ : Principal stress

σ_t : Tensile stress

σ_c : Compressive stress

τ : Shear stress

τ : Torsional stress

F: Load

P: Pressure

A: Cross-sectional area

Table II-A. 4 (7) Conditions of Packaging Structure Design and Analysis Method

Requirement	Condition	Analysis Item	Design Requirements						Analysis Method		Remark
			Reference drawing	Material	Temperature	Design load			Applicable equation or factor	Analysis Criteria	
						Type	Safety factor	Factor			
Package containing fissile material	Normal conditions of transport	Water spray									Evaluate these items referring to the analysis results on the above normal conditions of transport.
		Free drop									
		Stacking compression of external cylinder									
		Penetration									

II-A-12

Description of Symbols

σ : Principal stress
 σ_t : Tensile stress
 σ_c : Compressive stress
 τ : Shear stress
 τ_t : Torsional stress
F: Load
P: Pressure
A: Cross-sectional area

Table II-A. 4 (8) Conditions of Packaging Structure Design and Analysis Method

Requirement	Condition	Analysis Item	Design Requirements						Analysis Method		Remark
			Reference drawing	Material	Temperature	Design load			Applicable equation or factor	Analysis Criteria	
						Type	Safety factor	Factor			
Package containing fissile material	Hypothetical accident conditions of transport	Drop test I									
		Top end vertical drop									
		(a) Amount of deformation of outer shell	Fig. II-A. 40	-	-	9m top end vertical drop	1	Amount of deformation	$\delta_o = \delta_o' - (\delta H_i + \delta H_o)$	δ_o'	δ_o' = Thickness before deformation δH_i = Amount of inside deformation δH_o = Amount of outside deformation
		(b) Stress calculation									
		(i) Jack screw	Table II-A. 32	SCM435	73°C	9m top end vertical drop	1	Shear stress	Thread shear fracture equation	$0.6S_u$	
		(ii) Fixed frame	Table II-A. 32	SS400	73°C	9m top end vertical drop	1	Bending stress	$\sigma_b = M/Z$	S_u	
		Bottom end vertical drop									
		(a) Amount of deformation of outer shell	Fig. II-A. 41	-	-	9m bottom end vertical drop	1	Amount of deformation	$\delta_o = \delta_o' - (\delta H_i + \delta H_o)$	δ_o'	δ_o' = Thickness before deformation δH_i = Amount of inside deformation δH_o = Amount of outside deformation
		(b) Stress calculation									
		(i) Pivot mount fixing bolt	Table II-A. 32	SS400	73°C	9m bottom end vertical drop	1	Combined stress	$\sigma = 1/2 (\sigma_t + \sqrt{\sigma_t^2 + 4\tau^2})$ ($\sigma_t = F/A$) ($\tau = P/nA \times N$)	S_u	
		(ii) Skin	Table II-A. 32	Boron stainless steel	73°C	9m bottom end vertical drop	1	Compressive stress	$\sigma_c = m/A \times N$	S_u	

II-A-13

Description of Symbols

σ : Principal stress
 σ_t : Tensile stress
 σ_c : Compressive stress
 τ : Shear stress
 τ_t : Torsional stress
F: Load
P: Pressure
A: Cross-sectional area

Table II-A. 4 (9) Conditions of Packaging Structure Design and Analysis Method

Requirement	Condition	Analysis Item	Design Requirements						Analysis Method		Remark	
			Reference drawing	Material	Temperature	Design load			Applicable equation or factor	Analysis Criteria		
						Type	Safety factor	Factor				
Package containing fissile material	Hypothetical accident conditions of transport	(iii) Skeleton assembly	Table II-A. 32	Zircaloy-4	73°C	9m bottom end vertical drop	1	Compressive stress	$\sigma_c = \Sigma m / nA \times N$	S_u		
		(iv) Fuel rod cladding	Table II-A. 32	Zircaloy-4 MDA and ZIRLO	73°C	9m bottom end vertical drop	1	Compressive stress Buckling	$\sigma_c = P/A$ $P = m \cdot N$	S_u P_k		
		Horizontal drop	Fig. II-A. 42	-	-	9m horizontal drop	1	Amount of deformation	$\delta_o = \delta_o' - (\delta H_i + \delta H_o)$	δ_o'		δ_o' = Thickness before deformation δH_i = Amount of inside deformation δH_o = Amount of outside deformation
		(a) Amount of deformation of outer shell										
		(b) Stress calculation										
		(i) Clamping frame	Table II-A. 32	SS400	73°C	9m horizontal drop	1	Bending stress	$\sigma_b = M/Z$	S_u		
(ii) Skin	Table II-A. 32	Boron stainless steel	73°C	9m horizontal drop	1	Bending stress	Circumferentially simple supported flat plate equation	S_u				
(iii) Fuel rod cladding	Table II-A. 32	Zircaloy-4 MDA and ZIRLO	73°C	9m horizontal drop	1	Combined stress	Simple supported beam equation	S_u				

Description of Symbols

σ : Principal stress
 σ_t : Tensile stress
 σ_c : Compressive stress
 τ : Shear stress

τ : Torsional stress
 F: Load
 P: Pressure
 A: Cross-sectional area

Table II-A. 4 (10) Conditions of Packaging Structure Design and Analysis Method

Requirement	Condition	Analysis Item	Design Requirements						Analysis Method		Remark
			Reference drawing	Material	Temperature	Design load			Applicable equation or factor	Analysis Criteria	
						Type	Safety factor	Factor			
Package containing fissile material	Hypothetical accident conditions of transport	Top end corner drop	Fig. II-A. 43	-	-	9m corner drop	1	Amount of deformation	$\delta_o = \delta_o' \cdot (\delta H_i + \delta H_o)$	δ_o'	δ_o' = Thickness before deformation δH_i = Amount of inside deformation δH_o = Amount of outside deformation
		Bottom end corner drop	Fig. II-A. 44	-	-	9m corner drop	1	Amount of deformation	Stress calculation For analysis, decompose into horizontal and vertical components. In this case, the factors and applicable equation used are the same as in A.5.3 Stress calculation	δ_o'	
	Drop test II Puncture	Table II-A. 31	SS400	73°C	1m drop impact	1	Evaluation based on the prototype test results		Presence or absence of puncture		
	Thermal test	-	-	440°C	Inner pressure	1	Combined stress	Equation for thin wall cylinder	S_u		
		Immersion	-	-	73°C	0.009MPa·G	1	External pressure	Presence or absence of sealing function	15.0MPa·G	

II-A-15

A.2 Weight and Center of Gravity

The weight of the package shall be as shown in Table II-A. 5. The gravity center of the package is shown in Fig. II-A. 1.

Table II-A. 5 Maximum Weight of Each Part

Unit: kg

Component		Type of Content		type	type	type	type
				14 × 14 10 feet	14 × 14 12 feet	15 × 15 12 feet	17 × 17 12 feet
Contents		Fuel assembly/unit ^(Note)		490	600	680	690
		Non-nuclear bearing component/unit		49	58	75	68
		Contents (2 units)		1,078	1,316	1,510	1,516
Packaging	Cradle assembly	Shock mount frame		165			
		Cross frame		546	764	764	764
		Shock mounts		53			
	Outer shell	Upper cover		950			
		Lower Container		1,055	2,040	2,040	2,040
		Auxiliary devices		35			
Maximum weight of package				3,900	4,120	4,320	4,320

Note: The weight per fuel assembly shows the maximum weight of each type.

A.3 Mechanical Properties of Materials

The mechanical properties of the materials used for analysis are shown in Table II-A. 6. The mechanical properties of the material used as analysis criteria are shown in Table II-A. 7.

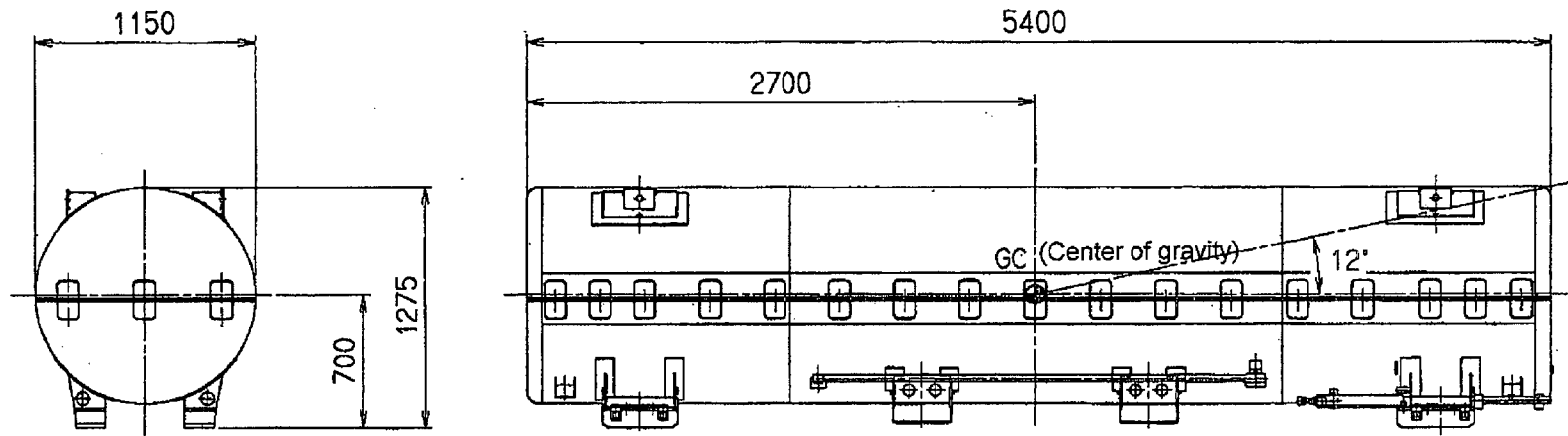
Changes in mechanical properties of carbon steel, alloy steel, Zircaloy-4, MDA and ZIRLO against temperature are shown in Fig. II-A. 2, Fig. II-A. 3, and Fig. II-A. 4, respectively.

These figures show that a yield stress tends to decrease against rise in temperature. The thermal analysis under normal conditions of transport shows that the maximum temperature of the package is 73°C. Therefore, a design yield strength at 80°C which is more conservative than at 73°C shall be used as an analysis criterion.

The compressive deformation stress of balsa wood used as shock absorber is shown in Table II-A. 8.

In addition, the dynamic spring constants of the shock mounts used for the cradle assembly are shown in Table II-A. 9.

II-A-17



Unit : mm

Fig. II-A. 1 Center of Gravity of Package

Proprietary Information Withheld Pursuant to 10 CFR 2.390

II-A-18

Proprietary Information Withheld Pursuant to 10 CFR 2.390

Proprietary Information Withheld Pursuant to 10 CFR 2.390

II-A-21

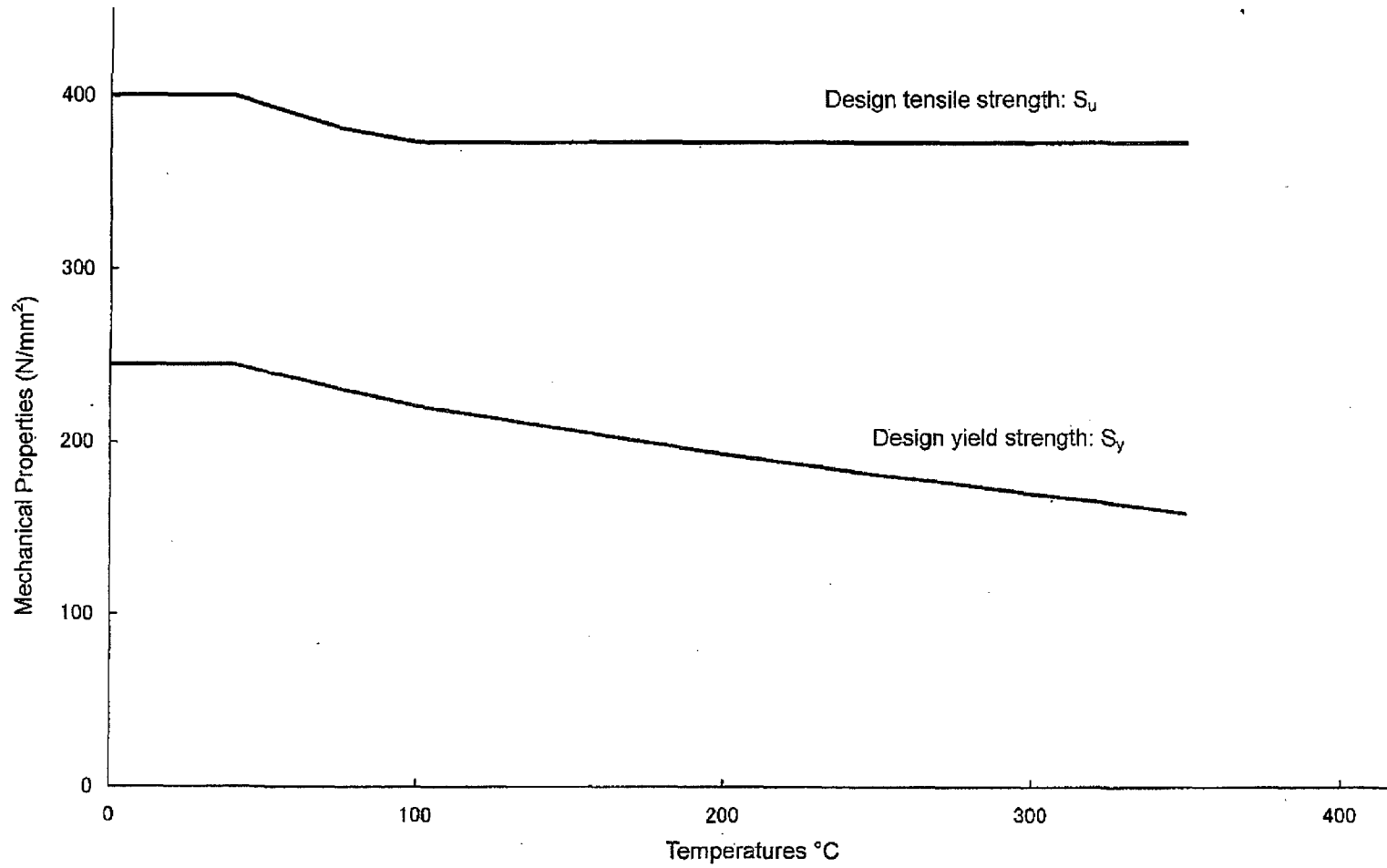


Fig. II-A. 2 Change of Mechanical Properties of SS400 for Temperatures

II-A-22

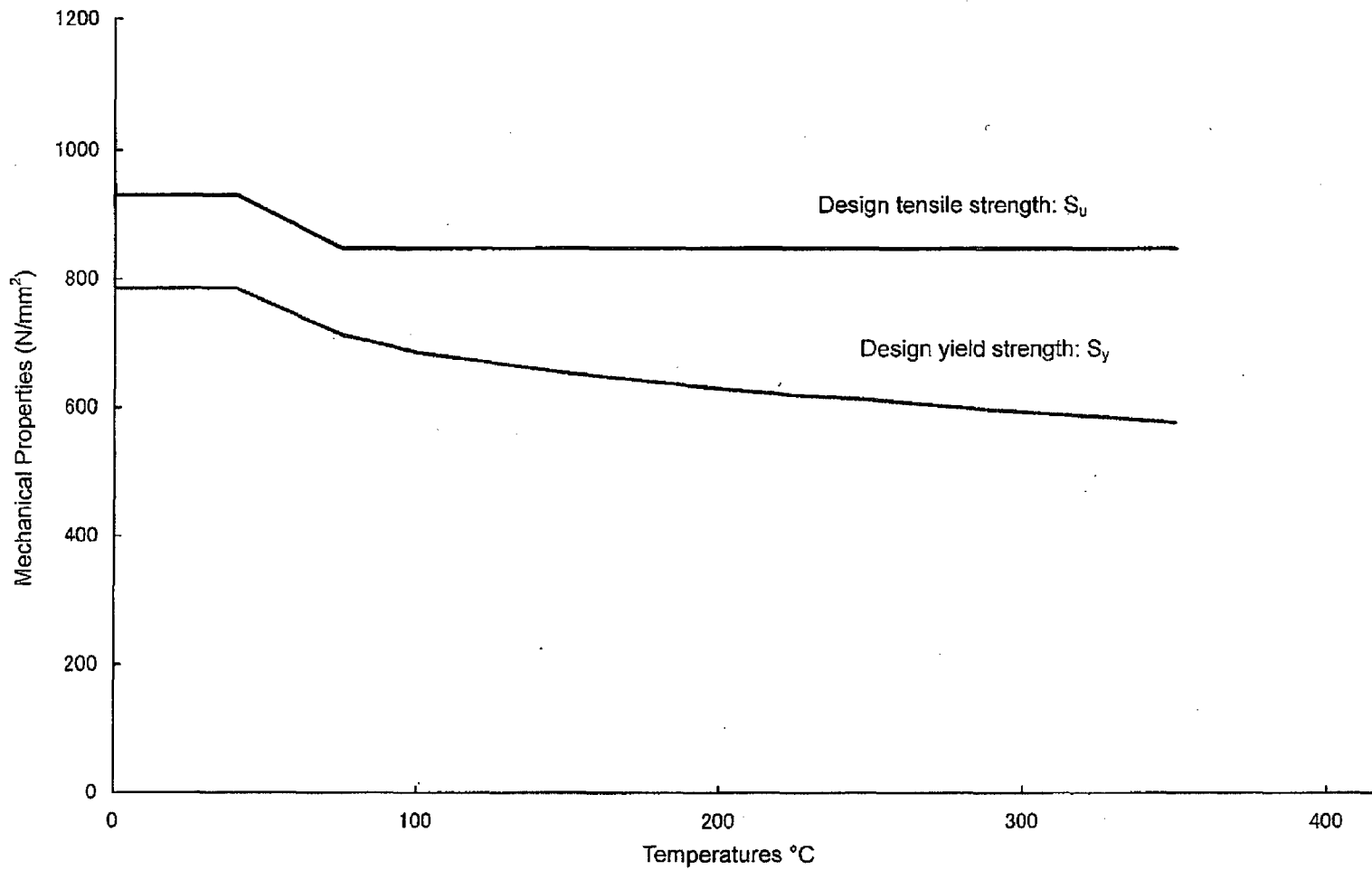


Fig. II-A. 3 Change of Mechanical Properties of SCM435 for Temperatures

Proprietary Information Withheld Pursuant to 10 CFR 2.390

II-A-23

A.4 General Standards of Package

A.4.1 Chemical and Galvanic Reactions

Those different materials of the package which are made in contact with each other are shown in Table II-A. 10.

The different materials used for the package are those stabilized chemically in air and, therefore, they will not react chemically or galvanically even if they are brought in contact with each other.

Table II-A. 10 List of Different Materials in Contact

Parts in Contact	Contact Material
External cylinder } Internal cylinder } -Shock absorber	Carbon steel-Wood
External cylinder } Internal cylinder } -O-ring	Carbon steel-Neoprene rubber
Internal cylinder } Shock mount frame } -Shock mount	Carbon steel-Polybutadiene rubber
Skin -Cross frame	Boron stainless steel-Carbon steel
Skin cushion	Boron stainless steel-Ethylene polyethylene rubber
Bottom plate -Cushion	Carbon steel- Ethylene polyethylene rubber
Protective board -Cushion	Carbon board- Ethylene polyethylene rubber
Protective board -Protective sheet	Carbon board-Polyethylene
Fuel assembly	
Top nozzle } Bottom nozzle } -Protective sheet	Stainless-steel-Polyethylene
Fuel rod cladding -Protective sheet	Zircaloy-4, MDA or ZIRLO-Polyethylene
Fuel rod cladding -Fuel pellets	Zircaloy-4, MDA or ZIRLO-Uranium dioxide Zircaloy-4, MDA or ZIRLO-Gadolinia -Uranium dioxide

A.4.2 Cold Strength

Table II-A. 11 ^[9] shows the minimum atmospheric temperature at each area. In Table II-A. 11, the minimum atmospheric temperature of -15.7°C is registered at Sutsu area. Therefore the design temperature has been set at -20°C.

Table II-A. 11 Minimum Atmospheric Temperature at Each Area

	Minimum Atmospheric Temperature (°C)	Place Name
Sendai	-6.7	Kagoshima
Genkai	-8.2	Fukuoka
Ikata	-8.3	Matsuyama
Takahama Ooi Mihama Tsuruga	-15.1	Fukui
Tomari	-15.7	Sutsu

The materials of major components which constitute the package are shown in Table II-A. 12. Also the mechanical properties of carbon steel at low temperatures are shown in Fig. II-A. 5.

As shown in Table II-A. 12, when the temperature of each part of the package is as low as -20°C, no problem occurs with the strength under low temperatures because it is above the brittleness transient temperature or minimum service temperature of each material.

Table II-A. 12 Material of Main Component

Component	Material	Type	Remark
Outer shell	Carbon steel	SS400	C: 0.23% or less
	Low-alloy steel	SCM435	Transient temperature: -30°C or less
	Rubber	Neoprene	Service temperature range: -50°C ~ -150°C ^[16]
Cradle assembly	Carbon steel	SS400	C: 0.23% or less
		SM490A	C: 0.20% or less
	Low-alloy steel	SCM435	Transient temperature: -30°C or less
	Rubber	Polybutadiene	Service temperature range: -50°C ~ -150°C ^[16]
Fuel assembly	Stainless steel	SUS304	Minimum service temperature: -198°C ^[17]
	Non-ferrous alloy	Zircaloy-4 MDA and ZIRLO	Transient temperature: -25°C or less

As shown in Table II-A. 12, the carbon content of the carbon steel which constitutes the package is 0.23% or less. Also, as shown in Fig. II-A. 5, a brittleness fracture of the carbon steel will not occur at a temperature of as low as -20°C. For low-alloy steel, stainless steel, Zircaloy-4, MDA and ZIRLO also a brittleness fracture will not occur at a temperature of as low as -20°C. In addition, the service temperature of the rubber is -50 to 150°C, therefore, it functions even under a temperature of as low as -20°C.

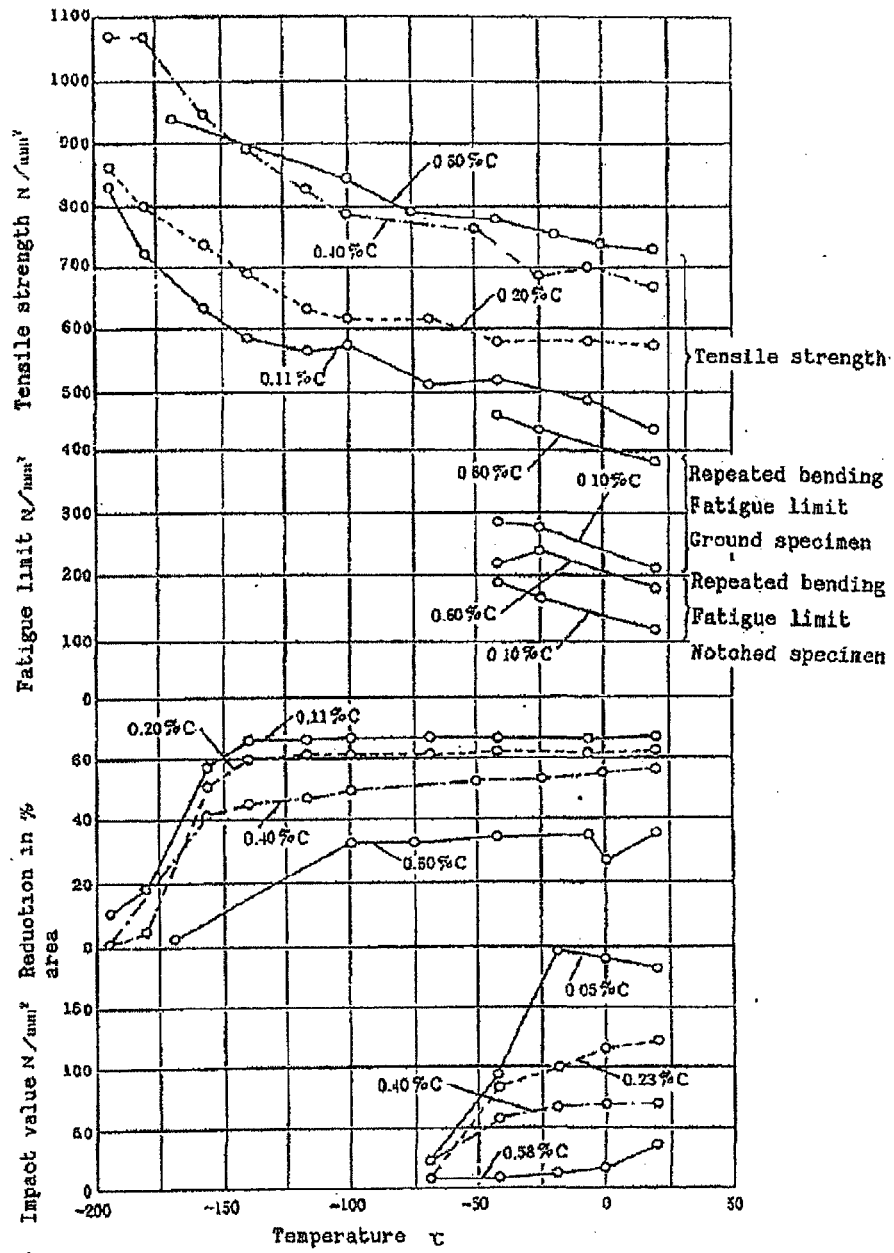


Fig. II-A. 5 Mechanical Properties of Carbon Steel at Low Temperatures

A.4.3 Containment System

A seal which cannot be broken easily is attached on the outer surfaces of the package at positions between the upper cover and the lower container so that the packaging cannot be opened easily.

Therefore, if the packaging is opened, it can be recognized easily.

The upper cover is fixed to the lower container with 40 bolts and locked by bolt supports and, therefore, it will not be easily loosened or opened accidentally or by the internal pressure of the package. Because the fuel rod acts as the sealing boundary of the radioactive contents any valve through which the radioactive contents may drain to the outside is not installed on the packaging. In order to avoid the air pressure inside the packaging from rising, a relief valve for pressure regulation is installed on the packaging. On the packaging, no component of the containment system is installed, and also any containment system which can be removed from it is not installed.

A.4.4 Lifting Devices

The structure of the lifting devices for the package is as shown in Fig. II-A. 6, and the devices are named as brackets. The brackets are welded to the upper cover main body in box shape, and their sling attaching part is 16.5mm thick with a hole through it by combining steel plates.

The brackets can safely handle the package by a mechanical means, and have sufficiently safe structure to withstand a load of three times as much as the full weight of the package so that they can withstand even if the package is lifted abruptly.

The strengths of the components of the brackets below have been analyzed and it has been found that any component has not lost its strength. The evaluation has been performed under the severest conditions where the weight of the package is maximum in consideration of a weight of a type 17 × 17 fuel (including non-nuclear fuel core internals).

(1) Lifting devices

- (a) Bracket hole part (Shear stress)
- (b) Bracket weld (Bending stress + Membrane stress)
- (c) External cylinder (Bending stress + Shear stress)

(2) Tightening bolt

- (a) Tightening bolt (Tensile stress + Shear stress)
- (b) Cross pin (Bending stress + Shear stress)

An analysis load shall be as follows.

An analysis load (W_a) shall be 3 times the maximum lifting weight.

$$W_a = m \times 3 \times g$$

W_a : Analysis load (N)

m: Maximum weight of package 4,320 (kg)

$$\begin{aligned} W_a &= 4,320 \times 3 \times 9.81 \\ &= 1.27 \times 10^5 \text{ (N)} \end{aligned}$$

The load (P) acting on the brackets while the package is lifted by them is supported by four brackets. Therefore the load (P) supported by each of the brackets is 1/4 of the analysis load (W_a).

$$P = W_a / N$$

P : Load (N)

W_a : Analysis load 1.27 × 10⁵ (N)

N : Number of brackets 4

$$P = 1.27 \times 10^5 / 4 = 3.18 \times 10^4 \text{ (N)}$$

Let us obtain the stresses produced in the components when the load (P) is applied to the brackets, and examine the strengths of the components.

A.4.4.1 Brackets for Lifting up Container

As shown in Fig. II-A. 6, force acting on the brackets for lifting up the container acts on them at a lifting wire angle of 45° .

(1) Shear stress at bracket hole part

A shear stress (τ) produced in the bracket has been obtained using the following equation.

$$\tau = F/A$$

F : Load acting on bracket = P/sin 45°(N)

P : Load = 3.18 × 10⁴ (N)

A : Area of bracket where shearing is applied (mm²)

$$A = h \times t$$

h: Length of cross-section where shearing is applied

$$\begin{aligned} h &= \sqrt{2} \times 52 - 1/2 \times 32 \\ &= 57.5 \text{ (mm)} \end{aligned}$$

t: Plate thickness 16.5(mm)

$$\begin{aligned} A &= 57.5 \times 16.5 \\ &= 949.4 \text{ (mm}^2\text{)} \end{aligned}$$

Substituting the values above,

$$\tau = (3.18 \times 10^4) / (\sin 45^\circ / 949.4) = 47.4 \text{ (N/mm}^2\text{)}$$

When a design yield strength $S_y = 229\text{N/mm}^2$ of brackets (SS400) is used considering the coefficient of 0.6 because it is a shear stress, the following equation is obtained:

$$0.6 \times S_y = 0.6 \times 229 = 137\text{N/mm}^2$$

The safety margin M_s is as follows.

$$\begin{aligned} M_s &= 0.6S_y / \tau - 1 \\ &= 137/47.4 - 1 \\ &= 1.89 \end{aligned}$$

Because the M_s is positive, the integrity of the bracket hole part will not be impaired.

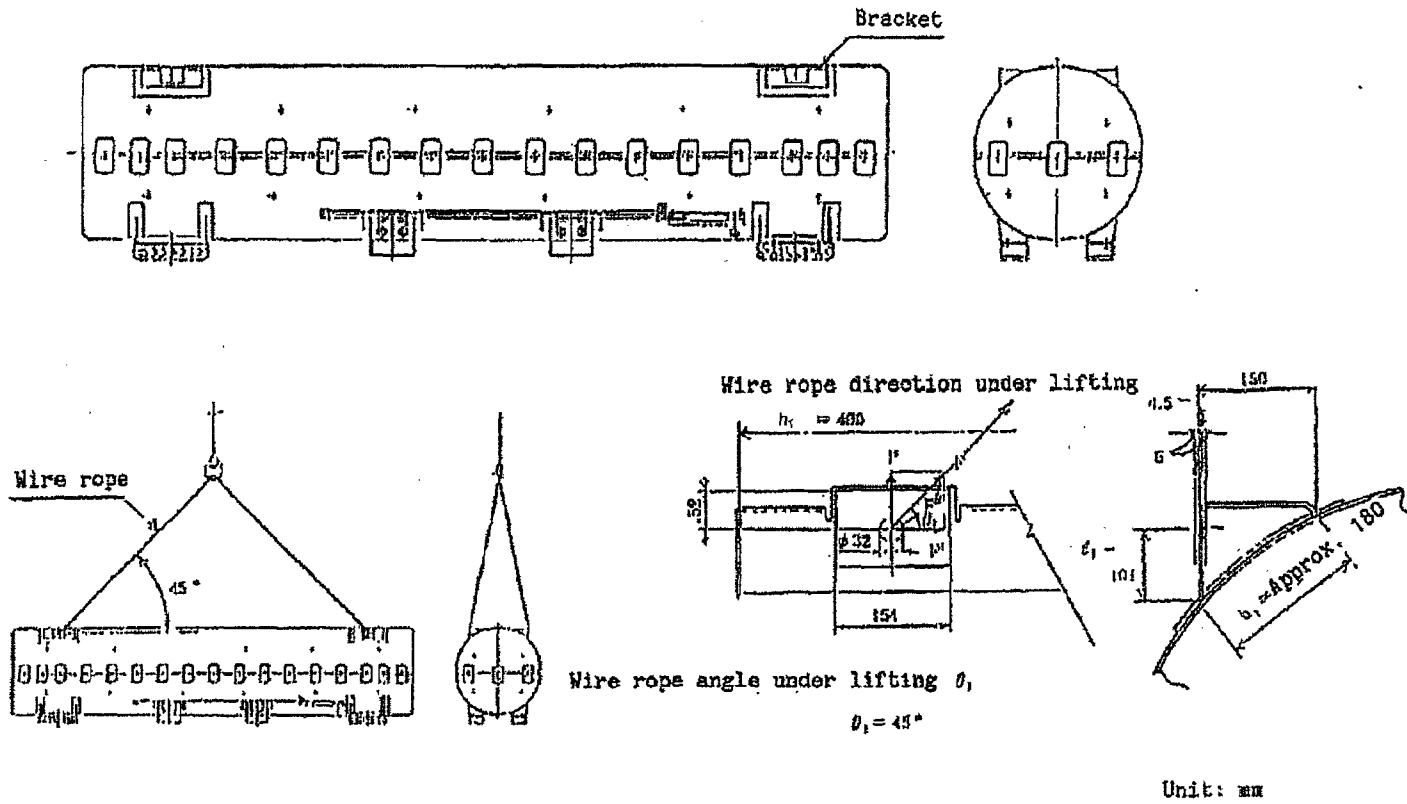


Fig. II-A. 6 Lifting Devices

(2) Bending stress at bracket weld

A stress produced at the weld of the bracket (σ_b), which is the sum of a bending stress and membrane stress, has been obtained using the following equation. The shape of the weld is as shown in Fig. II-A. 7.

$$\sigma_b = (M/Z + P/A)$$

M: Bending moment produced at weld

$$M = F \cos 45^\circ \times \ell_1$$

$$F : \text{Load acting on bracket} = P/\sin 45^\circ (\text{N})$$

$$P : \text{Load} = 3.18 \times 10^4 (\text{N})$$

$$\ell_1 : \text{Moment arm} = 101 (\text{mm})$$

$$\begin{aligned} M &= 3.18 \times 10^4 / \sin 45^\circ \times \cos 45^\circ \times 101 \\ &= 3.21 \times 10^6 (\text{N}\cdot\text{mm}) \end{aligned}$$

I: Second moment of area at bracket weld

Z: Section modulus of bracket at weld

$$I = 1/12 \{ (b_1 + 2a/\sqrt{2}) \times (h_1 + 2a/\sqrt{2})^3 - b_1 \times h_1^3 \}$$

$$= 1/12 \{ (180 + 2 \times 4/\sqrt{2}) \times (400 + 2 \times 4/\sqrt{2})^3 - 180 \times 400^3 \}$$

$$= 7.28 \times 10^7 (\text{mm}^4)$$

$$Z = I / (h_1/2 + a/\sqrt{2}) = 7.28 \times 10^7 / (400/2 + 4/\sqrt{2})$$

$$= 3.59 \times 10^5 (\text{mm}^3)$$

$$a : \text{Welding leg length} = 4 (\text{mm})$$

$$b_1 : \text{Bracket width} = 180 (\text{mm})$$

$$h_1 : \text{Bracket length} = 400 (\text{mm})$$

A: Area of bracket welded part

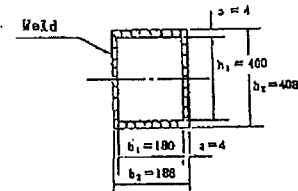
$$\begin{aligned} A &= (b_1 + 2a/\sqrt{2}) \times (h_1 + 2a/\sqrt{2}) - b_1 \times h_1 \\ &= (180 + 2 \times 4/\sqrt{2}) \times (400 + 2 \times 4/\sqrt{2}) - 180 \times 400 \\ &= 3.31 \times 10^3 (\text{mm}^2) \end{aligned}$$

Substituting the values above,

$$\begin{aligned} \sigma_b &= (3.21 \times 10^6) / (3.59 \times 10^5) + (3.18 \times 10^4) / (3.31 \times 10^3) \\ &= 18.6 (\text{N}/\text{mm}^2) \end{aligned}$$

A shear stress (τ) can be obtained by the following equation.

$$\begin{aligned} \tau &= P/A \\ &= (3.18 \times 10^4) / (3.31 \times 10^3) \\ &= 9.60 (\text{N}/\text{mm}^2) \end{aligned}$$



Unit: mm

Fig. II-A. 7 Bracket Welds

However,

$$P = F \times \cos 45^\circ = 3.18 \times 10^4 \text{ (N)}$$

$$A = 3.31 \times 10^3 \text{ (mm}^2\text{)}$$

The combined stress (σ) of the above produced stress (σ_b) and the shear stress (τ) can be obtained by the following equation.

$$\begin{aligned}\sigma &= 1/2(\sigma_b + \sqrt{\sigma_b^2 + 4\tau^2}) \\ &= 1/2(18.6 + \sqrt{18.6^2 + 4 \times 9.60^2}) \\ &= 22.7 \text{ (N/mm}^2\text{)}\end{aligned}$$

When a design yield strength $S_y = 229 \text{ N/mm}^2$ of brackets (SS400) is used considering the weld efficiency ($\eta = 0.6$), the safety margin M_s is as follows:

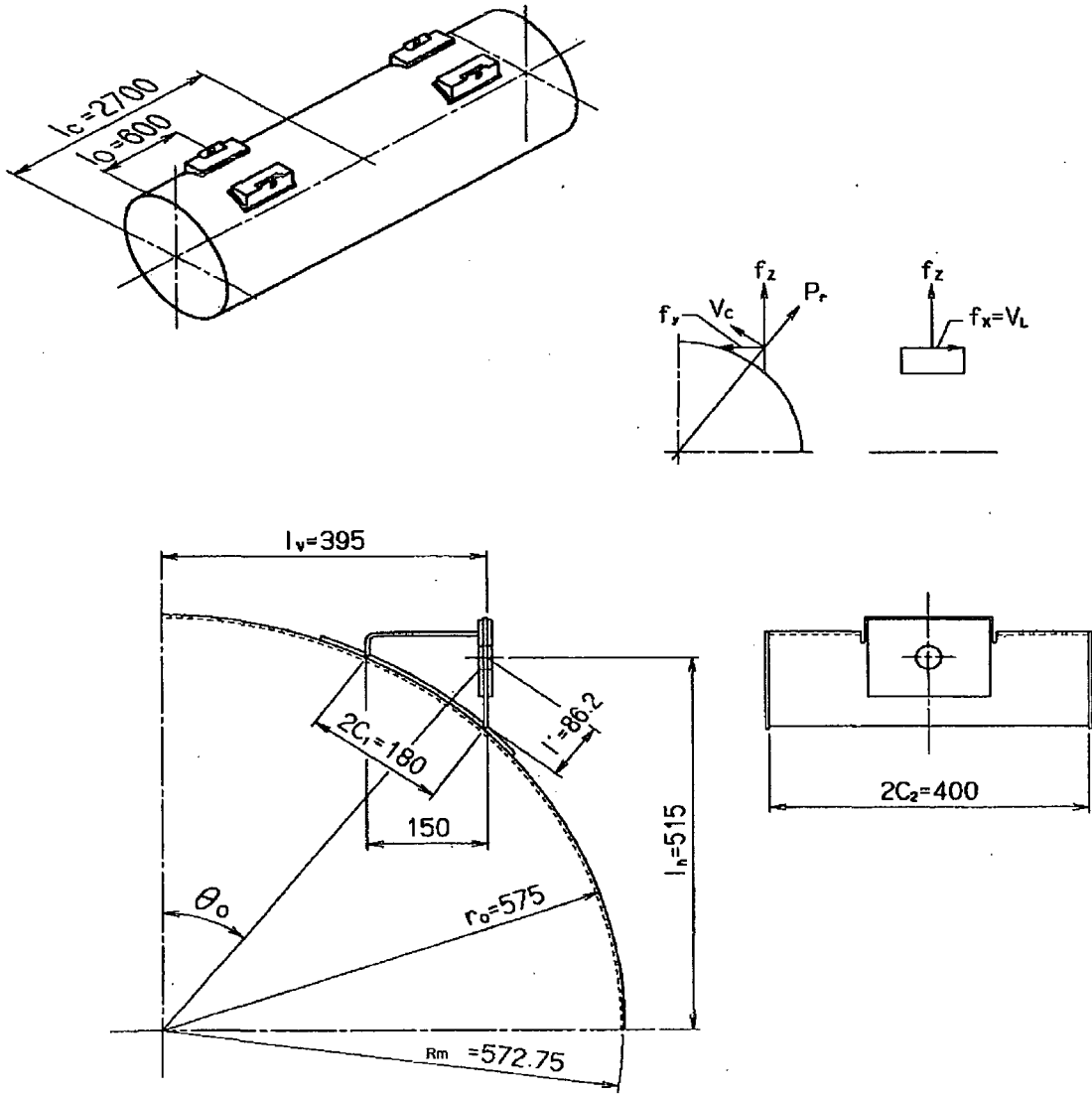
$$\begin{aligned}M_s &= \eta \times S_y / \sigma - 1 \\ &= (0.6 \times 229) / 22.7 - 1 \\ &= 5.05\end{aligned}$$

Because the M_s is positive, the integrity of the bracket weld will not be impaired.

(3) External cylinder

A stress produced in the external cylinder by a load acting on it when the package is lifted has been analyzed.

The load conditions of the external cylinder are as show in Fig. II-A. 8.

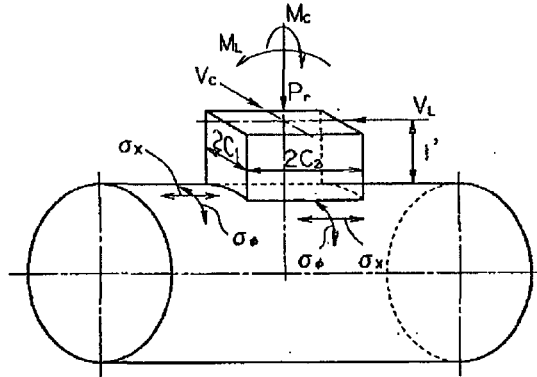


Unit: mm

Fig. II-A. 8 Load Conditions

(a) Stress evaluation position of on external cylinder

Stress evaluation position on the external cylinder is shown in Fig. II-A. 9.



P_r	: Load in the radial direction	(N)
M_c	: External moment in the circumferential direction	(N · mm)
M_L	: External moment in the axial direction	(N · mm)
V_c	: Shearing load in the circumferential direction	(N)
V_L	: Shearing load in the axial direction	(N)
σ_x	: Stress in the axial direction	(N/mm ²)
σ_ϕ	: Stress in the circumferential direction	(N/mm ²)
C_1	: Half length in the circumferential direction of rectangular load region	(mm)
C_2	: Half length in the axial direction of rectangular load region	(mm)
θ'	: Distance between a point of application of load and the plate	(mm)

Fig. II-A. 9 Stress Evaluation Position and Analysis Model

(b) Calculation of load conditions

Load conditions acting on the bracket are obtained from the following equation based on Fig. II-A. 8.

Inclination (θ_o) of radial load (P_r)

$$\theta_o = \tan^{-1} (\theta_v / \theta_h) = \tan^{-1} (395/515)$$

$$= 37.5^\circ$$

$$= 0.654 \text{ (rad)}$$

• Radial load (P_r)

$$P_r = f_z \cos \theta_o - f_y \sin \theta_o = 3.18 \times 10^4 \times \cos 37.5^\circ - 6.18 \times 10^3 \times \sin 37.5^\circ$$

$$= 2.15 \times 10^4 \text{ (N)}$$

- Circumferential load (V_c)

$$V_c = f_z \sin \theta_o + f_y \cos \theta_o = 3.18 \times 10^4 \times \sin 37.5^\circ + 6.18 \times 10^3 \times \cos 37.5^\circ$$

$$= 2.42 \times 10^4 \text{ (N)}$$
- Axial load (V_L)

$$V_L = f_x$$

$$= 3.18 \times 10^4 \text{ (N)}$$

Where,

f_x : Axial load acting on the bracket

$$f_x = W_a/4 \times \tan \theta_1 = 3.18 \times 10^4 \text{ (N)}$$

W_a : Analysis load = 1.27×10^5 (N)

θ_1 : Angle of a wire in the axial direction = $45^\circ = 0.785$ (rad)

f_y : Horizontal load acting on the bracket

$$f_y = W_a/4 \times \tan \theta_2 = (1.27 \times 10^5)/4 \times \tan 11^\circ = 6.18 \times 10^3 \text{ (N)}$$

θ_2 : Angle of a wire in the radial direction = $11^\circ = 0.192$ (rad)

f_z : Vertical load acting on the bracket

$$f_z = W_a/4 = 3.18 \times 10^4 \text{ (N)}$$

l_v : Horizontal bracket dimension after mounting = 395 (mm)

l_h : Vertical bracket dimension after mounting = 515 (mm)

(c) Calculation of profile coefficients

Profile coefficients, α , γ and β to obtain membrane force and bending moment acting on the external cylinder are respectively given by the following equation [6].

(i) Profile coefficient, α

Relational coefficient of a distance between bracket position and outer shell end

$$\alpha = l/R_m \text{ (however, } l_o \neq l/2)$$

$$l = 4l_o (l_c - l_o)/l_c \text{ (however, } l_o \geq R_m/2)$$

l_c : Length of outer shell = 2,700 (mm)

l_o : Distance between the center of load region and the outer shell end = 600mm

l : Length equivalent to the outer shell

R_m : Average radius of the outer shell

Therefore,

$$\alpha = 1,867/572.75 = 3.26$$

However,

$$l = 4 \times 600 \times (2,700 - 600)/2,700 = 1,867 \text{ (mm)}$$

(ii) Profile coefficient, γ

$$\gamma = R_m/\Gamma$$

R_m : Average radius of the cylindrical shell = 572.75 (mm)

T : Total thickness of the outer shell plate and the seat plate = 10.5 (mm)

$$\gamma = 572.75/10.5 = 54.5$$

(iii) Profile coefficient, β

$$\beta_1 = C_1 / R_m$$

$$\beta_2 = C_2 / R_m$$

C_1 : Half length in the circumferential direction of rectangular load region
= 90 (mm)

C_2 : Half length in the axial direction of rectangular load region = 200(mm)

$$\beta_1 = 90/572.75 = 0.157$$

$$\beta_2 = 200/572.75 = 0.349$$

(iv) Load in the radial direction P_r

In case of $4 \geq \beta_1/\beta_2 > 1$,

$$\beta = \{1 - 1/3 (\beta_1/\beta_2 - 1) (1 - K_1)\} \sqrt{\beta_1 \times \beta_2}$$

In case of $1 > \beta_1/\beta_2 \geq 0.25$

$$\beta = \{1 - 4/3 (1 - \beta_1/\beta_2) (1 - K_2)\} \sqrt{\beta_1 \times \beta_2}$$

K_1 and K_2 are given in Table II-A. 13.

$$\beta_1/\beta_2 = C_1/C_2 = 0.157/0.349 = 0.45 < 1$$

Table II-A. 13 K_1 and K_2 in Acting of Radial Load

	N_ϕ	N_x	M_ϕ	M_x
K_1	0.91	1.68	1.76	1.20
K_2	1.48	1.20	0.88	1.25
β	0.317	0.269	0.214	0.277

(v) External moment in the circumferential direction M_c

For membrane force N_ϕ and N_x ,

$$\beta = (\beta_1^2 \times \beta_2)^{1/3} = 0.205$$

For bending moment M_ϕ and M_x ,

$$\beta = K_c (\beta_1^2 \times \beta_2)^{1/3}$$

K_c is given in Table II-A. 14.

Table II-A. 14 C_c and K_c in Acting of Circumferential External Moment

β_1/β_2	γ	C_c in acting on N_ϕ	C_c in acting on N_x	K_c in acting on M_ϕ	K_c in acting on M_x	K_c in acting on θ
1/4	15	0.31	0.49	1.31	1.84	1.09
	50	0.21	0.46	1.24	1.62	1.04
	100	0.15	0.44	1.16	1.45	0.97
	300	0.09	0.46	1.02	1.17	0.92
1/2	15	0.64	0.75	1.09	1.36	1.00
	50	0.57	0.75	1.08	1.31	0.98
	100	0.51	0.76	1.04	1.26	0.94
	300	0.39	0.77	0.99	1.13	0.95
2	15	(1.7)	(1.3)	(1.20)	(0.97)	(1.00)
	100	1.43	1.12	1.10	0.95	1.19
	300	(1.3)	(1.00)	(1.00)	(0.90)	-
4	15	(1.75)	(1.31)	(1.47)	(1.08)	(1.00)
	100	1.49	0.81	1.38	1.06	1.49
	300	(1.36)	(0.74)	(1.27)	(0.88)	-

Remark: Values shown in parentheses are approximate values.

For M_ϕ , $\beta = 1.11 \times 0.205 = 0.227$

$K_c = 1.11$

For M_x , $\beta = 1.37 \times 0.205 = 0.280$

$K_c = 1.37$

(vi) External moment in the axial direction M_L

For membrane force N_ϕ and N_x ,

$$\beta = (\beta_1 \times \beta_2^2)^{1/3} = 0.268$$

For bending moment M_ϕ and M_x ,

$$\beta = K_L (\beta_1 \times \beta_2^2)^{1/3}$$

K_L is given in Table II-A. 15.

Table II-A. 15 C_L and K_L in Acting of Axial External Moment

β_1/β_2	γ	C_L in acting on N_x	C_L in acting on N_ϕ	K_L in acting on M_x	K_L in acting on M_ϕ	K_L in acting on θ
1/4	15	0.75	0.43	1.80	1.24	1.14
	50	0.77	0.33	1.65	1.16	1.13
	100	0.80	0.24	1.59	1.11	1.18
	300	0.90	0.07	1.56	1.11	1.31
1/2	15	(0.90)	(0.76)	(1.08)	(1.04)	(1.00)
	100	0.97	0.68	1.07	1.02	1.00
	300	(1.10)	(0.60)	(1.05)	(1.02)	(1.00)
2	15	(0.87)	(1.30)	(0.94)	(1.12)	-
	100	0.81	1.15	0.89	1.07	1.09
	300	(0.80)	(1.50)	(0.79)	(0.90)	-
4	15	0.68	1.20	0.90	1.24	1.39
	100	0.51	1.03	0.81	1.12	1.18
	300	(0.50)	(1.33)	(0.64)	(0.83)	-

Remark: Values shown in parentheses are approximate values.

For M_ϕ , $\beta = 1.19 \times 0.268 = 0.318$

$K_L = 1.19$

For M_x , $\beta = 1.06 \times 0.268 = 0.282$

$K_L = 1.06$

(d) Stress analysis

(i) Radial force acting on outer shell (see Fig. II-A. 9)

When radial load (P_r) acts, stress on the cylindrical shell is given by the following equation:

$$\sigma_x = N_x/T \pm 6M_x/T^2 \dots\dots\dots (A.4-1)$$

$$\sigma_\phi = N_\phi/T \pm 6M_\phi/T^2 \dots\dots\dots (A.4-2)$$

σ_x : Axial stress on the outer shell (N/mm²)

σ_ϕ : Circumferential stress on the outer shell (N/mm²)

M_x : Axial bending moment on the outer shell (N·mm/mm)

M_ϕ : Circumferential bending moment on the outer shell (N·mm/mm)

N_x : Axial membrane force on the outer shell (N/mm)

N_ϕ : Circumferential membrane force on the outer shell (N/mm)

T : Total thickness of the outer shell plate and the seat plate (mm)

1. Axial stress: σ_x

The above equation (A.4-1) deriving axial stress σ_x (N/mm²) is given by the following equation:

$$N_x / T = K_{N_x} (N_x / (P_r / R_m)) \times (P_r / R_m \cdot T) \dots \dots \dots (A.4-3)$$

$$6 M_x / T^2 = K_{M_x} (M_x / P_r) \times (6 P_r / T^2) \dots \dots \dots (A.4-4)$$

Where,

- T : 10.5 (mm)
- P_r : 2.15 × 10⁴ (N)
- R_m : 572.75 (mm)

K_{N_x} and K_{M_x} are given in Fig. II-A. 10.

In case of $\gamma = 50$,

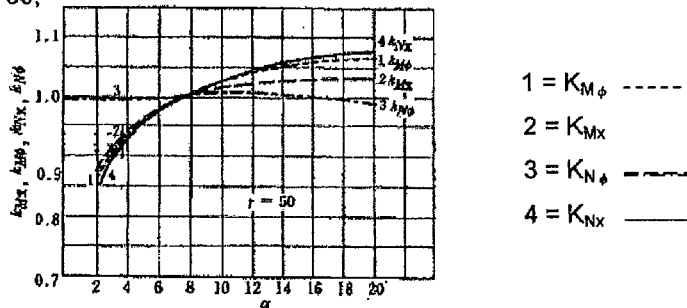


Fig. II-A. 10 Relationship between M_x, M_φ, N_x, N_φ and α in Acting of Radial Load (considering α = 8 as a criterion)

K_{N_x}: Influence coefficient = 0.88

K_{M_x}: Influence coefficient = 0.92

Therefore, the following values are obtained:

$$P_r / R_m T = 2.15 \times 10^4 / (572.75 \times 10.5) = 3.57$$

$$6 P_r / T^2 = 6 \times 2.15 \times 10^4 / 10.5^2 = 1168$$

The following values are obtained from Fig. II-A. 45 and Fig. II-A. 46 in A.10.2.

$$N_x / (P_r / R_m) = 6.3 \quad (\beta = 0.269 \text{ in the table})$$

$$M_x / P_r = 0.014 \quad (\beta = 0.277 \text{ in the table})$$

Based on the above equations, (A.4-3) and (A.4-4) are obtained as follows:

$$N_x / T = 0.88 \times 6.3 \times 3.57 = 19.8 \text{ (N/mm}^2\text{)}$$

$$6 M_x / T^2 = 0.92 \times 0.014 \times 1168 = 15.1 \text{ (N/mm}^2\text{)}$$

Therefore, axial stress σ_x (N/mm²) is as follows:

$$\begin{aligned} \sigma_x &= 19.8 \pm 15.1 \\ &= 34.9 \text{ (N/mm}^2\text{) (outer surfaces) or} \\ &= 4.8 \text{ (N/mm}^2\text{) (inner surfaces)} \end{aligned}$$

2 Circumferential stress: σ_ϕ

The above equation (A.4-2) deriving axial stress σ_x (N/mm²) is given by the following equation:

$$N_\phi/T = K_{N_\phi} (N_\phi / (P_r/R_m)) \times (P_r / R_m \cdot T) \dots\dots\dots (A.4-5)$$

$$6 M_\phi/T^2 = K_{M_\phi} (M_\phi / P_r) \times (6P_r/T^2) \dots\dots\dots (A.4-6)$$

K_{N_ϕ} and K_{M_ϕ} are given in Fig. II-A. 10.

Where,

K_{N_ϕ} : Influence coefficient = 0.99

K_{M_ϕ} : Influence coefficient = 0.90

Therefore, the following values are obtained:

First, the following values are obtained based on Fig. II-A. 47 and Fig. II-A. 48 in A.10.2:

$$N_\phi / (P_r/R_m) = 2.2 \quad (\beta = 0.317 \text{ in the table})$$

$$M_\phi / P_r = 0.054 \quad (\beta = 0.214 \text{ in the table})$$

Based on the above equations, (A.4-5) and (A.4-6) are obtained as follows:

$$N_\phi/T = 0.99 \times 2.2 \times 3.57 = 7.78 \text{ (N/mm}^2\text{)}$$

$$6M_\phi/T^2 = 0.90 \times 0.054 \times 1168 = 56.8 \text{ (N/mm}^2\text{)}$$

Therefore, circumferential stress σ_ϕ (N/mm²) is as follows:

$$\begin{aligned} \sigma_\phi &= 7.78 \pm 56.8 \\ &= 64.6 \text{ (N/mm}^2\text{) (outer surfaces) or} \\ &= -49.0 \text{ (N/mm}^2\text{) (inner surfaces)} \end{aligned}$$

(ii) Axial bending moment to a container acting on outer shell (see Fig. II-A. 9)

When axial bending moment (M_L) acts, stress on the cylindrical shell is given by the following equation:

$$\sigma_x = N_x/T \pm 6M_x/T^2 \dots\dots\dots (A.4-7)$$

$$\sigma_\phi = N_\phi/T \pm 6M_\phi/T^2 \dots\dots\dots (A.4-8)$$

σ_x : Axial stress on the outer shell (N/mm²)

σ_ϕ : Circumferential stress on the outer shell (N/mm²)

M_x : Axial bending moment on the outer shell (N·mm/mm)

M_ϕ : Circumferential bending moment on the outer shell (N·mm/mm)

N_x : Axial membrane force on the outer shell (N/mm)

N_ϕ : Circumferential membrane force on the outer shell (N/mm)

T : Total thickness of the outer shell plate and the seat plate(mm)

1 Axial stress: σ_x

The above equation (A.4-7) deriving axial stress σ_x (N/mm²) is given by the following equation:

$$N_x/T = (N_x/(M_L/R_m^2\beta)) \times (M_L/(R_m^2\beta T)) \dots\dots\dots(A.4-9)$$

$$6 M_x/T^2 = (M_x/(M_L/R_m^2\beta)) \times (6 M_L/R_m\beta T^2) \dots\dots\dots(A.4-10)$$

Where,

M_L : Axial bending moment (= $V_L \ell'$) (N·mm)

V_L : Acting load = 3.18×10^4 (N)

ℓ' : Distance between a point of application of load and the plate = 86.2 (mm)

$R_m = 572.75$ (mm)

$T = 10.5$ (mm)

For membrane force N_x , $\beta = 0.268$

For bending moment M_x , $\beta = 0.282$

$\gamma = 54.5$

Therefore, the following values are obtained:

$$M_L/R_m^2\beta T = (3.18 \times 10^4 \times 86.2)/(572.75^2 \times 0.268 \times 10.5) = 2.97$$

$$6M_x/R_m\beta T^2 = (6 \times 3.18 \times 10^4 \times 86.2)/(572.75 \times 0.282 \times 10.5^2) = 922$$

The following values are obtained based on Fig. II-A. 49 and Fig. II-A. 50 in A.10.2:

$$N_x/(M_L/R_m^2\beta) = 1.9 \quad (\beta = 0.268 \text{ in the table})$$

$$M_x/(M_L/R_m\beta) = 0.023 \quad (\beta = 0.282 \text{ in the table})$$

Based on the above equations, (A.4-9) and (A.4-10) are obtained as follows:

$$N_x/T = 1.9 \times 2.97 = 5.65 \text{ (N/mm}^2\text{)}$$

$$6M_x/T^2 = 0.023 \times 922 = 21.2 \text{ (N/mm}^2\text{)}$$

Therefore, axial stress σ_x (N/mm²) is as follows:

$$\begin{aligned} \sigma_x &= 5.65 \pm 21.2 \\ &= 26.9 \text{ (N/mm}^2\text{) (outer surfaces) or} \\ &= -15.6 \text{ (N/mm}^2\text{) (inner surfaces)} \end{aligned}$$

2 Circumferential stress: σ_ϕ

The above equation (A.4-8) deriving circumferential stress σ_ϕ (N/mm²) is given by the following equation:

$$N_\phi/T = (N_\phi/(M_L/R_m^2\beta)) \times (M_L/R_m^2\beta T) \dots\dots\dots(A.4-11)$$

$$6 M_\phi/T^2 = M_\phi/(M_L/R_m\beta) \times (6 M_L/R_m\beta T^2) \dots\dots\dots(A.4-12)$$

Where,

For membrane force N_ϕ , $\beta = 0.268$

For bending moment M_x , $\beta = 0.318$

$$M_x/R_m^2\beta T = (3.18 \times 10^4 \times 86.2)/(572.75^2 \times 0.268 \times 10.5) = 2.97$$

$$6M_x/R_m\beta T^2 = (6 \times 3.18 \times 10^4 \times 86.2)/(572.75 \times 0.318 \times 10.5^2) = 818$$

The following values are obtained based on Fig. II-A. 51 and Fig. II-A. 52 in A.10.2:

$$N_x/(M_x/R_m^2\beta) = 4.1 \quad (\beta = 0.268 \text{ in the table})$$

$$M_x/(M_x/R_m\beta) = 0.012 \quad (\beta = 0.318 \text{ in the table})$$

Therefore, (A.4-11) and (A.4-12) are obtained as follows:

$$N_x/T = 4.1 \times 2.97 = 12.2 \text{ (N/mm}^2\text{)}$$

$$6M_x/T^2 = 0.012 \times 818 = 9.82 \text{ (N/mm}^2\text{)}$$

Therefore, circumferential stress σ_x (N/mm²) is as follows:

$$\begin{aligned} \sigma_x &= 12.2 \pm 9.82 \\ &= 22.1 \text{ (N/mm}^2\text{) (outer surfaces) or} \\ &= 2.4 \text{ (N/mm}^2\text{) (inner surfaces)} \end{aligned}$$

- (iii) Circumferential bending moment to a container acting on outer shell (see Fig. II-A. 9)

When circumferential bending moment (M_C) acts, stress on the cylindrical shell is given by the following equation:

$$\sigma_x = N_x/T \pm 6M_x/T^2 \dots\dots\dots (A.4-13)$$

$$\sigma_x = N_x/T \pm 6M_x/T^2 \dots\dots\dots (A.4-14)$$

Where

- σ_x : Axial stress on the outer shell (N/mm²)
- σ_x : Circumferential stress on the outer shell (N/mm²)
- M_x : Axial bending moment on the outer shell (N·mm/mm)
- M_x : Circumferential bending moment on the outer shell (N·mm/mm)
- N_x : Axial membrane force on the outer shell (N/mm)
- N_x : Circumferential membrane force on the outer shell (N/mm)
- T : Total thickness of the outer shell plate and the seat plate (mm)

1 Axial stress: σ_x

The above equation (A.4-13) deriving axial stress σ_x (N/mm²) is given by the following equation:

$$N_x/T = (N_x/(M_C/R_m^2\beta)) \times (M_C/(R_m^2\beta T)) \dots\dots\dots (A.4-15)$$

$$6M_x/T^2 = (M_x/(M_C/R_m\beta)) \times (6M_C/R_m\beta T^2) \dots\dots\dots (A.4-16)$$

M_C : Circumferential bending moment (= $V_C l'$) (N·mm)

V_C : Acting load = 2.42×10^4 (N)

\varnothing' : Distance between a point of application of load and the plate = 86.2 (mm)

$$R_m = 572.75 \text{ (mm)}$$

$$T = 10.5 \text{ (mm)}$$

For membrane force N_x , $\beta = 0.205$

For bending moment M_x , $\beta = 0.280$

$$\gamma = 54.5$$

$$M_C/R_m^2\beta T = (2.42 \times 10^4 \times 86.2)/(572.75^2 \times 0.205 \times 10.5) = 2.96$$

$$6M_C/R_m\beta T^2 = (6 \times 2.42 \times 10^4 \times 86.2)/(572.75 \times 0.280 \times 10.5^2) = 709$$

The following values are obtained based on Fig. II-A. 53 and Fig. II-A. 54 in A.10.2:

$$N_x/(M_C/R_m^2\beta) = 4.6 \quad (\beta = 0.205 \text{ in the table})$$

$$M_x/(M_C/R_m\beta) = 0.024 \quad (\beta = 0.280 \text{ in the table})$$

Based on the above equations, (A.4-15) and (A.4-16) are obtained as follows:

$$N_x/T = 4.6 \times 2.96 = 13.7 \text{ (N/mm}^2\text{)}$$

$$6M_x/T^2 = 0.024 \times 709 = 17.1 \text{ (N/mm}^2\text{)}$$

Therefore, axial stress σ_x (N/mm²) is as follows:

$$\begin{aligned} \sigma_x &= 13.7 \pm 17.1 \\ &= 30.7 \text{ (N/mm}^2\text{) (outer surfaces) or} \\ &= -3.5 \text{ (N/mm}^2\text{) (inner surfaces)} \end{aligned}$$

2 Circumferential stress: σ_ϕ

The above equation (A.4-14) deriving circumferential stress σ_ϕ (N/mm²) is given by the following equation:

$$N_\phi/T = (N_\phi/(M_C/R_m^2\beta)) \times (M_C/R_m^2\beta T) \dots \dots \dots \text{(A.4-17)}$$

$$6M_\phi/T^2 = M_\phi/(M_C/R_m\beta) \times (6M_C/R_m\beta T^2) \dots \dots \dots \text{(A.4-18)}$$

Where,

For membrane force N_ϕ , $\beta = 0.205$

For bending moment M_ϕ , $\beta = 0.227$

$$M_C/R_m^2\beta T = (2.42 \times 10^4 \times 86.2)/(572.75^2 \times 0.205 \times 10.5) = 2.96$$

$$6M_C/R_m\beta T^2 = (6 \times 2.42 \times 10^4 \times 86.2)/(572.75 \times 0.227 \times 10.5^2) = 874$$

The following values are obtained based on Fig. II-A. 55 and Fig. II-A. 56 in A.10.2:

$$N_\phi/(M_C/R_m^2\beta) = 2.1 \quad (\beta = 0.205 \text{ in the table})$$

$$M_\phi/(M_C/R_m\beta) = 0.064 \quad (\beta = 0.227 \text{ in the table})$$

Therefore, (A.4-17) and (A.4-18) are obtained as follows:

$$N_\phi/T = 2.1 \times 2.96 = 6.22 \text{ (N/mm}^2\text{)}$$

$$6M_s/T^2 = 0.064 \times 874 = 56.0 \text{ (N/mm}^2\text{)}$$

Therefore, circumferential stress σ_s (N/mm²) is as follows:

$$\begin{aligned}\sigma_s &= 6.22 \pm 56.0 \\ &= 62.2 \text{ (N/mm}^2\text{) (outer surfaces) or} \\ &= -49.8 \text{ (N/mm}^2\text{) (inner surfaces)}\end{aligned}$$

(iv) Shearing load acting on outer shell (see Fig. II-A. 9)

1 Axial shear stress τ_L

Axial shear stress τ_L is given by the following equation:

$$\tau_L = V_L / (4C_2T)$$

Where,

V_L : Shearing load in the axial direction = 3.18×10^4 (N)

C_2 : Half length in the axial direction of rectangular load region = 200 (mm)

T : Total thickness of the outer shell plate and seat plate = 10.5 (mm)

$$\begin{aligned}\tau_L &= (3.18 \times 10^4) / (4 \times 200 \times 10.5) \\ &= 3.79 \text{ (N/mm}^2\text{)}\end{aligned}$$

2 Circumferential shear stress τ_C

Circumferential shear stress τ_C is given by the following equation:

$$\tau_C = V_C / (4C_1T)$$

Where,

V_C : Shearing load in the circumferential direction = 2.42×10^4 (N)

C_1 : Half length in the circumferential direction of rectangular load region
= 90 (mm)

$$\begin{aligned}\tau_C &= (2.42 \times 10^4) / (4 \times 90 \times 10.5) \\ &= 6.42 \text{ (N/mm}^2\text{)}\end{aligned}$$

(v) Stress evaluation

Stress on the outer shell is summarized in [Table II-A. 16](#).

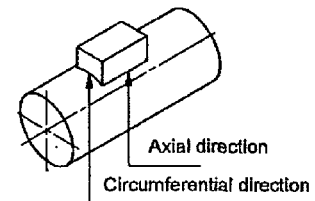


Table II-A. 16 Stress during Lifting

Unit N/mm²

Load items	Circumferential stress σ_{ϕ}		Axial stress σ_x		Shearing load τ	
	Axial direction	Direction perpendicular to axis	Axial direction	Direction perpendicular to axis	Axial direction	Direction perpendicular to axis
Radial load P_r	64.6	64.6	34.9	34.9		
	-49.0	-49.0	4.8	4.8		
Axial external moment M_L		22.1		26.9		
		2.4		-15.6		
Circumferential external moment M_C	62.2		30.7			
	-49.8		-3.5			
Axial shearing load V_L					3.79	
					3.79	
Circumferential shearing load V_C						6.42
						6.42
Total	126.8	86.7	65.6	61.8	3.79	6.42
	-99.8	-46.6	1.3	-10.8	3.79	6.42

Top cell – Outer surfaces

Bottom cell – Inner surfaces

Combined stress

$$\begin{aligned} \sigma &= 1/2[\sigma_{\phi} + \sigma_x + \{(\sigma_{\phi} - \sigma_x)^2 + 4\tau^2\}^{1/2}] \\ &= 1/2[126.8 + 65.6 + \{(126.8 - 65.6)^2 + 4 \times 3.79\}^{1/2}] \\ &= 127 \text{ (N/mm}^2\text{)} \end{aligned}$$

Design yield strength of the outer shell (SS400) is $S_y = 229 \text{ (N/mm}^2\text{)}$ and the safety margin is as follows:

$$\begin{aligned} M_s &= 229/127 - 1 \\ &= 0.80 \end{aligned}$$

Because the M_s is positive, the integrity of the outer shell during lifting will not be impaired.

A.4.4.2 Tightening Bolts

(1) Tightening bolts

A load at lifting shall be applied to the tightening bolts.

The tightening bolts have been analyzed under the load conditions that the overall weight of the package and maximum internal pressure are applied to the bolts. A tensile stress (σ_t) and shear stress (τ) produced in the tightening bolts can be obtained using the following equation. The tightening bolt is shown in Fig. II-A. 11.

$$\sigma_t = P_a / (nA)$$

$$\tau = T_{ff} / Z_p$$

Where

P_a : Tightening force (N)

$$\begin{aligned} P_a &= W_a + P \times \ell_1 \times \ell_2 \\ &= 1.27 \times 10^5 + 5.00 \times 10^{-2} \times 5,400 \times 1,134 = 4.33 \times 10^5 \text{ (N)} \end{aligned}$$

W_a : Analysis load = 1.27×10^5 (N)

P : Maximum internal pressure = 5.00×10^{-2} (MPa)

ℓ_1 : Length of packaging in longitudinal direction = 5,400 (mm)

ℓ_2 : Length of packaging in lateral direction = 1,134 (mm)

n : Number of tightening bolts = 40

A : Cross-section of a tightening bolt where tension is applied (mm^2)

$$\begin{aligned} A &= \pi / 4 (D_0^2 - D_1^2) - (D_0 - D_1) \times t \\ &= \pi / 4 (20.5^2 - 9.5^2) - (20.5 - 9.5) \times 6.3 \\ &= 189.9 \text{ mm}^2 \end{aligned}$$

D_0 : Outside diameter of tightening bolt = 20.5 (mm)

D_1 : Inside diameter of tightening bolt = 9.5 (mm)

t : Width of notch in tightening bolt = 6.3 (mm)

Substituting these values above,

$$\begin{aligned} \sigma_t &= (4.33 \times 10^5) / (40 \times 189.9) \\ &= 57.1 \text{ (N/mm}^2\text{)} \end{aligned}$$

Proprietary Information Withheld Pursuant to 10 CFR 2.390

II-A-48

A shear stress (τ) can be obtained using the following equation.

$$\tau = T_f / Z_p$$

Where

T_f : Torque load at tightening [7]

$$T_f = P_a / (2n) \{ d_2 \times (\tan \theta + \mu_s \sec \theta') + d_w \times \mu_w \}$$

P_a : Tightening force = 4.33×10^6 (N)

n : Number of the tightening bolts = 40

Z_p : Torsional section modulus = 514.1 mm^3 (Attached document A.10.3)

d_2 : Effective diameter of the cross pin

$$\begin{aligned} d_2 &= 2/3 \times (D_c^3 - D_p^3) / (D_c^2 - D_p^2) \\ &= 2/3 \times (30^3 - 22^3) / (30^2 - 22^2) \\ &= 26.2 \text{ (mm)} \end{aligned}$$

D_c : Outside diameter of the cross pin 30 (mm)

D_p : Inside diameter of tapered section 22 (mm)

d_w : Equivalent diameter for frictional torque on nut seat surface

$$\begin{aligned} d_w &= 2/3 \times (D_w^3 - D_i^3) / (D_w^2 - D_i^2) \\ &= 2/3 \times (30^3 - 22^3) / (30^2 - 22^2) \\ &= 26.2 \text{ (mm)} \end{aligned}$$

D_w : Outside diameter of the nut seat surface 30 (mm)

D_i : Inside diameter of the nut seat surface 22 (mm)

θ : Lead angle at effective diameter of cross pin

$$\begin{aligned} \theta &= \tan^{-1} (P_c / (\ell_3 / 2)) \\ &= \tan^{-1} (3.5 / (33 / 2)) \\ &= 12^\circ \end{aligned}$$

P_c : Height of the bolt supporter 3.5 (mm)

ℓ_3 : Outside diameter of the bolt supporter 33 (mm)

θ' : Half angle of thread 0°

μ_s : Coefficient of friction on the thread face 0.15

μ_w : Coefficient of friction on the seat face 0.15

Substituting the values above,

$$\begin{aligned} T_f &= 4.33 \times 10^5 / 2 \times 40 \{ 26.2 \times (\tan 12^\circ + 0.15 \times \sec 0^\circ) + 26.2 \times 0.15 \} \\ &= 7.27 \times 10^4 \text{ (N}\cdot\text{mm)} \\ \tau &= 7.27 \times 10^4 / 514.1 = 142 \text{ (N/mm}^2\text{)} \end{aligned}$$

Combined stress:

The combined stress (σ) of the above tensile stress (σ_t) and shear stress (τ) can be obtained using the following equation.

$$\begin{aligned}\sigma &= 1/2(\sigma_t + \sqrt{\sigma_t^2 + 4\tau^2}) \\ &= 1/2 (57.1 + \sqrt{57.1^2 + 4 \times 142^2}) \\ &= 173 \text{ (N/mm}^2\text{)}\end{aligned}$$

When a design yield strength $S_y = 706 \text{ N/mm}^2$ of the tightening bolt (SCM435) is used, the safety margin M_s is as follows.

$$\begin{aligned}M_s &= 706/173 - 1 \\ &= 3.08\end{aligned}$$

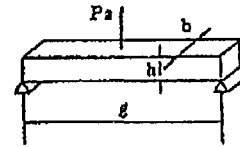
Because the M_s is positive, the integrity of the tightening bolts will not be impaired.

(2) Cross pin

The cross pin shall be analyzed under the condition that a load item (1) above is applied to it. A bending stress (σ_b) and shear stress (τ) produced in the cross pin can be obtained using the following equation. The analysis model is as shown in

Fig. II-A. 12.

$$\begin{aligned}\sigma_b &= M/Z \\ \tau &= P_a / (2nA)\end{aligned}$$



Where

M: Bending moment acting on the cross pin (N·mm)

$$\begin{aligned}M &= P_a \cdot l / 4 \times 1/n \\ &= 4.33 \times 10^5 \times 25.25 / 4 \times 1/40 \\ &= 6.84 \times 10^4 \text{ (N·mm)}\end{aligned}$$

Fig. II-A. 12 Cross Pin Analysis Model

P_a : Tightening force Based on the item (1) above = 4.33×10^5 (N)

n : Number of the tightening bolts = 40

l : Length of the cross pin where bending is applied = 25.25 (mm)

Z : Section modulus of the cross pin (mm^3)

$$Z = bh^2/6 = 6.2 \times 12.55^2/6 = 162.75 \text{ (mm}^3\text{)}$$

b : Thickness of the cross pin = 6.2 (mm)

h : Height of the cross pin = 12.55 (mm)

Substituting the values above,

$$\begin{aligned}\sigma_b &= 6.84 \times 10^4 / 162.75 \\ &= 421 \text{ (N/mm}^2\text{)}\end{aligned}$$

Next, let us obtain a shear stress (τ).

$$\tau = P_a / (2nA)$$

Where

A : Cross-section of the cross pin where shearing is applied

$$A = b \times h$$

$$= 6.2 \times 12.55 = 77.81 \text{ (mm}^2\text{)}$$

P_a : Tightening force = 4.33×10^5 (N)

n : Number of the tightening bolts = 40

b : Thickness of the cross pin = 6.2 (mm)

h : Height of the cross pin = 12.55 (mm)

Substituting the values above,

$$\begin{aligned}\tau &= 4.33 \times 10^5 / (2 \times 40 \times 77.81) \\ &= 69.7 \text{ (N/mm}^2\text{)}\end{aligned}$$

Combined stress:

The combined stress (σ) of the above bending stress (σ_b) and shear stress (τ) can be obtained using the following equation.

$$\begin{aligned}\sigma &= 1/2(\sigma_b + \sqrt{\sigma_b^2 + 4\tau^2}) \\ &= 1/2(421^2 + \sqrt{(421^2 + 4 \times 69.7^2)}) \\ &= 432 \text{ (N/mm}^2\text{)}\end{aligned}$$

When a design yield strength $S_y = 706 \text{ N/mm}^2$ of the cross pin (SCM435) is used, the safety margin M_s is as follows.

$$\begin{aligned}M_s &= 706/432 - 1 \\ &= 0.63\end{aligned}$$

Because the M_s is positive, the integrity of the cross pin will not be impaired.

A.4.5 Tie-Down Devices

Because any tie-down device to fix the packaging is not provided on it, this item is not applicable to it.

A.4.6 Pressure

It must be taken into account that the atmospheric pressure may lower excessively. Therefore, let us study about the influence given on the packaging when the atmospheric pressure is lowered to 60 kPa. When the atmospheric pressure lowers to 60 kPa, an internal pressure of $(19.0 + 101) - 60 = 60\text{kPa}$ acts on the packaging.

In this case, because the internal pressure regulating a relief valve (open at the maximum pressure of 49 kPa·G) provided on the packaging operates, a pressure difference of 49 kPa acts on the inside of the packaging.

A stress has been analyzed in item A.5.1.3 "Stress Calculation" under the condition that the internal pressure acting on the packaging is 50 kPa·G in order to verify the integrity of the packaging. Therefore a stress analysis shall be omitted here.

A.4.7 Vibration

The frequency band applied to the platform of a package carrying truck under the normal conditions is 0 to 10Hz^[1]. Let us obtain the natural frequency of the package to show that it will not cause sympathetic vibration.

Because the package is fixed to the platform of the truck with wire ropes, let us analyze the package by approximating it to a supported beam which is supported as shown in Fig. II-A. 14.

The natural frequency f (Hz) can be obtained using the following equation.

$$f = a_1 / (2\pi) \sqrt{E \cdot I \cdot g / w \cdot \ell^4}$$

a_1 : Primary mode coefficient = 15.8

(Using Fig. II-A. 13,

$$\alpha = a\ell / \ell = 600 / 5,400 = 0.11)$$

E : Young's modulus = 2.06×10^6 (N/mm²)

ℓ : Overall length of the packaging
= 5,400 (mm)

a : Extended length from the pivot
= 600 (mm)

w : Weight per unit length (N/mm)

$$w = m \cdot g / \ell = 4.32 \times 10^3 \times 9.81 / 5,400 \\ = 7.85 \text{ (N/mm)}$$

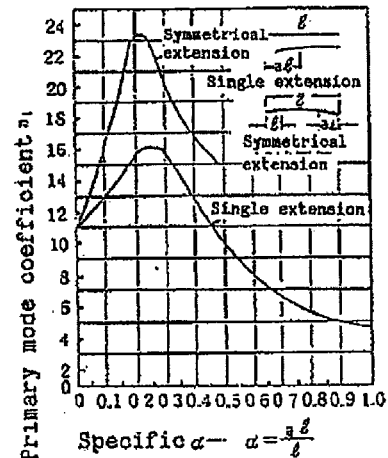


Fig. II-A. 13 Primary Mode Coefficient

g : Acceleration of gravity

$$= 9.81 \times 10^3 \text{ (mm/s}^2\text{)}$$

m: Weight of the package = 4.32×10^3 (kg)

I: Moment of inertia of area of the packaging

$$I = \pi/64 (D_1^4 - D_2^4)$$

$$= \pi/64 (1,150^4 - 1,141^4)$$

$$= 2.66 \times 10^9 \text{ (mm}^4\text{)}$$

D₁: Outside diameter of the outer shell: 1,150 (mm)

D₂: Inside diameter of the outer shell: 1,141 (mm)

Thus the following result can be obtained.

$$f = 15.8/(2 \pi) \sqrt{2.06 \times 10^2 \times 2.66 \times 10^9 \times 9.81 \times 10^3 / (7.85 \times 5,400^4)}$$

$$= 71.3 \text{ (Hz)}$$

The natural frequency of 71.3Hz is out of the frequency zone of 0 to 10 Hz which is applied to the packaging carrying truck and, therefore, the packaging will not cause sympathetic vibration.

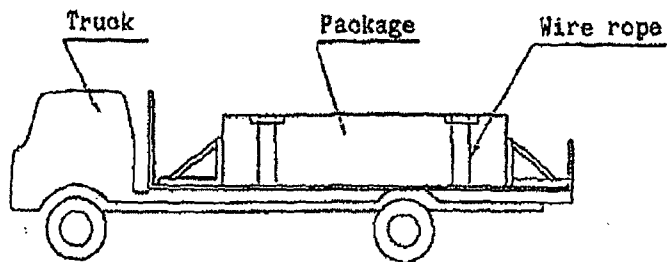
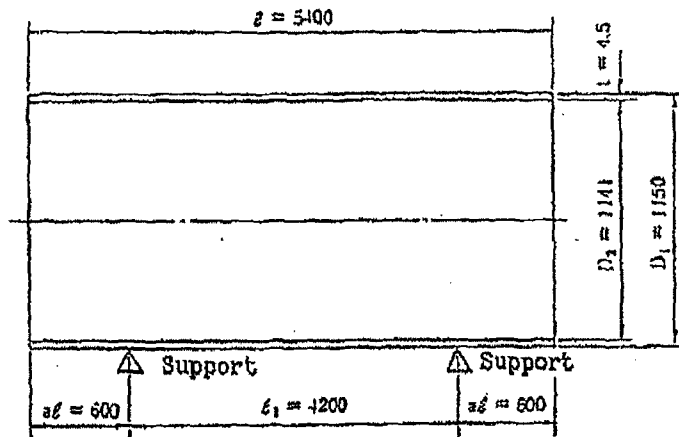


Fig. II-A. 14 Tie-down State of Package and Natural Frequency Analysis Model

A.5 Normal Conditions of Transport

A.5.1 Thermal Test

The thermal evaluation of the package taking into consideration of the solar radiation is shown in the thermal evaluation under B.4 Normal Conditions of Transport.

A.5.1.1 Summary of Pressure and Temperatures

The highest temperature of the package is obtained on the assumption that the solar radiation has the heat transfer amount of maximum 400w/m^2 (on the curved surface) for 12 hours a day on the surface of the package when the environmental temperature is highest, i.e., 38°C as described in B.4. The result is 73°C on the surface of the external cylinder. As there is no decay heat, the lowest temperature of the package is -20°C which is the lowest environmental temperature.

On the other hand, the temperature of the inside container is evaluated on the assumption that it is same as that on the surface of the outer shell. The temperature at each part is shown in Table II-A.17.

Table II-A.17 Temperature at Each Part

Summary	Temperature ($^\circ\text{C}$)	
	Minimum	Maximum
Environmental temperature	-20	38
Surface of outer shell of container	-20	73
Inside container	-20	73

The maximum internal pressure on the container and the fuel rod in this condition is $0.019\text{ MPa}\cdot\text{G}$ and $3.73\text{ MPa}\cdot\text{G}$ respectively as described in B.4.4, and the maximum internal pressure on the container is $0.05\text{ MPa}\cdot\text{G}$ from the value in A.4.6 "Pressure".

A.5.1.2 Thermal Expansion

The cradle assembly is suspended from the outer shell, and no components can be restricted by the thermal expansion of the package.

Thus, no thermal stress is produced due to the thermal expansion.

A.5.1.3 Stress Calculation

The stress produced in each part due to the rise of the internal pressure on the container and the fuel rod under the normal condition of transport is examined.

(1) External cylinder under maximum internal pressure

The tensile stress (σ_a) produced in the external cylinder under the internal pressure is obtained from the following equation.

$$\sigma_a = PD/(2t)$$

P	: Maximum internal pressure of the container	0.05 (MPa)
D	: Maximum inner diameter of the container	1,141 (mm)
t	: Wall thickness of the container	4.5 (mm)

Substituting the values above,

$$\begin{aligned}\sigma_a &= 0.05 \times 1,141 / (2 \times 4.5) \\ &= 6.34 \text{ (N/mm}^2\text{)}\end{aligned}$$

The design yield point of the container itself (SS400) is $S_y = 229 \text{ N/mm}^2$.

Thus, the safety margin M_s considering the weld efficiency (=0.6) is as follows.

$$\begin{aligned}M_s &= 229 \times 0.6 / 6.34 - 1 \\ &= 20.6\end{aligned}$$

Because the safety margin is positive, the integrity of the body part of the container is not damaged by the internal pressure.

(2) Container dome plate under maximum internal pressure

When the container is under the internal pressure, the bending stress (σ_b) associated with the strain and the membrane stress (σ_o) due to the in-plane force are produced in the dome plate, and the combined stress (σ) is obtained by the following equation.

Examination is made using the model on the safety side in which the flange part of the dome plate of the container is neglected.

$$\sigma = \sigma_b + \sigma_o \text{ [8]}$$

When the disk with its circumference fixed is subject to the uniformly distributed load, the relationship between the maximum strain (ω) produced in the center of the disk and the distributed load (p) is obtained by the following equation.

$$\omega/t + A (\omega/t)^3 = B \cdot p/E (\gamma/t)^4 \text{ [8]}$$

t	: Thickness of the dome plate	9(mm)
p	: Distributed load (maximum internal pressure)	0.05 (MPa)

γ : Radius of the dome plate	575 (mm)
E : Young's modulus	2.06×10^5 (N/mm ²)
A : Strain factor in the formula of large deflection theory for the disk under the uniformly distributed load (displacement in the radial direction: restricted)	0.471
B : Same as A	0.171

Substituting the values above in the formula, the following equation is obtained.

$$\omega^3 + 171.97\omega - 1070.3 = 0$$

ω is calculated as follows.

$$\omega = 5.34 \text{ (mm)}$$

The bending stress (σ_b) and the membrane stress (σ_o) are obtained by the following equations.

$$\sigma_b = \beta_\gamma \cdot E \cdot t \cdot \omega / \gamma^2$$

$$\sigma_o = \alpha_\gamma \cdot E \cdot \omega^2 / \gamma^2$$

Where,

β_γ : Stress factor (at the center) in the formula of the maximum deflection theory for the disk under the uniformly distributed load 2.86

α_γ : Same as β_γ 0.976

E : Young's modulus 2.06×10^5 (N/mm²)

t : Thickness of the dome plate 9 (mm)

ω : Maximum strain produced in the center of disk 5.34 (mm)

γ : Radius of the dome plate 575 (mm)

Substituting the values above,

$$\begin{aligned} \sigma_b &= 2.86 \times 2.06 \times 10^5 \times 9 \times 5.34 / 575^2 \\ &= 85.7 \text{ (N/mm}^2\text{)} \end{aligned}$$

$$\begin{aligned} \sigma_o &= 0.976 \times 2.06 \times 10^5 \times 5.34^2 / 575^2 \\ &= 17.4 \text{ (N/mm}^2\text{)} \end{aligned}$$

Thus, the combine stress (σ)

$$\begin{aligned} \sigma &= 85.7 + 17.4 \\ &= 103 \text{ (N/mm}^2\text{)} \end{aligned}$$

The design yield point of the dome plate (SS400) is $S_y = 229 \text{ N/mm}^2$.

Thus, the safety margin M_s is as follows.

$$\begin{aligned} M_s &= 229 / 103 - 1 \\ &= 1.22 \end{aligned}$$

Proprietary Information Withheld Pursuant to 10 CFR 2.390

Proprietary Information Withheld Pursuant to 10 CFR 2.390

Proprietary Information Withheld Pursuant to 10 CFR 2.390

1/14

Table II-A. 20 Comparison with Allowable Stress

Condition	Items of analysis	Analysis criteria	Reference value for analysis	Result of analysis	Design margin
Routine transport conditions	Chemical and electric reaction				
	Chemical reaction	Presence or absence of activity	Activity: None	Activity: None	In compliance with the standard
	Electric reaction	Presence or absence of water content	Water content: None	Water content: None	In compliance with the standard
	Sealing device				
	Fuel rod	Presence or absence of sealing performance	Sealing performance: Present	Sealing performance: Present	In compliance with the standard
	Lifting device				
	1. Bracket				
	(1) Bracket hole				
	Shear stress	$0.6 S_y$	137 (N/mm ²)	47.4 (N/mm ²)	1.89
	(2) Bracket weld				
Combined stress	$S_y \cdot \eta^*$	$229 \times 0.6 =$ 137.4(N/mm ²)	22.7 (N/mm ²)	5.05	
2. External cylinder					
Combined stress	S_y	229 (N/mm ²)	127 (N/mm ²)	0.80	
3. Tightening bolt					
Combined stress	S_y	706 (N/mm ²)	173 (N/mm ²)	3.08	
4. Cross pin					
Combined stress	S_y	706 (N/mm ²)	432 (N/mm ²)	0.63	
Normal conditions of transport	Thermal test				
	Stress calculation				
	1. External cylinder				
	Tensile stress	$S_y \cdot \eta^*$	$229 \times 0.6 =$ 137.4(N/mm ²)	6.34 (N/mm ²)	20.6
2. Dome plate					
Combined stress	S_y	229 (N/mm ²)	103 (N/mm ²)	1.22	
3. Fuel rod cladding					
Primary membrane stress	S_m	239 (N/mm ²)	31.1 (N/mm ²)	6.68	

* η : Weld efficiency (=0.6)

A.5.2 Water Spray Test

The outer shell of the container is a cylindrical container, and of the shape so as for water not to be collected, and its surface is coated and no water is absorbed. The flange part of the outer shell of the container is of watertight structure, and no water enters the container.

A.5.3 Free Drop Test

The package is evaluated in accordance with the requirements of the Type A Package based on the regulation, and its free drop is 1.2m under the normal conditions of transport because the maximum weight of the package is 4320kg, which is below 5000kg.

Because the package is tested with the water spray before this drop test and demonstrated to be watertight, no water enters the container, or no weight of the package is changed, and the package is evaluated to be completely free from the effect by water spray.

(a) Analysis model

The evaluation of the package during the 1.2m free drop test is analyzed. Its appropriateness is demonstrated by the comparative verification of the result of the 9m free drop test using the prototype container to evaluate the package during the 1.2m free drop. Examination is performed for three drop orientations as follows.

- (i) Horizontal drop
- (ii) Vertical drop (upper part and lower part)
- (iii) Corner drop (upper and lower part)

(1) Analysis method and results

The acceleration and the deformation of the package during the 1.2m free drop test are analyzed based on the following conditions.

- a The colliding surface is a rigid body, and the drop energy of the package is totally absorbed by the plastic deformation of the container.
- b Because the cradle assembly of the package is suspended by the shock mounts, the assembly is dropped in the restricted condition by the outer shell through the shock mounts.
- c The weight of the package to be used in the analysis is described in "A.2 Weight and Center of Gravity", and the drop energy for each component is as follows.

$$E_{ai} = E_{vi} = m_i \times g \times h$$

$$E_{ao} = E_{vo} = m_o \times g \times h$$

Where,

E_{ai} : Absorbed energy by the outer shell of the cradle assembly side (J)

E_{vi} : Drop energy of the cradle assembly side (J)

E_{ao} : Absorbed energy by the outer shell of the package container (J)

E_{vo} : Drop energy of the outer shell of the package container (J)

m : Weight of package = 4,320kg

$$m = m_i + m_o$$

m_i : Weight of the cradle assembly = 2,280 (kg)

m_o : Weight of the outer shell = 2,040 (kg)

h : Drop height = 1.2 (m)

g : Acceleration of gravity = 9.81 (m/s²)

The following values are obtained.

$$\begin{aligned} E_{ai} = E_{vi} &= 2,280 \times 9.81 \times 1.2 \\ &= 2.68 \times 10^4 \text{ (J)} = 2.68 \times 10^7 \text{ (N}\cdot\text{mm)} \end{aligned}$$

$$\begin{aligned} E_{ao} = E_{vo} &= 2,040 \times 9.81 \times 1.2 \\ &= 2.40 \times 10^4 \text{ (J)} = 2.40 \times 10^7 \text{ (N}\cdot\text{mm)} \end{aligned}$$

The total drop energy E_T is obtained from the following equation.

$$E_T = E_{vi} + E_{vo} = 5.08 \times 10^7 \text{ (N}\cdot\text{mm)}$$

- d The analysis results of the impact acceleration and the deformation amount produced in the Type A package obtained using the SHOCK code are shown in Table II-A. 39 of Annex A.10.5.

(b) Tests of prototype

The 9m drop tests of the prototype using the prototype container are carried out to check the safety of the fuel assemblies as contents, and confirm the suitability of the analysis method.

The prototype container is that for "Model MFC-1 Package", and equivalent to the actual container in which only the alternative is used for the fuel assembly as contents. As described in Chapter I-C, the prototype container consists of the outer shell composed of the upper cover and the lower container, and the cradle assembly composed of the shock mount frame, the cross frame, etc., and the outer dimension is about 5,400mm in length, about 1,150mm in outer diameter, and 1,275mm in height, and the total weight of the package is about 4,300kg.

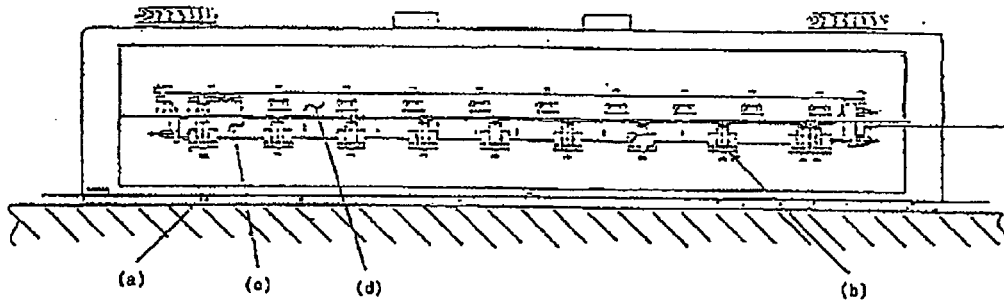
The vertical drop test and the corner drop test (by #1 prototype) and the horizontal drop test (by #2 prototype) were carried out using 2 sets of the prototype containers. Refer to II-F "Test Report of Prototype Packaging for Model MFC-1 Container ZEG-3222".

- (c) Model test
Not applicable.

(2) Strength evaluation of package during free drop

- (A) Horizontal drop with the top half downward from a height of 1.2m

The evaluation item during the 1.2m horizontal drop is shown in Fig. II-A. 16.



Symbol	Evaluation item	With/without evaluation
(a)	Deformation amount	○
(b)	Clamping frame	○
(c)	Skin	○
(d)	Fuel rod cladding	○

Fig. II-A. 16 Evaluation Item during 1.2m Horizontal Drop

- (a) Deformation amount of outer shell

It is proved that the thickness of the outer shell remains even when the outer shell is deformed during the 1.2m horizontal drop. The analysis model is shown in Fig. II-A. 17.

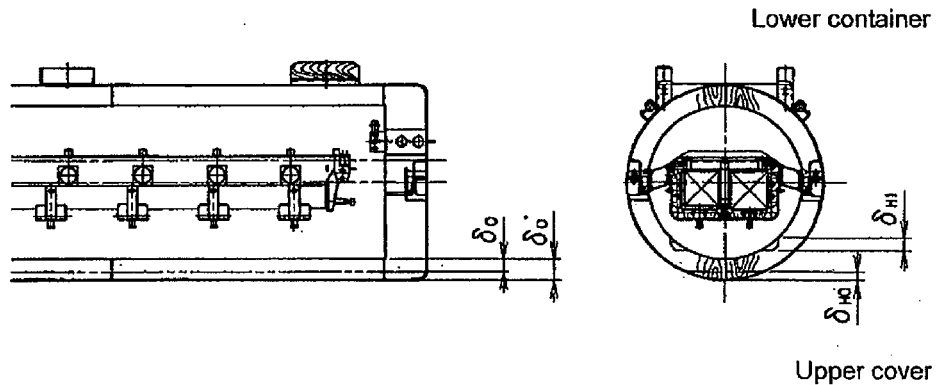


Fig. II-A. 17 Deformation Amount Analysis Model of Outer Shell during 1.2m Horizontal Drop

Proprietary Information on Pages II-A-65 through II-A-69
Withheld Pursuant to 10 CFR 2.390

(a) Deformation Amount of Outer Shell

It is proved from the vertical drop with the top end wall downward from a height of 1.2m that the thickness of the outer shell remains even when the outer shell is deformed. The analysis model is shown in Fig. II-A. 23.

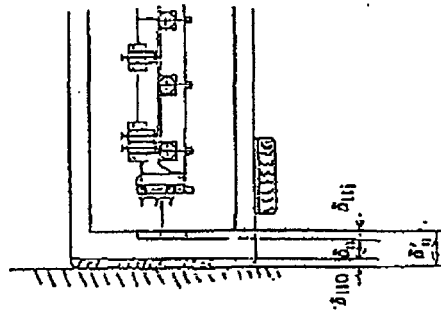


Fig. II-A. 23 Deformation Amount Analysis Model of Outer Shell during 1.2m Top End Vertical Drop

The deformation amount and the remaining amount of the package container after the 1.2m top end vertical drop are given by the following equation from Fig. II-A. 23.

$$\delta_o = \delta_o' - (\delta_{Hi} + \delta_{Ho})$$

Where,

δ_o' : Thickness before deformation = 250 (mm)

δ_{Hi} : Deformation inside the outer shell = 0 (mm)

δ_{Ho} : Deformation outside the outer shell = 9.5 (mm)

Thus, the deformation amount is give as follows.

$$\delta_o = 250 - 9.5 = 240.5 \text{ (mm)}$$

Thus, only the outer shell is deformed during the 1.2m top end vertical drop, and the cradle assembly is not directly collided on the drop base.

(b) Jack-screw

When the package is dropped from the height of 1.2m, the jack-screw is dropped downward. Then, the impact force of the fuel assemblies is applied to the jack-screw. The critical buckling load and the compressive load of the jack-screw and the shearing strength of the screw part are obtained to demonstrate that the jack-screw is not broken. The analysis model is shown in Fig. II-A. 24.

Proprietary Information on Pages II-A-71 through II-A-80
Withheld Pursuant to 10 CFR 2.390

(a) Deformation amount of outer shell

It is proved from the 1.2m bottom end vertical drop that the thickness of the outer shell remains even when the outer shell is deformed. The analysis model is shown in Fig. II-A. 30.

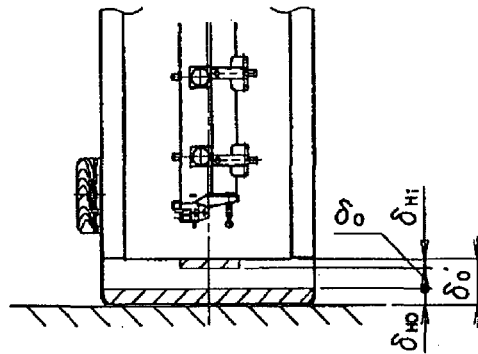


Fig. II-A. 30 Analysis Model of Deformation Amount of Outer Shell during 1.2m Bottom End Vertical Drop

The deformation amount and the remaining amount of the container after the 1.2m bottom end vertical drop as shown in Fig. II-A. 30 are given by the following equation.

$$\delta_o = \delta_o' - (\delta_{HI} + \delta_{HO})$$

Where,

δ_o' : Thickness before deformation = 250 (mm)

δ_{HI} : Deformation inside the outer shell = 0 (mm)

δ_{HO} : Deformation outside the outer shell = 9.5 (mm)

Thus, the following value is obtained.

$$\delta_o = 250 - 9.5 = 240.5 \text{ (mm)}$$

Only the outer shell is deformed during the 1.2m bottom end vertical drop, and the cradle assembly is not directly collided with the drop base.

(b) Pivot mount attaching bolt

The impact load is applied due to the self-weight of the clamping frame during the 1.2m vertical drop.

The tensile stress (σ_t) and the shear stress (τ) produced in the attaching bolt part due to the impact load are given by the following equations.

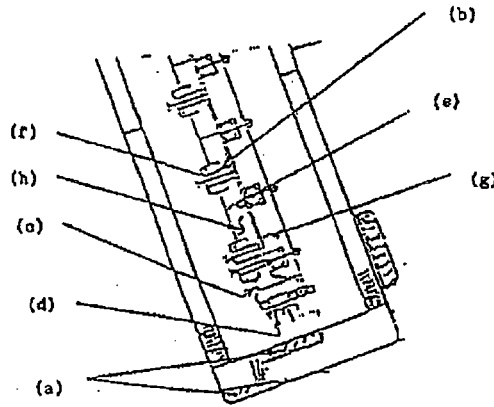
The analysis model is shown in Fig. II-A. 31.

$$\sigma_t = F_2/A \text{ (N/mm}^2\text{)}$$

Proprietary Information on Pages II-A-82 through II-A-86
Withheld Pursuant to 10 CFR 2.390

(a) Evaluation Item

Evaluation during the 1.2m corner drop is performed at the following items. The evaluation positions of stress during the 1.2m corner drop are shown in Fig. II-A. 33.



Symbol	Evaluation item	With/without evaluation
(a)	Deformation amount	○
(b)	Clamping frame	○
(c)	Jack screw	○
(d)	Fixed frame	○
(e)	Skeleton assembly	○
(f)	Pivot mount attaching bolt	○
(g)	Skin	○
(h)	Fuel rod cladding	○

Fig. II-A. 33 Evaluation Item during 1.2m Corner Drop

(b) Deformation Amount of Outer Shell

It is proved from the 1.2m corner drop that the thickness of the outer shell remains even when the outer shell is deformed. The analysis model is shown in Fig. II-A. 34.

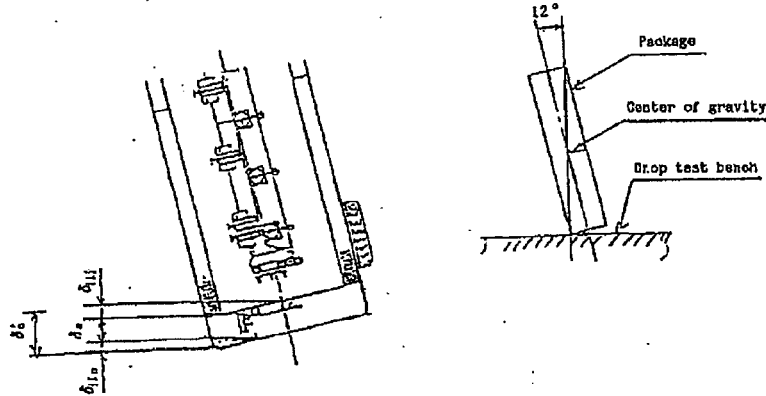


Fig. II-A. 34 Deformation Amount Analysis Model of Outer Shell during 1.2m Corner Drop

The deformation amount and the remaining amount of the outer shell after the 1.2m corner drop are given by the following equation as shown in Fig. II-A. 34.

$$\delta_o = \delta_o - (\delta_{HI} + \delta_{HO})$$

Where,

δ_o : Thickness before deformation = 375 (mm)

δ_{HI} : Deformation of the inner side of the outer shell = 0 (mm)

δ_{HO} : Deformation of the outer side of the outer shell = 71 (mm)

Thus,

$$\delta_o = 375 - (0 + 71) = 304 \text{ (mm)}$$

Only the outer shell is deformed and the cradle assembly is not directly collided with the drop base.

(c) Stresses produced in Cradle Assembly and Contents

It is shown from Table II-A. 26 that the acceleration component in each direction is larger than the acceleration produced during the vertical drop. In this paragraph, the stress produced in each part in each direction is obtained to perform evaluation individually or in a combined manner according to the condition of application of the load. The stress produced in each part is analyzed by the same method at the same evaluation positions as described in "A.5.3 (2) (a), (b) and (c) Horizontal Drop and Vertical Drop". The analysis results are indicated in Table II-A. 27.

Table II-A. 27 (1) Analysis Result of 1.2m Corner Drop

Requirement	Condition	Items for Analysis	Reference value in analysis	Results of analysis			Design margin	
				Vertical component of stress	Horizontal component of stress	Combined stress		
Type A Package	Top end corner drop	(1) Clamping frame Bending stress	$S_y = 229$ (N/mm ²)	-	7.31 (N/mm ²)	-	30.3	
		(2) Fuel rod cladding a. Bending stress + Stress due to internal pressure + Compressive stress (15 x 15 Type, 12ft) b. Buckling load	$1.5 S_m = 358$ (N/mm ²)	$\sigma_\theta = 28.5$ (N/mm ²) $\sigma_z = -24.3$ (N/mm ²) $\sigma_r = -1.75$ (N/mm ²)	-	$ \sigma_\theta - \sigma_z = 52.7$ (N/mm ²)	-	5.79
		(3) Jack screw (SCM435) a. Buckling load	$P_k = 2.19 \times 10^3$ (N)	96.2 (N)	-	-	-	21.7
		b. Shear stress at thread	$P_k = 7.94 \times 10^5$ (N)	3.65×10^4 (N)	-	-	-	20.7
		(4) Fixed frame (SS400) a. Shear stress at thread	$0.6 S_y = 423$ (N/mm ²)	24.5 (N/mm ²)	-	-	-	16.2
		b. Body Combined stress	$0.6 S_y = 137$ (N/mm ²)	19.1 (N/mm ²)	-	-	6.17	
		(5) Skin (boron stainless steel) Bending stress + Compressive stress	$S_y = 229$ (N/mm ²)	172 (N/mm ²)	-	-	0.33	
			$S_y = 207$ (N/mm ²)	14.1 (N/mm ²)	1.74 (N/mm ²)	15.9 (N/mm ²)	12.0	

Table II-A.27 (2) Analysis Result of 1.2m Corner Drop

Requirement	Condition	Items for Analysis	Reference value in analysis	Results of analysis			Design margin
				Vertical component of stress	Horizontal component of stress	Combined stress	
Type A Package	Bottom end corner drop	(1) Skeleton assembly (zircaloy 4) Bending stress + Compressive stress	$S_y = 555$ (N/mm ²)				8.06
		1. Type 14 × 14 (10ft) 2. Type 14 × 14 (12ft) 3. Type 15 × 15 (12ft) 4. Type 17 × 17 (12ft)		48.1 (N/mm ²) 55.3 (N/mm ²) 54.9 N/mm ²) 53.2 (N/mm ²)	5.84 (N/mm ²) 5.90 (N/mm ²) 5.81 (N/mm ²) 3.95 (N/mm ²)	54.0 (N/mm ²) 61.2 (N/mm ²) 60.7 (N/mm ²) 57.1 (N/mm ²)	Type 14 × 14 (12ft)
		(2) Pivot mount attaching bolt (SS400) Combined stress	$S_y = 229$ (N/mm ²)	35.9 (N/mm ²)	-	-	5.37

II-A-90

A.5.4 Stacking Test

In this paragraph, the case in which the load prescribed in the regulation is applied to the package is examined. The compressive load (F_1) 5 times the weight of the package in accordance with the regulation is compared with the load (F_2) which is the product of the perpendicular projected area of the package with 13kPa, and the stress to be produced in the package when the larger load of the two is applied is analyzed.

- (1) Load (F_1) 5 times the weight of package

$$F_1 = 5 \cdot m$$

$$= 5 \times 4,320 \times 9.81$$

$$= 2.12 \times 10^5 \text{ (N)}$$

$$m : \text{Maximum weight of the package} \quad 4,320 \text{ (kg)}$$

- (2) Load (F_2) which is the product of the perpendicular projected area of the package with 13kPa

$$F_2 = 13 \times 10^{-3} \times D \times L$$

$$= 13 \times 10^{-3} \times 1,150 \times 5,400$$

$$= 8.07 \times 10^4 \text{ (N)}$$

$$D : \text{Width of the container} \quad 1,150 \text{ (mm)}$$

$$L : \text{Length of the container} \quad 5,400 \text{ (mm)}$$

Because $F_1 = 2.12 \times 10^5 \text{ (N)} > F_2 = 8.07 \times 10^4 \text{ (N)}$, the compressive load applied to the container is $2.12 \times 10^5 \text{ (N)}$.

The load applied to the package is the self-weight of the package plus the load (F_1), and the load $F = 2.54 \times 10^5 \text{ (N)}$. The bending stress produced in the outer shell is obtained to demonstrate the integrity of the outer shell.

When the load (F) is applied to the package, the outer shell is modeled as the simply supported beam. The analysis model is shown in Fig. II-A. 35. The bending stress (σ_b) produced in the outer shell is given by the following equation.

$$\sigma_b = M/Z$$

M: Bending moment

$$M = FL/8$$

$$M = 2.54 \times 10^5 \times 5,400/8$$

$$= 1.72 \times 10^8 \text{ (N}\cdot\text{mm)}$$

$$F: \text{Load} \quad 2.54 \times 10^5 \text{ (N)}$$

$$L: \text{Length of the container} \quad 5,400 \text{ (mm)}$$

Z: Section modulus of the container

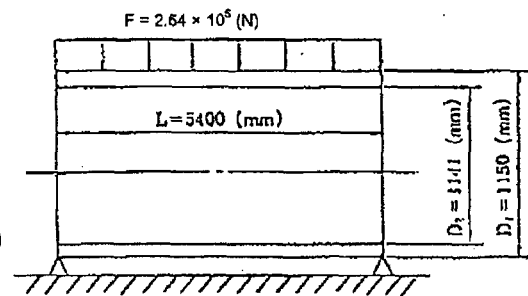


Fig. II-A. 35 Bending Stress Analysis Model

$$\begin{aligned}
 Z &= \pi/32 \times (D_1^4 - D_2^4)/D_1 \\
 &= \pi/32 \times (1,150^4 - 1,141^4)/1,150 \\
 &= 4.62 \times 10^6 \text{ (mm}^3\text{)}
 \end{aligned}$$

D_1 : Outer diameter of the external cylinder = 1,150 (mm)

D_2 : Inner diameter of the external cylinder = 1,141 (mm)

Substituting the values above, the bending stress (σ_b) is obtained as follows.

$$\begin{aligned}
 \sigma_b &= 1.72 \times 10^8 / (4.62 \times 10^6) \\
 &= 37.2 \text{ (N/mm}^2\text{)}
 \end{aligned}$$

The design yield strength of the external cylinder (SS400) is $S_y = 229 \text{ (N/mm}^2\text{)}$.

The safety margin M_s is given as follows.

$$\begin{aligned}
 M_s &= 229/37.2 - 1 \\
 &= 5.15
 \end{aligned}$$

Because the safety margin is positive, the integrity of the package is not damaged by the compressive load which is 5 times its self-weight.

A.5.5 Penetration Test

The integrity of the package is demonstrated by analysis even in the case in which a steel rod of 6kg in weight and 32mm in diameter is dropped on the weakest part of the package from the height of 1m with the semi-spherical tip downward and the major axis perpendicular as the test condition of the paragraph.

The important containment boundary of the package is fuel rods, which the fuel assembly consists of is contained in the upper cover and the lower container which are the outer shell. The thickness of the external cylinder of the outer shell is at least 4.5mm.

The case in which the rod directly hits the external cylinder is explained to demonstrate that the external cylinder is not penetrated by the rod.

Explanation is given for the case in which the rod is collided with the outer shell of 4.5mm in thickness in the most easily penetrating position as indicated in Fig. II-A. 36.

The potential energy E_1 (N·mm) of the rod before the drop is given by the following equation.

$$E_1 = m \cdot h \cdot g$$

Where,

m: Weight of the rod = 6 (kg)

h: Drop height = 1,000 (mm)

g: Acceleration of gravity = 9.81 (m/s²)

Thus, the potential energy is given as follows:

$$E_1 = 5.89 \times 10^4 \text{ (N} \cdot \text{mm)}$$

The energy E_2 (N·mm) required for the rod to penetrate the external cylinder of 4.5mm in thickness is given by the following equation.

The analysis model is shown in Fig. II-A. 37.

$$E_2 = \int_0^t \tau_{cr} \cdot \pi \cdot d \cdot (t - y) \cdot dy$$

Where,

τ_{cr} : Shear stress in external cylinder (N/mm²)

$$\begin{aligned} \tau_{cr} &= 0.6S_u = 0.6 \times 379 \\ &= 227 \text{ (N/mm}^2\text{)} \end{aligned}$$

d : Diameter of the rod = 32 (mm)

t : Thickness of the external cylinder = 4.5 (mm)

Implementing the integration and substituting the values above,

$$E_2 = \tau_{cr} \cdot \pi \cdot d \times 1/2 \times t^2$$

$$\begin{aligned}
 &= 227 \times \pi \times 32 \times 1/2 \times 4.5^2 \\
 &= 2.31 \times 10^5 \text{ (N}\cdot\text{mm)} \\
 E_1 &= 5.89 \times 10^4 \text{ N}\cdot\text{mm} < E_2 = 2.31 \times 10^5 \text{ N}\cdot\text{mm}
 \end{aligned}$$

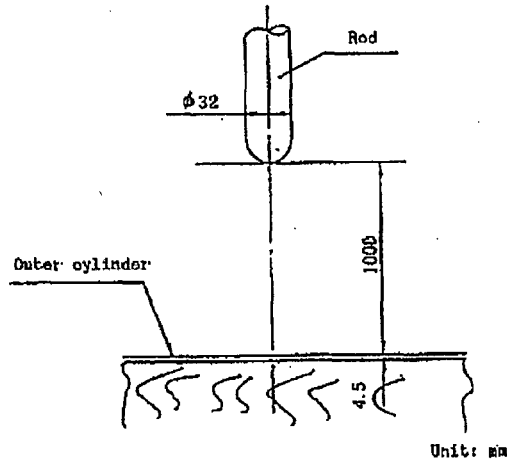


Fig. II-A. 36 Penetration Model

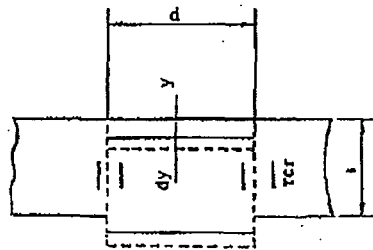


Fig. II-A. 37 Shear Model

Thus, the external cylinder of the outer shell is not penetrated by the rod.

Only the energy by the shear in the external cylinder is taken into consideration in the above-mentioned energy E_2 , but in reality, the energy is required for the bending of the external cylinder and for the compression of wood for the rod to penetrate the external cylinder, and E_2 is further increased, and the above analysis is made on the safety side. As described above, the containment boundary is not affected by the drop of the rod, and the integrity of the package is not damaged either.

A.5.6 Corner or Edge Drop

The weight of this package is up to 4,320kg, which is not applicable.

A.5.7 Summary of Results and Evaluation

The summary of the package under the normal conditions of transport is described for each test item.

(1) 1.2m drop

The deformation amount of the external cylinder of the container during the 1.2m drop in each case is proved to be 9.5mm (horizontal drop) through 71mm (corner drop), and the deformation in any drop orientation does not reach the cradle assembly. The impact acceleration with the fuel rod loaded is 298G-55G for the external cylinder of the container, and 72G-17G for the cradle assembly, and the stress produced in the fuel rod cladding which is the containment boundary is below the reference value of analysis, and the fuel rod cladding tube keeps its integrity, and its containment-ability is kept.

(2) Other summary

The strength and containment-ability of the fuel rod cladding which is the containment boundary are kept in the analyses on the free drop, other pressure, vibration, water spray, and stacking test.

(3) Comparison with allowable stress

The analysis results based on the design conditions in A.1.2 satisfy the design criteria in A.1.2, and the results are compared with the reference values of analysis by the analysis item, and indicated in Table II-A. 28 (1)-(3). The stresses produced are below the reference values of analysis in any cases as indicated in the table, and the integrity of the fuel rod cladding tube which is the containment boundary is not damaged and its containment-ability is kept.

Table II-A. 28 (1) Comparison with Allowable Stress

Requirement	Condition	Items for Analysis	Analysis criteria	Reference value in analysis	Results of analysis	Design margin	
Type A Package	Normal conditions of transport	Water spray					
		1. Water absorbing property	None	None	None	In compliance with the standard Same as above	
		2. Water drainage property	Present	Present	Present		
		Free drop					
		1. 1.2m horizontal drop					
		(1) Clamping frame					
		(a) Bending stress	S_y	229 (N/mm ²)	126 (N/mm ²)	0.81	
		(2) Skin					
		(a) Bending stress	S_y	207 (N/mm ²)	29.8 (N/mm ²)	5.94	
		(3) Fuel rod cladding					
		Combination of Bending + Internal pressure	$1.5 S_m$	358 (N/mm ²)	156 (N/mm ²)	1.29	
		2. 1.2m top end vertical drop					
		(1) Jack screw					
		(a) Buckling load	P_k	7.94×10^5 (N)	3.17×10^4 (N)	24.0	
(b) Shear stress of thread	$0.6 S_y$	423 (N/mm ²)	21.2 (N/mm ²)	18.9			
(2) Fixed frame							
(a) Combined stress (bending + shearing)	S_y	229 (N/mm ²)	149 (N/mm ²)	0.53			
(b) Shear stress of thread	$0.6 S_y$	137 (N/mm ²)	16.6 (N/mm ²)	7.25			
(3) Skin							
(a) Compressive stress	S_y	207 (N/mm ²)	12.3 (N/mm ²)	15.8			
(4) Fuel rod cladding							
(a) Combination of compression + Internal pressure	S_m	239 (N/mm ²)	40.5 (N/mm ²)	4.90			
(b) Buckling load	P_k	2.19×10^3 (N)	83.4 (N)	25.2			

II-A-96

Table II-A. 28 (2) Comparison with Allowable Stress

Requirement	Condition	Items for Analysis	Analysis criteria	Reference value in analysis	Results of analysis	Design margin
Type A Package	Normal conditions of transport	3. 1.2m bottom end vertical drop				
		(1) Pivot mount attaching bolt				
		(a) Combined stress (tensile + shearing)	S_y	229 (N/mm ²)	31.2 (N/mm ²)	6.33
		(2) Skeleton assembly				
		(a) Compressive stress	S_y	555 (N/mm ²)	48.0 (N/mm ²)	10.5
		4. 1.2m top end corner drop				
		(1) Clamping frame				
		(a) Bending stress	S_y	229 (N/mm ²)	7.31 (N/mm ²)	30.3
		(2) Fuel rod cladding				
		(a) Combination of Bending + Compression + Internal pressure	$1.5 S_m$	358 (N/mm ²)	52.7 (N/mm ²)	5.79
		(b) Buckling load	P_k	2.19×10^3 (N)	96.2 (N)	21.7
		(3) Jack screw				
		(a) Buckling load	P_k	7.94×10^5 (N)	3.65×10^4 (N)	20.7
		(b) Shear stress of thread	$0.6 S_y$	423 (N/mm ²)	24.5 (N/mm ²)	16.2
		(4) Fixed frame				
(a) Shear stress of thread	$0.6 S_y$	137 (N/mm ²)	19.1 (N/mm ²)	6.17		
(b) Combined stress of body (bending + shearing)	S_y	229 (N/mm ²)	172 (N/mm ²)	0.33		
(5) Skin						
(a) Combination of Bending + Compression	S_y	207 (N/mm ²)	15.9 (N/mm ²)	12.0		
5. 1.2m bottom end corner drop						
(1) Skeleton assembly (Type 14 × 14 (12ft))						
(a) Combination of Bending + Compression	S_y	555 (N/mm ²)	61.2 (N/mm ²)	8.06		
(2) Pivot mount attaching bolt						
(a) Combined stress (tensile + shearing)	S_y	229 (N/mm ²)	35.9 (N/mm ²)	5.37		

II-A-97

Table II-A. 28 (3) Comparison with Allowable Stress

Requirement	Condition	Items for Analysis	Analysis criteria	Reference value in analysis	Results of analysis	Design margin
Type A Package	Normal condition of transport	Stacking test 1. External cylinder (a) Bending stress	S_y	229 (N/mm ²)	37.2 (N/mm ²)	5.15
		Penetration 1. External cylinder (minimum thickness part)	Critical penetration energy	2.31×10^5 (N/mm ²)	5.89×10^4 (N/mm ²)	2.92

II-A-98

A.6 Hypothetical Accident Conditions of Transport

This package does not fall under the category of this paragraph as the requirement for Type A package.

A.7 Reinforced Immersion Test

Amount of radioactivity of this package does not fall under the category of this paragraph as it does not exceed 100 thousand times the A_2 value.

A.8 Radioactive Contents

The contents of this package are fuel assemblies (which could include non-nuclear fuel core internals). The fuel assemblies consist of, as indicated in Chapter I-D, fuel rod, grid assembly, adapter plate, top and bottom nozzles, guide thimble for instrumentation within reactor, guide thimble for control rod.

The radioactive contents of this package consist of uranium dioxide pellets or gadolinia - uranium dioxide pellets.

The uranium dioxide pellets or gadolinia - uranium dioxide pellets are housed in a fuel rod cladding tube which constitutes a fuel rod and is made of zircaloy alloy (zircaloy-4, MDA, or ZIRLO) having heat resistance and corrosion resistance, and both ends of the fuel rod cladding tube are sealed with end plugs by welding. Also, the fuel rod cladding tube is filled with helium between 2.35 MPa·G and 3.14 MPa·G.

The density of the fuel pellets is about 97% of the theoretical density, and the maximum charging amount of uranium is about 540kg/fuel assembly (17 × 17 type, 12 feet), while the enrichment is 5wt% or less.

Also, the fuel rod cladding tube, which constitutes containment boundary, retains its integrity in a free drop test from a height of 1.2m, thus maintaining its containment properties.

A.9 Fissile Materials Package

This package is to be evaluated based on the regulations, following the requirement of the fissile materials package. The package is free from the possibility of causing cracks or damages under ambient temperature conditions between -20 and 38 °C, as shown in A. 4.2.

A.9.1 Normal Conditions of Transport for Fissile Materials Package

As the normal conditions of transport for fissile material package, the safety features are evaluated in view of the cumulative effects by the test procedures shown in Fig. II-A. 38 (water spray test, free drop test from a height of 1.2m, stacking test and steel rod penetration test).

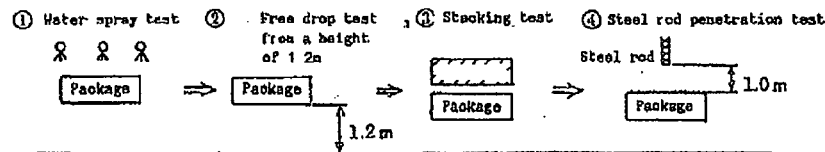


Fig. II-A. 38 Test Procedures in Normal Conditions of Transport

A.9.1.1 Water Spray Test (Re: Para. 721 of IAEA regulations)

Like A.5.2, an outer shell of this packaging is a container of a cylindrical shape, a form being difficult for water to stay thereon, and its surface is coated, thus having no water absorbing nature, also a flange part on the outer shell of container is of a watertight structure, thus water can not go into the container.

A.9.1.2 Free Drop (Re: Para. 722)

Like A.5.3, the deformation is limited to the outer shell. Thus no deformation takes place at the cradle assembly. Also, fuel rods constituting the containment boundary keep their integrity.

A.9.1.3 Stacking Test (Re: Para. 723)

As in A.5.4, the package keeps its integrity.

A.9.1.4 Penetration Test (Re: Para. 724)

As in A5.5, the rod of 6kg that is unlikely to break easily does not penetrate the package.

A.9.2 Hypothetical Accident Conditions of Transport for Fissile Materials Package

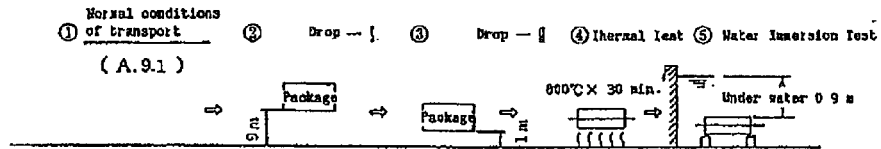
Concerning the accident conditions of transport for fissile material package, the two types of test procedures are shown in Fig. II-A. 39.

(A) Damaged state after a test under normal conditions of transport + 9m drop test + 1m puncture test + thermal test (800 °C x 30 minutes) + 0.9m water immersion test

(B) Damaged state after a test under normal conditions of transport + 15m water immersion test

The conditions of (A) is taken up as this test procedure including both of the drop tests from a height of 9m which has a significant influence over the criticality system and the thermal test in which distances between fuel assemblies become shorter by loss of shock absorber by fire in the test, where both tests bring out cumulative effects, and the safety features are evaluated.

[A]



[B]

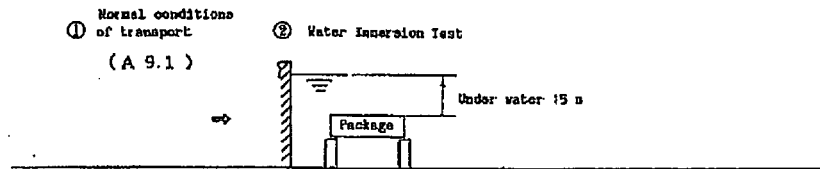


Fig. II-A. 39 Test Procedures in Hypothetical Accident Conditions of Transport

The hypothetical accident conditions of transport which are applied to this package are as shown below. Here, while the packaging is deformed under the normal conditions of transport, the integrity of the package is maintained without being impaired.

1. Strength test

- Drop test I
- Drop test II

An evaluation of structure of this package under the strength test is made: for Drop test I, by analysis partially using the results of test of prototype packaging, and for Drop test II, by using the results of test of prototype packaging.

First, studies are made on the influence received by the fuel assembly which is the contents and on the deformation of the container when the package is dropped from a height of 9m in the drop tests I and II, under which the package is subject to the risk of receiving the maximum damage.

In the strength test, the order of performing the drop test I and the drop test II constitutes a problem. For example, when the drop test II is made succeeding the drop test I, the manner of the deformation in the packaging will be such that local deformations superimpose over the uniform deformation. On the other hand, if reverse order is made, the local deformation generated by the drop test II will not be superimposing on the uniform deformation in drop test I but will be buried in the latter.

Therefore, here, a case of performing drop test II after the drop test I will be taken up, that is, taking up the procedure where the degree of deformation is made larger.

2. Thermal test

Thermal tests will be described under Chapter II-B, Thermal Analysis, which will be shown later.

3. Water immersion test

Concerning the water immersion test, containment properties will be studied by comparison with an external pressure bearing on the fuel assembly.

A.9.2.1 Strength Test/Drop Test I (as drop is made from a height of 9m) (Re. Para. 727 (a))

(1) Evaluation method

An evaluation is to be made on this package with the drop from a height of 9m in view of the deformation taking place in the free drop under normal conditions of transport (1.2m) based on the regulation, taking place in each drop orientation of the package.

Here, as to the drop orientations of the package, the following four orientations will be taken up:

- (i) Vertical (end) drop (with the upper cover downward; and with the lower container downward)
- (ii) Horizontal (side) drop
- (iii) Corner drop (with the upper cover downward; and with the lower container downward)
- (iv) Slanting (oblique) drop

(2) Method of analysis and results

The method of analysis was same as the method in A.5.3 and the results were obtained by using SHOCK code. The impact acceleration generated in the fissile material package and the analysis results of the deformation in the package are shown in Table II-A. 39 in the Annex A. 10. 5.

(a) Vertical drop with the upper cover downward from a height of 9m

1. Deformation amount of outer shell

It is shown that even if a deformation was generated on the outer shell by the vertical drop with the top of container downward from a height of 9m, the outer shell retained its thickness. An analysis model is shown in Fig. II-A. 40.

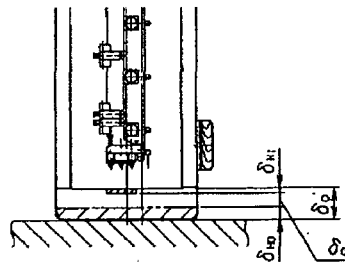


Fig. II-A. 40 Deformation Amount Analysis Model of Outer Shell during 9m Vertical Drop (with the upper cover downward)

The deformation amount and the remaining amount of thickness in the outer shell after the vertical drop test with the upper cover downward from a height of 9m are given by the following equation based on Fig. II-A. 40.

$$\delta_o = \delta_o' - (\delta_{HI} + \delta_{HO})$$

Where,

δ_o' : Thickness before deformation = 240.5 (mm)

(Deformation amounts after 1.2m drop were taken into consideration (Re: A.5.3 (2) (b))

δ_{HI} : Deformation amount inside of the outer shell = 102 (mm)

δ_{HO} : Deformation amount outside of the outer shell = 56.5 (mm)

Therefore, the following value is obtained:

$$\delta_o = 240.5 - (102 + 56.5) = 82 \text{ (mm)}$$

Thus, a deformation by the vertical drop with the upper cover downward from a height of 9m will be taking place only on the outer shell and the cradle assembly will not collide directly with the drop base.

2. Evaluation of strength of packaging and contents

An analysis was made with the same method and at the same evaluation items as those described in the paragraph A.5.3. Results of evaluation are shown in Table II-A. 32.

(b) Vertical drop with the lower container downward from a height of 9m

1. Deformation amount of outer shell

It is shown that even if deformation takes place at the outer shell by the vertical drop with the bottom of container downward from a height of 9m, the outer shell retained its thickness. An analysis model is shown in Fig. II-A. 41.

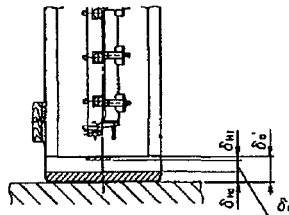


Fig. II-A. 41 Deformation Amount Analysis Model of Outer Shell during 9m Vertical Drop (with the lower container downward)

Deformation amount and the remaining amount of thickness after the vertical drop with the lower container downward from a height of 9m are given by the following equation based on Fig. II-A. 41.

$$\delta_o = \delta_o' - (\delta_{HI} + \delta_{Ho})$$

Where,

δ_o' : Thickness before deformation = 240.5 (mm)

(Deformation amounts after 1.2m drop were taken into consideration (Re: A.5.3 (2) (c).)

δ_{HI} : Deformation amount inside of the outer shell = 92 (mm)

δ_{Ho} : Deformation amount outside of the outer shell = 58.5 (mm)

Therefore, the following value is obtained:

$$\delta_o = 240.5 - (92 + 58.5) = 90 \text{ (mm)}$$

Thus, a deformation by the vertical drop with the lower container downward from a height of 9m will be taking place only on the outer shell and the cradle assembly will not collide directly with the drop base.

2. Evaluation of strength of packaging and contents

An analysis was made with the same method and at the same evaluation items as those described in the paragraph A.5.3. Results of analysis are shown in Table II-A. 32.

(c) Horizontal drop from a height of 9m

1. Deformation amount of packaging

It is shown that even if a deformation was generated on the outer shell by the horizontal drop from a height of 9m, the outer shell retained its thickness. An analysis model is shown in Fig. II-A. 42.

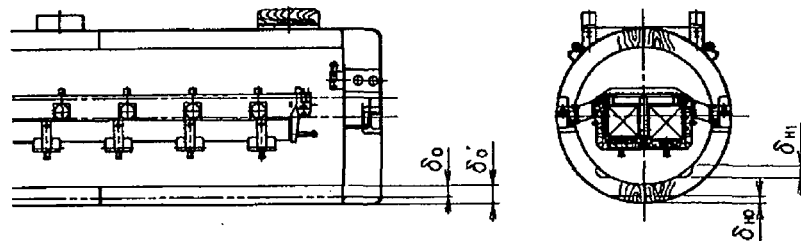


Fig. II-A. 42 Deformation Amount Analysis Model of Outer Shell during 9m Horizontal Drop (with the upper cover downward)

Deformation amount and the remaining amount of thickness after the horizontal drop from a height of 9m are given by the following equation based on Fig. II-A. 42.

$$\delta_o = \delta_o' - \delta_{Ho}$$

(Refer to a presence/absence of deformation amount in A.10.8)

Where,

δ_o' : Thickness before deformation = 115.5 (mm)

(Deformation amounts after 1.2m drop were taken into consideration (Re: A.5.3 (2) (a).)

δ_{Hi} : Deformation amount inside of the outer shell = 50 (mm)

δ_{Ho} : Deformation amount outside of the outer shell = 19.5 (mm)

Therefore, the following value is obtained:

$$\delta_o = 115.5 - 19.5 = 96 \text{ (mm)}$$

Thus, a deformation by the horizontal drop from a height of 9m will be taking place only on the outer shell and the cradle assembly will not collide directly with the drop base.

2. Evaluation of strength of packaging and contents

An analysis was made with the same method and at the same evaluation items as those described in the paragraph A.5.3. Results of evaluation are shown in Table II-A. 32.

(d) Corner drop test with the top of container downward from a height of 9m

1. Deformation amount of outer shell

It is shown that even if a deformation was generated on the outer shell by the corner drop with the upper cover downward from a height of 9m, the outer shell retained its thickness. An analysis model is shown in Fig. II-A. 43.

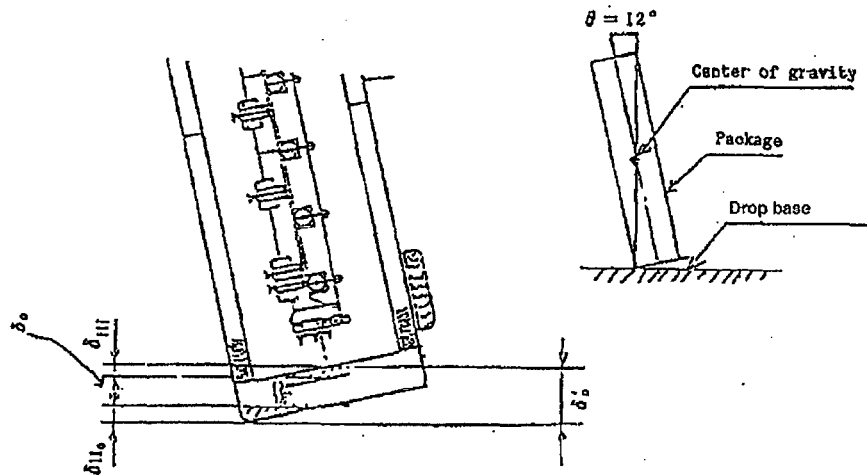


Fig. II-A. 43 Deformation Amount Analysis Model of Outer Shell during 9m Corner Drop
(with the upper cover downward)

Deformation amount and the remaining amount of thickness after the corner drop with the top of container downward from a height of 9m are given by the following equation based on Fig. II-A. 43.

$$\delta_o = \delta_o' - (\delta_{HI} + \delta_{HO})$$

Where,

δ_o' : Thickness before deformation = 304 (mm)

(Deformation amounts after 1.2m drop were taken into consideration (Re: A.5.3 (2) (d).)

δ_{HI} : Deformation amount inside of the outer shell = 97 (mm)

δ_{HO} : Deformation amount outside of the outer shell = 29 (mm)

Therefore, the following value is obtained:

$$\delta_o = 304 - (97 + 29) = 178 \text{ (mm)}$$

Thus, a deformation by the corner drop with the top of container downward from a height of 9m will be taking place only on the outer shell and the cradle assembly will not collide directly with the drop base.

2. Stress generated at cradle assembly and contents

The acceleration was broken down to a vertical component and a horizontal component based on Table II-A. 39 and thus broken down components are shown in Table II-A. 29. The angle was $\theta = 12^\circ$ as shown in Fig. II-A. 43.

Table II-A. 29 Analysis Acceleration during Corner Drop

(Unit $g(m/s^2)$)

Drop orientations	Acceleration in drop direction (N)		Acceleration in vertical direction ($N_V = N\cos\theta$)		Acceleration in horizontal direction ($N_H = N\sin\theta$)	
	Outer shell of packaging	Cradle assembly	Outer shell of packaging	Cradle assembly	Outer shell of packaging	Cradle assembly
Corner drop	216	169	211	165	44.9	35.1

Table II-A. 39 shows that the acceleration components in each direction become larger than the acceleration generated at the time of vertical drop. Therefore, the stress generated at each part was obtained here by each direction, with the evaluation being based on the combined stress.

The stress generated at each part was analyzed by the same method and at the same evaluation items as described in the paragraph of "A.5.3 Free Drop". The results of analysis are shown in Table II-A. 32.

Here, the design safety margin M_s at the evaluation item of each part was in positive value, thus the package tested will not be broken.

(e) Corner drop with the bottom of container downward from a height of 9m

1. Deformation amount of outer shell

It was to show that even if a deformation was generated on the outer shell by the corner drop with the lower container downward from a height of 9m, the outer shell retained its thickness. An analysis model is shown in Fig. II-A. 44.

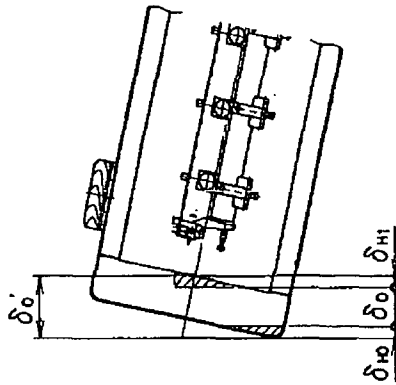


Fig. II-A. 44 Deformation Amount Analysis Model of Outer Shell during 9m Corner Drop
(with the lower container downward)

Deformation amount and the remaining amount of thickness after the corner drop with the lower container downward from a height of 9m are given by the following equation based on Fig. II-A. 44.

$$\delta_o = \delta_o' - (\delta_{Hi} + \delta_{Ho})$$

Where,

δ_o' : Thickness before deformation = 304 (mm)

(Deformation amounts after 1.2m drop were taken into consideration (Re: A.5.3 (2) (d).)

δ_{Hi} : Deformation amount inside of the outer shell = 98 (mm)

δ_{Ho} : Deformation amount outside of the outer shell = 29 (mm)

Therefore, the following value is obtained:

$$\delta_o = 304 - (98 + 29) = 177 \text{ (mm)}$$

Thus, a deformation by the corner drop with the bottom of container downward from a height of 9m will be taking place only on the outer shell and the cradle assembly will not collide directly with the drop base.

2. Stress generated at cradle assembly and contents

The acceleration was broken down to a vertical component and a horizontal component based on Table II-A. 39 and thus broken down components are shown in Table II-A. 30 The angle was $\theta = 12^\circ$ as shown in Fig. II-A. 43.

Table II-A. 30 Analysis Acceleration during Corner Drop

(Unit: $g(m/s^2)$)

Drop orientations	Acceleration in drop direction (N)		Acceleration in vertical direction ($N_v = N \cos \theta$)		Acceleration in horizontal direction ($N_H = N \sin \theta$)	
	Outer shell of packaging	Cradle assembly	Outer shell of packaging	Cradle assembly	Outer shell of packaging	Cradle assembly
Corner drop	216	166	211	162	44.9	34.5

Table II-A. 39 shows that the acceleration components in each direction become larger than the acceleration generated at the time of vertical drop. Therefore, the stress generated at each part was obtained here by each direction, with the evaluation being based on the combined stress. The stress generated was analyzed by the same method and at the same evaluation items as described in the paragraph of "A.5.3 Free Drop". The results of analysis are shown in Table II-A. 32.

Here, the design safety margin M_s at the evaluation item of each part was in positive value, thus the package tested will not be broken.

(f) Slanting drop

When a slanting drop of a package is made from a height of 9m, the center of gravity of the package comes to a position which is away from the plumb line either to left or right, thus a force to rotate the package works with the impact point serving as the fulcrum. Therefore, the impact force generated at the time of impact will be reduced to lower level than that of a corner drop which is a drop on the plumb line which goes through the center of gravity of the package, thus a calculation of strength will be omitted.

(3) Summary of results

(a) Vertical drop with the upper cover downward

In the case of a vertical drop with the upper cover downward, the total deformation of the external cylinder is 168mm. The impact acceleration is $110 \cdot g(m/s^2)$ at the cradle assembly, and the fuel rod cladding tube which constitutes a containment boundary at this time keeps its integrity, thus maintains the containment properties of the fuel rod.

(b) Vertical drop with the lower container downward

In the case of a vertical drop with the lower container downward, the total deformation of the external cylinder is 160mm. The impact acceleration is $111 \cdot g(m/s^2)$ at the cradle assembly, and the fuel rod cladding tube which constitutes a containment boundary at this time keeps its integrity, thus maintains the containment properties of the fuel rod.

(c) Horizontal drop with the direction of 0° in the lower container downward

In the case of a horizontal drop with the direction of 0° in the lower container downward, the total deformation of the external cylinder is 29mm. The impact acceleration is $333 \cdot g$ at the cradle assembly (the maximum impact acceleration is $350 \cdot g$ with the direction of 180°) (m/s^2), and the fuel rod cladding tube which constitutes a containment boundary at this time keeps its integrity, thus maintains the containment properties of the fuel rod.

(d) Corner drop with the upper cover downward

In the case of a corner drop with the upper cover downward, the total deformation of the external cylinder is 197mm. The impact acceleration is $169 \cdot g(m/s^2)$ at the cradle assembly ($165 \cdot g m/s^2$ in vertical direction and $35.1 \cdot g m/s^2$ in horizontal direction), but the fuel rod cladding tube which constitutes a containment boundary at this time keeps its integrity, thus maintains the containment properties of the fuel rod.

(e) Corner drop with the lower container downward

In the case of a corner drop with the lower container downward, the total deformation of the external cylinder is 198mm. The impact acceleration is $166 \cdot g$ (m/s^2) at the cradle assembly ($162 \cdot g$ m/s^2 in vertical direction and $34.5 \cdot g$ m/s^2 in horizontal direction), but the fuel rod cladding tube which constitutes a containment boundary at this time keeps its integrity, thus maintains the containment properties of the fuel rod.

(f) Comparison of analysis results and test results of prototype

The deformation amount in any drop orientation is smaller than that in the analysis results corresponding to the test, based on Table II-A. 40 of the Annex A.10.6. Therefore, results of this analysis are regarded as being at a safe side.

Also, the impact acceleration at any drop orientation is, as in the deformation amount, smaller than the analysis results, thus the analysis results are regarded as being at a safe side.

(g) As has been explained above, the outer shell of container in any drop orientation makes a plastic deformation, but the fuel rod cladding tube, which constitutes a containment boundary, keeps its integrity, thus the containment properties of the fuel rod is secured.

A.9.2.2 Strength Test/Drop Test II (drop from a height of 1m)

(Re: Para. 727 (b))

Drop test II is a test in which the package is dropped from a height of 1m for causing the package the maximum breakage onto a round steel rod with a diameter of 150mm and a length of more than 200mm.

The evaluation of deformation and breakage of package by the drop test II is all made by using results of the test of prototype.

Deformation amount and impact acceleration in the strength test, i.e. drop test II, of the prototype are shown in Table II-A. 31.

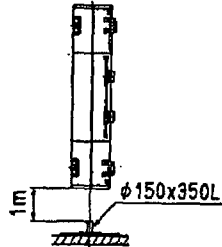
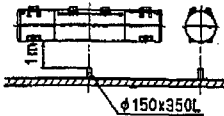
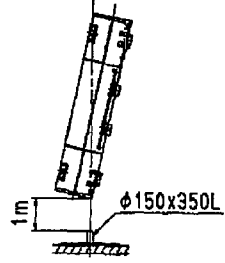
It can be confirmed from Table II-A. 31 that the impact acceleration generated at the outer shell and cradle assembly is smaller than the impact acceleration in the drop test I (drop from a height of 9m) of Table II-A. 39, also the package has been confirmed that it will not be broken even in the drop test I which has greater acceleration generated therein, thus the evaluation of the drop test II will be omitted.

(1) Summary of results and studies thereon

Results of deformation amount, impact acceleration in drop test II of the test of prototype are shown in Table II-A. 31.

Even if a deformation is generated on the external cylinder of packaging under the drop conditions which cause the maximum breakage, the fuel rod cladding tube which constitutes the containment boundary retains its containment properties intact in the evaluation in the drop test I (drop from a height of 9m) with a larger acceleration generate therein. Thus the fuel rod cladding tube which is the containment boundary will keep its containment properties in the drop test II.

Table II-A. 31 Results of Drop Test II of Prototype Test (1)

Drop orientations		Vertical drop (with the lower container downward)	Horizontal drop (with the direction of 0° downward)	Corner drop (with the direction of 0° in the upper cover downward)
Impact acceleration × g (m/s ²)	Outer shell	30	20	36
	Cradle assembly	35	15	20
Deformation amount of container (mm)	Deformation amount	31	104	21
	Width of influence of deformation	900	1,800	-
Presence or absence of puncture		None	None	None
Outline drawing				

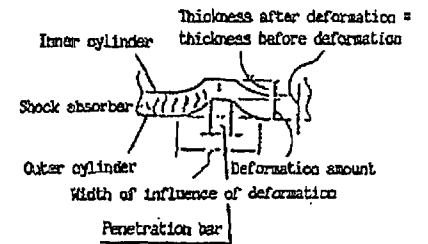
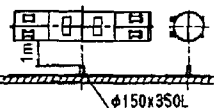
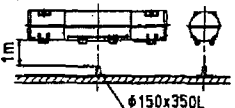
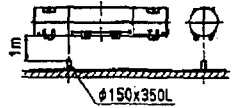
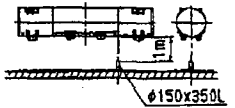
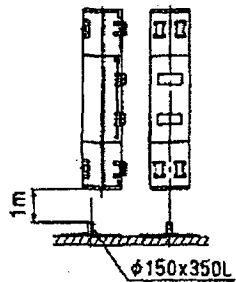


Table II-A.31 Results of Drop Test II of Prototype Test (2)

Drop orientations		Horizontal drop (with the direction of 90° downward)	Horizontal drop (with the direction of 180° downward)	Horizontal drop (with the direction of 180° downward)	Horizontal drop (with the direction of 180° downward)	Vertical drop (with the lower container downward)
Impact acceleration × g (m/s ²)	Outer shell	35	10	15	15	35
	Cradle assembly	30	35	5	15	-
Deformation amount of container (mm)	Deformation amount	62	94	62	63	39
	Width of influence of deformation	1,250	1,800	1,250	1,100	700
Presence or absence of puncture		None	None	None	None	None
Outline drawing				(Welded part of external cylinder) 	(A part of external cylinder with a thickness of 4.5mm) 	(Center part of the semicircular) 

A.9.2.3 Thermal Test

An evaluation of the thermal test is made in Chapter II-B Thermal Analysis.

(1) Summary of temperature and pressure

It was revealed as a result of test under hypothetical accident conditions of transport, II-B.5 that the fuel rod cladding tube which constitutes containment boundary will not have its containment properties impaired even if it is placed in an atmosphere of 440 °C, the severest condition.

(2) Thermal expansion

Thermal stress due to thermal expansion will not be generated as the entire package is heated and there will be no difference in temperature among components and at the same time there will be no constraint.

(3) Comparison with allowable stress

An analysis made based on the design conditions shown in the paragraph A.1.2, the design conditions of this A.1.2 were satisfied in every item involved, and the results thereof were compared with the values of analytical criterion by the analysis items, and are shown in Table II-A. 32, (1) ~ (2). As indicated in these tables, any stress generated in every case was below the values of analytical criterion, thus the integrity of the fuel rod which constitutes the containment boundary is maintained and its containment properties remained intact.

A.9.2.4 Water Immersion Test

Since the fuel assembly, the contents are so designed as withstanding 150 atmospheric pressure even when it is placed under an immersed state under a depth of 0.9m of water (0.009MPa), after the test under hypothetical accident conditions of transport (Drop test I, Drop test II and Thermal test), the fuel rod keeps its strength and its containment properties remained intact.

A.9.2.5 Summary of Results and their Evaluation

Summary of damages received by this package under hypothetical accident conditions of transport will be described by each test item.

(1) Drop test I (Drop from a height of 9m) (Re: Para. 727(a))

The total deformation amount of the external cylinder of container at the time of drop was, based on the paragraph A.9.2.1, 29mm (horizontal drop) ~ 198mm (corner drop), and these deformations do not reach the cradle assembly in any drop orientations. The impact acceleration was $110 \times g$ (m/s^2) ~ $350 \times g$ (m/s^2) at the cradle assembly ($216 \times g$ (m/s^2) ~ $552 \times g$ (m/s^2) at the external cylinder of container), and the stress generated at this time at the fuel rod cladding tube is below the values of analytical criterion, thus the fuel rod kept its integrity and its containment properties remained intact.

(2) Drop test II (Drop from a height of 1m) (Re: Para. 727 (b))

The deformation amount of the external cylinder of container at the time of drop was, based on the paragraph A.9.2.2, 21mm ~ 104mm, and even if a deformation is generated at the external cylinder of container, the stress generated at this time at the fuel rod cladding tube which is the containment boundary was below the value of the criterion, thus the fuel rod kept its strength and its containment properties remained intact.

(3) Thermal test (800 °C, 30 minutes)(Re: Para. 728)

When this package is placed in an atmosphere of 800 °C for 30 minutes, based on the paragraph B.5.6, the temperature of the fuel assembly reaches 440°C. Even at this temperature, the fuel rod, which is the containment boundary, keeps its strength and its containment properties remained intact.

(4) Water immersion (0.009MPa, 8 hours) (Re: Para. 733)

Even when fuel assembly is placed in a state immersed in water of 0.9m depth, based on the paragraph A.9.2.4, the fuel rod cladding tube, which is the containment boundary, keeps its strength, and its containment properties remained intact.

Table II-A. 32 (1) Comparison with Allowable Stress

Subject item	Condition	Items for Analysis	Analysis criteria	Reference value for analysis	Result of analysis	Design margin	
Fissile material package	Hypothetical accident conditions of transport	Drop test I					
		1. Vertical drop with the upper cover downward from a height of 9m					
		(1) Jack screw					
		(a) Buckling load	P_k	$7.94 \times 10^5 (N)$	$2.05 \times 10^5 (N)$	2.87	
		(b) Shear stress of screw thread	$0.6S_u$	$508 (N/mm^2)$	$138 (N/mm^2)$	2.68	
		(2) Fixed frame					
		(a) Bending stress	S_u	$379 (N/mm^2)$	$155 (N/mm^2)$	1.44	
		(b) Shear stress of screw thread	$0.6S_u$	$227 (N/mm^2)$	$107 (N/mm^2)$	1.12	
		2. Vertical drop with the lower container downward from a height of 9m					
		(1) Pivot mount attaching bolt					
		(a) Combined stress (tensile + shearing)	S_u	$379 (N/mm^2)$	$204 (N/mm^2)$	0.85	
		(2) Skeleton assembly					
		(a) Compressive stress	S_u	$719 (N/mm^2)$	$313 (N/mm^2)$	1.29	
		(3) Skin					
		(a) Compressive stress	S_u	$460 (N/mm^2)$	$79.8 (N/mm^2)$	4.76	
(4) Fuel rod cladding tube (Type 14×14 (12ft), Type 15×15 (12ft))							
(a) Combination of compression + internal pressure	$2/3 S_u$	$479 (N/mm^2)$	$186 (N/mm^2)$	1.57			
(b) Buckling load	P_k	$2.19 \times 10^3 (N)$	$545 (N)$	3.01			
3. 9m Horizontal drop							
(1) Clamping frame							
(a) Bending stress	S_u	$379 (N/mm^2)$	$148 (N/mm^2)$	1.56			
(2) Skin							
(a) Bending stress	S_u	$460 (N/mm^2)$	$145 (N/mm^2)$	2.17			
(3) Fuel rod cladding tube (14×14 type, 12ft, 15×15 type, 12ft)							
(a) Combination of bending + internal pressure	S_u	$719 (N/mm^2)$	$694 (N/mm^2)$	0.03			

II-A-118

Table II-A.32 (2) Comparison with Allowable stress

Subject item	Condition	Items for Analysis	Analysis criteria	Reference value for analysis	Result of analysis	Design margin
Fissile material package	Hypothetical accident conditions of transport	4. 9m Corner drop with the upper cover downward				
		(1) Jack screw				
		(a) Buckling load	P_k	$7.94 \times 10^5 (N)$	$3.07 \times 10^5 (N)$	1.58
		(b) Shear stress of screw thread	$0.6S_u$	$508 (N/mm^2)$	$206 (N/mm^2)$	1.46
		(2) Fixed frame				
		(a) Bending stress	S_u	$379 (N/mm^2)$	$232 (N/mm^2)$	0.63
		(b) Shear stress of screw thread	$0.6S_u$	$227 (N/mm^2)$	$161 (N/mm^2)$	0.40
		5. 9m Corner drop with the lower container downward				
		(1) Pivot mount attaching bolt				
		(a) Combined stress (tensile + shearing)	S_u	$379 (N/mm^2)$	$297 (N/mm^2)$	0.27
		(2) Clamping frame				
		(a) Bending stress	S_u	$379 (N/mm^2)$	$60.0 (N/mm^2)$	5.31
		(3) Skin				
		(a) Combination of compression + bending	S_u	$460 (N/mm^2)$	$131 (N/mm^2)$	2.51
(4) Skeleton						
(a) Combination of compression + bending	S_u	$719 (N/mm^2)$	$505 (N/mm^2)$	0.42		
(3) Fuel rod cladding tube						
(a) Combination of internal pressure + bending + compression	S_u	$719 (N/mm^2)$	$332 (N/mm^2)$	1.16		
	Drop test II					
	1. Puncture test		Presence of puncture	No puncture	No puncture (from test result of prototype)	Criterion is satisfied.
	Water Immersion		Depth of water:			
	2. External pressure		0.9m	15.0 (MPa · G)	0.009 (MPa)	1665

II-A-119

A.10 Annex

A.10.1 Reference

- [1] Technical standards on structures, etc. related to nuclear facilities for power generation (Notification No. 501, 1980)
- [2] Evaluating Strength and Ductility of Irradiated Zircaloy (Task⁶¹) (BMI-NUREG-1948)
- [3] MATPRO VERSION 09.
- [4] Internal data, Mitsubishi Heavy Industries, Ltd.
- [5] Internal data, Mitsubishi Heavy Industries, Ltd.
- [6] "Local Stress in Spherical and Cylindrical Shells due to External Loading" K.R.Wichman, A.G. Hopper and J.L. Mershon.
- [7] JSME Mechanical Engineer's Handbook 6th revision, the Japan Society of Mechanical Engineers, P7 – 35
- [8] JSME Mechanical Engineer's Handbook 6th revision, the Japan Society of Mechanical Engineers, P4 – 78
- [9] National Astronomical Observatory "RIKA NENNPYO (Science Reference Book)", Maruzen Co., Ltd. (1980)
- [10] JSME Mechanical Engineer's Handbook 6th revision, the Japan Society of Mechanical Engineers, P5 – 22
- [11] Internal data, Mitsubishi Nuclear Fuel Company, Ltd.
- [12] JSME Mechanical Engineer's Handbook 6th revision, the Japan Society of Mechanical Engineers, P4 – 83
- [13] JSME Mechanical Engineer's Handbook 6th revision, the Japan Society of Mechanical Engineers, P7 – 36
- [14] Garbrielson.V.K., Reese, R.T. "Shock Code User's Manual: A Computer Code to Solve the Dynamic Response of Lamped-Mass Systems "Sandia Laboratories Report SCL-DR-69-98,1969.
- [15] Investigation & Research Report on Safe Transport Criteria of Radioactive Material in the 28th Basic Research Meeting, Shipbuilding Yard Research Institute
- [16] KAGAKU KOUGAKU BINRAN (Chemical Engineer's Handbook) 3th revision, The Society of Chemical Engineers, Japan P1338
- [17] JIS B8243 (Construction of Pressure Vessels) Japanese Standards Association (1975)
- [18] Internal data, Mitsubishi Heavy Industries, Ltd.
- [19] Internal data, Mitsubishi Heavy Industries, Ltd.

A.10.2 Dimensionless Curve to Cylindrical Shell ^[6]

Dimensionless curves to the cylindrical shell obtained in A.4.4.1 (3) are shown in Fig. II-A. 45 to Fig. II-A. 56.

Proprietary Information on Pages II-A-122 through II-A-133
Withheld Pursuant to 10 CFR 2.390

A.10.3 Searing Section Modulus of Tightening Bolts

An analysis model is shown in Fig. II-A. 57.

The tightening bolt is of a hollow cylindrical shape, and as parts shown with hatched line in Fig. II-A. 57 are bored.

- (1) The section polar modulus of hollow circle (Z_p) is obtained by the following equation:

$$Z_p = I_z / r_o \text{ (mm}^3\text{)}$$

I_z : Secondary polar moment of section

$$I_z = I_{z0} - I_s$$

I_{z0} : Secondary polar moment of hollow circular section

$$\begin{aligned} I_{z0} &= 1/4 A_o \times (r_o^2 + r_i^2) \\ &= \pi / 4 \times (r_o^4 - r_i^4) \\ &= \pi / 4 \times (10.25^4 - 4.4^4) = 8.37 \times 10^3 \text{ (mm}^4\text{)} \end{aligned}$$

I_s : Secondary polar moment of hatched part of section

$$\begin{aligned} I_s &= \{(\ell + 2t)^2 + h^2\} / 12 \times A_1 - (\ell^2 + h^2) / 12 \times A^2 \\ &= \{(\ell + 2t)^2 + h^2\} / 12 \times \{h \times (\ell + 2t)\} - (\ell^2 + h^2) / 12 \times \ell \times h \\ &= \{(6.14 + 2 \times 5.85)^2 + 6.3^2\} \times \{6.3 \times (6.14 + 2 \times 5.85)\} / 12 \\ &\quad - (6.14^2 + 6.3^2) \times 6.14 \times 6.3 / 12 \\ &= 3.10 \times 10^3 \text{ (mm}^4\text{)} \end{aligned}$$

r_o : Outer radius of the tightening bolt : 10.25 (mm)

r_i : Hollow inner radius of the tightening bolt : 4.4 (mm)

h : Length of chord at outside of cutout : 6.3 (mm)

ℓ : Distance between chords at inside of cutout

$$\ell = 2 \sqrt{\{r_i^2 - (h/2)^2\}} = 6.14 \text{ (mm)}$$

t : Head thickness of the tightening bolt

$$t = r_o - r_i$$

Therefore,

$$\begin{aligned} I_z &= 8.37 \times 10^3 - 3.10 \times 10^3 = 5.27 \times 10^3 \text{ (mm}^4\text{)} \\ Z_p &= 5.27 \times 10^3 / 10.25 = 514.1 \text{ (mm}^3\text{)} \end{aligned}$$

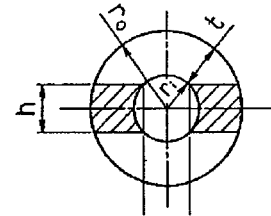


Fig. II-A. 57 Tightening Bolt Analysis Model

A.10.4 Impact Response Analysis Code by Non-Linear Spring –Mass System Model
"SHOCK" ^[14]

(1) Outline

"SHOCK", which is a calculation code used for evaluating the strength when a package makes a free drop, is a program to convert a structure to various linear, non-linear spring, mass system model, and to calculate the generating speed, speed, displacement of each mass point when an impact load works on the structure, as well as the time history of the force bearing on each mass point, *relative displacement, etc. by a time integration method based on Runge-Kutta-Gill method*, and has been developed in 1969 by SANDIA LABORATORY.

(2) Function

"SHOCK" can handle not only initial value matters in which initial speed and initial displacement are given on a dynamic response of a structure on which any impact load may work, but also the matters on which dynamic external force works.

It can also handle two kinds of problems, i.e. a case when the placement and displacement of springs are parallel and a case when they are vertical.

Also, the types of springs used in SHOCK code are as follows:

- (a) Linear spring: What is expressed by an ordinary $F \text{ (load)} = kx$ (displacement)
- (b) Compression · tensile spring: Axle spring which works only for compression or tension, and can handle play or backlash.
- (c) Non-linear spring: Load displacement relationship may be expressed by multiple curves approximation.
- (d) Non-linear-irreversible spring: Curves for loading and those unloading in multiple curves approximation are different from each other.

"SHOCK" can handle not only structures made of metal material which exhibits elastic-plastic deformation, but also structures consisting of material which exhibits anisotropy such as soil type, concrete, timber, etc. Also, when a structure is replaced by a spring and mass point system, up to 100 pieces of mass points and up to 200 pieces of springs may be used.

(3) Example of analysis of 9m drop of packaging by "SHOCK" code ^[15]

As an example of an evaluation with "SHOCK" code, a case of analysis with "SHOCK" code of a 9m vertical drop of 1/3 scale model of a typical packaging for used fuel rod (TN-12A) will be shown here.

First, a form to be computed and analysis model are shown in Fig. II-A. 58. Table II-A. 33, shows their analyzed results and experimentation values. It may be said from these that:

- (a) As to a deformation amount, the analyzed values by "SHOCK" code are larger than experimentation values, thus an evaluation at safe side is made.
- (b) Concerning the acceleration also, like in the deformation amount, the analyzed values by "SHOCK" code are larger than experimentation values, thus an evaluation at safe side is made.

It can be said from these results that the free drop analysis with "SHOCK" code can make an evaluation with sufficient safety margin.

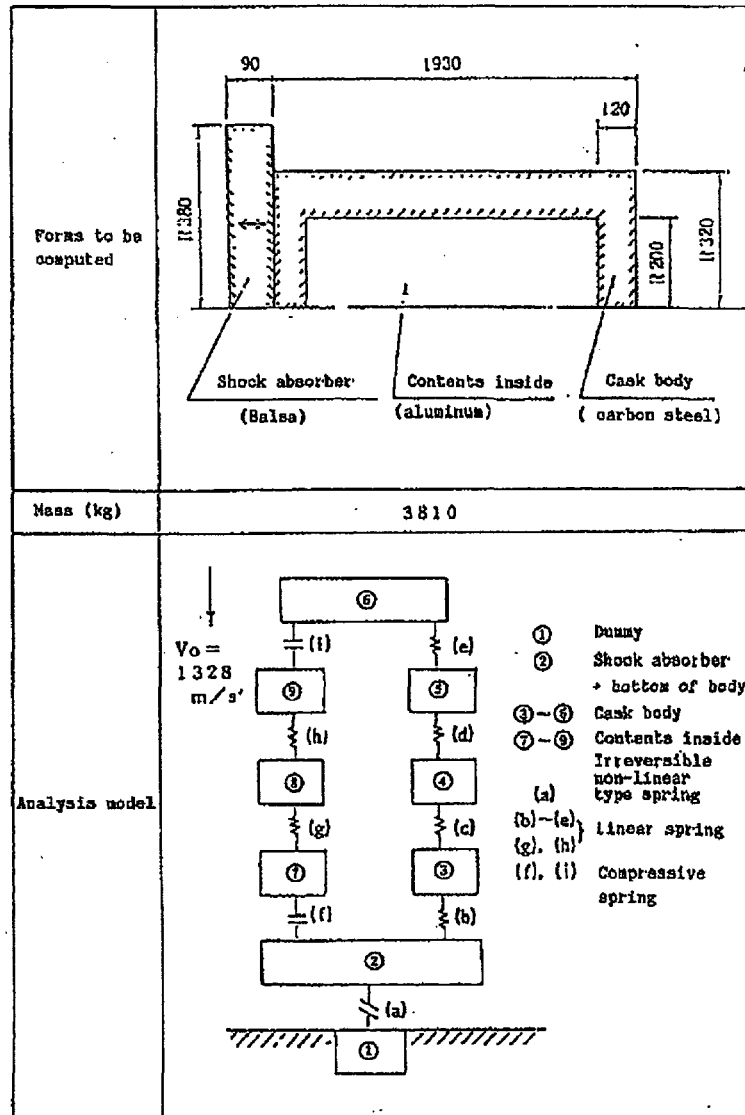


Fig. II-A. 58 Analysis Evaluation Model for "SHOCK" Code

Table II-A. 33 Comparison between Experiment Value and Analytical Value

Acceleration (x g)			Deformation amount (mm)		
Analyzed value	Experimental value	Comparison	Analyzed value	Experimental value	Comparison
350	260	1.34	32	13 ~ 27	2.46 ~ 1.18

Proprietary Information on Pages II-A-138 through II-A-146
Withheld Pursuant to 10 CFR 2.390

Table II-A. 39 Drop Analysis Result
 (Evaluation as Type A Package)
 (Evaluation as Fissile Material Package)

Subject item	Drop orientations		Vertical drop with the lower container downward	Vertical drop with the upper cover downward	Horizontal drop with the direction of 0° in the lower container downward	Horizontal drop with the direction of 90° in the lower container downward	1 drop with the direction of 180° in the lower container downward	Corner drop with the upper cover downward	Corner drop with the lower container downward	
										Evaluation item
Type A package (Individual evaluation)	Drop from a height of 1.2m	Acceleration (xg)	Outer shell	298	298	199	193	199	55	55
			Cradle assembly	17	17	72	55	24	20	20
		Deformation amount (mm)	Outside of outer shell	9.5	9.5	9.5	9.5	9.5	71	71
			Cradle assembly (Note 1, 2)	0	0	23	1.2	0	0	0
Fissile material package (Evaluation with cumulative effects)	Drop from a height of 1.2m	Acceleration (xg)	Outer shell	298	298	199	193	199	55	55
			Cradle assembly	17	17	72	55	24	20	20
		Deformation amount (mm)	Outside of outer shell	9.5	9.5	9.5	9.5	9.5	71	71
			Cradle assembly (Note 1, 2)	0	0	23	1.2	0	0	0
	Drop from a height of 9m (Note 3)	Acceleration (xg)	Outer shell	381	381	552	539	552	216	216
			Cradle assembly	111	110	333	343	350	169	166
		Deformation amount (mm)	Outside of outer shell	58.5 (68)	56.5 (66)	19.5 (29)	19.5 (29)	19.5 (29)	29 (100)	29 (100)
			Cradle assembly (Note 1)	92	102	40.5 (50)	31.5 (41)	32	97	98

Note 1 The deformation amount of the cradle assembly shows the deformation amount of the outer shell when the cradle assembly moves and collides with the inner plane of the outer shell.

Note 2 The deformation amount of 0mm as shown for the cradle assembly means that the cradle assembly and the outer shell do not collide with each other.

Note 3 (1) The drop from a height of 9m is evaluated in consideration of the deformation of the drop from the height of 1.2m.

(2) The deformation amount in () indicates the aggregate deformation amount considering from the condition where its integrity is maintained.

A.10.6 Adequacy of Analysis of Free Drop of Model MFC-1 Package by "SHOCK" Code

An adequacy of evaluation of the analysis of the free drop from a height of 9m using "SHOCK" code shown in A.10.4 will be explained by comparison with the results of the drop test with the prototype container.

The comparison of the analysis of the drop from the height of 9m by "SHOCK" code and the test results with the prototype container is shown in Table II-A. 40.

The calculated values in both of the acceleration and deformation amount show higher values than the experimentation values, indicating the results with safety margin.

Table II-A. 40 Comparison between Analysis Value and Experiment Value for 9m Drop

Evaluation items			Drop orientations				
			Vertical drop with the lower container downward	Horizontal drop with the direction of 0° in the lower container downward	Horizontal drop with the direction of 90° in the lower container downward	Horizontal drop with the direction of 180° in the lower container downward	Corner drop with the upper cover downward
Acceleration (xg)	Outer shell	Calculation results	357	500	475	500	174
		Test results	340	230	230	220	174
		Comparison (calculation/test)	1.05	2.17	2.07	2.27	1.00
	Cradle assembly	Calculation results	112	332	345	342	152
		Test results	110	320	340	160	123
		Comparison (calculation/test)	1.02	1.04	1.01	2.14	1.24
Deformation amount (mm)	Outer shell	Calculation results	64	35	35	35	170
		Test results	32	27	-	-	142
		Comparison (calculation/test)	2.00	1.30	-	-	1.20
	Cradle assembly	Calculation results	95	59	40	33	98
		Test results	95	25	-	-	65
		Comparison (calculation/test)	1.00	2.36	-	-	1.51

Proprietary Information Withheld Pursuant to 10 CFR 2.390

Proprietary Information Withheld Pursuant to 10 CFR 2.390

A.10.8 Presence of Interference by Deformation Amount to Packaging

This paragraph deals with the deformation generated in the outer shell by horizontal drop from a height of 1.2m and 9m. The relationship between deformation inside and outside of the outer shell is shown in Fig. II-A. 72.

Presence or absence of interference by the deformation amount can be obtained by the following equation based on Fig. II-A. 72.

$$\ell = \ell_3 - \ell_4$$

Results of analysis are shown in Table II-A. 42.

ℓ : Interfering dimension of the deformed part

ℓ_3 : Width of inside deformation

$$\ell_3 = 2 \times \sqrt{r_i^2 - (\Delta H + \delta_{Hi})^2}$$

ΔH : Distance between inner wall
of the cradle assembly and the center

r_i : Inner diameter of outer shell

δ_{Hi} : Deformation amount inside of the outer shell

ℓ_4 : Width of deformation outside

$$\ell_4 = 2 \times \sqrt{r_o^2 - (r_o + \delta_{Ho})^2}$$

r_o : Outer diameter of the outer shell

δ_{Ho} : Deformation amount outside of the outer shell

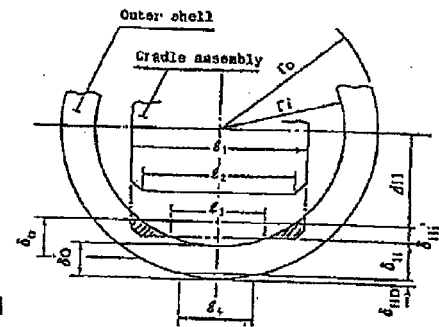


Fig. II-A. 72 Analysis Model of Deformation Amount in Outer Shell

Table II-A. 42 shows that there will be no interference by the deformation inside or outside of the packaging at the time of horizontal drop from a height of 1.2m. The interfering width (ℓ) of the deformation inside and outside at the time of horizontal drop from a height of 9m is about 20mm at one side. Also, amount of remaining thickness (δ_{Hi} =128mm) at the interfered part after the deformation of outer shell is thicker than the thickness before deformation (δ_o = 125mm), therefore it is deemed that there is no interference taking place.

Next, concerning an evaluation of the part of the outer shell where a thickness is left (amount of thickness left by deformation inside (ΔH_i) and amount of thickness left by deformation outside (ΔH_o)), the amount of thickness left by the deformation on the outside is smaller in each case. Therefore, the amount of thickness left is considered as being represented by the amount of thickness left by the amount of deformation outside of the outer shell (ΔH_o).

Table II-A. 42 Analysis Result of Deformation Width during Horizontal Drop

Analysis items	Height of drop	Horizontal drop from a height of 1.2m	Horizontal drop from a height of 9m
Outer diameter of outer shell	r_o (mm)	575	575
Inner diameter of outer shell	r_i (mm)	450	450
The maximum width of cradle assembly	l_1 (mm)	628	628
Width of initial impact part of cradle assembly	l_2 (mm)	558	558
Center of container and height of impact part	ΔH (mm)	353	353
Deformation amount on the inside	δ_{Hi} (mm)	23	50
Deformation amount on the outside	δ_{Ho} (mm)	9.5	29
Width of deformed part on the inside	l_3 (mm)	494.2	400.2
Width of deformed part on the outside	l_4 (mm)	208.2	360.6
Amount of interference by deformation width ($l_3 - l_4$)	l (mm)	286.1	39.6
Amount of thickness left by deformation on the inside ($\delta_{oi} - \delta_{Hi}$)	ΔH_i (mm)	126.7	99.7
Amount of thickness left by deformation on the outside ($\delta_{oo} - \delta_{Ho}$)	ΔH_o (mm)	115.5	96.0

II-B THERMAL ANALYSIS

Proprietary Information Withheld Pursuant to 10 CFR 2.390

B.1.2 Thermal Analysis

The thermal analyses were performed for the package under normal conditions of transport and under hypothetical accident conditions of transport.

- (1) The thermal properties under normal conditions of transport are as follows (Re: Para. 545 and 546 of IAEA Regulations for Safe Transport of Radioactive Material, 2005 Edition TS-R-1, hereinafter referred to as "2005 IAEA Regulations" or referred to only its paragraph as "Para*"):
 - (a) The package shall be subject to ambient temperature of 38 °C.
 - (b) The package receives the solar insolation.
- (2) The thermal conditions under hypothetical accident conditions of transport are as follows (Re: Para. 628):
 - (a) The package is exposed to the environment of 800°C for a period of 30 minutes with the atmosphere radiation factor of 0.9. In this case, the radiation factor on the package surface is 0.8.
 - (b) After exposed to the conditions of (a),
 - (i) The package is left for one week in the atmosphere of 38°C.
 - (ii) The package receives the solar insolation.

II-B-3

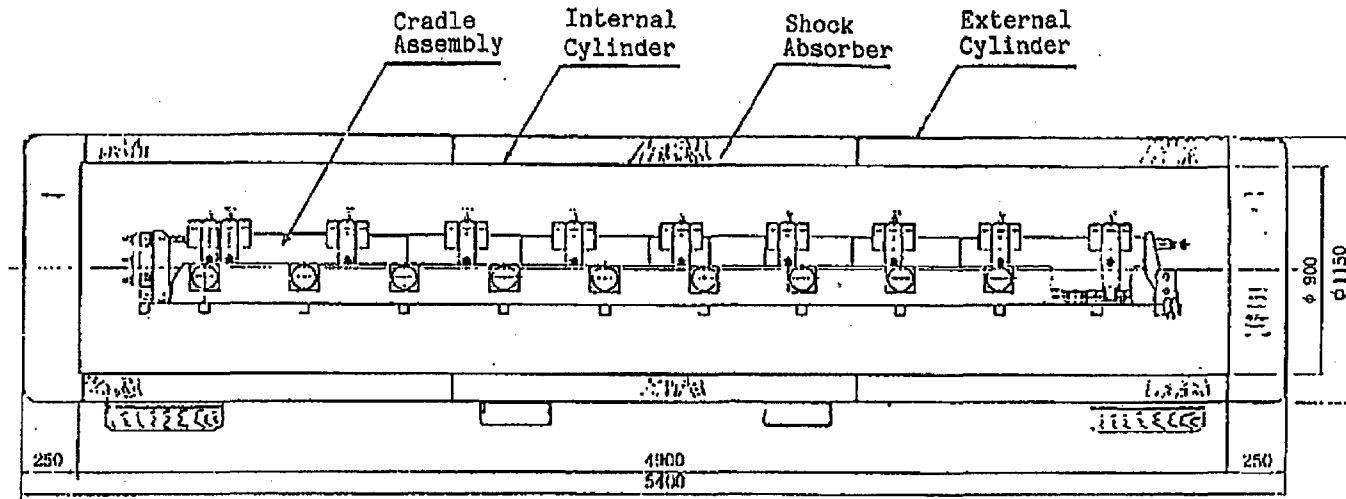


Fig. II-B. 1 Package Component Drawing

Proprietary Information on Pages II-B-4 through II-B-10 Withheld
Pursuant to 10 CFR 2.390

B.4.6 Summary of Results and Evaluation

- (1) The sealing performance of the packaging can be maintained because of the following reasons:
 - Under normal conditions of transport, the maximum temperature of the package is 73°C, and its minimum temperature is -20°C.
 - The internal pressure rise of the packaging at the maximum temperature is 0.019 MPa.
 - Since the temperature of the packaging in use is within the usable temperature range of O-rings between -50°C and 150°C.
- (2) The leak-tightness of the content can be maintained under normal conditions of transport because of the following reasons:
 - The integrity of the fuel rod that is content can be maintained, as the internal pressure becomes 3.73 MPa.
 - No thermal stress can be produced since there is nothing to restrict the thermal expansion.
 - At the minimum temperature (-20°C), the fuel cladding (Zircaloy-4, MDA and ZIRLO), which forms the containment boundary, will not break due to cold brittleness.

B.5 Hypothetical Accident Conditions of Transport

This package has to be evaluated in accordance with the requirements of the fissile material package.

B.5.1 Thermal Analysis Code

The thermal evaluation under hypothetical accident conditions of transport is carried out using Three-Dimensional Non-Steady Thermal Analysis Code TRUMP.

B.5.1.1 Analysis Model

The following items used for the calculations by TRUMP are described below:

(1) Model geometry

Local deformations on this packaging could be caused during drop test I and drop test II under hypothetical accident conditions of transport, as shown in the conditions of the fissile material package of A.9.2 in II-A Structural Analysis.

Deformation could be caused at the whole length of the external cylinder and the internal cylinder by drop test I, and local deformations could be caused by drop test II.

Deformation due to drop shall be considered for the thermal analysis model in accordance with the requirements for the fissile material package. Therefore, the thermal analysis model is established on the conservative side taking into account the internal and external deformation over the whole length as shown in Fig. II-B. 2.

In this case, the balsa wood still has thickness of approx. 26mm.

The deformation due to drop test II can be neglected in the thermal analysis, since there were no significance differences of the reached temperature on the internal surface of the outer shell during the fire test between the part which is subject to the impact due to the drop test II (cross section A-A) and the part which is subject to no impact due to the drop test II (cross section B-B) based on the result of the proto type packaging test shown in Annex B.6.8.

Proprietary Information on Pages II-B-13 through II-B-16
Withheld Pursuant to 10 CFR 2.390

B.5.1.2 Test Model

Not applied.

B.5.2 Evaluation Conditions of Package

The analysis was performed taking into consideration the deformation of the package produced due to the mechanical test under hypothetical accident conditions of transport as shown in Fig. II-B. 3 and further under the following conditions

- (1) It is assumed that there is no shock mount or cross frame. It is difficult to transfer heat from the internal cylinder to the contents because of bad thermal conduction of the shock mounts. Furthermore the heat capacities of the shock mounts, the cross frame, etc. rods are not taken in to consideration, thus the temperature of the fuel rods are to be evaluated at higher temperature on the conservative side.
- (2) The initial temperature of the thermal test is to be 73°C for the whole region of the package, based on the calculation results of temperature (equilibrium temperature subjected to solar insolation) under normal conditions of transport.
- (3) Although the thermal conductivity and the specific heat of balsa wood depend upon the temperature, only the specific heat during cooling is assumed to be maintained as the specific heat at the temperature at the termination of fire. The temperature of the fuel rods is to be evaluated as higher temperature on the conservative side, taking into consideration the reduction of heat capacity due to the carbonization.

B.5.3 Temperatures of Package

Fig. II-B.4 shows the calculation result based on the analysis model described in B.5.1.1. This is the temperature histories of the package under the thermal test conditions.

As understood from Fig. II-B.4 of the temperature distribution, the temperature of the fuel reaches the maximum temperature in two minutes after cooling, which is 440°C

B.5.4 Maximum Internal Pressures

By exposure of the package for a period of 30 minutes to the temperature of 800°C followed by leaving to the environment under the conditions of an ambient temperature of 38°C, the maximum temperature of the fuel rods becomes 440°C. At that time, the internal pressure rises, due to the reduction of the void volume by thermal expansion of the claddings and the UO₂ pellets and due to the temperature rise of the gas in the fuel rods.

The relationship between temperature and internal pressure is given by the following equation according to the Boyle-Charle's law:

$$PV/T = P_0V_0/T_0 \dots\dots\dots(B.5-1)$$

Where,

P: Internal pressure of cladding at maximum temperature of fuel rod (MPa)

V: Void volume at maximum temperature of fuel rod (cm³)

T: Temperature (K)

P₀: Initial pressure (MPa)

V₀: Initial void volume (cm³)

T₀: Initial temperature (K)

The void volume can be calculated by the following equation:

$$\begin{aligned} V - V_0 &= (V_T - V_F) - (V_{T0} - V_{F0}) \\ &= (V_T - V_{T0}) - (V_F - V_{F0}) \\ &= 3 \alpha_T \Delta T V_{T0} - 3 \alpha_F \Delta T V_{F0} \dots\dots\dots(B.5-2) \end{aligned}$$

V_T: Volume of cladding (cm³)

V_F: Volume of UO₂ pellet (cm³)

V_{T0}: Volume of cladding at initial temperature (cm³)

V_{F0}: Volume of UO₂ pellet at initial temperature (cm³)

α_T: Coefficient of thermal expansion of cladding (1/°C)

α_F: Coefficient of thermal expansion of UO₂ pellet (1/°C)

ΔT: Temperature difference (°C)

The maximum internal pressure obtained by the above equation of (B.5-2) becomes 7.79 MPa·G. The circumferential stress of cladding (σ) can be calculated by the following equation:

$$\sigma = P \times d/2t$$

P: Internal pressure (MPa·G)

d: Inner diameter of cladding (mm)

t: Thickness of cladding (mm)

The maximum stress for each type of fuel assemblies is 57.2 (N/mm²) as shown in Annex B. 6.9. This is sufficiently lower value, in comparison with 282 N/mm², which is the design criterion of the fuel cladding tube (Zircaloy-4, MDA and ZIRLO) at 440°C.

B.5.5 Maximum Thermal Stresses

Thermal stresses cannot be produced, since there is nothing to restrict thermal expansion under the hypothetical accident conditions.

B.5.6 Summary of Results and Evaluation

The performance of the package under hypothetical accident conditions of transport was evaluated assuming that the package was exposed to the fire of 800°C for a period of 30 minutes under the conditions of an ambient temperature of 38°C with calorific value of 0W. The temperature change of each part of the package is shown in Fig. II-B.4.

(1) Analysis result

The following describes the temperature of each part of the package and the internal pressure generated within the void space in the package and in the fuel rods under the conditions shown in B.1.2.

(a) Temperature

Table II-B.11 shows the temperature of each part of the package under normal and accident conditions of transport. Fig. II-B.4 shows the temperature histories of each part of the package under hypothetical accident conditions of transport.

Under normal conditions of transport, the surface temperature of the package is 73°C. Temperature of O-rings remains within the service temperature range (between -50 and 150°C). Since the fuel rod temperature is 73°C, no special heat removal system is required.

Under hypothetical accident conditions of transport, the temperature of the fuel rods is 440°C, which is lower than their allowable temperature (approx. 860°C).

Table II-B.11 Maximum Temperature of Each Part of Package
under Normal and Accident Conditions of Transport

Position \ Item	Normal Conditions of Transport	Hypothetical Accident Conditions of Transport	
		Temperature	Period
Fuel rod surface	73°C	440°C	0.53 h
Internal cylinder surface	73°C	656°C	0.53 h
External cylinder surface	73°C	793°C	0.5 h

(b) Pressure

Table II-B.12 shows the maximum pressure in the fuel rods and in the void space in the packaging under normal and accident conditions of transport.

Table II-B.12 Maximum Pressure in Fuel Rods and in Packaging
under Normal and Accident Conditions of Transport

(Unit: MPa·G)

Position \ Item	Pressure under Normal Conditions of Transport	Pressure under Hypothetical Accident Conditions of Transport
Fuel rod	3.73	7.79
Space in packaging	0.019	-

Table II-B.11 shows the maximum temperature of each part shown in Fig. II-B.4 and the period between occurrence of the fire and achieving of the maximum temperature. Then, the maximum pressure of the fuel rods that are the containment boundary is as shown in Table II-B.12.

Table II-B.13 shows integrity evaluation of the package under hypothetical accident conditions of transport.

These results show that the fuel rods that form containment boundary of this package maintain its integrity even under hypothetical accident conditions of transport.

Table II-B.13 Integrity of Package under Hypothetical Accident Conditions of Transport

Item	Criteria	Result	Remarks
Maximum temperature			
Fuel rod	860°C	440°C	Acceptable
Internal cylinder	-	656°C	
External cylinder	-	793°C	
Maximum stress			
Cladding of fuel rod (Zircaloy-4, MDA and ZIRLO)	282 N/mm ²	57.2 N/mm ²	Acceptable

Proprietary Information Withheld Pursuant to 10 CFR 2.390

11-B-22

B.6 Annex

B.6.1 Reference

- [1] Safety Standards on Transport of Radioactive Materials etc., Atomic Energy Commission of Japan (January 21, 1975)
- [2] Edwards A.L., Trump; A COMPUTER PROGRAM FOR TRANSIENT AND STEADY STATE TEMPERATURE DISTRIBUTIONS IN MULTIDIMENSIONAL SYSTEMS, Lawrence Radiation Laboratory, University of California Livermore (May 1, 1968)
- [3] Goldsmith A et al.; "Handbook of Thermo Physical Properties of Solid Materials" "Revised Edition, Vol.II, The MacMillan Company, New York (1961)
- [4] Heat Transfer Engineering Data, Revised Edition No.3, Japan Society of Mechanical Engineers (1975)
- [5] R.O.Wooton & H.M.Epstein : "Heat Transfer from a Parallel Rod Fuel Element in a Shipping container" Battelle Memorial Institute (1963)
- [6] Hasegawa et al, "Nuclear Reactor Material Handbook", Daily Industry Newspaper (1977)
- [7] Research Subcommittee for Cask Heat Transfer Characteristics Evaluation Code "Design and Evaluation of Spent Fuel Transport Packaging of Fast Breeder Reactor", Japan Society of Mechanical Engineers (December, 1977)
- [8] "THERMAL CONDUCTIVITY" IFI/PLENUM NEW YORK-WASHINGTON (1970)
- [9] "Chemical Engineering Handbook", Revised Edition No.4
- [10] Heat Exchanger Design Handbook, Engineering Book Co., Ltd. (1974)
- [11] Property Values and Calculation Book necessary for Fuel Design, JAERI-M4881
- [12] In-house Data of Mitsubishi Heavy Industries, Co., Ltd.

Proprietary Information Withheld Pursuant to 10 CFR 2.390

Proprietary Information Withheld Pursuant to 10 CFR 2.390

B.6.3 Outline of Heat Transfer General-Purpose Program "TRUMP"

(1) Outline

TRUMP is a heat transfer calculation program based upon the node method, which was developed by Lawrence Radiation Laboratory in 1968.

(2) Function

TRUMP can calculate heat transfer involving heat generation, chemical reaction, phase change and mass transfer. Also, TRUMP can analyze a body of three-dimensional shape by dividing the body into meshes using rectangular coordinates, circular cylindrical coordinates, revolution body coordinates or spherical coordinates.

Thermal conductivity and specific heat can be expressed as a function of temperature or time.

In the program, the heat transfer due to conduction, natural convection, forced convection and radiation are considered for heat transfer between the meshes, while natural convection, forced convection and radiation are considered for the boundary conditions. The boundary temperature can be expressed as a function of time. The initial temperature can depend on the locations in the void space. As an output of TRUMP, heat balance as well as the hourly temperature distribution can be obtained.

(3) Calculation method [refer to [Fig. II-B. 5](#)]

TRUMP can solve simultaneous partial differential equations including 4 independent variables for space coordinates and time, and 3 dependent variables in total, that is, temperature and 2 reactant concentrations.

Equations of heat generation, heat transfer involving chemical reaction and mass transfer can be expressed by a vector arithmetic expression in the case of three dimensions as follows:

$$\begin{aligned} DT/Dt &= \partial T / \partial t + v \cdot \Delta T \\ &= 1/\rho C \cdot \Delta \cdot k \Delta T + G - Qa/C \cdot \partial a / \partial t - Qb/C \cdot \partial b / \partial t \end{aligned}$$

$$\begin{aligned} Da/Dt &= \partial a / \partial t + v \cdot \Delta a \\ &= -a \cdot \exp(Za - Ea/R \cdot T) \end{aligned}$$

$$k_1 \cdot (\partial T_1 / \partial r)_i = h_{i2} \cdot (T_{2i} - T_{1i}) = k_2 \cdot (\partial T_2 / \partial r)_i$$

$$h_i = h_{i0} + h_{ic} \cdot [(T_{2i} - T_{1i})^2]^{p/2} + \sigma \cdot F_i \cdot (T_{1i} + T_{2i}) \cdot (T_{1i}^2 - T_{2i}^2)$$

Conductance on the boundary surface h_i is obtained from the equation considering contact conductance, natural convection, enforced convection and radiation. σ is Stefan-Boltzmann constant, and F is a total radiation factor.

$$k \cdot (\partial T / \partial t)_s = U_{sb} \cdot (T_b - T_s)$$

Where, U_b = External temperature

U_{sb} = Surface conductance

U_{sb} can be expressed in the same manner as the case of a material phase as follows:

$$U_{sb} = h_{so} + h_{sc} \cdot [(T_b - T_s)^2]^{ps/2} + \sigma \cdot F_b \cdot (T_s + T_b) \cdot (T_s^2 + T_b^2)$$

TRUMP actually solves the equations for small time intervals. The above-mentioned equation can be solved by substituting time differential $\partial u / \partial t$ for $(u' - u) / \Delta t$. Here, u' and u show values at start and end of time interval Δt , respectively.

(4) TRUMP Achievement

TRUMP developed by Lawrence Radiation Laboratory is now used by a number of laboratories in the United States.

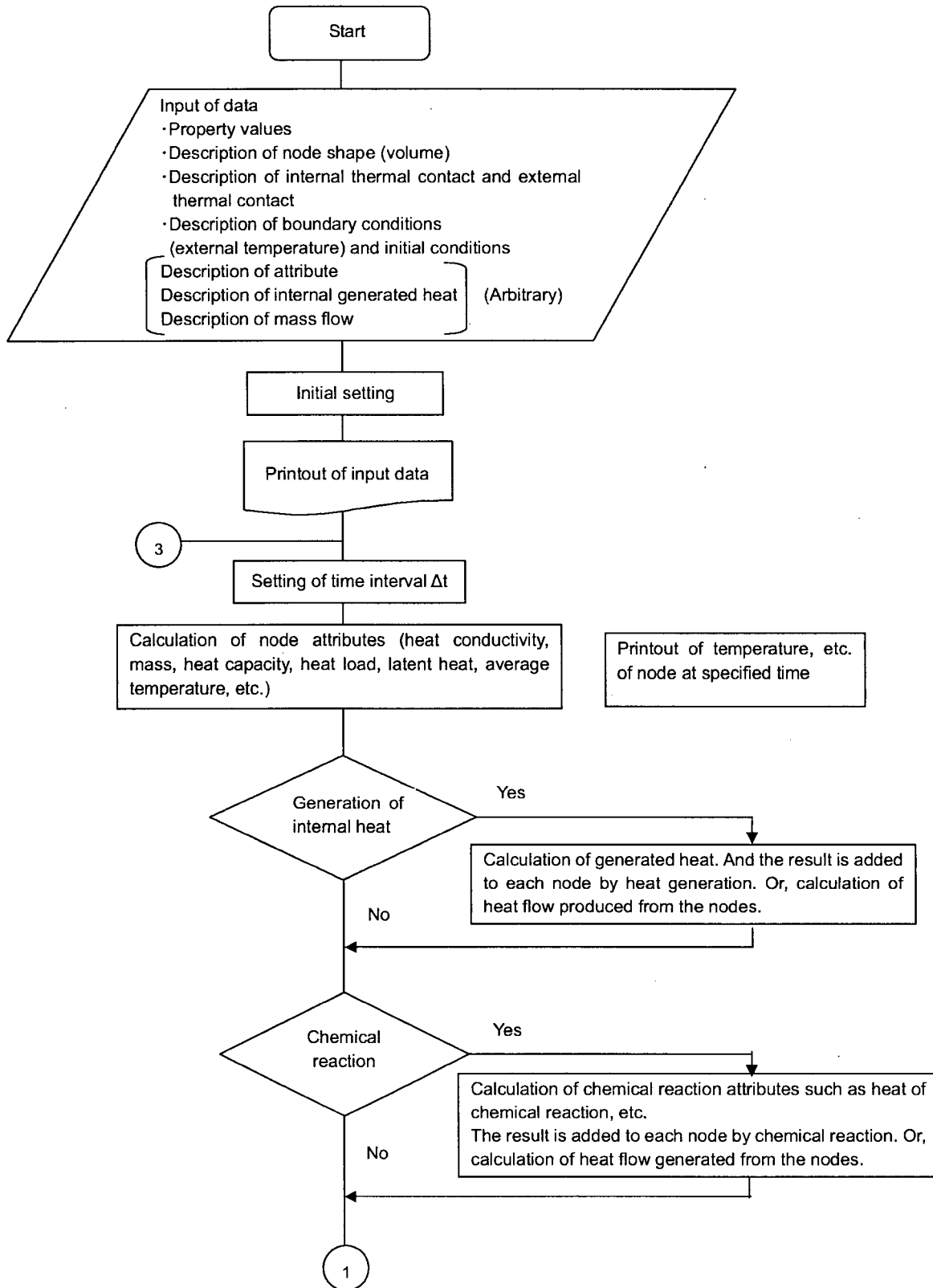


Fig. II-B. 5 TRUMP Flow Chart (1/3)

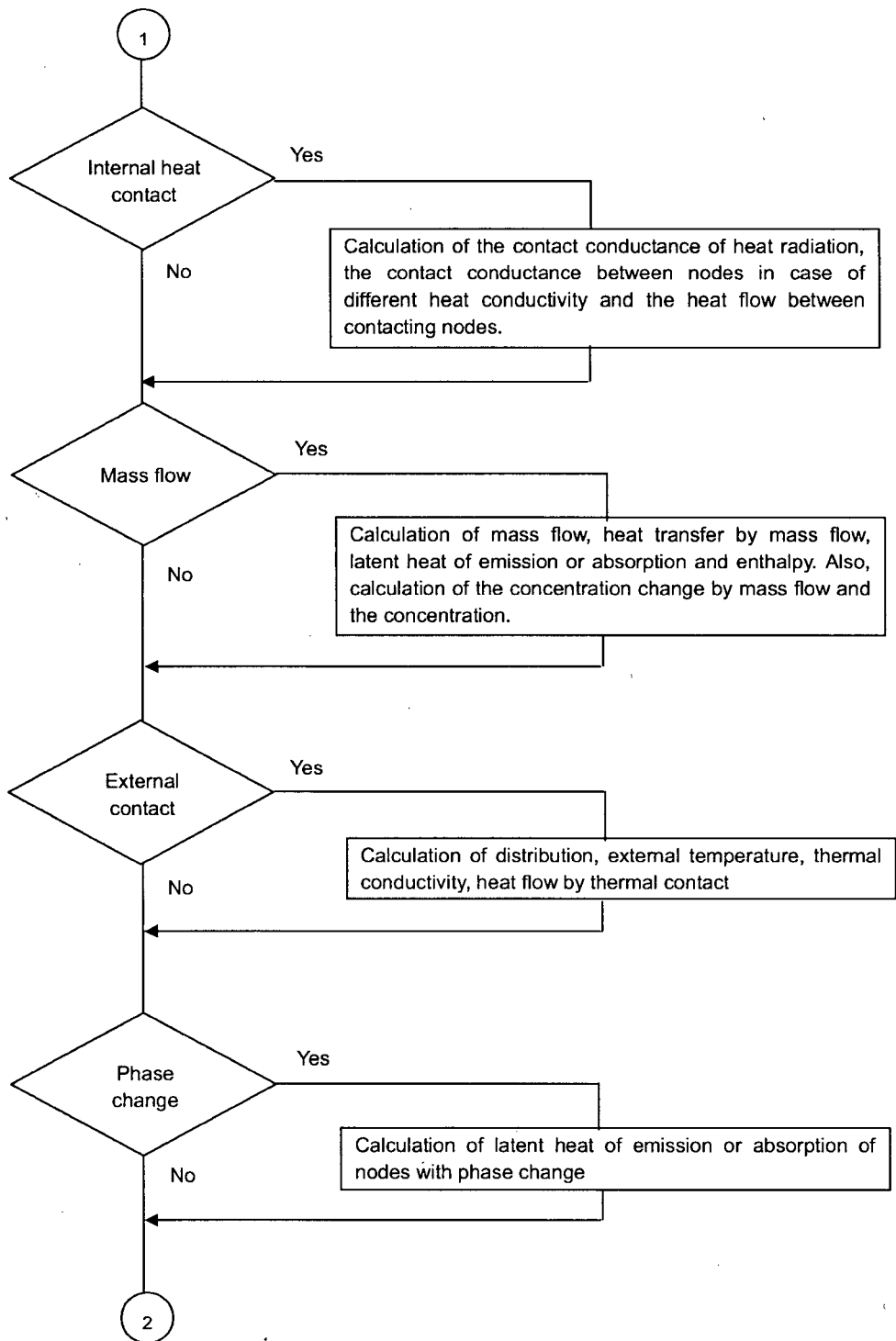


Fig. II-B.5 TRUMP Flow Chart (2/3)

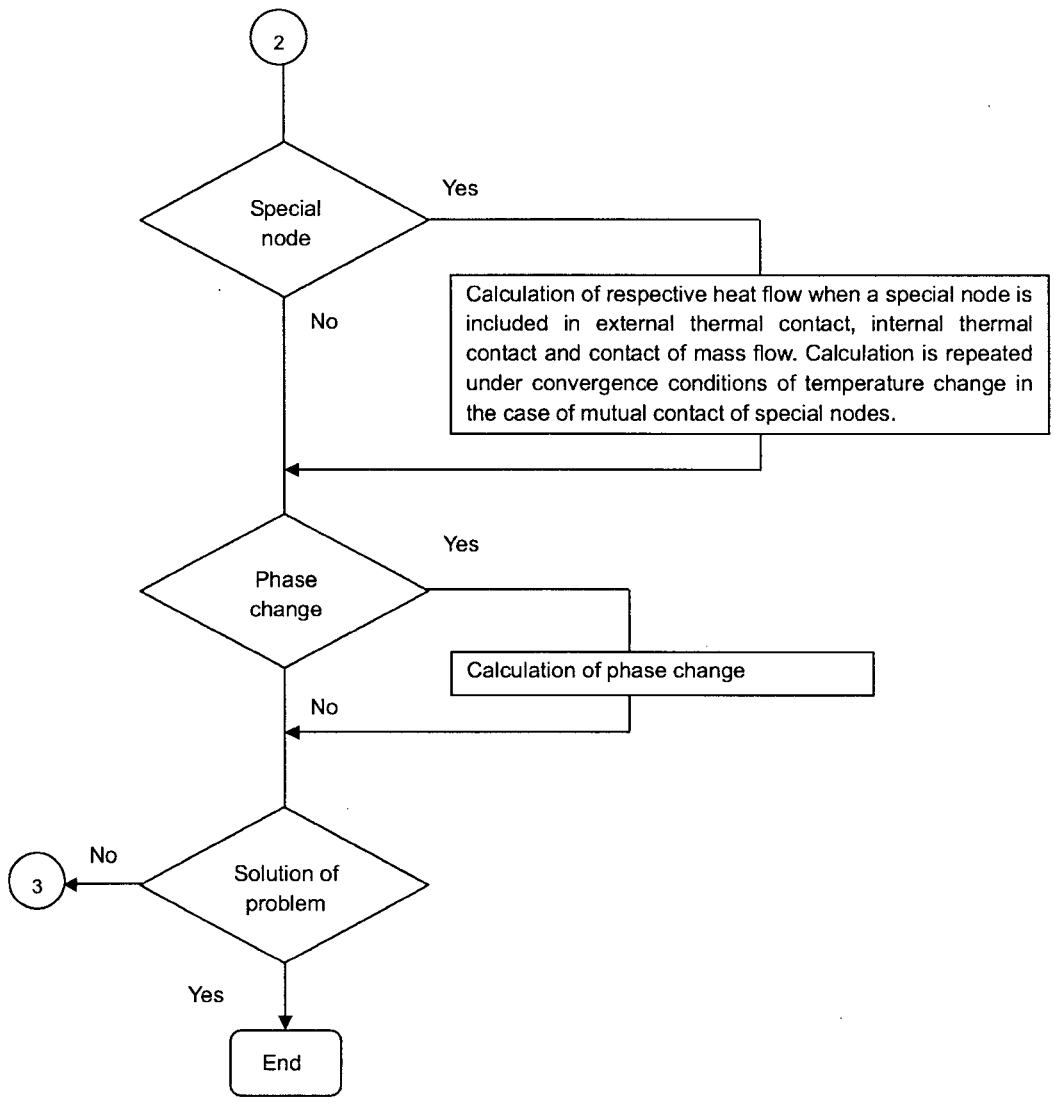


Fig. II-B.5 TRUMP Flow Chart (3/3)

Proprietary Information on Pages II-B-31 through II-B-40
Withheld Pursuant to 10 CFR 2.390

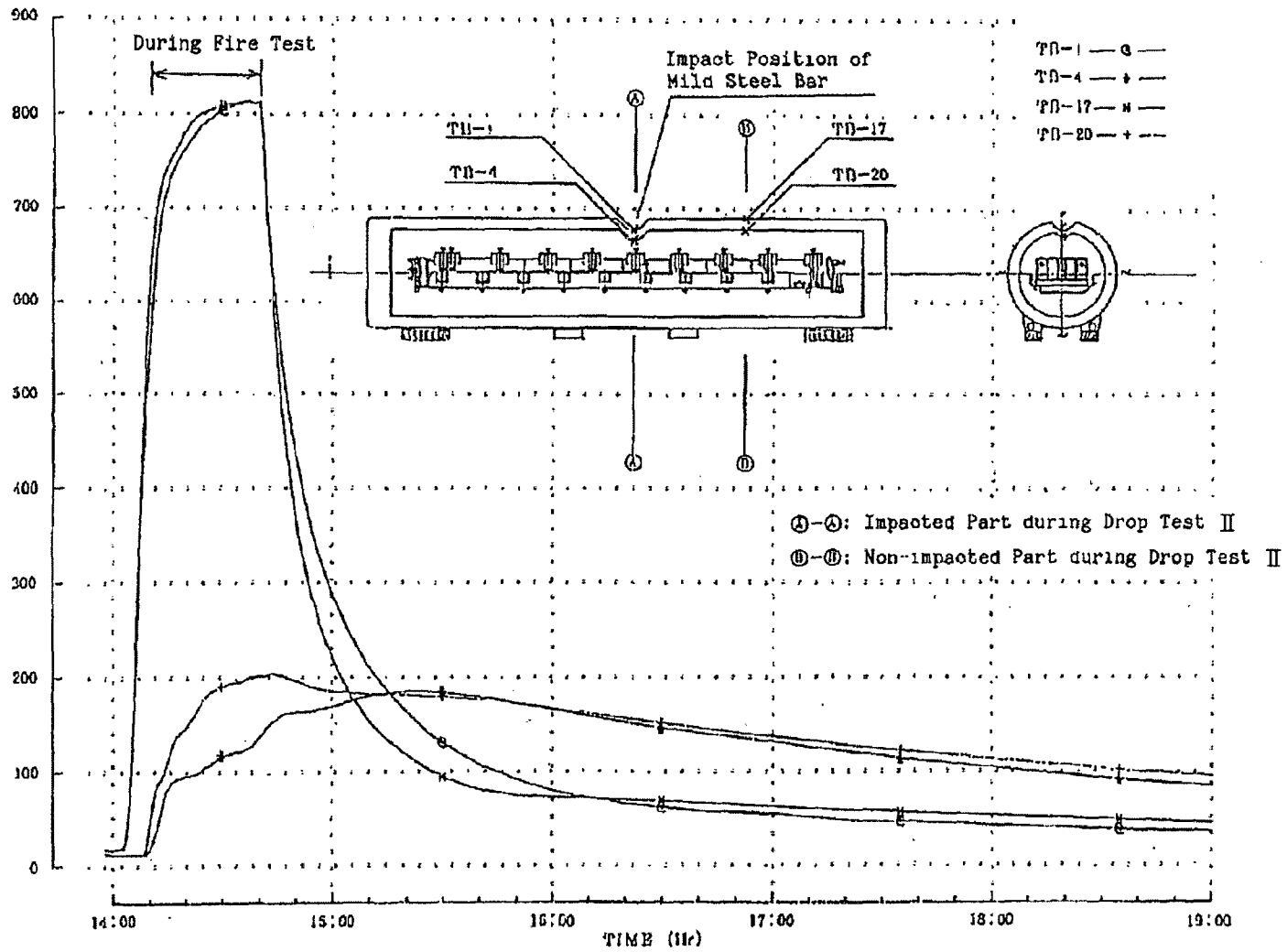


Fig. II-B. 10 Effect of Drop Test II at Fire Test at 800°C for 30 Minutes on Thermal Analyses

Proprietary Information Withheld Pursuant to 10 CFR 2.390

Proprietary Information Withheld Pursuant to 10 CFR 2.390

II-C CONTAINMENT ANALYSIS

II-C Containment Analysis

C.1 Outline

The containment system for the package consists of the fuel rods. The fuel rod cladding and the fuel rod end plugs seal-welded at both ends which are components of every fuel rod form a containment boundary, the sealing performance of which shall be analyzed.

The integrity of the containment boundary of the fuel rods has been confirmed based on the results of the structural analysis and the thermal analysis of this package under normal and accident conditions of transport, and the test results of the drop test I, the drop test II and the fire test under the hypothetical accident conditions of transport with two prototype packagings.

C.2 Containment System

C.2.1 Containment System

This packaging has no component as a containment system, and the fuel rod cladding and the fuel rod end plugs which are components of every fuel rod form the containment boundary as shown in Fig. I-D.10 through Fig. I-D.12. A general drawing of fuel rods as a containment boundary is shown in Fig.II-C. 1.

The design specifications of the fuel rods as a containment boundary are shown below. Maximum temperatures and pressures under normal and accident conditions of transport are summarized in Table II-C. 1 of Annex C.6.1.

(1) Design specification of fuel rod

The fuel rod is so designed that it can maintain the leak-tightness even after it has been used in the pressurized water type reactor under the high temperature of approx. 400°C and the high pressure of 15MPa for approx. 3 years.

Helium gas is filled and pressurized to up to 3.14MPa · G at room temperature (20°C) in the fuel rod as shown in Table I-D.9.

C.2.2 Penetration of Containment System

The fuel rod cladding and the fuel rod end plugs which form a containment boundary are sealed with welding, and there is no penetration.

C.2.3 Gaskets and Welds of Containment System

There is no gasket used for a containment boundary.

Welding positions of the fuel rod are shown in Fig. II-C.2. All the welded parts shall be inspected with visual inspection (macroscopic observation method) Furthermore, the integrity of the welded parts shall be confirmed with helium leak tests. Leakage of 1.0×10^{-8} cm³/s or more is not allowed in the leak test of the fuel rod.

The leak-tightness of welded area is maintained without being damaged even at the maximum pressure of 3.73 MPa·G at the expected maximum temperature of 73°C under the normal conditions of transport, and also, even at the pressure of 7.79MPa·G at the fuel rod temperature (440°C) during the fire test of 800°C as mentioned in Chapter II-B.

C.2.4 Closure System

There is no closure system.

C.3 Normal Conditions of Transport

C.3.1 Leakage of Radioactive Materials (Re: Para. 537 (a))

As mentioned in A.5, there is no influence on the containment boundary of fuel rods for the pressure and the thermal expansion of each part at the maximum temperature of 73°C in the package under normal conditions of transport. Even if subjected to the water spray test, the free drop test, the stacking test or the penetration test, the integrity of the fuel rods can be maintained and there is no leakage of radioactive materials.

(1) Water spray test

There is no possibility that the water infiltrates into the packaging even when the package is exposed to rainfall of approximately 5cm per hour for one hour, as per evaluated in A.5.2. Furthermore, the fuel rods that are a containment boundary are designed to endure in the water of approximately 15MPa for a long period when used in the reactor. Therefore, there is no possibility that the water infiltrates even when subjected to the water spray test.

(2) Free drop test

As mentioned in A.5.3, the drop energy can be absorbed by the deformation of outer shell of the packaging during the free drop test from a height of 1.2m, and the integrity of the fuel rod can be maintained. Therefore, the integrity of the package can be maintained even during the free drop test.

(3) Stacking test

As analyzed in A.5.4, the packaging has integrity even after the stacking test with a compressive load equal to 5 times the mass of the package. Therefore, the leak-tightness of the fuel rod can be maintained even when subjected to the stacking test.

(4) Penetration test

As analyzed in A.5.5, the external cylinder of the packaging would not penetrate, even when a bar of ϕ 3.2cm in diameter and 6 kg is dropped from a height of 1m. Therefore, the leak-tightness of the fuel rod can be maintained even when subjected to the penetration test.

C.3.2 External Pressure on Containment System

The fuel rod inside is pressurized with helium gas (refer to C.2.1). FP gas could not be produced since the pellets are made of unirradiated sintered uranium dioxide. Only very small amount of vapor could be included inside the fuel rods. The maximum internal pressure at the temperature of 73°C of the content under normal conditions of transport is below the maximum allowable working pressure as shown in Annex C.6.1. Therefore, the leak-tightness can be maintained without damaging the fuel rod that is the containment boundary, since the stress generated in the fuel rods is below the criteria as shown in A.5.7 of Structural Evaluation.

C.3.3 Contamination of Coolant Materials

This requirement is not applied, as the coolant is not used in this package.

C.3.4 Loss of Coolant Materials

This requirement is not applied, as the coolant is not used in this package.

C.4 Hypothetical Accident Conditions of Transport

C.4.1 Nuclear Fission Gas

The content of this package does not contain fission gas.

C.4.2 Leakage of Radioactive Materials

As mentioned in II-A.9.2 of Structural Evaluation, the leak-tightness can be assured without any damage of the fuel rods. Also, in the case mentioned in B.5.6 of Thermal Analysis, the leak-tightness can be maintained without any damage of the fuel rods, under the environment of 440°C. The maximum internal pressure generated in the fuel rods is below the maximum allowable working pressure, and the leak-tightness of the fuel rods that are a containment boundary can be maintained.

Furthermore, it has been confirmed by performing the prototype tests (drop test I, II and fire test) that the fuel rods would not be damaged. Therefore, there should be no leakage of the radioactive material from this package.

C.5 Summary of Results and Evaluation

As mentioned in II-A.5.3 and II-A.9.2 of Structural Evaluation, the leak-tightness can be assured without any damage of the fuel rods, under normal conditions of transport and hypothetical accident conditions of transport.

Also, as mentioned in B.4.4 of Thermal Evaluation, the internal pressure at the maximum temperature of 73°C on the fuel rods could become 3.73MPa·G. The general membrane stress generated in the fuel rods could be 31.1N/mm², which is sufficiently smaller than the design stress strength of Zircaloy-4, 239 N/mm². Thus, the leak-tightness can be maintained.

As analyzed in A.9.2 of Structural Evaluation and as demonstrated in the prototype test (refer to II-F Test Report of Prototype Packaging for Model MFC-1 Container), the integrity of the containment boundary can be maintained against the drop impact of 9m under hypothetical accident conditions of transport.

Furthermore, as analyzed in B.5.4 of Thermal Evaluation, the leak-tightness can be maintained without any damage of the fuel rods under the environment of 800°C for a period of 30 minutes under hypothetical accident conditions of transport.

Proprietary Information Withheld Pursuant to 10 CFR 2.390

11-C-5

Proprietary Information Withheld Pursuant to 10 CFR 2.390

11-C-6

C.6 Annex

C.6.1 Containment Boundary

Maximum temperatures and internal pressures of the containment boundary of the fuel rods are shown in Table II-C. 1.

Table II-C. 1 Maximum Temperature of Containment Boundary (1/2)

Type	Component name	Temperature (°C)					
		Current fuel			High burnup fuel		
		Normal conditions of transport	Hypothetical accident conditions of transport	Maximum allowable working temperature ⁽¹⁾	Normal conditions of transport	Hypothetical accident conditions of transport	Maximum allowable working temperature ⁽¹⁾
Type 14 × 14 10 feet	Fuel rod cladding tube Fuel rod end plugs	73	440	860 ⁽¹⁾	-	-	-
Type 14 × 14 Type 15 × 15 12 feet	Fuel rod cladding tube Fuel rod end plugs	73	440	860 ⁽¹⁾	73	440	860 ⁽¹⁾
Type 17 × 17 12 feet	Fuel rod cladding tube Fuel rod end plugs	73	440	860 ⁽¹⁾	73	440	860 ⁽¹⁾

Table II-C.1 Maximum Pressure of Containment Boundary (2/2)

Type	Component name	Pressure (MPa·G)					
		Current fuel			High burnup fuel		
		Normal conditions of transport	Hypothetical accident conditions of transport	Maximum allowable working pressure ⁽²⁾	Normal conditions of transport	Hypothetical accident conditions of transport	Maximum allowable working pressure ⁽²⁾
Type 14×14, 10 Feet	Fuel rod cladding tube Fuel rod end plugs	3.25	6.81	Normal conditions: 66.2 ⁽²⁾ Accident conditions: 34.5	—	—	—
Type 14×14, 12 Feet	Fuel rod cladding tube Fuel rod end plugs	3.40	7.10	Normal conditions: 66.2 ⁽²⁾ Accident conditions: 34.5	2.79	5.86	Normal conditions: 66.2 ⁽²⁾ Accident conditions: 34.5
Type 15×15, 12 Feet	Fuel rod cladding tube Fuel rod end plugs	3.49	7.30	Normal conditions: 66.2 ⁽²⁾ Accident conditions: 34.5	2.79	5.86	Normal conditions: 66.2 ⁽²⁾ Accident conditions: 34.5
Type 17×17, 12 Feet	Fuel rod cladding tube Fuel rod end plugs	3.73	7.79	Normal conditions: 68.8 ⁽²⁾ Accident conditions: 35.9	2.79	5.86	Normal conditions: 68.8 ⁽²⁾ Accident conditions: 35.9

(1) Maximum allowable working temperature is set to β transformation temperature derived from the characteristics of the material (Zircaloy-4, MDA and ZIRLO). The melting temperature of the material is 1,855°C.

(2) Under normal conditions of transport, maximum allowable working pressure is set to the internal pressure where the hoop stress generated in cladding becomes 540N/mm² (at 73°C).

Under hypothetical accident conditions of transport, maximum allowable working pressure is set to the internal pressure where the hoop stress generated in cladding becomes 282 N/mm² (at 440°C).

II-D SHIELDING ANALYSIS

II-D Shielding Analysis

D.1 Outline

The content of this package is uranium dioxide fuel assemblies. Therefore, uranium and its daughter nuclides shall be considered as radiation sources.

The enrichment of uranium dioxide fuel assemblies that are the content is equal to or less than 5wt%. Therefore, the fuel enrichment is set as 5.0 wt% in the shielding analysis.

For the radioactivity and the source terms, those with higher enrichment are bigger and their dose rate becomes also higher. Accordingly, the shielding analysis is performed using the uranium isotopic composition of the maximum enrichment of 5.0wt%.

Under both the routine transport conditions and the normal conditions of transport, dose-equivalent rate is evaluated in the radial direction of the package, considering only the fuel assemblies and the external cylinder of the package with the minimum distance between the fuel assembly and the package surface.

The maximum displacement of the cradle assembly due to the free drop test is considered in the shielding analysis under the normal conditions of transport.

D.2 Specifications of Source Terms

D.2.1 Gamma Emission Rate

The uranium dioxide fuel that is the content of this package includes the uranium isotopes and their daughter nuclides and the decay gamma radiation shall be considered.

The calculation of the gamma is carried out based upon the uranium isotopic composition of 5.0wt% enrichment assuming a period of 10 years until the transport on a conservative side by using the burnup calculation code, ORIGEN-2 (refer to II-D.6.1).

Gamma emission rate from the uranium dioxide fuel calculated by using the ORIGEN-2 Code is shown in Table II-D. 1. The radioactivity of major nuclides is as shown in Table II-D. 2.

D.2.2 Neutrons Source

Spontaneous fission of uranium isotopes and (α , n) reaction between alpha decay nuclides and oxygen consist of emission of neutrons from the content of uranium dioxide assembly. However, neutrons source can be negligible and much smaller than the gamma emission rate.

Table II-D. 1 Gamma Emission Rate

(per Package)

Energy group	Average energy (MeV)	Gamma emission rate of contents (γ /sec)
1	0.01	2.63×10^{10}
2	0.025	1.83×10^8
3	0.0375	8.24×10^8
4	0.0575	1.82×10^9
5	0.085	2.14×10^9
6	0.125	1.17×10^9
7	0.225	2.80×10^9
8	0.375	2.96×10^8
9	0.575	1.83×10^8
10	0.85	1.14×10^8
11	1.25	7.25×10^7
12	1.75	1.34×10^7
13	2.25	5.09×10^3
14	2.75	2.35×10^7
15	3.5	1.66×10^3
16	5.0	7.09×10^2
17	7.0	8.14×10^1
18	9.5	9.34×10^0
Total		3.76×10^{10}

* When two fuel assemblies are accommodated

Table II-D. 2 Radioactivity of Major Nuclides

(per Fuel Assembly)

Major nuclide	Radioactivity (Bq)
Tl 208	1.24×10^7
Pb 212	3.45×10^7
Bi 212	3.45×10^7
Po 212	2.21×10^7
Po 216	3.45×10^7
Rn 220	3.45×10^7
Ra 224	3.45×10^7
Th 228	3.44×10^7
Th 231	1.92×10^9
Th 234	5.67×10^9
Pa 234m	5.67×10^9
U 232	3.45×10^7
U 234	5.54×10^{10}
U 235	1.92×10^9
U 236	2.87×10^8
U 238	5.67×10^9
Total	7.68×10^{10}

Proprietary Information on Pages II-D-4 through II-D-7
Withheld Pursuant to 10 CFR 2.390

D.4 Shielding Analysis

D.4.1 Routine Transport Conditions

The shielding analysis under routine transport conditions is performed by means of one-dimensional transport calculation code ANISN using the analysis model as shown in Fig. II-D. 2, and the dose-equivalent rate can be obtained by multiplying the result by the number of accommodated assemblies (two). As shown in D.3.1, this method is sufficiently conservative, because the minimum distance between the fuel assembly and the package surface is assumed, the internal cylinder and the balsa wood between the internal cylinder and the external cylinder are ignored, and the finite length of radiation source is modeled with infinite length of cylinder in ANISN calculation.

II-D.6.2 shows the description of ANISN code.

P_3 transport constant data set of gamma radiation group No. 18 in DLC23E/CASK Library is used as a neutron cross section. Table II-D. 5 shows the dose-equivalent rate conversion coefficient used to determine this energy group structure and the dose-equivalent rate.

The dose-equivalent rate conversion coefficient is based on ICRP Publication 74.

ANISN calculation is carried out using S-8 Division Point Set of Data.

Table II-D. 6 shows the result of the shielding analysis under routine transport conditions of this package.

D.4.2 Normal Conditions of Transport

The shielding analysis under normal conditions of transport is performed using the same method as that of routine transport conditions taking into consideration the maximum displacement of the cradle assembly.

Table II-D. 6 shows the result of the shielding analysis under normal conditions of transport.

The dose-equivalent rates under normal conditions of transport show no significant increase in comparison with those under routine transport conditions as shown in Table II-D. 6. The analysis results of the dose rates are small enough to satisfy the criteria.

Table II-D. 5 γ -ray Energy Group Structure and Conversion Coefficient of Dose-Equivalent Rate

Energy group	Upper limit energy (MeV)	Dose-equivalent rate conversion coefficient (mSv/h)/(γ /cm ² ·s)
1	10.0	8.49×10^{-5}
2	8.0	7.24×10^{-5}
3	6.5	6.15×10^{-5}
4	5.0	5.20×10^{-5}
5	4.0	4.42×10^{-5}
6	3.0	3.78×10^{-5}
7	2.5	3.34×10^{-5}
8	2.0	2.90×10^{-5}
9	1.66	2.48×10^{-5}
10	1.33	2.08×10^{-5}
11	1.0	1.73×10^{-6}
12	0.8	1.41×10^{-6}
13	0.6	1.05×10^{-5}
14	0.4	7.53×10^{-6}
15	0.3	5.41×10^{-6}
16	0.2	3.22×10^{-6}
17	0.1	1.93×10^{-6}
18	0.05 (0.01)	2.70×10^{-6}

D.5 Summary of Results and Assessment

Table II-D. 6 shows the result of dose rates obtained by the shielding analysis of this package and gives a conservative result because of the following points:

- (1) Burnup calculation code ORIGEN-2 and transport calculation ANISN whose code reliability and validity are widely recognized are used for the calculation of source terms and the calculation of shielding respectively.

Furthermore, the source terms are evaluated assuming a period of 10 years until the transport on a conservative side based on the uranium isotopic composition of 5.0wt% of the maximum enrichment.

- (2) The analysis model is conservatively set as shown below.
 - (a) The minimum distance between the fuel assembly and the package surface is assumed, and the dose rate based on one fuel assembly is multiplied by the number of the accommodated assemblies (two).
 - (b) The internal cylinder (1.2mm in thickness) of the package and the balsa wood (119mm in thickness) between the external cylinder and the internal cylinder are ignored.
 - (c) The minimum thickness is applied to the shielding thickness of the external cylinder, taking into consideration the tolerance of the plate thickness.
 - (d) The cylindrical radiation source with infinite length is modeled as a radiation source with finite length in one-dimensional cylindrical shape.

Based on the result of Table II-D. 6, all the dose rates obtained from this analysis satisfy the criteria.

Table II-D. 6 Summary of Maximum Dose Rate

(Unit: mSv/h)

	Routine transport conditions		Under normal conditions of transport
	Package surface	Location at 1m from package surface	Package surface
Gamma	0.022	0.006	0.029
Neutrons	-	-	-
Total	0.022	0.006	0.029
Criteria	≤ 2.0	≤ 0.1	≤ 2.0

D.6 Annex

D.6.1 Description of ORIGEN-2 Code

(1) Outline

ORIGEN-2 code, which was developed by ORNL of the United States, is the depletion and decay analysis module.

Precise reactor physics codes with multi-group neutron cross sections in a function of time and space are generally used for the burnup calculation of the nuclear fuel in the reactor. These codes are complicated and can be used only for the calculation of limited nuclides. On the other hand, ORIGEN-2 code can be used for a wide variety of calculation such as spent fuel characterization, isotopic inventory, radiation source terms, and decay heat for research and design on nuclear fuel cycles. It also performs the burnup calculation with effective one-group cross sections with depletion controlled either by power or irradiation flux level. Thus, the neutron cross sections are obtained from other precise reactor physics codes, which possess the neutron cross sections corresponding to several reactor type models as library data.

(2) Calculation method of ORIGEN-2

(a) Basic equation

The change of nuclide i during irradiation and decay is calculated by the following equation:

$$\frac{dX_i}{dt} = \sum_{j=1}^N \ell_{ij} \lambda_j X_j + \phi \sum_{k=1}^N f_{ik} \sigma_k X_k - (\lambda_i + \phi \sigma_i + r_i) X_i + F_i$$

$i = 1 \sim N$ (D.6.1 - 1)

Where,

X_i : Atom density of nuclide i

N : Number of nuclides

ℓ_{ij} : Ratio at which nuclide i is generated by decay of nuclide j

λ_i : Decay constant

ϕ : Neutron flux (space and energy average)

f_{ik} : Ratio at which nuclide i is generated by neutron absorption of nuclide k

σ_k : Spectral average neutron cross section of nuclide k

r_i : Continuous removal ratio of nuclide i from system

F_i : Continuous supply amount of nuclide i

In the equation (D.6.1-1), ϕ is an average neutron flux of space and energy. The equation (D.6.1-1) is a non-linear equation since the neutron flux and cross section vary with time depending upon the composition change of the fuel. As changes of the neutron flux and cross section according to time are small in a short time, the equation (D.6.1-1) becomes simultaneous linear differential equations with constant coefficients, assuming the neutron flux and cross section are constant in the short time of Δt . Thus, this equation can be given as follows:

$$X = \tilde{A} \cdot X + F \quad (D.6.1-2)$$

Where,

$$X = \{X_i\} \quad i = 1 \sim N$$

$$\tilde{A} = \{a_{ij}\} \quad i, j = 1 \sim N$$

$$a_{ij} = \lambda_{ij} + \phi f_{jk} \cdot \sigma_j - (\lambda_i + \phi \cdot \sigma_i + \Gamma) \delta_{ij}$$

$$\delta_{ij}: \text{when } i = j, \sigma_{ij} = 1$$

$$\text{When } i \neq j, \sigma_{ij} = 0$$

$$F = \{F_i\} \quad i = 1 \sim N$$

In the solution of the equation (D.6.1-1) or the equation (D.6.1-2), matrix index method is used in ORIGIN-2, and the Bateman equation and the radiation equilibrium are used as for the short-lived nuclides.

(3) Library of ORIGIN-2

ORIGIN-2 is a code to calculate various characteristics of nuclides caused by irradiation and decay of nuclear materials, and it possesses the data required to calculate their characteristic values as a library. The data required by ORIGIN-2 is mainly classified into the following three categories:

- (a) Data on decay: Half-life period (decay constant), decay ratio in decay series and heat load during decay. (Natural isotopic composition and allowable concentration are given, as well.)
- (b) Data on photon: γ -ray involved in decay, γ -ray by (α , n) reaction, γ -ray during spontaneous fission, bremsstrahlung X-ray by β -ray of each nuclide in 3 kinds of materials
- (c) Data on cross section: Various reaction cross sections of neutron and fission yield

D.6.2 Description of ANISN Code

(1) Outline

ANISN code solves the one-dimensional Boltzmann transport equation for neutrons or gamma rays in slab sphere, or cylinder geometry, which was developed by ORNL* of the United States.

The transport equation describes the statistical distribution of one particle in a fluid, which is given by the following equation:

$$\begin{aligned} & \Omega \cdot \nabla \phi(r, E, \Omega) + \sigma_t(r, E) \phi(r, E, \Omega) \\ & = \iint \phi(r, E', \Omega') \sigma_s(r, E' \rightarrow E, \Omega' \rightarrow \Omega) dE' d\Omega' + S(r, E, \Omega) \end{aligned} \quad (D.6.2-1)$$

Where,

$\phi(r, E, \Omega)$: Angular neutron flux

$\sigma_t(r, E)$: Total cross section

$\sigma_s(r, E' \rightarrow E, \Omega' \rightarrow \Omega)$: Scattering cross section or generated cross section of secondary gamma-ray by neutron

$S(r, E, \Omega)$: External radiation source

Sn Method is a numerical calculation technique to solve discrete ordinates transport equation using iteration calculation methods.

If a one-dimensional transport equation is expressed with neighboring Fundamental cell determined by (r_i, r_{i+1}) , $(\mu_{n-1/2}, \mu_{n+1/2})$ mesh, the following is obtained:

$$\begin{aligned} & W \cdot \mu \cdot (A_{i+1} N_{i+1} - A_i N_i) + \alpha_{n+1/2} N_{n+1/2} - \alpha_{n-1/2} N_{n-1/2} \\ & = V \cdot (S - \Sigma_t) \cdot N \cdot W \end{aligned} \quad (D.6.2-2)$$

* ORNL/RSIC COMPUTER CODE COLLECTION-ANISN-W "A-ONE DIMENSIONAL DISCRETE ORDINATES TRANSPORT CODE" CCC-82

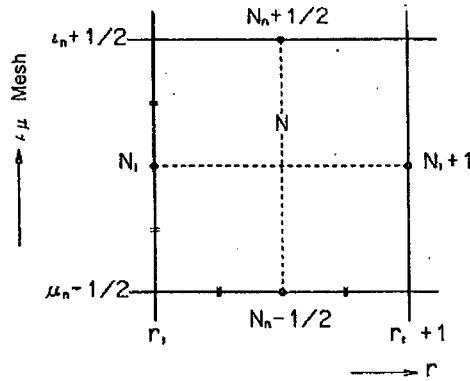


Fig. II-D. 5 Mesh Division Drawing

Where,

N : Neutron flux (including angular distribution for each energy group)

μ : Direction cosine

A : Area element

$$\begin{cases} 1.0 & \text{for flat plate shape} \\ 2 \pi r & \text{for cylinder shape} \\ 4 \pi r^2 & \text{for sphere shape} \end{cases}$$

W : Weight of direction cosine μ : $\sum_{\mu} W = 1.0$

V : Volume element

$$\begin{cases} r_{i+1} - r_i & \text{for flat plate shape} \\ \pi (r_{i+1}^2 - r_i^2) & \text{for cylinder shape} \\ 4/3 \pi (r_{i+1}^3 - r_i^3) & \text{for sphere shape} \end{cases}$$

Σ_t : Total cross section

S : Radiation source term (external radiation source + scattering integral term)

α Value determined by the following equation:

$$\alpha_{n+1/2} = \alpha_{n-1/2} - W \cdot \mu \cdot (A_{i+1} - A_i)$$

$$\alpha_{1/2} = 0.0$$

The equation (D.6.2-2) can be obtained by integrating that obtained when the equation (D.6.2-1) is multiplied by phase volume, and replacing the differential by the finite difference.

To reduce unknown variables (N , N_i , N_{i+1} , $N_{n-1/2}$, $N_{n+1/2}$) included in the equation

(D.6.2-2), diamond finite difference method and step function approximation are used. Diamond step differential method: Linear approximation between adjacent meshes

$$N = 1/2 (N_{i+1} + N_i) \\ = 1/2 (N_{n-1/2} + N_{n+1/2})$$

Step function approximation:

$$N = N_i = N_{n+1/2} \text{ for } \mu < 0 \\ N = N_{i+1} = N_{n+1/2} \text{ for } \mu > 0$$

For $\mu > 0$ when diamond finite difference method is used,

$$N = 2\mu AN_i + 2\alpha / WN_{n-1/2} + SV/2\mu A + 2\alpha / W + \Sigma_t V \quad (D.6.2 - 3)$$

Where

$$\alpha = 1/2 (\alpha_{n+1/2} \alpha_{n-1/2}) \\ A = 1/2 (A_{i+1} + A_i)$$

This step difference equation performs calculation until the convergence by Iteration Method, giving properly the initial values.

These calculations are a basic solution method.

II-E CRITICALITY ANALYSIS

II-E Criticality Analysis

E.1 Outline

As for the evaluation of subcriticality relating to this fissile material package, the evaluation is to be carried out to confirm that the criticality is not reached for any following condition: (1) individual undamaged package in isolation, (2) individual damaged package in isolation, (3) damaged package arrays (Ref: Para. 678, 679, 681 and 682)

Undamaged packages are assumed to be incident free packages subject to routine conditions of transport. Damaged package are assumed to be packages taking into account the maximum damage under hypothetical accident conditions superimposed on the damage under normal conditions of transport.

The subcriticality of damaged package arrays under hypothetical accident conditions of transport is confirmed, which is the most conservative model of the above-mentioned three evaluation conditions.

The criticality calculation method and nuclear data are verified and validated by the benchmark test based on a criticality evaluation of the criticality experiments by Battelle laboratory.

The fuel enrichment of the uranium dioxide that is the content is 5.0wt% or less, and then fuel enrichment of 5.0wt% is used in the subcriticality evaluation.

E.2 Objects of Analysis

E.2.1 Contents

Two fresh fuel assemblies can be accommodated per package. These two fresh fuel assemblies are arranged so that they may not approach within 62mm each other with the structure of cross frame. The specifications of the fuel assemblies are shown in Table II-E. 1. The fuel enrichment is set as 5.0wt% to perform the criticality evaluation.

Though a burnable poison which is to suppress an initial reactivity is, in some cases, contained in the fuel, this burnable poison is ignored to perform the criticality analysis on the conservative side.

E.2.2 Packaging

Two fresh fuel assemblies [type 14 × 14, type 15 × 15 and type 17 × 17] can be accommodated in this packaging.

These fresh fuel assemblies are arranged so that they may not approach within 62mm each other with the structure of cross frame (refer to Fig. II-E. 1).

- (1) The distances from the outer surface of a fuel assembly to the packaging surface subject to routine transport conditions, normal conditions of transport (Fig. II-A.17) and hypothetical accident conditions of transport (Fig. II-A.42), obtained from the structural analysis, are summarized in Table II-E. 2. As clearly shown in this table, the deformation amount under the routine transport conditions (undamaged packages) is smaller than that in the case subject to hypothetical accident conditions (damaged packages) following the normal conditions of transport. Therefore, to perform the criticality evaluation with damaged packages is sufficiently conservative.
- (2) Under hypothetical accident conditions of transport (damaged packages), it is necessary to consider the fact that the clearances between the contents become smaller due to the deformation of the packages than those under routine transport conditions (undamaged packages). As a severer situation than individual package in isolation, it is assumed that the deformed packagings are facing one other and an infinite number of packages are arranged in array, although it is impossible that such a situation occurs actually. Furthermore, it is assumed that the water exists both inside and outside the package and the accommodated fuel assemblies are completely flooded with the water, but no water leaks into the fuel rods because the integrity of the containment system (fuel rods) can be maintained.

E.2.3 Neutron Absorbers

As a neutron absorber, two boronated stainless steel plates (with the boron at 1 wt%) are allocated between two fuel assemblies in the packaging. These neutron absorbers are fixed on the structural material, which can be kept even under hypothetical accident conditions of transport. Since the neutron source is as small as negligible as described in the Shielding Analysis, it can be well assumed that no attenuation of neutron absorbing capability of boronated stainless steel is caused. In addition, the external cylinder has also neutron absorbing capability.

E.3 Specification of Model

E.3.1 Analysis Model

Two fresh fuel assemblies (type 14 × 14, type 15 × 15 and type 17 × 17) are accommodated in this packaging.

These fresh fuel assemblies are arranged so that they do not approach each other within 62mm by the package. Both actual packages and analysis models for the following conditions are described: (1) individual undamaged package in isolation, (2) individual damaged package in isolation and (3) damaged package arrays.

(1) Individual undamaged package in isolation

As shown in Table II-E. 2, as the clearance between fuel assemblies of undamaged packages is sufficiently big in comparison with that of damaged packages, the conditions of the damaged package arrays are severer than this condition, as far as the criticality safety is concerned.

(2) Individual damaged package in isolation

There is only one package in isolation. Therefore there is no neutron mutual interference between the packages. The condition of the damaged package arrays is severer than this condition because the neutron mutual interference exists in the packages in array, as far as the criticality safety is concerned.

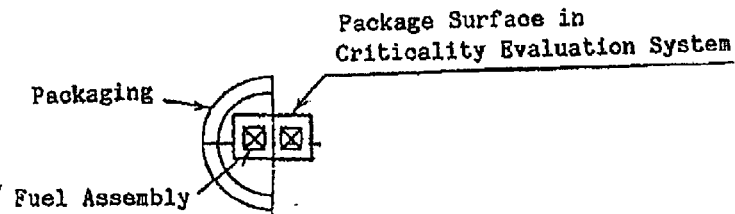
(3) Damaged package arrays

As for damaged package arrays, it is necessary to consider that the clearance between the contents due to the deformation of packagings is smaller than that of undamaged packages. Although the situation does not occur actually, it is assumed that the deformed packages face one other as shown in Fig. II-E. 1, and the infinite number of packages are arranged in array.

As the fuel assemblies to be accommodated are of type 14 × 14, type 15×15 and type 17× 17, the analysis was performed for each type of fuel assembly. Fig. II-E. 2, Fig. II-E. 3 and Fig. II-E. 4 show the cross sections of each type of fuel assemblies respectively.

The boundary condition is complete reflection on all boundaries shown in Fig. II-E. 1, and it is simulated that the infinite number of packages are in array under this assumption. Also, the absorption effect of boronated stainless steel (with the boron at 1wt%) and steel plate of packaging external cylinder is taken into consideration.

It is determined to consider that the deformed situation of the packaging under the hypothetical accident conditions of transport following the normal conditions of transport is considered as for the geometry of damaged packages, while the geometry of the undamaged packages is assumed to be a geometry without deformation of the packaging under the routine transport conditions. In the criticality evaluation, the geometry is considered that the clearance between the package surface and the fuel assembly is the smallest (analysis model) as shown in the figure below, although the situation cannot occur actually.



E.3.2 Atomic Number Densities in Each Region of Analysis Model

Table II-E. 3 shows the atomic number density in each region, which is used for criticality calculation. The fuel enrichment is set to 5.0wt% for fuel assemblies.

The surrounding water density is set to 1.0g/cm³.

E.4 Subcriticality Evaluation

E.4.1. Calculation Conditions

(1) Content

The evaluation is carried out for the fuel with enriched uranium of 5.0wt% shown in Table II-E. 4.

(2) Packaging

The distances from the fuel assembly surface to the packaging surface in criticality evaluation is shown in Table II-E. 2. It is sufficiently conservative to perform the analysis and evaluation under hypothetical accident conditions of transport, and the evaluation is performed with the geometry shown in Fig. II-E. 1.

(3) Neutron absorber

Two boronated stainless steel plates (with the Boron at 1wt%) are allocated between two fuel assemblies in the packaging for criticality evaluation, and these neutron absorbers are fixed by structural materials of cross frame. As these plates can be kept even under hypothetical accident conditions of transport, they are evaluated as neutron absorbers in the criticality evaluation.

E.4.2. Assumption of Water Leakage into Package

The effective multiplication factor under hypothetical accident conditions is calculated assuming the water exists both inside and outside the packages which are arranged closely in array.

The water density is set to 1.0g/cm^3 , which gives the highest effective multiplication factor.

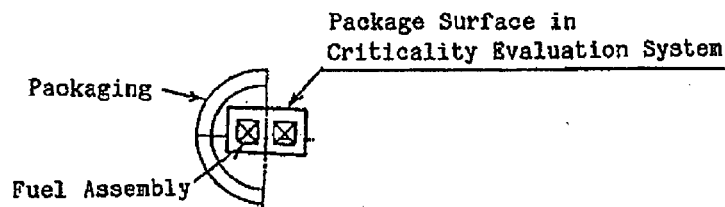
E.4.3. Calculation Procedures

The criticality calculation is carried out using SCALE^[1], which is a code system developed in Oak Ridge National Laboratory of the United States. It contains codes required for the criticality analysis, particularly multi-group Monte Carlo Calculation Code KENO-V.a^[2].

In this criticality analysis, the set of ENDF/B-V 238 Group Neutron Cross Section Data^[3] included in SCALE is used as nuclear data library. The resonance absorption is processed with the method of Bondarenko by BONAMI^[4] for ^{235}U and ^{238}U , and the result is inputted into KENO-V.a. The calculation flow is shown in Fig. II-E. 5.

E.4.4. Results of Calculation

In the case where the packages are subjected to hypothetical accident conditions of transport as specified in the regulations, the outer surface of the packaging, which is out of the damaged package model in the criticality analysis, is only deformed as shown in the figure below, and there is no effect on reduction rate of the volume and cavity of the structural part which are basis of criticality evaluation. In this criticality evaluation, it is considered that the surface of packages is close to the fuel assembly in the cross section direction, as shown in the figure below. Furthermore, an infinite model in axial direction is applied. The effective multiplication factor is calculated assuming the water leakage into the packages in this criticality evaluation.



The subcriticality evaluation relating to the fissile material package is carried out regarding the following three cases:

(1) Individual undamaged package in isolation, (2) Individual damaged package in isolation, (3) Damaged package arrays

As for the package arrays, all the neutrons reaching the package surface are reflected, while in individual package in isolation, some of neutrons are absorbed by the water, since reflection by 20cm of water around one package is assumed. Therefore, the condition for package arrays is severer in the viewpoint of criticality evaluation.

Since the distance between the contents in damaged package arrays is smaller than that in undamaged package arrays and the neutron mutual interference effect between contents of damaged package arrays is bigger, the condition of the damaged package arrays is severer than that of undamaged package arrays in the viewpoint of criticality evaluation.

Therefore, the subcriticality is evaluated under the most severe condition, (3) Damaged package arrays (infinite number packages in array under hypothetical accident conditions of transport).

The calculation results of effective multiplication factors in damaged package arrays are shown in Table II-E. 4.

3

Proprietary Information Withheld Pursuant to 10 CFR 2.390

Proprietary Information Withheld Pursuant to 10 CFR 2.390

E.5 Summary of Results and Evaluation

The analysis results are as shown in Table II-E. 4, and the subcriticality is assured even under the most severe hypothetical accident conditions of transport (damaged package arrays). Therefore, subcriticality is maintained under either of the above three conditions.

Table II-E. 4 Criticality Analysis Conditions and Analysis Results

Fuel assembly type		Type 14×14	Type 15×15	Type 17×17
Analysis conditions	Number of packaging	Infinite number	Same as left	Same as left
	Fuel data	Enrichment : 5.0wt% Cross section dimensions : 197mm×197mm Refer to Table II-E. 1 for detailed data. 2 assemblies per packaging	Enrichment : 5.0wt% Cross section dimensions : 214mm×214mm Refer to Table II-E. 1 for detailed data. 2 assemblies per packaging	Same as left
	Structural materials	Boronated stainless steel plate of 4.5mm Steel plate of external cylinder of packaging	Same as left	Same as left
	Calculation condition	Calculation of one packaging completely under the water, and array an infinite number of packagings in each direction.	Same as left	Same as left
Result	Effective multiplication factor ($k_{eff} + 3\sigma$)	0.873	0.936	0.934

II-E-10

Proprietary Information on Pages II-E-11 through II-E-14
Withheld Pursuant to 10 CFR 2.390

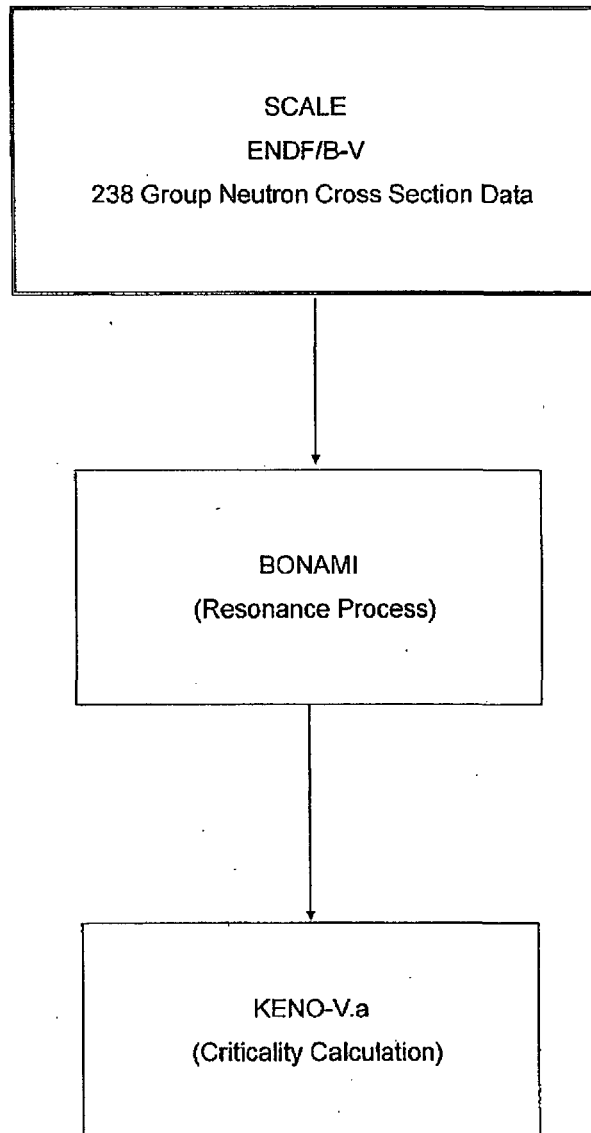


Fig. II-E. 5 Flow of Criticality Calculation

E.6 Annex

E.6.1 Reference

- [1] "SCALE: A Modular Code System for Performing Standardized Computer Analyses for Licensing Evaluation," NUREG/CR-0200, Rev. 6 (ORNL/NUREG/CSD-2/R6), Vols. I, II, and III (1999).
- [2] L.M.Petrie and N.F.Landers, "KENO V.a: AN IMPROVED MONTE CARLO CRITICALITY PROGRAM WITH SUPER GROUPING," NUREG/CR-0200, Rev. 6, Vol. 2, Sec. F11 (ORNL/NUREG/CSD-2/R6) (1998).
- [3] W.C.Jordan and S.M.Bowman, "SCALE CROSS-SECTION LIBRARIES," NUREG/CR-0200, Rev. 6, Vol. 3, Sec. M4 (ORNL/NUREG/CSD-2/V3/R6) (1998).
- [4] M.N.Greene, "BONAMI: RESONANCE SELF-SHIELDING BY THE BONDARENKO METHOD," NUREG/CR-0200, Rev. 6, Vol. 2, Sec. F1 (ORNL/NUREG/CSD-2/V2/R6) (1998).
- [5] S.R.Biermann, et al., "Critical Separation Between Subcritical Clusters of 2.35 wt% Enriched UO₂ Rods in Water with Fixed Neutron Poisons", PNL-2438 (1977)
- [6] S.R.Biermann, et al., "Criticality Experiments with Subcritical Cluster of 2.35 wt% and 4.29 wt% ²³⁵U Enriched UO₂ Rods in Water with Uranium or Lead Reflecting Walls", NUREG/CR-0796 PNL-2827 (1979)
- [7] V.F.Dean "WATER-MODERATED U(2.35) O₂ FUEL RODS IN 2.032-CM SQUARE-PITCHED ARRAYS" NEA/NSC/DOC(95)03/IV VOL.IV LEU-COMP-THERM-001 (1999)
- [8] S.S.Kim and V.F.Dean "WATER-MODERATED RECTANGULAR CLUSTERS OF U(2.35)O₂ FUEL RODS (2.032-CM PITCH) SEPARATED BY STEEL, BORAL, COPPER, COADOMIUM, ALMINIUM, OR ZIRCALOY-4, PLATES" NEA/NSC/DOC(95)03/IV VOL.IV LEU-COMP-THERM-016 (1999)
- [9] S.S.Kim and V.F.Dean "WATER-MODERATED U(2.35) O₂ FUEL RODS REFLECTED BY TWO LEAD, URANIUM, OR STEEL WALLS" NEA/NSC/DOC(95)03/IV VOL.IV LEU-COMP-THERM-017 (1999)
- [10] J.T.Thomas, Ed. "Nuclear Safety Guide TID-7016 Rev.2" NUREG/CR-0095 (1978)

E.6.2 Description of KENO-V.a Code

KENO-V.a is a calculation code based upon multi-group Monte Carlo method developed by Oak Ridge National Laboratory of the United States, which can calculate neutron multiplication factors of a complicated system.

In this code, the probabilistic weight of neutron is treated assuming that it decreases according to the absorption rate in the neutron range hysteresis. The annihilation of neutron is determined with Russian R oulette when the neutron weight becomes below a certain value. The neutron effective multiplication factor k_{eff} is calculated by the following equation:

$$k_{\text{eff}} = \frac{\sum_{j=1}^{\text{NPB}} \sum_{i=1}^{\text{NCOLL}} W T_{ij} (v \Sigma_f / \Sigma_t)}{\sum_{j=1}^{\text{NPB}} W T_{0j}}$$

Where,

- NPB : Number of neutrons generated in one batch
- NCOLL : Number of collisions of neutrons
- WT_{ij} : Weight that neutron had when fission occurred
- WT_{0j} : Weight that generated neutron had
- v : Number of neutrons generated in one fission
- Σ_f : Macroscopic fission cross section area
- Σ_t : Macroscopic total cross section area

E.6.3 Bench Mark Test

E.6.3.1 Outline of Test

In order to prove the appropriateness of the calculation method and nuclear data used in this analysis, the effective multiplication factor of each system was determined by selecting 3 kinds of criticality systems from the criticality experiments in Battelle^{[5][6]}, and using the same calculation method and nuclear data.

E.6.3.2 Details of Test

Fig. II-E. 6 shows the fuel rod specification used for the criticality experiment in Battelle and Fig. II-E. 7 shows the experiment system.

The content of each criticality experiment is as follows:

(1) Criticality Experiment-1 ^{[5][7]}

20 × 18 fuel rods are in the array of square grid of 2.032cm pitch. There is only one fuel cluster, and there is no neutron absorbing plate or reflecting wall.

(2) Criticality Experiment-2 ^{[5][8]}

There is a boron plate as a neutron absorbing plate, and 3 fuel clusters are in the array, sandwiching this plate. There is no reflecting wall. The criticality dimensions are as shown in Table II-E. 5.

(3) Criticality Experiment-3 ^{[6][9]}

Lead is used as a reflecting wall. There is no neutron absorbing plate, and the array is 3 fuel clusters in series.

The criticality dimensions are as shown in Table II-E. 5. Furthermore, Table II-E. 6 shows the densities and atomic number densities of the materials used for each criticality experiment.

In the criticality calculation, acrylic board, aluminum angles, aluminum channel and aluminum bars are ignored, and water is substituted for them.

Also, the calculation was performed assuming that water of 20cm (in the case where the reflecting wall exists, this value shall be 30.5cm including the reflecting wall) surrounds the outside of the fuel cluster and vacuum exists outside the water.

E.6.3.3 Results of Test and Evaluation

Table II-E. 7 shows the analysis result of the criticality test, which proves the validity of the calculation method and nuclear data used for this analysis.

Table II-E. 5 Criticality Dimensions in Criticality Experiment

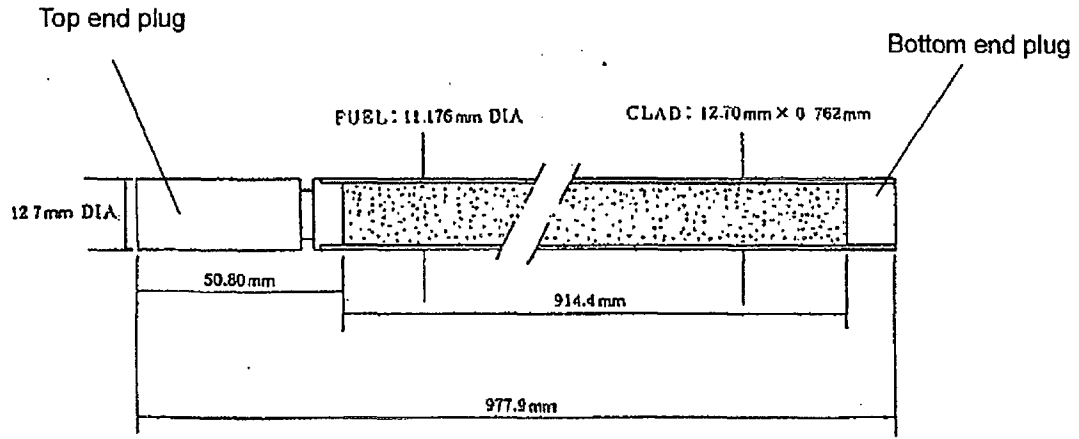
Criticality dimensions Experiment No.	Fuel rod array in cluster ⁽¹⁾ LENGTH x WIDTH	Neutron absorbing plate		Reflecting wall				X _c ⁽³⁾ (mm)
		t _p ⁽²⁾ (mm)	G (mm)	t _B (mm)	L (mm)	H (mm)	Y ⁽³⁾ (mm)	
Criticality Experiment-1	20×18	—	—	—	—	—	—	—
Criticality Experiment-2	20×17	7.13	6.45	—	—	—	—	63.4
Criticality Experiment-3	19×16	—	—	102.0	1,640	1,234	26.16	105.1

- (1) Only Criticality-Experiment-1 has one cluster. Other experiments have 3 clusters in series. The fuel rod pitch is 20.32mm.
- (2) Plate thickness including 1.02mm thick aluminum cladding material on both sides.
- (3) Distance from cell boundary of cluster.

Proprietary Information Withheld Pursuant to 10 CFR 2.390

Table II-E. 7 Results of Criticality Experiment Analysis

Case	$k_{\text{eff}} \pm \sigma$
1	0.995±0.001
2	0.993±0.001
3	0.998±0.001



Cladding and End Plug: Aluminum

Fuel: UO_2 Powder

UO_2 Weight = 825g/Fuel Rod

^{235}U Enrichment = 2.35 wt%

UO_2 Density = 9.20 g/cm³

Fig. II-E. 6 Specification of Fuel Rod used for Criticality Experiment

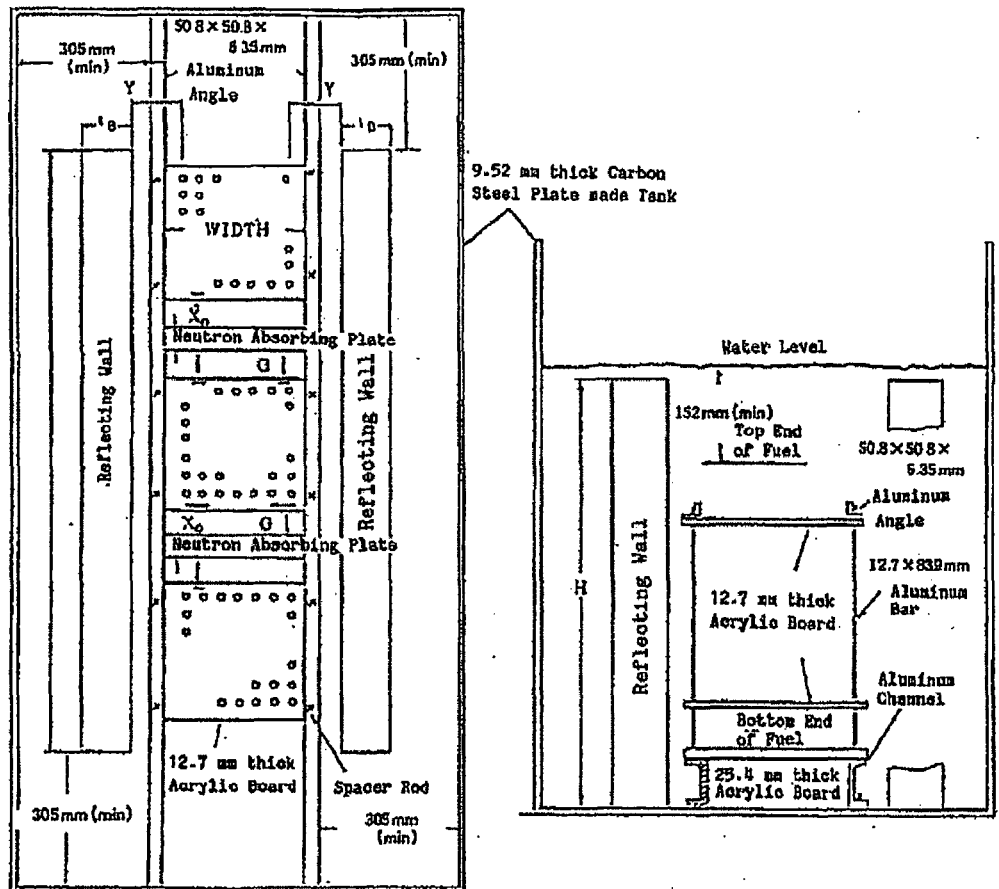


Fig. II-E. 7 Criticality Experiment System

**II-F TEST REPORT OF PROTOTYPE PACKAGING FOR
MODEL MFC-1 CONTAINER**

ZEG-3222

May 1985

Table of contents

1. Outline	II-F-1
2. Test item	II-F-1
3. Test place and schedule	II-F-1
4. Used equipments	II-F-5
4.1 Test article	II-F-5
4.2 Used equipments	II-F-11
4.2.1 Mechanical test	II-F-11
4.2.2 Thermal test	II-F-12
4.2.3 Inspection for containment-ability of fuel assembly	II-F-12
4.3 Used tools	II-F-12
5. Mechanical test	II-F-20
5.1 Test procedure	II-F-20
5.2 Adjustment of drop orientation	II-F-21
5.3 Measurement items and measurement points	II-F-28
5.4 Test results	II-F-30
5.4.1 Vertical drop (bottom downward orientation)	II-F-30
5.4.2 Horizontal drop (0° direction downward orientation)	II-F-31
5.4.3 Corner drop (top 0° direction downward orientation)	II-F-31
5.4.4 Horizontal drop (180° direction downward orientation)	II-F-32
5.4.5 Horizontal drop (90° direction downward orientation)	II-F-33
5.4.6 1m horizontal puncture test	II-F-33
(mechanical test II, 180° direction downward orientation)	
5.4.7 1m vertical puncture test	II-F-34
(mechanical test II, bottom downward orientation)	
6. Thermal test	II-F-42
6.1 Test procedure	II-F-42
6.2 Measuring method	II-F-42
6.3 Test condition and measurement results	II-F-42
6.4 Condition after completion of test	II-F-43

7. Inspection for containment-ability of fuel assembly	II-F-51
7.1 Outline of test	II-F-51
7.2 Test article	II-F-51
7.3 Used equipments	II-F-51
7.4 Test method	II-F-52
7.4.1 Taking out of dummy fuel rod	II-F-52
7.4.2 Helium leak test	II-F-52
7.5 Test results	II-F-52
8. Evaluation of test results	II-F-54
9. 9m drop test of skin part model used boronated stainless steel	II-F-55

1. Outline

In this time, the following tests were carried out by using 2 prototype packagings to confirm the soundness of packaging and its contents for development of MFC-1 type packaging.

- (1) Strength test (drop test I, drop test II) (Re : Para. 627(a) and (b))
- (2) Thermal test (Re : Para. 628)
- (3) Inspection for containment-ability of fuel assembly (Re : Para. 633)

2. Test item

The test items carried out in this time are shown as follows.

- (1) Drop test I (9m drop) (free drop from a height of 9m)
 - (a) Vertical drop
 - (b) Horizontal drop
 - (c) Corner drop
- (2) Drop test II (1m drop) (free drop from a height of 1m onto the specified steel round bar or puncture drop)
 - (a) Vertical drop
 - (b) Horizontal drop
 - (c) Corner drop
- (3) Thermal test
 - Furnace test - Method II (left in the environmental condition of 800°C for 30 min.)
- (4) Inspection for containment-ability of fuel assembly (= fuel rods)
 - Confirmation of He gas leak

3. Test place and schedule

- (1) Test place
 - (a) Strength test
Takasago Research & Development Center, Mitsubishi Heavy Industries, Ltd.
1-1, Shinhama 2 Chome, Arai Machi, Takasago City, Hyogo Prefecture
 - (b) Thermal test
Kobe Shipyard & Machinery Works, Mitsubishi Heavy Industries, Ltd.
1-1, Wadasaki Cho, Hyogo-ku, Kobe City, Hyogo Prefecture
 - (c) Inspection for containment-ability of fuel assembly
Tokai Plant, Mitsubishi Nuclear Fuel Co., Ltd.
622, Oaza Funaishigawa, Tokai Village, Naka-Gun, Ibaragi Prefecture
- (2) Schedule
The test schedule is shown on Table II-F.1.

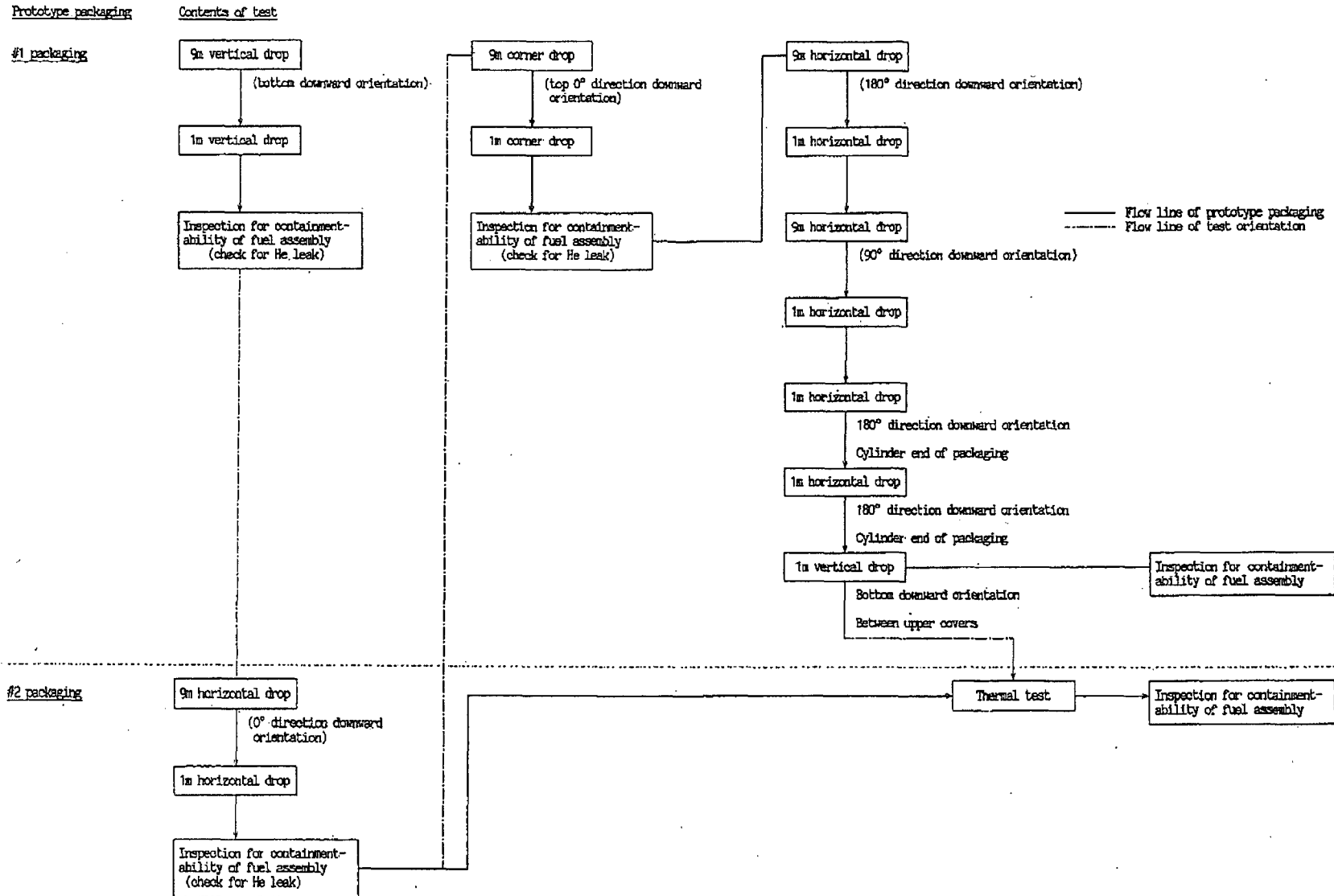
(3) Test procedure

The test procedure is shown on Table II-F.2.

Table II-F.1 Test schedule of Model MFC-1 packaging

	1984			1985									
	December			January			February			March			April
	1	11	21	1	11	21	1	11	21	1	11	21	i
1 Preparation of prototype packaging													
(1) Fabrication													
• Model MFC-1 packaging													
• Dummy fuel assembly													
• Dummy weight													
(2) Preparation of test													
2 Prototype packaging test													
(1) Drop test													
(2) Thermal test													
(3) Inspection for containment-ability of dummy fuel assembly													
(4) Report													

Table II-F-2 Test procedure of prototype packaging



4. Used equipments

4.1 Test article

(1) Prototype packaging 2 pcs [see Fig. II-F.1]

2 prototype packagings similar to actual packaging were fabricated as a test article for strength and thermal tests. The dimensions, weight and material of major parts of prototype and actual packgings are shown on Table II-F.3.

(2) Dummy fuel assembly 2 pcs [see Fig. II-F.2]

Dummy fuel assembly has the same dimensions and shape as those of actual 15×15 type fuel assembly. Only fuel pellet is different from the actual fuel assembly, and Pb-Sb made one is used for the drop test and W-Ni-Cu made one is used for the thermal test.

(3) Dummy weight 2 pcs [see Fig. II-F.3]

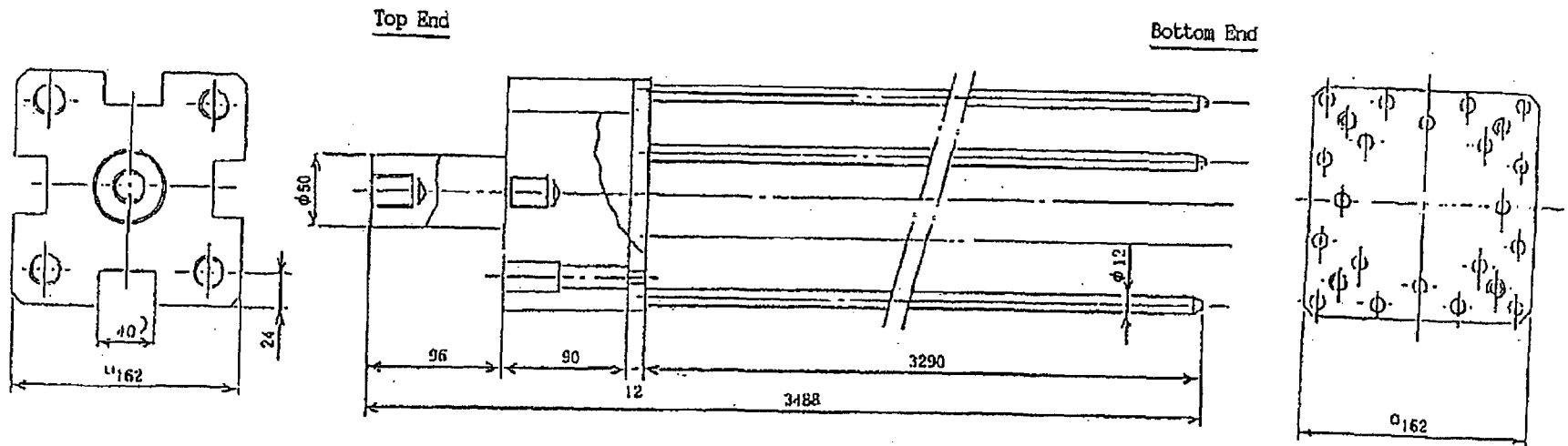
The shape is same as that of 15×15 type 12 feet dummy fuel assembly and the weight is same as that of 17×17 type 12 feet dummy fuel assembly. One piece is loaded in each prototype packaging.

(4) Weight for adjustment 2 pcs [see Fig. II-F.4]

This is to adjust the weight of dummy fuel assembly so that it becomes same as the weight of 17×17 type 12 feet fuel assembly.

Proprietary Information on Pages II-F-6 through II-F-8
Withheld Pursuant to 10 CFR 2.390

II-F-10



Unit : mm

Fig. II-F.4 Weight for adjustment of dummy fuel assembly

4.2 Used equipments

4.2.1 Mechanical test

(1) Target for drop tests

The used target for drop tests is formed with a ferro-concrete block of 7m length×4m breadth×1.5m depth and a steel plate of 6m×3m×50mm laid on the block. Total weight of target is about 99.5 tons and approx. 20 times the weight of prototype packaging. [see Fig. II -F.5, Photo 1]

(2) Cutting-off device

The cutting-off device is shown on Fig. II -F.6. The cutting-off device is operated electromagnetically and the maximum lifting capacity is 5 tons. (see Photo 2)

(3) Puncture bar (drop test II)

The penetration bar with 150mm×350mm in dimension is made of steel and mounted rigidly on the drop target by bolts. [see Fig. II -F.7, Photo 3]

(4) Crane vehicle

A crane vehicle with lift 30m and lifting capacity 35 tons was used. [see Fig. II -F.8]

(5) Acceleration converter

Acceleration converters for single axis and 3 axes [type : AS-1000A (single axis), AS-1000TA (3 axes), capacity 1000×g] were used. Data were recorded by a data recorder through an amplifier, and printed on a chart sheet.

(6) High speed camera

Phtographs were taken at high speed (500 pictures/sec) for each drop posture to investigate the behavior before/after touching the drop target. (type : 16HD, manufacturer : Nack Co.)

(7) Video

Video was taken for each drop posture to record the behavior and deformation before/after touching the drop target, measuring condition, etc.

Camera	type : CV-S-101	Manufacturer : Victor
Deck	type : Macload NV-10000	Manufacturer : National

(8) Measuring tools

Straight scale	: 1.5m, 1m, 15cm
Tape measure	: 5m, 3m
Vernier caliper	: 1.5m
Radius measure	: 300R, 350R
Gage for angle adjustment	: 12° , 25°

Others

4.2.2 Thermal test

(1) Thermal test furnace

The heat treatment furnace owned by Kobe Shipyard & Machinery Works, 8m×8m, 16m length, was used for thermal test. [see Fig. II-F.9]

(2) Sheath thermo-couple

The sheath thermo-couples, ϕ 1.6CA, 10m length, non-grounded type, were used for thermal test to measure the temperature on each part.

4.2.3 Inspection for containment-ability of fuel assembly

(1) Helium gas leak indicator

4.3 Used tools

Welding machine, gas cutter, torque wrench, spanner, hammer, others

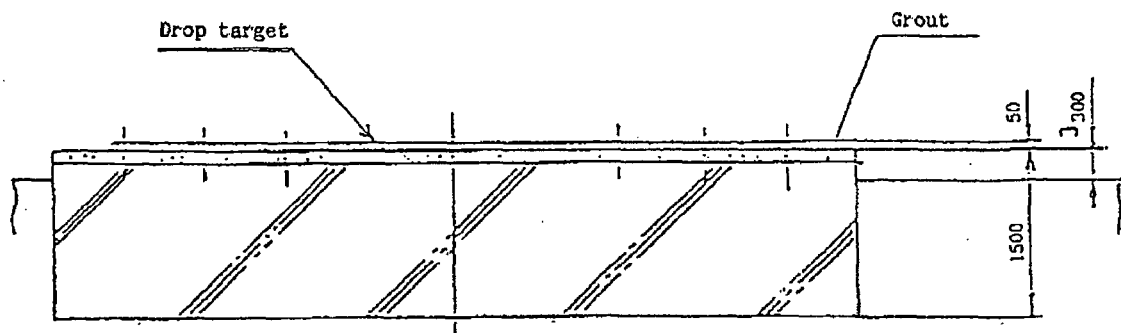
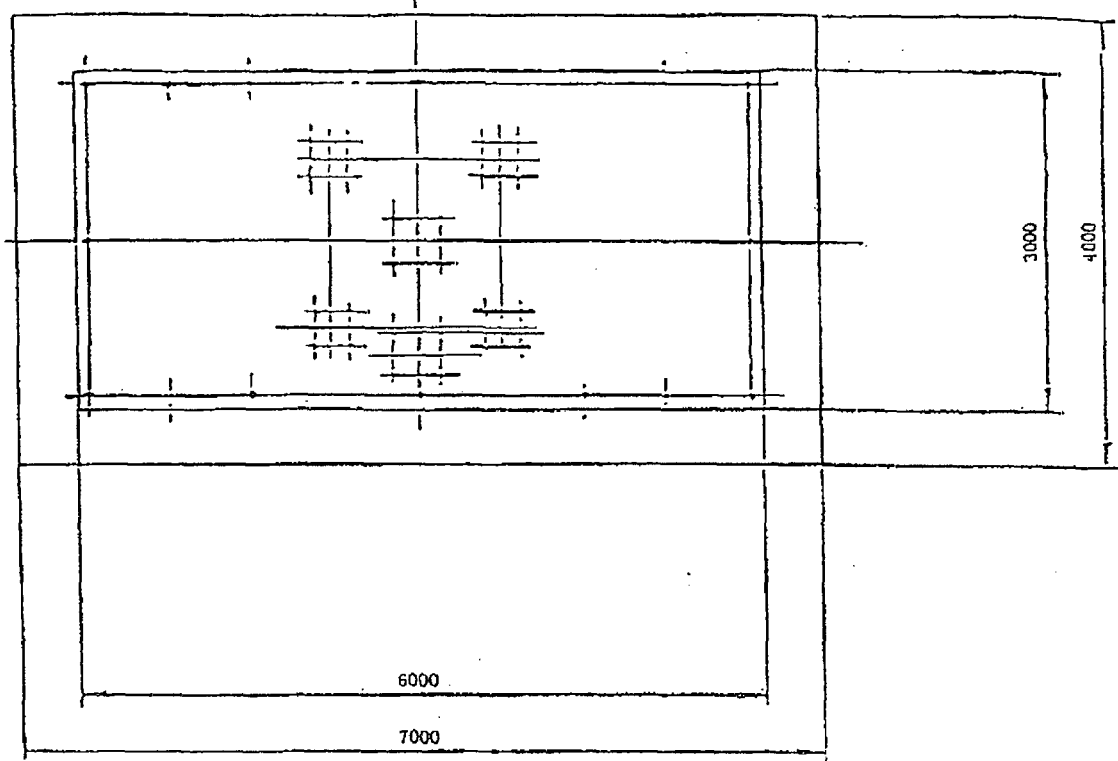


Fig. II-F-5 Target for drop tests

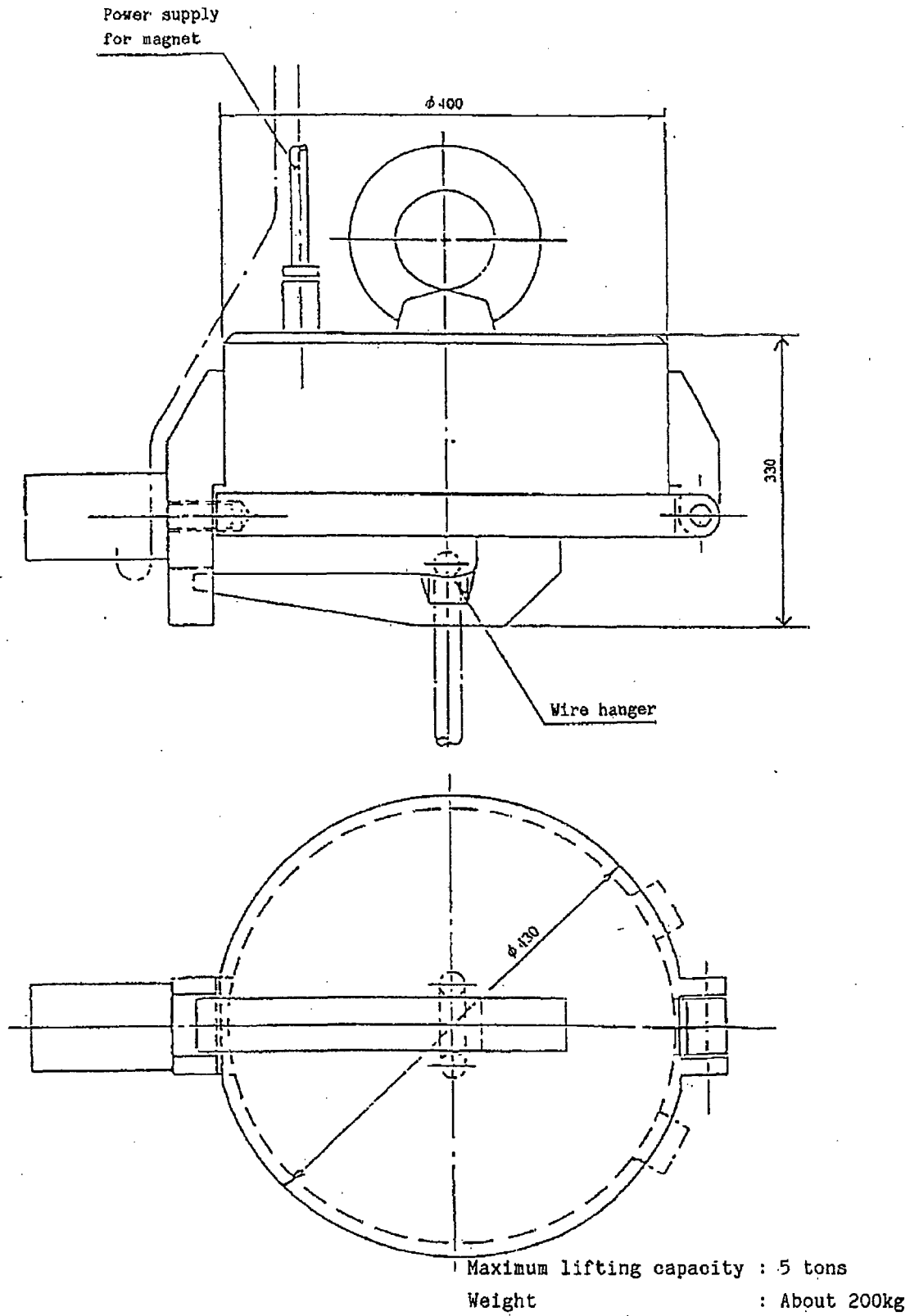


Fig. II -F.6 Cutting-off device

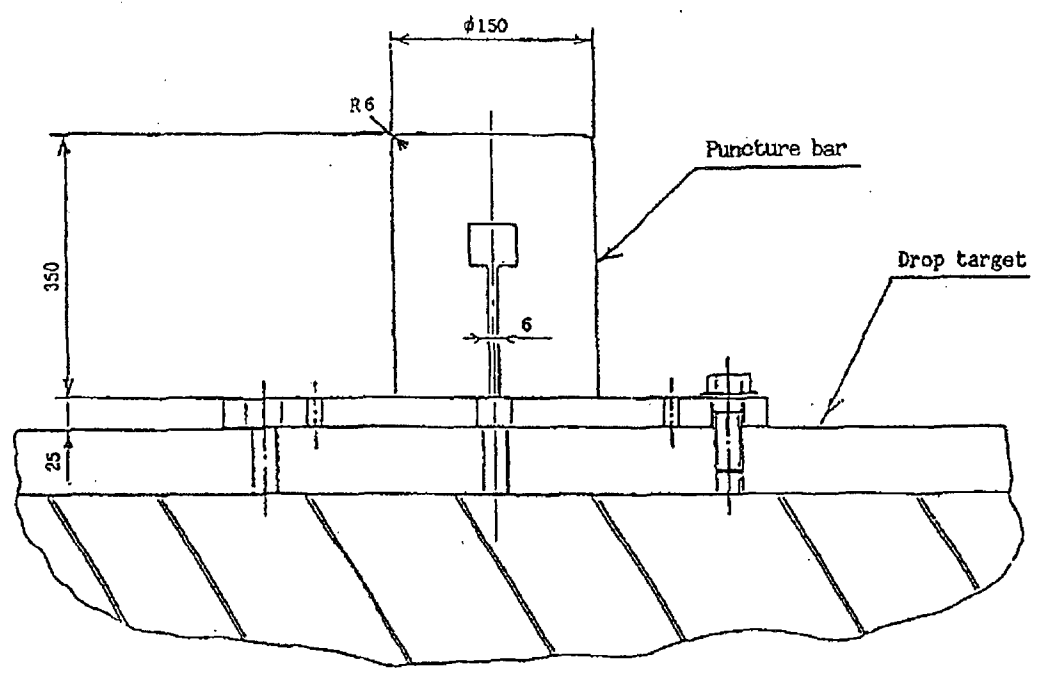
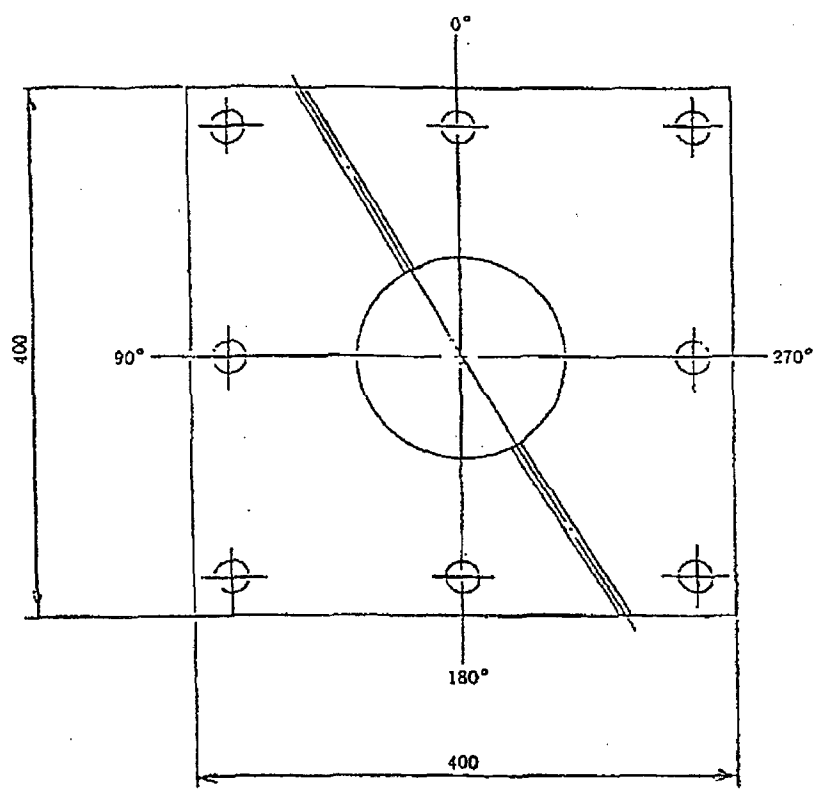


Fig. II-F.7 Puncture Bar

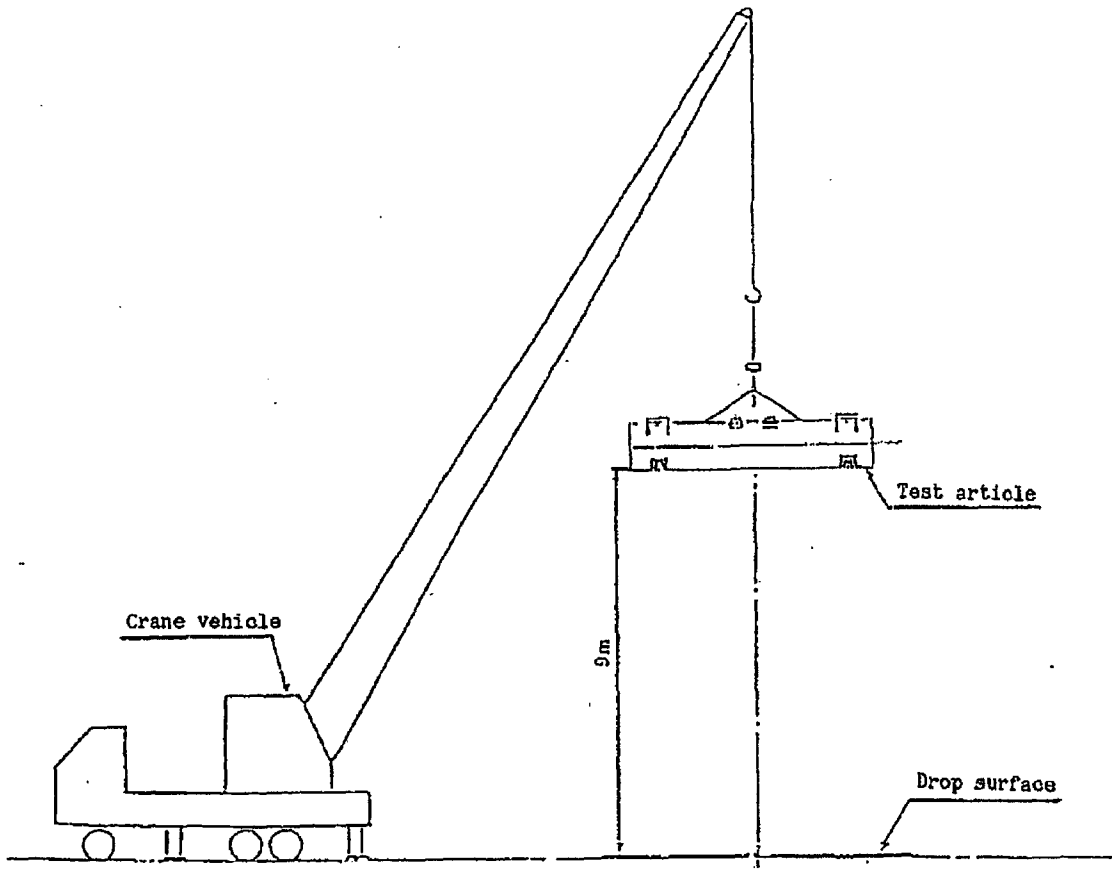


Fig. II-F.8 Crane vehicle

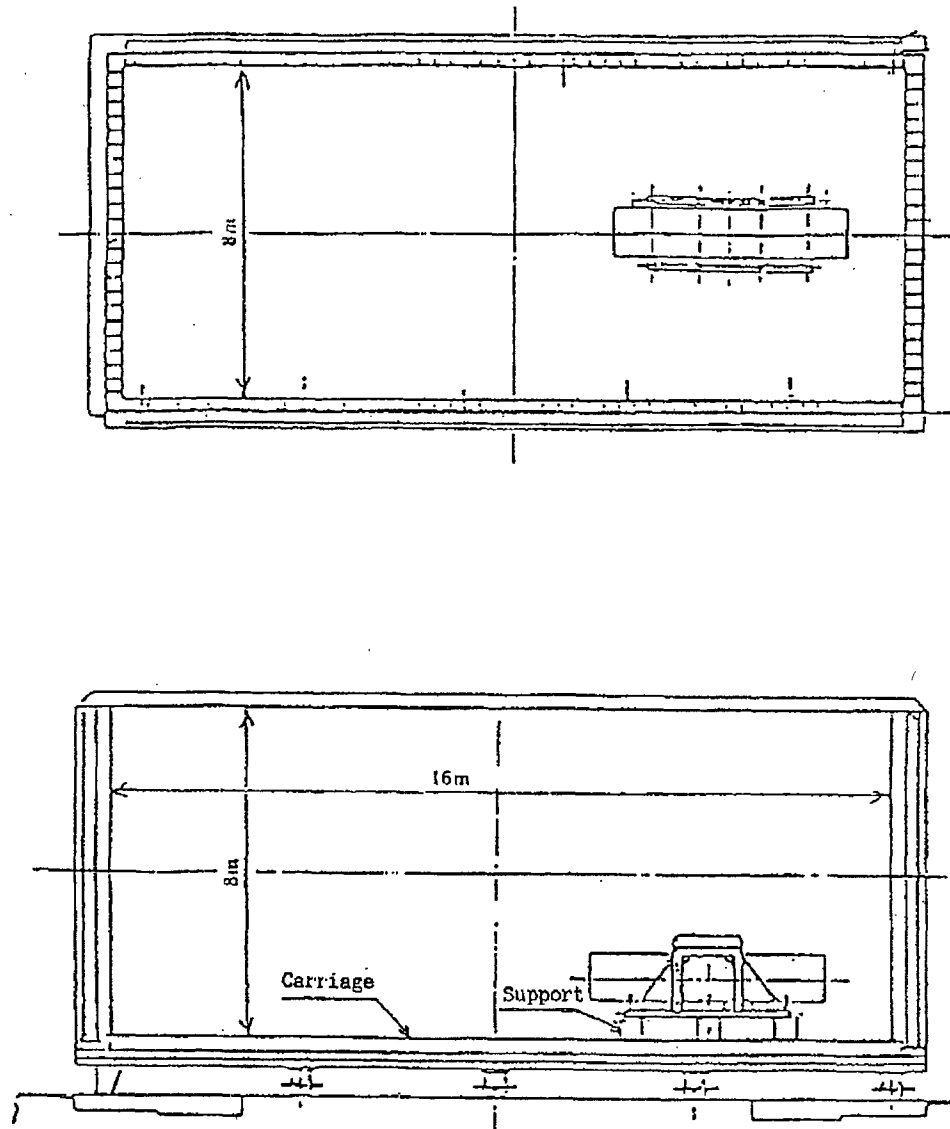


Fig. II -F.9 Thermal test furnace

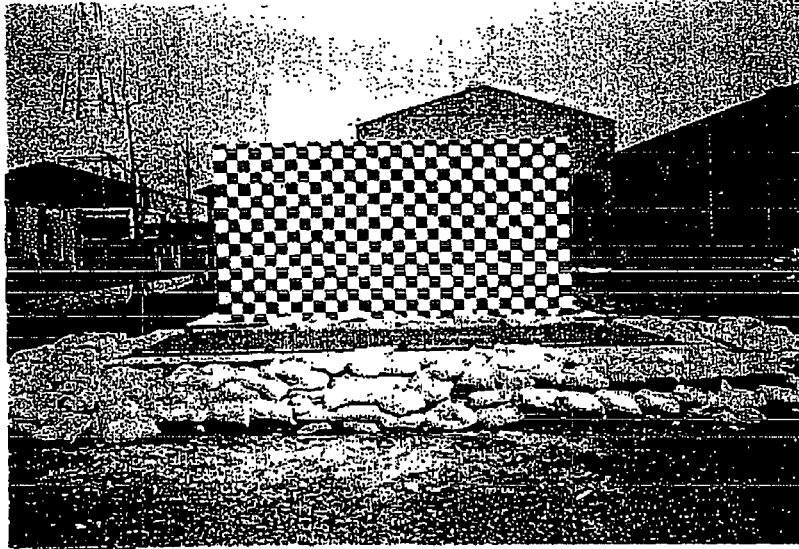


Photo 1 Target for drop tests

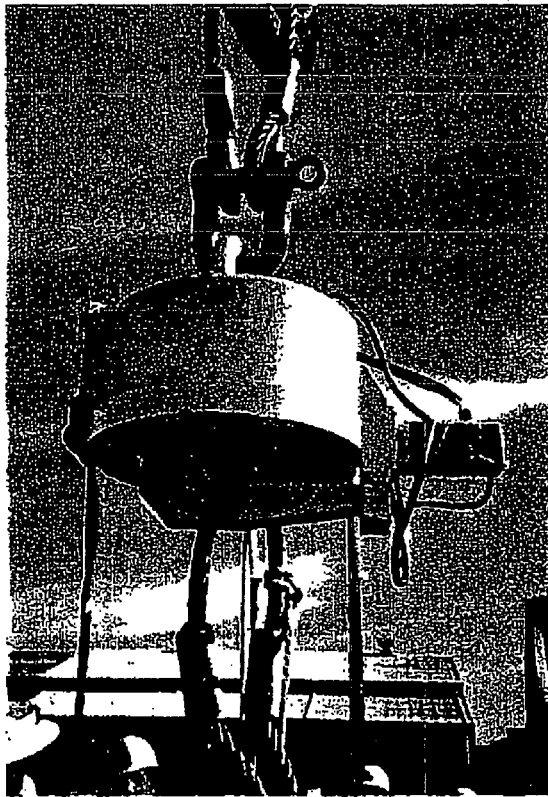


Photo 2 Cutting-off device

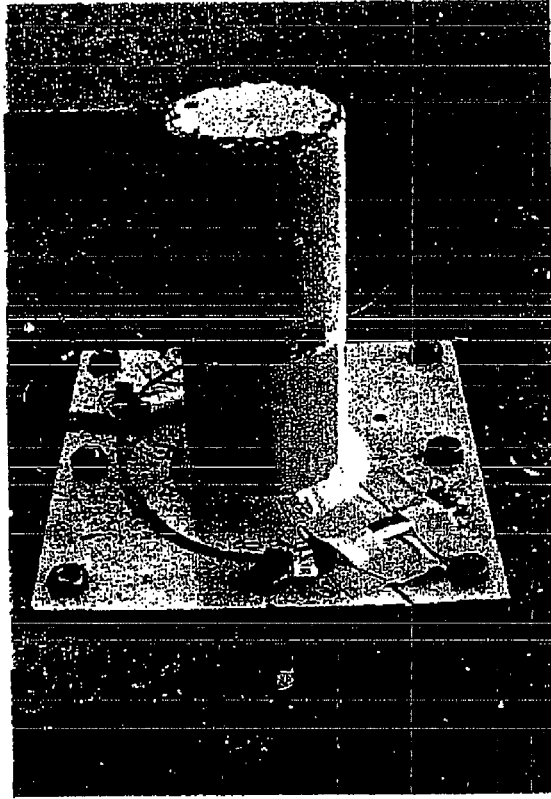


Photo 3 Punoture bar

5. Mechanical test

5.1 Test procedure

(1) 9m drop test (strength test I)

9m drop test is a test to drop the packaging from a height of 9m onto the rigid and non-damageable floor so as to suffer the largest damage on the package. 9m drop test procedure is shown on Fig. II-F.10.

The tests were carried out in the vertical, horizontal and corner postures. The corner drop posture means such posture that the corner of package and the center of gravity of cask are aligned on the perpendicular line.

(2) 1m puncture test (strength test II)

1m puncture test is a test to drop the packaging from a height of 1m onto the puncture bar with 150mm of diameter and 350mm of length rigidly mounted on the floor. The tests were carried out in the vertical, horizontal and corner orientations.

The test procedure is shown on Fig. II-F.11.

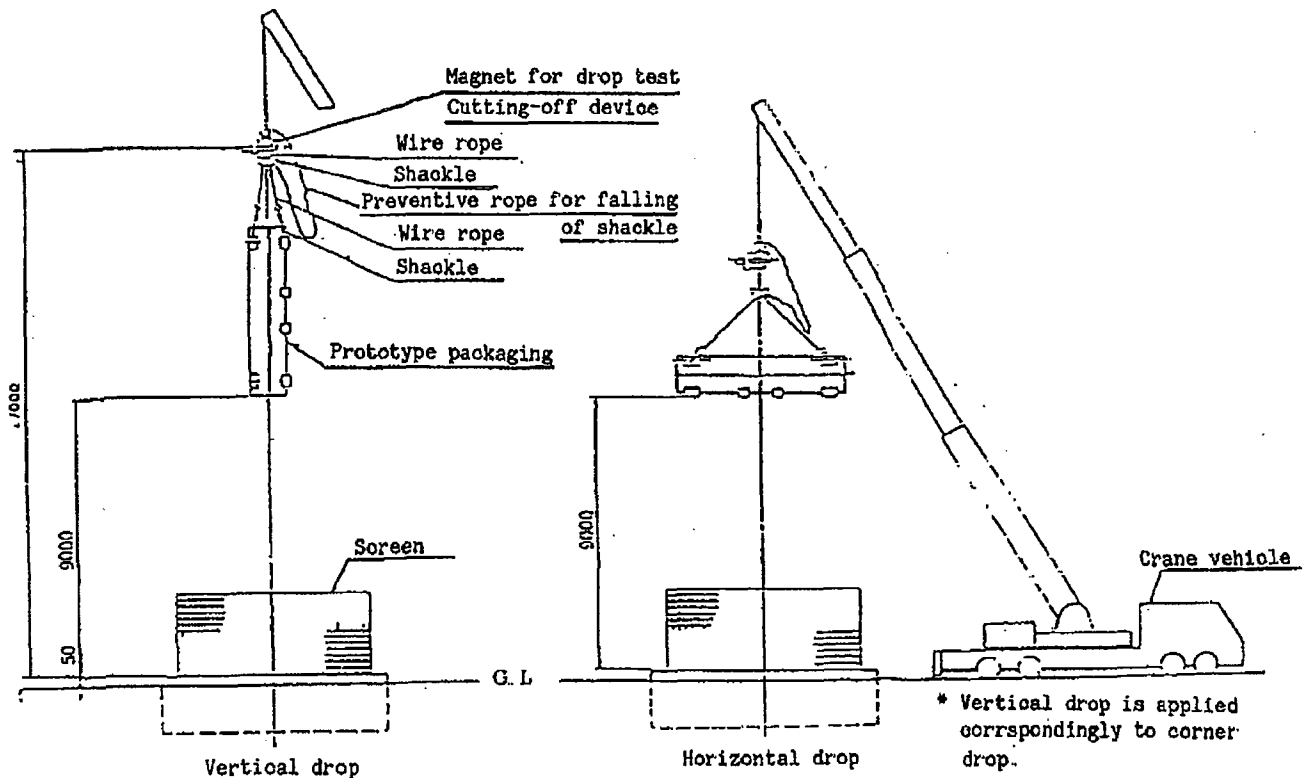


Fig. II-F.10 Drop Test Procedure Drawing (9m Drop Test)

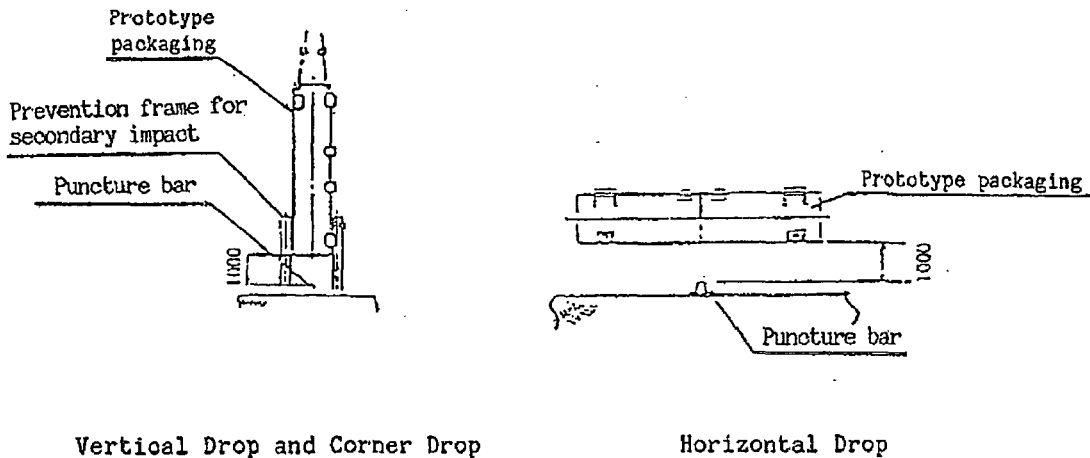


Fig. II -F.11 Outline of Drop Orientation (1m Puncture Test)

5.2 Adjustment of drop orientation

- (1) Vertical drop (#1 packaging, bottom downward orientation) : TEST 1, TEST 2

Vertical drop orientation was adjusted by using 2 eye-plates, which are installed on the inside (top side) of sleeper attachment on the lower part of packaging, and the lifting wire guided through the bracket assembly on the upper cover.

Outline of drop orientation and lifting condition of packaging are shown on Fig. II -F.12 and Photo 4 respectively.

- (2) Horizontal drop (#2 packaging, 0° direction downward orientation) : TEST 3, TEST 4

Horizontal drop orientation was adjusted by using 4 eye-plates, which are installed on the inside of sleeper attachment on the lower part of packaging, and the lifting wire.

Outline of drop orientation and lifting condition of packaging are shown on Fig. II -F.13 and Photo 5 respectively.

- (3) Corner drop (#1 packaging, top 0° direction downward orientation) : TEST 5, TEST 6

Corner drop orientation was adjusted by using each 2 eye-plates, which are installed on the bracket assembly for the inside (bottom side) of sleeper attachment on the lower part of packaging and the upper cover, and the lifting wire.

Outline of drop orientation is shown on Fig. II -F.14.

- (4) Horizontal drop (#1 packaging, 180° direction downward orientation) : TEST 7, TEST 8

Horizontal drop orientation was adjusted by using the lifting wire guided through the bracket assembly on the upper cover side.

Outline of drop orientation is shown on Fig. II-F.15.

(5) Horizontal drop (#1 packaging, 90° direction downward orientation) :
TEST 9, TEST 10

Horizontal drop orientation was adjusted by using each 2 eye-plates, which are installed on the bracket assembly for the inside (270° side) of sleeper attachment on the lower part of packaging and the upper cover, and the lifting wire.

Outline of drop orientation is shown on Fig. II-F.16.

(6) 1m horizontal drop (#1 packaging, 180° direction downward orientation):
TEST 11

Drop orientation was adjusted so that the puncture bar will hit the welds by shifting about 1,300mm the hitting point from the middle of prototype packaging to the top side.

Outline of drop orientation is shown on Fig. II-F.17.

(7) 1m horizontal drop (#1 packaging, 180° direction downward orientation):
TEST 12

Drop orientation was adjusted so that the puncture bar will hit the part between the edge and the welds (steel plate with 6mm thick) by shifting about 1,500mm the hitting point from the middle of prototype packaging to the bottom side.

Outline of drop orientation is shown on Fig. II-F.18.

(8) 1m vertical drop (#1 packaging, bottom downward orientation) : TEST 13

Drop orientation was adjusted so that the puncture bar will hit the middle part between the circumferential edge and the flange (steel plate with 9mm thick).

Outline of drop orientation is shown on Fig. II-F.19.

Verticality and horizontality of drop orientation were confirmed by a transit and the prototype packaging was lifted to a height of 9m or 1m after adjustment.

Drop height was confirmed by fitting a plumb bob (tied weight and string), which is previously adjusted to 9m and 1m in length, on the prototype packaging.

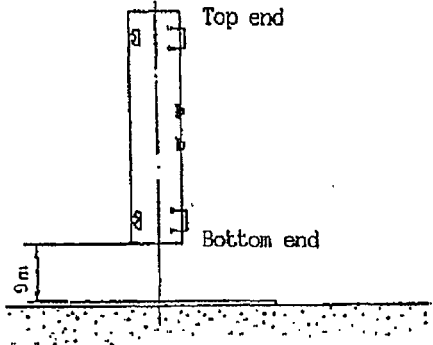
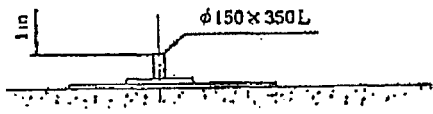
Test article No.	Drop orientation		Test No.
I	9m vertical drop (bottom downward orientation)		Test 1
	1m vertical drop (center of packaging)		Test 2

Fig. II-F.12 Outline of drop orientation

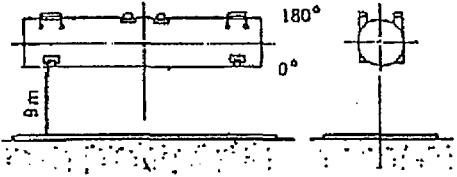
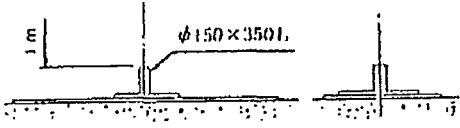
Test article No.	Drop orientation		Test No.
I	9m vertical drop (0° direction downward orientation)		Test 3
	1m horizontal drop (center of packaging)		Test 4

Fig. II-F.13 Outline of drop orientation

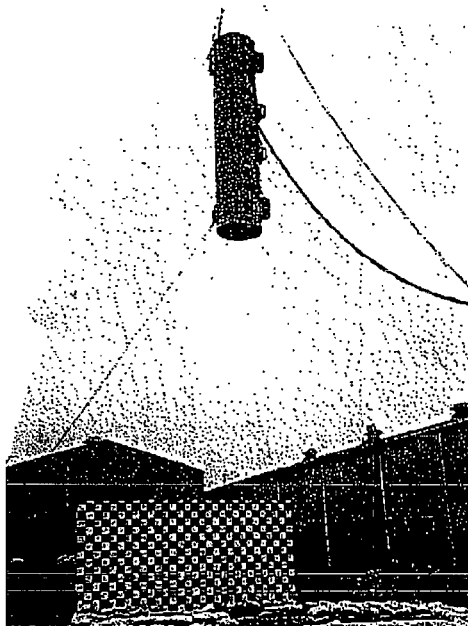
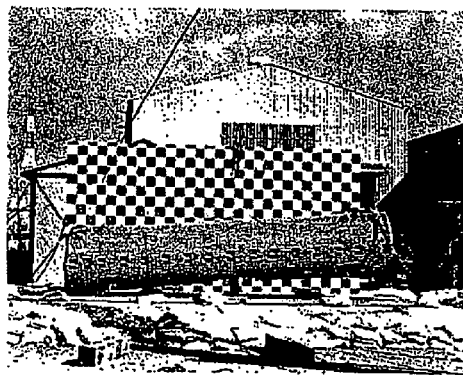
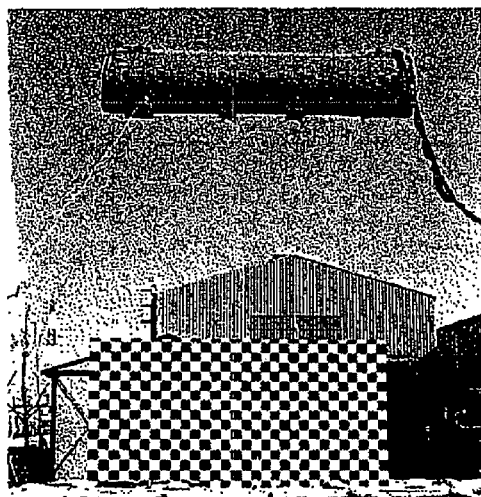


Photo 4 Vertical Drop from a Hight of 9m



(a) Horizontal Drop from a Hight of 9m (b) Puncture Drop from a Hight of 1m

Photo 5

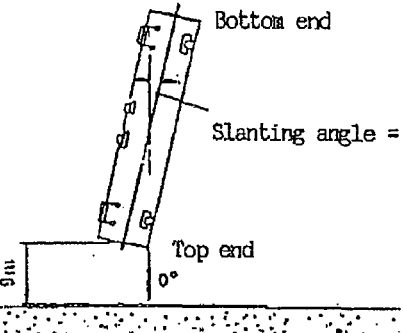
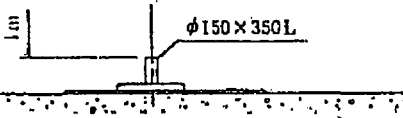
Test article No.	Drop orientation		Test No.
I	9m corner drop (top 0° direction downward orientation)		Test 5
	1m corner drop		Test 6

Fig. II -F.14 Outline of drop orientation

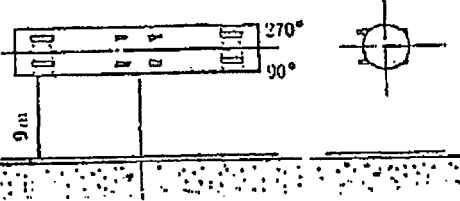
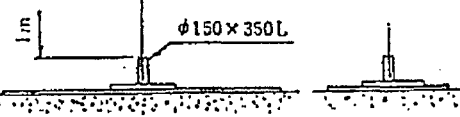
Test article No.	Drop orientation		Test No.
I	9m horizontal drop (180° direction downward orientation)		Test 7
	1m horizontal drop		Test 8

Fig. II -F.15 Outline of drop orientation

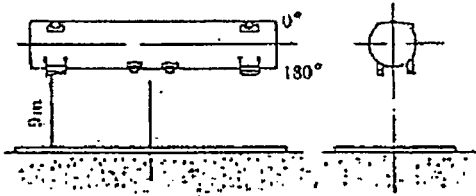
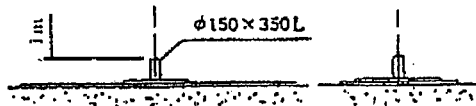
Test article No.	Drop orientation		Test No.
I	9m horizontal drop (90° direction downward orientation)		Test 9
	1m horizontal drop (center of packaging)		Test 10

Fig. II-F.16 Outline of drop orientation

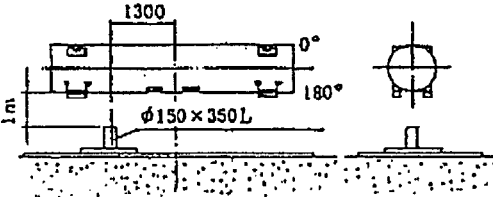
Test article No.	Drop orientation		Test No.
I	1m horizontal drop (180° direction downward orientation) Welds		Test 11

Fig. II-F.17 Outline of drop orientation

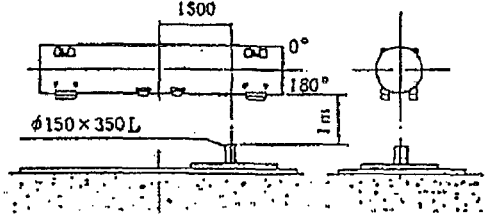
Test article No.	Drop orientation		Test No.
I	1m horizontal drop (180° direction downward orientation) Between the edge and the welds		Test 12

Fig. II-F.18 Outline of drop orientation

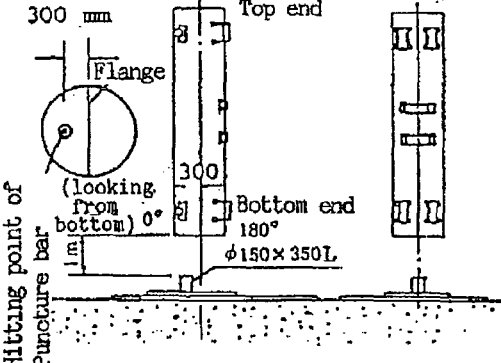
Test article No.	Drop orientation		Test No.
I	1m horizontal drop (bottom downward orientation) [Between the circumferential edge and the flange]		Test 13

Fig. II-F.19 Outline of drop orientation

5.3 Measurement items and measurement points

The measurement items and measurement points are shown on Table II-F.4

Table II-F.4 Measurement Items and Measurement Points

Measurement item	Measurement point
Acceleration	<ul style="list-style-type: none">• Packaging main body• Cross frame
Strain	<ul style="list-style-type: none">• Fuel rod
Residual deformation	<ul style="list-style-type: none">• Outside of packaging body• Inside of packaging body

Located points of accelerometer and strain gage are shown on Fig. II-F.20.

Proprietary Information Withheld Pursuant to 10 CFR 2.390

II - F-29

5.4 Test results

5.4.1 Vertical drop (bottom downward orientation)

(1) 9m drop test (mechanical test I) : TEST 1

(a) Drop condition

The prototype packaging dropped vertically in bottom downward orientation, and stopped with the drop orientation kept after bounding about 50mm on the drop target.

(b) State of prototype packaging

(i) The deformation of about 32mm in the axial direction was observed at the bottom edge of cylindrical part, but crack or fracture was not observed at the weld.

(ii) The upper cover and the flange of fastening bolt box located at the bottom edge of cylindrical part in lower part of packaging were bent, but the fastening bolts were not damaged.

(iii) The clearance at flange was about 6.5mm in the maximum.

(2) 1m puncture test (mechanical test II) : TEST 2

(a) Drop condition

After 9m drop test, 1m puncture test was carried out so that the puncture bar, external diameter 150mm × length 350mm, will hit the center part of circular bottom plate of packaging.

(b) State of prototype packaging

(i) The deformation of about 31mm caused by puncture bar was observed on the hitting part of prototype packaging, but the outer edge plate was not punctured.

(ii) The convex deformation of about 30mm on the bolt box enclosure plate, which is caused by the puncture bar hit the flange and fastening bolt box, was observed in the box inside. However, the clearance at flange was about 6mm in the maximum.

(3) Internal state of prototype packaging

(a) The dummy fuel rod on the bottom nozzle side of dummy fuel assembly was bent about 10mm, but it was confirmed by He leak test carried out after drop test that no crack, fracture, etc. were not generated.

(b) Any deformation was not observed on the clamping frame.

(c) Such behavior as the fuel rod projected from the bottom nozzle was not observed.

5.4.2 Horizontal drop (0° direction downward orientation)

(1) 9m drop test (mechanical test I) : TEST 3

(a) Drop condition

The prototype packaging dropped horizontally with 0° direction directed downward, and stopped with the horizontal drop orientation kept after bounding about 350mm on the drop target.

(b) State of prototype packaging

(i) The deformation of about 27mm was generated by hitting on the cylindrical part, but no crack, fracture, etc. were generated on the welds between the cylindrical part and the end plate.

(ii) The hoisting accessory is strong because it is thicker than the steel plate (t = 4.5mm) on the attachment of outer cylinder plate and its corner is bent at right angles, therefore, the cylinder part dented though any deformation was not observed. However, any crack and fracture was not observed on the welds at the attachment of hoisting accessory.

(iii) The clearance at flange was about 9.2mm in the maximum.

(2) 1m puncture test (mechanical test II) : TEST 4

(a) Drop condition

After 9m drop test, 1m puncture test was carried out so that the puncture bar, external diameter 150mm × length 350mm, will hit the axial center of packaging.

(b) State of prototype packaging

The deformation of about 104mm was observed on the part where the puncture bar hit, but any crack and fracture was not observed on the outer cylinder steel plate.

(3) Internal state of prototype packaging

(a) The whole dummy fuel assembly was slightly bent, but local deformation was not observed. It was confirmed by He leak test carried out after drop test that no crack, fracture, etc. were not generated on the dummy fuel rod.

(b) The clamping frame was partially bent due to plastic deformation, but the function to tie the contents was maintained.

5.4.3 Corner drop (top 0° direction downward orientation)

(1) 9m drop test (mechanical test I) : TEST 5

(a) Drop condition

The prototype packaging was lifted and dropped with top 0° direction directed downward so that the inclined angle of prototype packaging axis will be 12° by aligning the center of gravity of prototype packaging and the packaging corner vertically.

(b) State of prototype packaging

- (i) The hitting part of prototype packaging was deformed with the same inclined angle as the inclined angle 12° of packaging axis, and the deformation was about 42mm. Any crack etc. was not observed on the outer cylinder steel plate and the end plate welds.
- (ii) The fastening bolts were not damaged.
- (iii) The clearance at flange was about 5.5mm in the maximum.

(2) 1m puncture test (mechanical test II) : TEST 6

(a) Drop condition

After 9m drop test, the preventive frame for turnover of packaging was provided on the drop target, and then 1m puncture test was carried out so that the puncture bar, external diameter 150mm X length 350mm, will hit the corner in the top 0° direction of packaging.

(b) State of prototype packaging

The deformation of about 21mm was observed on the hitting part of prototype packaging, but any crack was not observed on the outer cylinder steel plate and the end plate.

(3) Internal state of prototype packaging

- (a) The top edge of dummy fuel assembly was partially bent due to plastic deformation, but the fastening function by jack screw was maintained.
- (b) It was confirmed by He leak test carried out after drop test that no crack, fracture, etc. were generated on the dummy fuel rod.
- (c) Such behavior as the fuel rod projected from the top nozzle was not observed.

5.4.4 Horizontal drop (180° direction downward orientation)

(1) 9m drop test (mechanical test I) : TEST 7

(a) Drop condition

The prototype packaging was dropped with top 180° direction directed downward, and bounded about 400mm after hitting.

(b) State of prototype packaging

The leg of prototype packaging was deformed, but no crack, fracture, etc. were observed on the welds of leg attachment.

(2) 1m puncture test (mechanical test II) : TEST 8

(a) Drop condition

After 9m drop test, 1m puncture test was carried out so that the puncture bar, external diameter 150mm X length 350mm, will hit the center part of packaging.

(b) State of prototype packaging

The deformation of about 294mm was observed on the part where the puncture bar hit, but any crack was not observed on the outer cylinder steel plate.

5.4.5 Horizontal drop (90° direction downward orientation)

(1) 9m drop test (mechanical test I) : TEST 9

(a) Drop condition

The prototype packaging was dropped with 90° direction directed downward in the nearly even condition, and bounded about 500mm at the top side and about 200mm at the bottom side after hitting.

(b) State of prototype packaging

The hit surface was deformed, but no crack was observed on the outer cylinder steel plate and the flange part.

(2) 1m puncture test (mechanical test II) : TEST 10

(a) Drop condition

After 9m drop test, 1m puncture test was carried out so that the puncture bar, external diameter 150mm × length 350mm, will hit the center part of packaging in the axial direction.

(b) State of prototype packaging

The deformation of about 62mm was observed on the part where the puncture bar hit, but any crack was not observed on the outer cylinder steel plate and the flange part.

5.4.6 1m horizontal puncture test (mechanical test II, 180° direction downward orientation)

(1) Eccentricity of 1,300mm from the center of gravity of prototype packaging to the top side : TEST 11

For the drop orientation, the prototype packaging was dropped so that the puncture bar will directly hit the middle part (thickness 6mm) and edge part of packaging and the welds of steel plate.

In this time, the packaging was deformed about 62mm, but no puncture and/or crack were generated.

(2) Eccentricity of 1,500mm from the center of gravity of prototype packaging to the bottom side : TEST 12

For the drop orientation, the prototype packaging was dropped so that the puncture bar will directly hit the steel plate with 4.5mm thick which was shifted by 1,500mm from the center of gravity of prototype packaging to the bottom side.

In this time, the prototype packaging was deformed about 63mm, but no puncture and/or crack were generated.

5.4.7 1m vertical puncture test (mechanical test II, bottom downward orientation) : TEST 13

For the drop orientation, the prototype packaging was dropped so that the puncture bar will directly hit the steel plate with 9mm thick which was shifted by 300mm from the center of gravity of prototype packaging in the 0° direction.

In this time, the prototype packaging was deformed about 39mm, but no puncture and/or crack were generated.

For TEST 1~13 carried out as above, the prototype packaging body was deformed on the hitting part in all cases, but no puncture and/or crack were generated.

In addition, the bend of dummy fuel rod, which is sealing boundary, was observed, but it was confirmed from the results of He leak test that no crack was generated.

For the above tests, the outline of deformed condition of prototype packaging are shown on Fig. II-F.21~Fig. II-F.28, and the impact acceleration and the outline of packaging deformation are shown on Table II-F.5.

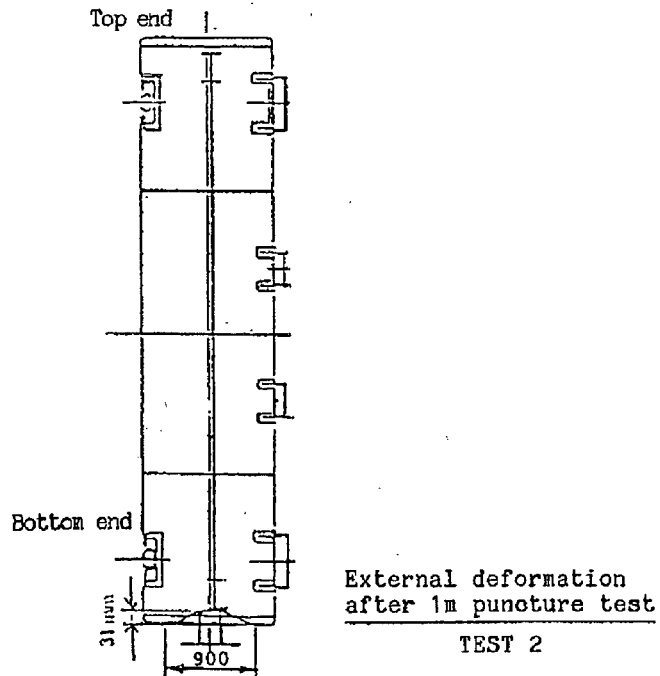
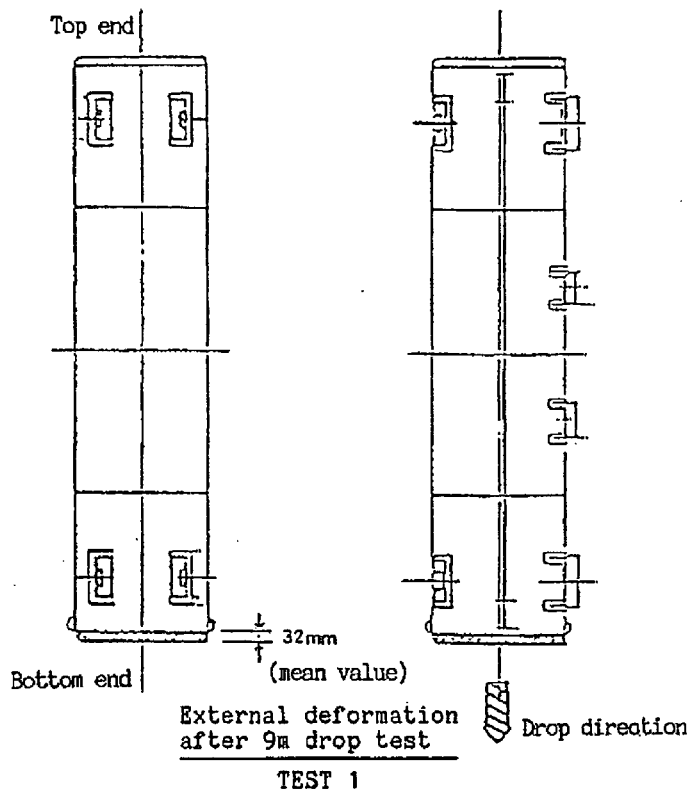
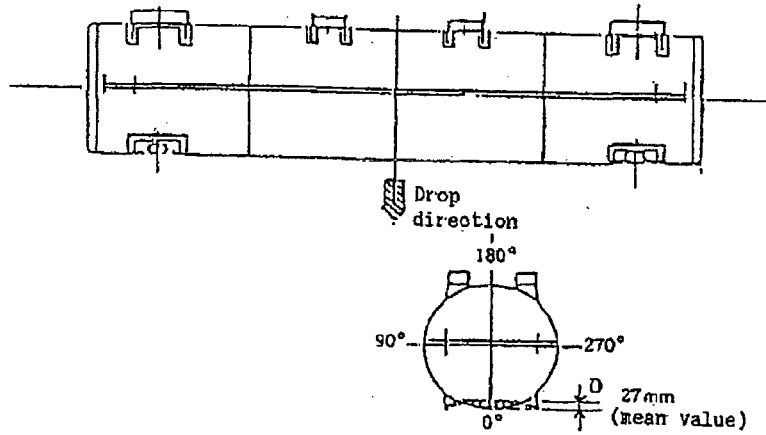
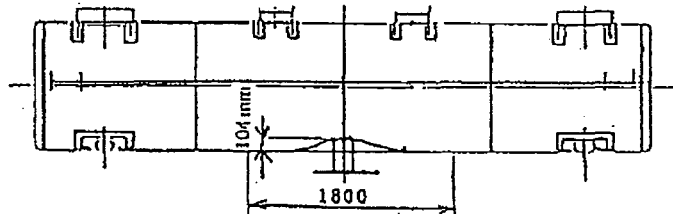


Fig. II -F.21 Vertical Drop Test (9m, 1m bottom downward orientation)
Packaging Main Body (outside)
Deformation Measurement Results (TEST 1, TEST 2)

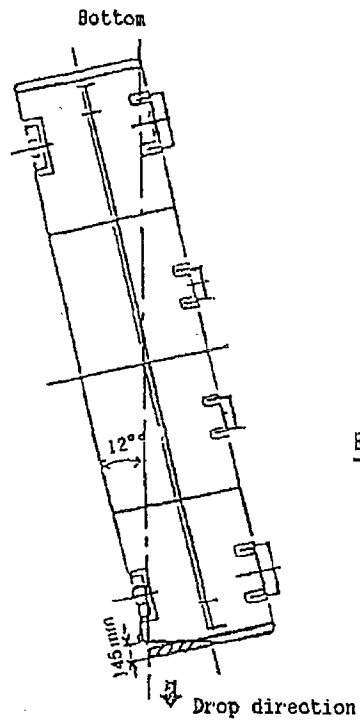


External Deformation after 9m Drop Test
TEST 3

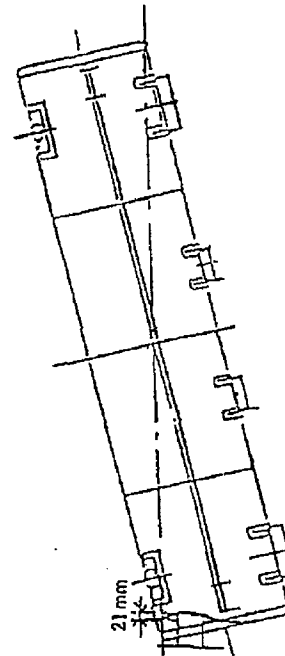


External Deformation after 1m Puncture Test
TEST 4

Fig. II -F-22 Horizontal Drop Test (9m, 1m 0° Direction Downward Orientation) Packaging Main Body (Outside) Deformation Measurement Results (TEST 3, TEST 4)



External Deformation after 9m Drop Test
TEST 5



External Deformation after 1m Puncture Test
TEST 6

Fig. II-F-23 Corner Drop Test (9m, 1m top 0° Direction Downward Orientation) Packaging Main Body (Outside) Deformation Measurement Results (TEST 5, TEST 6)

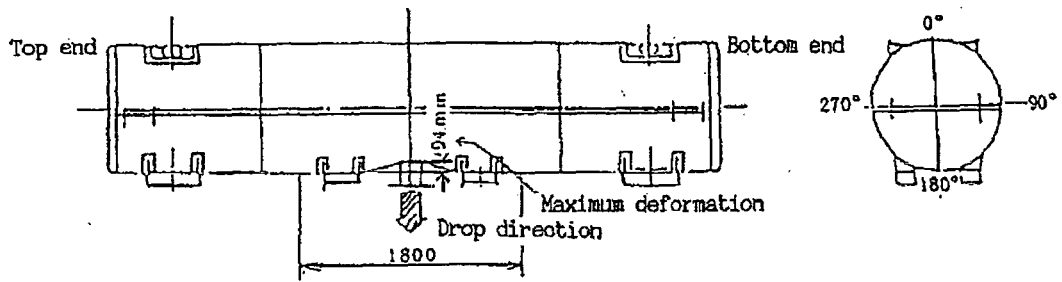


Fig. II -F.24 1m horizontal puncture test (180° direction downward orientation) Packaging main body (outside) Deformation measurement results (TEST 10)

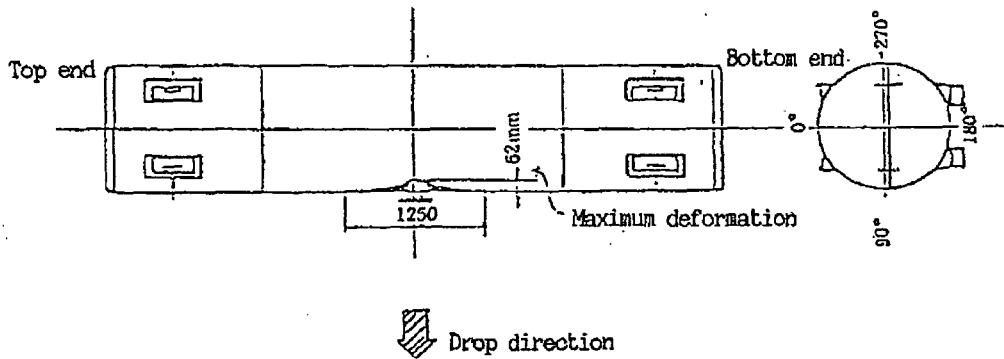


Fig. II -F.25 1m horizontal puncture test (90° direction downward orientation) Packaging main body (outside) Deformation measurement results (TEST 12)

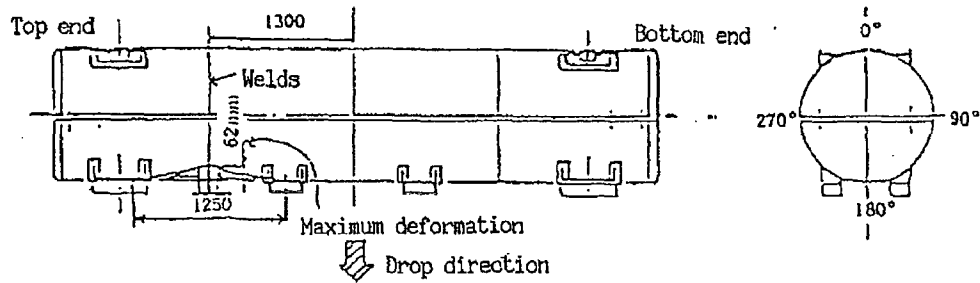


Fig. II-F.26 1m horizontal puncture test (eccentricity to top at 180° direction downward orientation) Packaging main body (outside) Deformation measurement results (TEST 13)

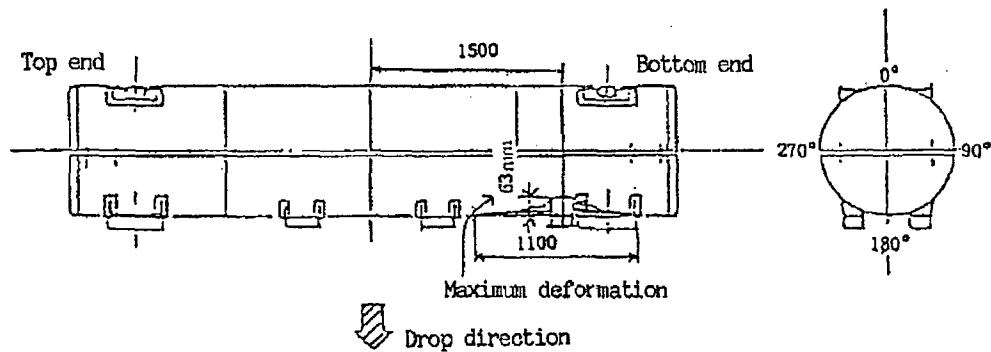


Fig. II-F.27 1m horizontal puncture test (eccentricity to bottom at 180° direction downward orientation) Packaging main body (outside) Deformation measurement results (TEST 14)

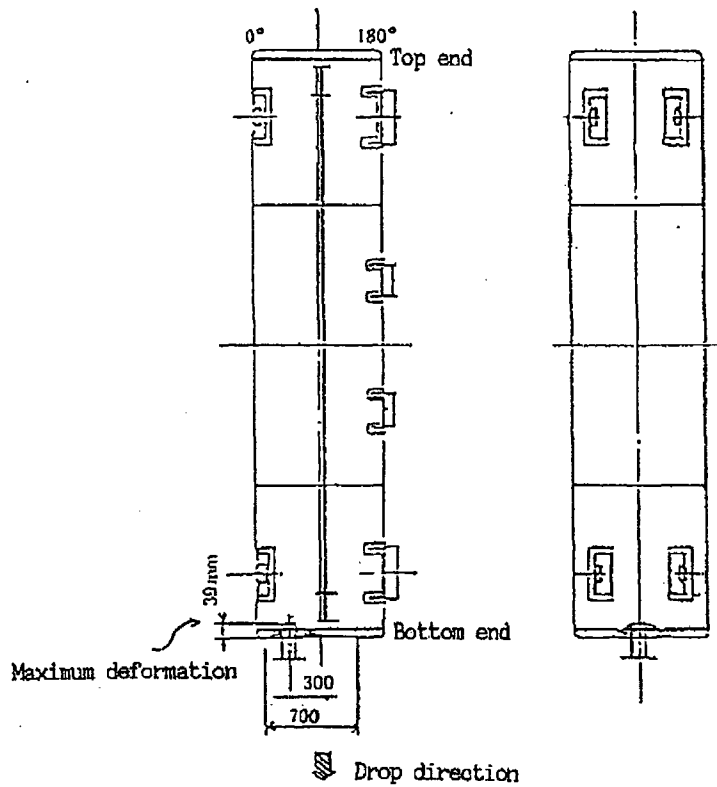


Fig. II -F.28 1m vertical puncture test (eccentricity to bottom direction downward orientation) Packaging main body (outside) Deformation measurement results (TEST 15)

Table II-F.5 Outline of Measurement Results

Test article No.	Test No.	Drop orientation	Drop height	Test value		Impact acceleration (Xg)		Packaging deformation (mm)		Stress at middle of fuel rod (N/mm ²)
				Outer shell	Cradle assembly (cross frame)	Outside	Inside			
#1 packaging	1	Vertical drop (bottom end downward orientation)	9m drop	340	110	32	95	177		
	2		1m puncture	30	35	31	** -	152		
#2 packaging	3	Horizontal drop (0° direction downward orientation)	9m drop	230	320	27	25	550		
	4		1m puncture	20	15	104	** -	-211		
#1 packaging	5	Corner drop (top end 0° direction downward orientation)	9m drop	*174	*123	*142	65	461		
	6		1m puncture	* 36	* 20	21	** -	-98.1		

* : Converted to the acceleration and displacement in the vertical direction.

** : Not measured.

II-F-41

6. Thermal test

6.1 Test procedure

The thermal test is a test to leave the prototype packaging in the environmental condition of 800°C for 30 minutes. The test procedure is shown on Fig. II -F.29.

6.2 Measuring method

CA thermocouple was used for all temperature measurements in the thermal test. The temperature measurements in the thermal test were carried out on the following positions. [see Fig. II -F.30]

- (1) Outside of prototype packaging main body
- (2) Inside of prototype packaging main body
- (3) Space in prototype packaging main body
- (4) O ring
- (5) Fuel assembly

The temperature in the furnace was controlled and recorded by the thermocouple for measuring the environmental temperature in the vicinity of the prototype packaging.

6.3 Test condition and measurement results

The temperature in the furnace was raised from early morning on the test day, and set so that the wall temperature will be 950°C after about 2.5 hours elapsed. The packaging was maintained at this temperature for about 2 hours to equalize the temperature in the furnace.

About 7 minutes was required for the works such as ① opening of furnace door, ② drawing out of carriage in the furnace, ③ mounting of prototype packaging on the carriage, ④ drawing in of carriage, ⑤ closing of furnace door, etc., therefore, the temperature in the furnace was dropped from 950°C to 570°C.

After closing the furnace door, the temperature in the furnace was raised again from 570°C to 800°C during about 5 minutes. Then the thermal test was carried out for 30 minutes with the temperature in the furnace maintained at $825^{\circ}\text{C} \pm 20^{\circ}\text{C}$.

After 30 minutes elapsed, the furnace door was opened and the carriage with prototype packaging was drawn out, then the prototype packaging was shifted to other place by lifting to keep out of heat radiation of carriage and naturally cool down.

The maximum temperature and required time at each measurement point are shown as follows.

- (1) Outside of prototype packaging main body - 812.1°C -
just after completion of thermal test

Proprietary Information Withheld Pursuant to 10 CFR 2.390

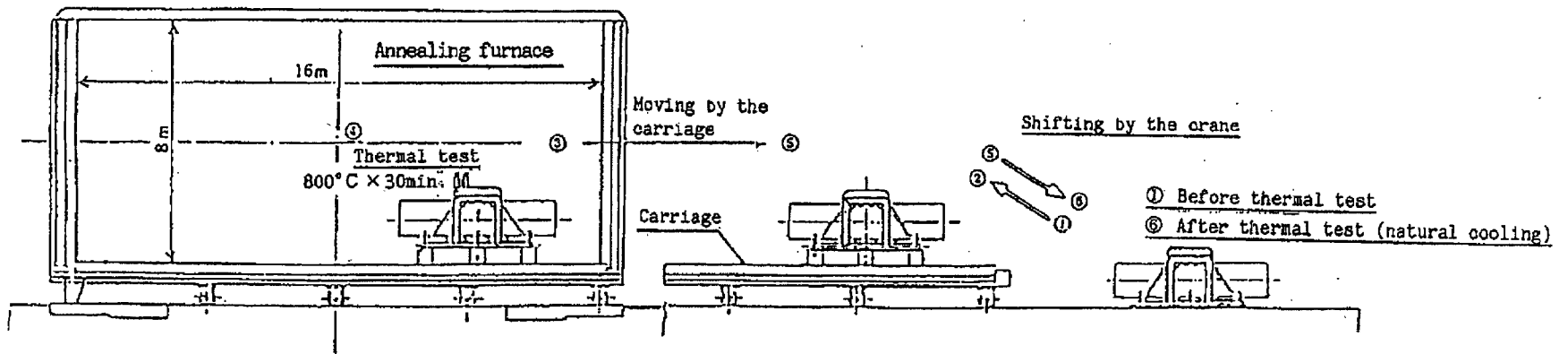
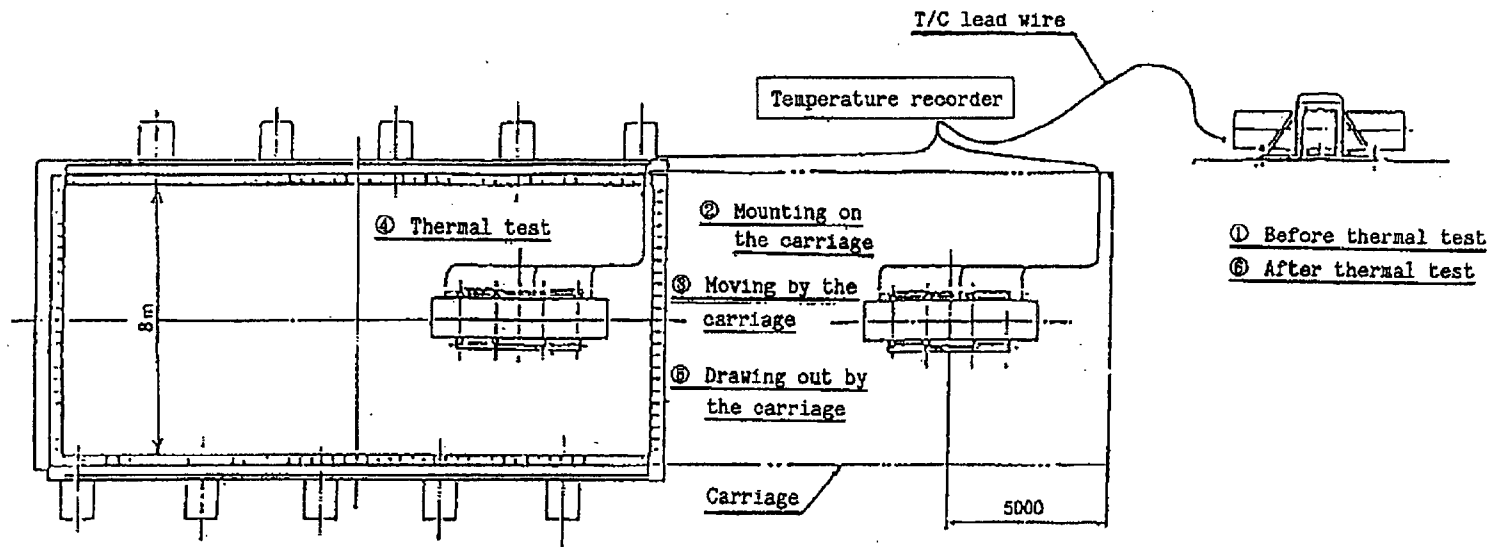


Fig. II.29 Thermal test procedure

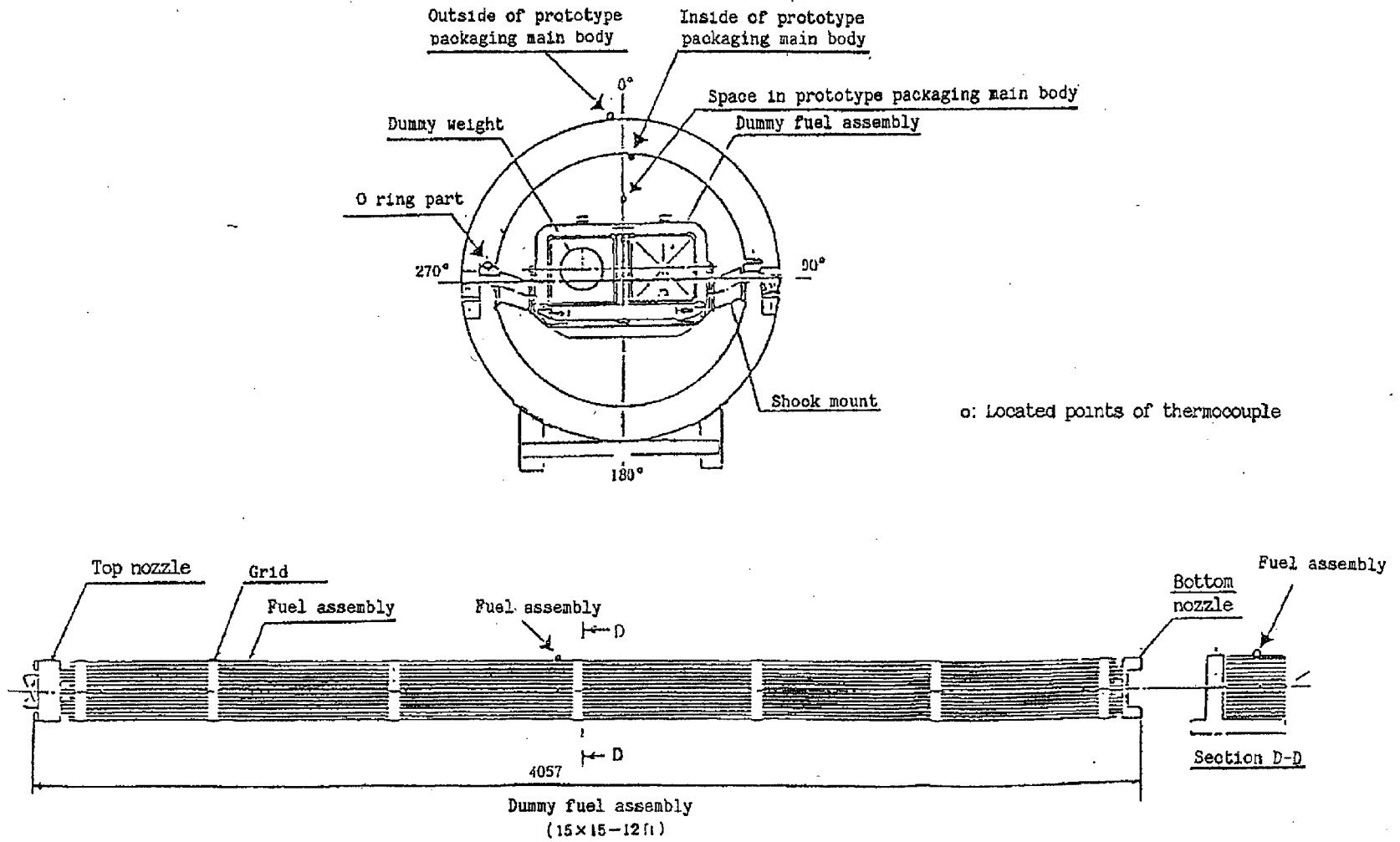


Fig. II-F.30 Temperature Measuring Points During Thermal Test

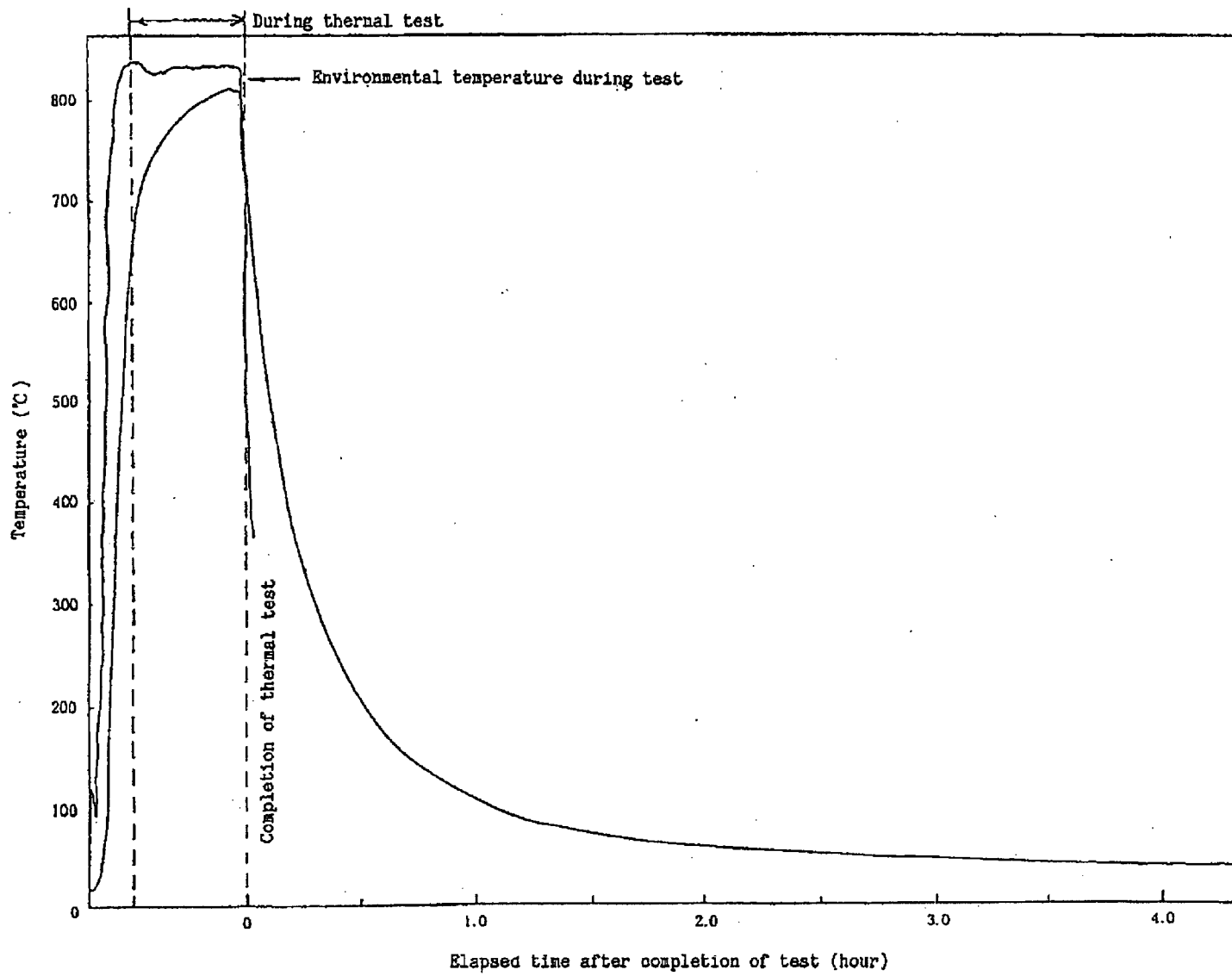


Fig. II-F.31 Thermal test temperature data
(outside of prototype packaging main body)

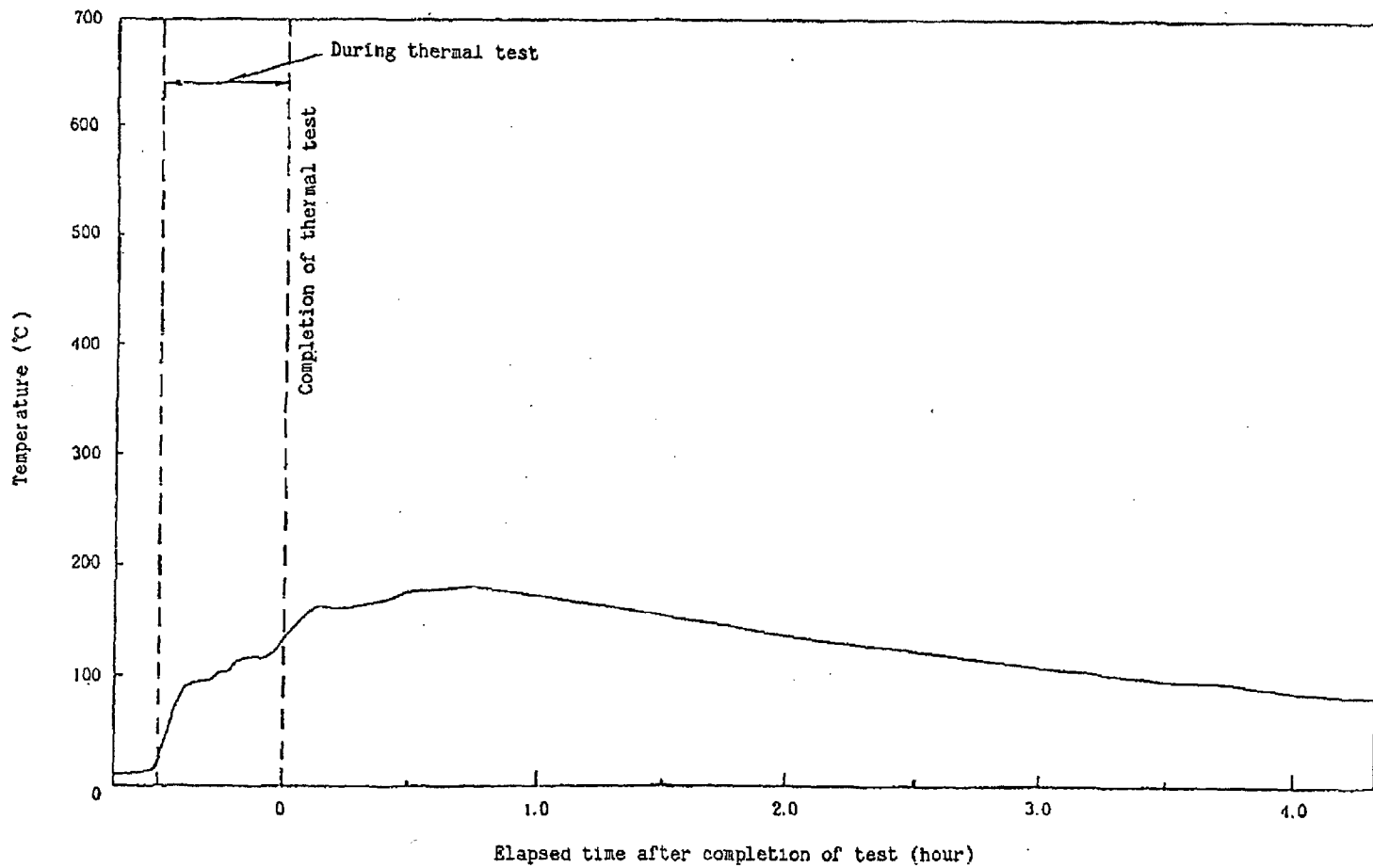


Fig. II-F.32 Thermal test temperature data
(inside of prototype packaging main body)

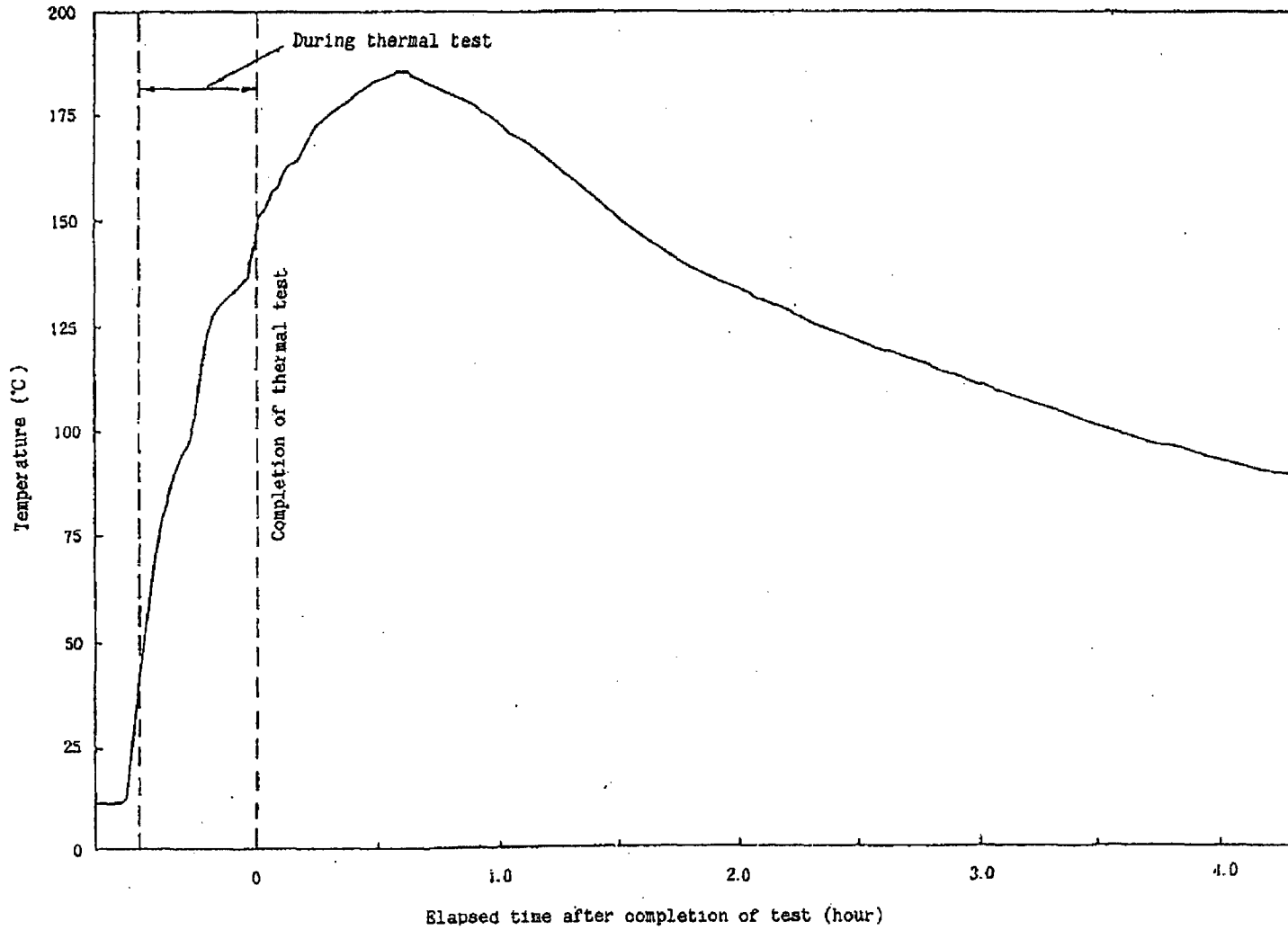


Fig. II-F.33 Thermal test temperature data
(space in prototype packaging main body)

II-F-49

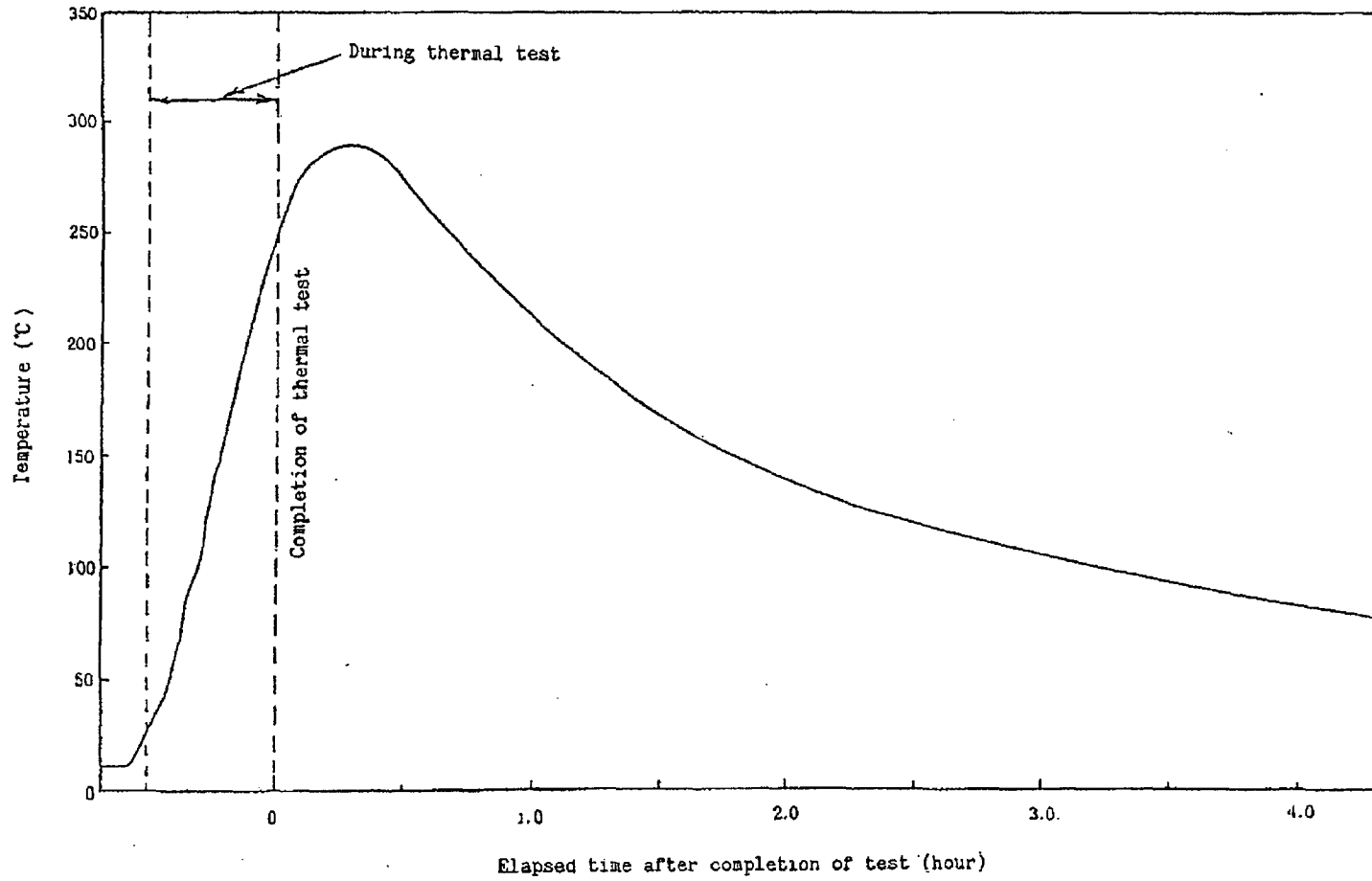


Fig. II-F.34 Thermal test temperature data (O ring part)

II-F-50

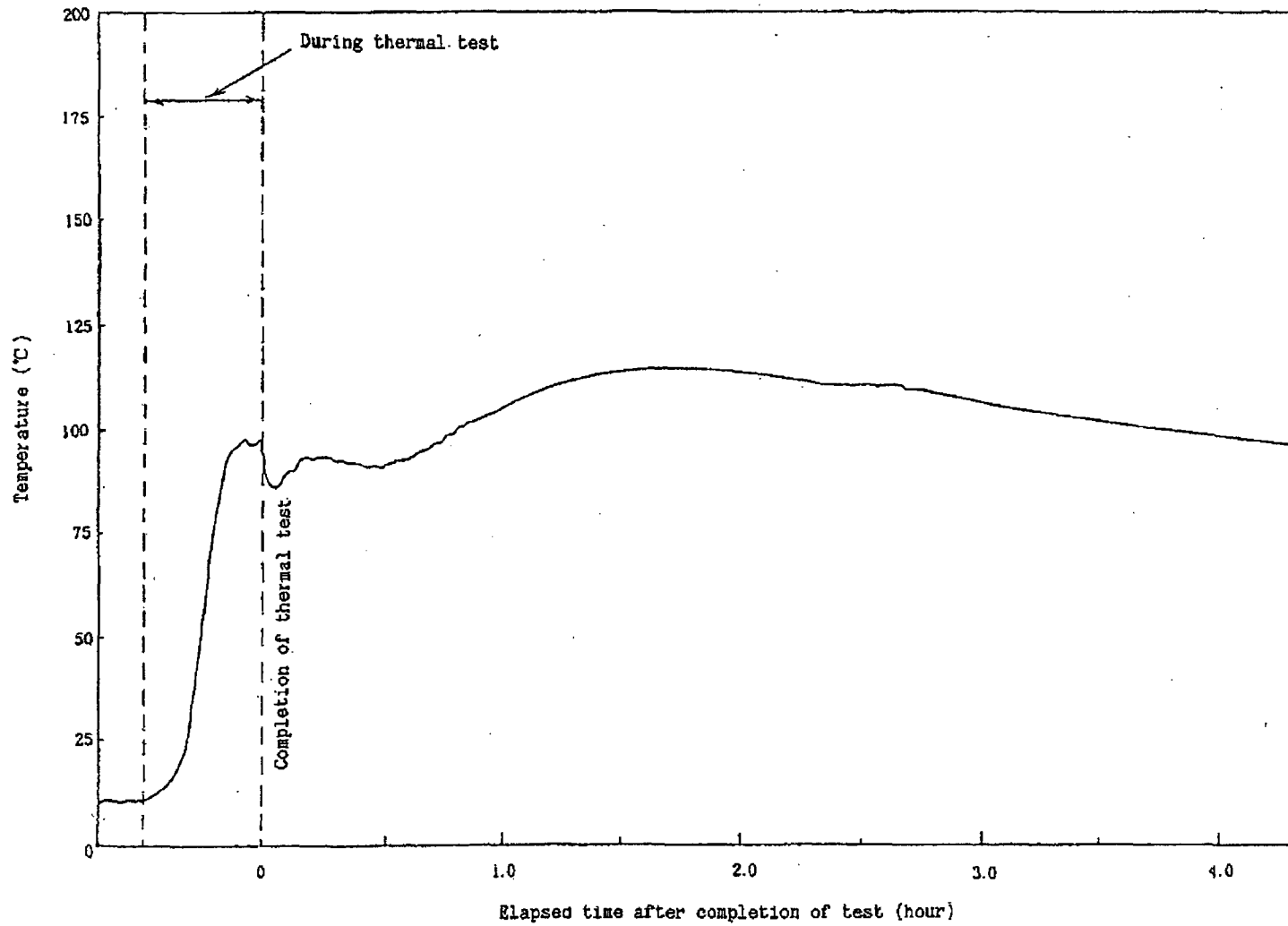


Fig. II-F.35 Thermal test temperature data (fuel assembly)

7. Inspection for containment-ability of fuel assembly

7.1 Outline of test

The He leak test was carried out on the dummy fuel rod used for the prototype packagings for drop test (#1) and thermal test (#2) in order to prove that the fuel rod, which is containment boundary, is not damaged under the prototype packaging tests (drop test I, drop test II, thermal test) for Model MFC-1 packaging. As a result, the leakage is nearly same as the background and considerably lower than the acceptable standard value in the case of new fuel, therefore, the containment-ability of dummy fuel assembly was verified.

7.2 Test article

The specification of dummy fuel rod is shown on Table II-F.6.

Table II-F.6 Specification of Dummy Fuel Rod

	For drop test (#1)	For thermal test (#2)
(Ass'y) No.	DM-47	DM-48
(Ass'y) Type	15×15 - 12 ft	Same as the left
Shield tube	Zircaloy-4	Same as the left
End plug	Zircaloy-4	Same as the left
Pellet	Pb-Sb	W-Ni-Cu
Charged pressure of He gas	3.10MPa · G	Same as the left
No. of fuel rods	30 pcs	30 pcs

7.3 Used equipments

- (1) Helium leak detector : 24-120B type (manufactured by Du Pont)
Maximum sensibility 2×10^{-10} atm · cm³/s
- (2) Vacuum chamber : $\phi 260 \times L 5,000$ mm

7.4 Test method

7.4.1 Taking out of dummy fuel rod

As shown on Fig. II-F.36, 30 dummy fuel rods in total were taken out from the dummy fuel assembly used for verification test, each 15 pcs from upper 2 lines (A, B), after cutting the grid by using a tinman's shear and cutting plier. After taking out, the dummy fuel rods were visually inspected on the surface table to confirm that no defect exists.

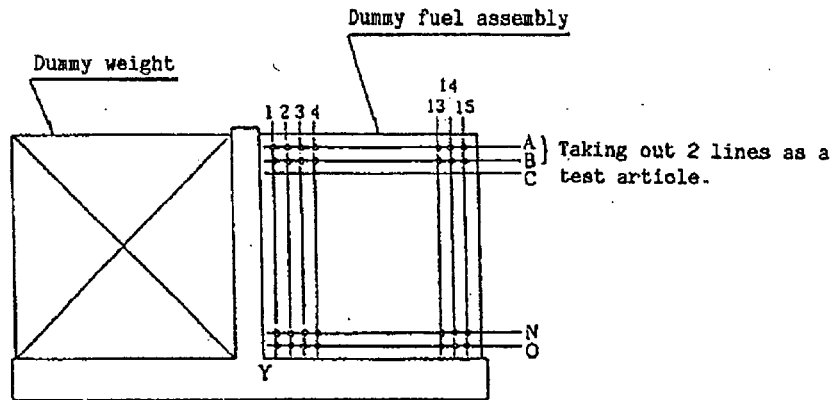


Fig. II-F.36 Taking out of dummy fuel rod

7.4.2 Helium leak test

The helium leak test was carried out after dividing the dummy fuel rods into the following groups and placing them in each channel.

- Ass'y No. DM-47
 - A line (1~ 15) : Group 1
 - B line (1~ 15) : Group 2

- Ass'y No. DM-48
 - A line (1~ 15) : Group 3
 - B line (1~ 15) : Group 4

7.5 Test results

The leakage on both of dummy fuel rod for drop test and thermal test is less than the acceptable standard value (1×10^{-8} atm · cm³/s) in the case of new fuel and nearly same as the background as shown on Table II-F.6, so that, it was confirmed that no leak exists.

Table II-F.7 Results of Helium Leak Test

Item		Group 1	Group 2	Group 3	Group 4
Date carried out		1985.2.22	1985.2.22	1985.2.22	1985.2.22
Time		10:00	10:00	11:20	11:20
Temperature		21°C	21°C	21°C	21°C
Standard helium leakage rate (atm · cm ³ /s)		2.83 × 10 ⁻⁸	2.83 × 10 ⁻⁸	2.83 × 10 ⁻⁸	2.83 × 10 ⁻⁸
Range of instrument		5	5	5	5
Graduation for standard leak		32	32	32	32
Graduation for background		2	2	2	2
Acceptable standard graduation		10	10	10	10
Acceptable standard value (atm · cm ³ /s)		(1 × 10 ⁻⁸)	(1 × 10 ⁻⁸)	(1 × 10 ⁻⁸)	(1 × 10 ⁻⁸)
Measured value	Read value	2	2	2	2

8. Evaluation of test results

As a result of 9m drop test and 1m puncture test, the dummy fuel assembly was in the normal condition though the surfaces of upper cover and lower part of packaging, which form the outer shell, was deformed. On the other hand, it was confirmed that the containment performance was maintained, because the dummy fuel rod, which is containment boundary, was slightly bent and moved in the longitudinal direction, but the helium leak was not observed in the helium leak test for the dummy fuel assembly carried out after drop test.

In addition, for the thermal test carried out subsequently, it was confirmed that the containment performance was maintained, because the helium leak was not observed in the helium leak test for the dummy fuel assembly carried out after test.

By the prototype packaging tests carried out in this time, it was confirmed that Model MFC-1 packaging can keep the safety performance sufficiently in the accident condition required in the regulation.

9. 9m drop test of skin part model used boronated stainless steel

9.1 Outline

This test was carried out to confirm whether the skin part model used boronated stainless steel is damaged or not by 9m dropping.

9.2 Drop test procedure

As a test model, the cross frame part model of actual packaging <dimensions : 472mm×230mm×4.5mm, weight : about 7kg> was used, and the test was carried out in the same condition as that in the verification test for drop height and drop orientation [see Fig. II-F.38 and Fig. II-F.39 for outline of drop orientation].

Unit weight of fuel assembly (only horizontal drop : about 62kg) was applied for dummy weight and wood was used for shock absorber*.

9.3 Outline of test results

Table II F.8 shows the results of 9m drop test for skin part model.

Table II -F.8 Results of Skin Part Model Test

Drop orientation	Cushioning material	Impact acceleration (×g)	Stress generated on skin (N/mm ²)
Horizontal drop	With	About 1,040	193
	Without	1,000 or more	245
Vertical drop	With	About 860	109
	Without	1,000 or more	150

9.4 Conclusion

As a result of PT inspection carried out after drop test, no crack was observed on the skin and welds, therefore, it was confirmed in the drop test of skin part model used boronated stainless steel that any damage was not generated by drop impact.

* Wood was placed on the drop target, and then the test article was dropped on the wood.

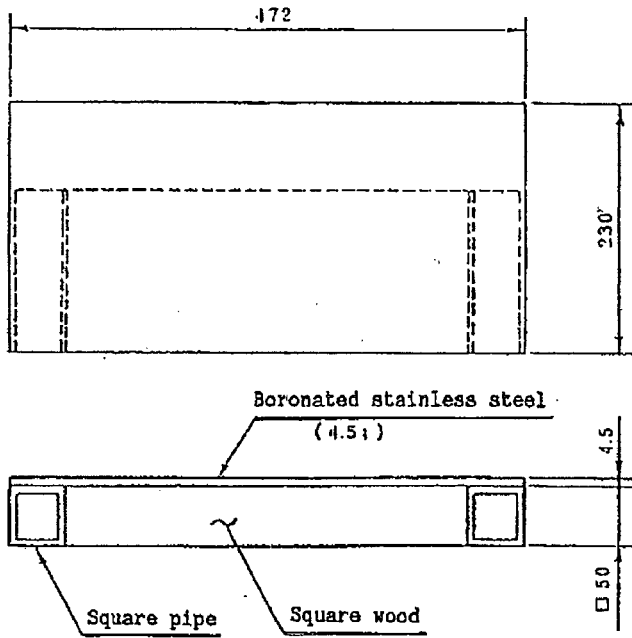


Fig. II-F.37 Sketch of Test Article

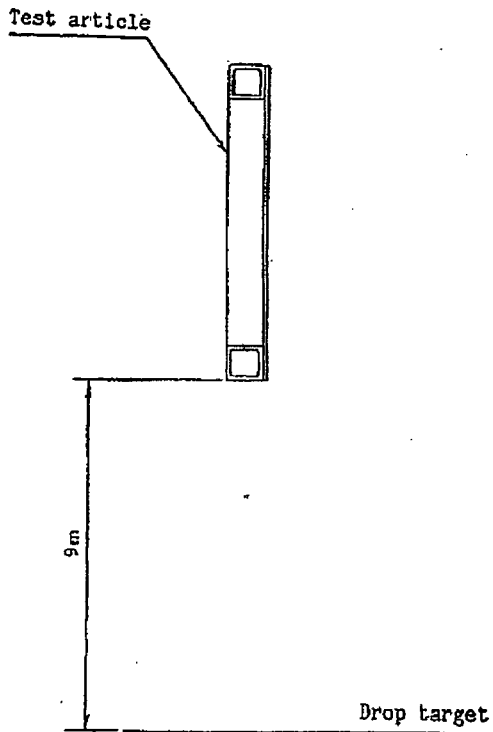


Fig. II-F.38 Sketch of Drop Orientation
(Vertical Drop)

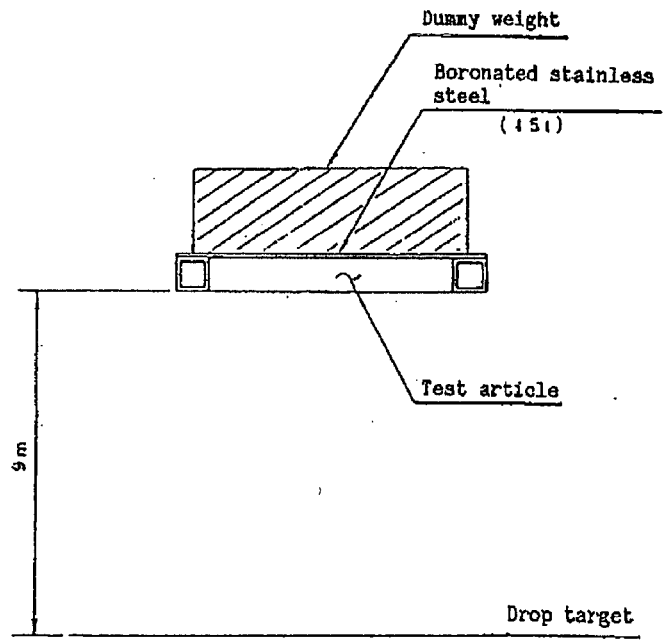


Fig. II-F.39 Sketch of Drop Orientation
(Horizontal Drop)

III QUALITY MANAGEMENT PRINCIPLES

Proprietary Information on Pages III-1 through III-22
Withheld Pursuant to 10 CFR 2.390

IV HANDLING PROCEDURES AND MAINTENANCE

CONDITIONS OF PACKAGE

IV-A HANDLING PROCEDURES OF PACKAGE

IV Handling Procedures and Maintenance Conditions of Package

Outline

This chapter describes preparation before loading contents (fuel assemblies) into a packaging, a loading procedure and their inspections, their unloading procedures from the packaging and their inspections to transport the package safely. It also describes test/inspection methods of the packaging and maintenance conditions after repeated use of the packaging. Fig. IV-A. 2 shows a fuel assembly loading flow, and Fig. IV-A. 11 shows a unloading flow.

IV-A Handling Procedures of Package

A.1 Loading Procedures

A.1.1 Preparation

The following operations must be conducted prior to loading contents (hereinafter called fuel assemblies) into a packaging.

- (1) Check of applied equipment and tools
 - (a) Check traveling performance of a hook of an overhead crane (lifting performance: 5 ton) and brake performance.
 - (b) Check thimbles attached to container lifting wires and both ends of the container for harmful damage, cracks, etc.
 - (c) Check a crane wire or a ring, especially for its detrimental loose. Also, check the ring for harmful damage, cracks, etc.
 - (d) Check shackles for harmful damage, cracks, etc.
 - (e) Check a skid for the top end, ropes, spanners, wrenches, torque wrenches, etc. for harmful damage, cracks, etc.
- (2) Cleaning and tidiness of the workplace
 - (a) Layout of the workplace
- (3) Preparation prior to loading
 - Preparation of an empty packaging (See Fig. IV-A. 1)
 - (a) Combine and install overhead crane container lifting wires, a crane wire and shackles
 - (b) Install one end of each shackle to each bracket on the top cover.
 - (c) Check on the condition of the wires, shackles, etc. by lifting up the hook of the overhead crane a little.
 - (d) Carry the empty packaging to the workplace.

- (e) Put the empty packaging softly down on the floor. (The floor shall be sufficiently horizontal.)
- (f) Lower the overhead crane hook until the container lifting wires are sufficiently loose. Then, hold the overhead crane in this position.

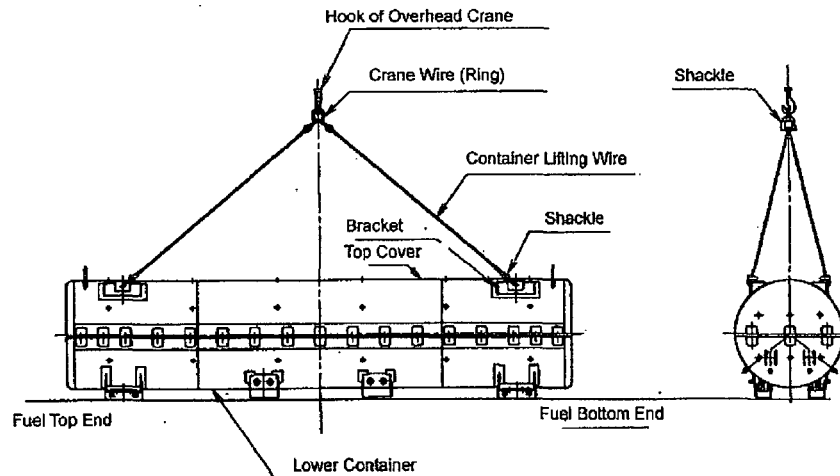


Fig. IV-A. 1 Preparation of Empty Packaging

A.1.2 Loading Procedures

The procedures from opening of the top cover of the packaging to loading of fuel assemblies are as follows:

- (1) Fixing of auxiliary legs (See Fig. IV-A. 3 and Fig. IV-A. 4)
Pull out the auxiliary legs housed underside of the lower container, and fix them in place.
- (2) Removal of the top cover
 - (a) Set a skid to put the top cover on in place.
 - (b) Unscrew the tightening bolts on flanges of the packaging using an offset wrench. (See Fig. IV-A. 5)
 - (c) Lift up the top cover with lifting jigs for use with containers by crane, and put the packaging on the skid.
- (3) Fixing of a crossbar (See Fig. IV-A. 9)
 - (a) Attach shackles and the container lifting wires to an axle cover on the bottom end of the shock mount frames.
 - (b) Attach the container lifting wires on one side and shackles and the crane wire on the other side, and hang them on the crane hook.

- (c) Lift up the packaging gently, and hold it with vibration absorbing rubber in a horizontal position.
 - (d) Remove pins under the shock mount frames.
 - (e) Slide out the crossbars to the right and left side, insert them into the crossbar fixing frames of the lower container, and fix them with locking bolts.
 - (f) Remove the above wires and shackles.
- (4) Erection of a cross frame (See Fig. IV-A. 10)
- (a) Remove hexagon socket bolts that are fixing the shock mount frames and a cross frame from the shock mount frames using a spanner with hexagonal bars and a socket wrench.
 - (b) Attach shackles and the crane wire to the lifting jigs for erection of the cross frame on the top end, and hang cotton ropes on the shackles.
 - (c) Hang the crane wire on the hook of the overhead crane.
 - (d) Lift up and erect the cross frame by gradually moving the overhead crane to the bottom end.
- (5) Fixing of stabilizing bars
- (a) Remove hexagon bolts on the top end of the stabilizing bars fixed on the outside of the lower container.
 - (b) Fix the stabilizing bars in place. (See Fig. IV-A. 10)
 - (c) Clean the inside of the container.
- (6) Loading of a fuel assembly
- (a) Remove ball-locking pins of pivot mounts on the top of the cross frame, and pull out the clamping frames. (See Fig. IV-A. 10)
 - (b) First, pull out the clamping frames on the side of the first loading fuel assembly. (See Fig. IV-A. 10)
 - (c) Attach fuel assembly jigs to the crane, and then install them to the fuel assembly surrounded by cardboards.
 - (d) Put the fuel assembly on the cross frame, and lower it softly until the bottom nozzle contacts the bottom support.
 - (e) Put back the clamping frames in place, fix the ball-locking pins, and fasten the bolts for the support grid pads.
 - (f) Remove the fuel assembly jigs from the fuel assembly, and tape the plastic bag with masking tape.
 - (g) Load the second fuel assembly according to the above (a) through (f) procedures.

- (h) Fix the hexagon bolts, and tighten the jackscrews for fixing nozzles on the top end.
- (7) Housing of cross frame
- (a) Install the wire attached to the crane to the eye plate above the cross frame with shackles.
 - (b) Remove the stabilizing bars from the cross frame, and fix them in place with hexagon bolts.
 - (c) Put back the cross frame in a horizontal position slowly, and put back the crossbar in place.
 - (d) Tighten and fix the hexagon bolts to the cradle assembly.
 - (e) Tighten the support grid pads on the top nozzle with the given torque using a torque wrench. Furthermore, tighten the fixing nuts not to loosen bolts.
 - (f) Tighten the support grid pads on the clamping frames with the given torque using a torque wrench. Furthermore, tighten the fixing nuts.
 - (g) Check the O-rings.
 - (h) A representative of Quality Assurance section shall inspect the results of a series of operations mentioned above.
- (8) Installation of the top cover
- (a) House the auxiliary legs in place, and fix them with hexagon bolts.
 - (b) Place the top cover on the lower container with lifting wires.
 - (c) Fasten the tightening bolts so that they are fixed by the bolt receptacle. (See Fig. IV-A. 5 and Fig. IV-A. 6)
 - (d) Quality Assurance section shall confirm the tightening condition in the above (c).
 - (e) Put the seal in place to show loading completion.
- (9) Measurement of dose equivalent rates
- Quality Assurance section shall measure dose equivalent rates on the surfaces and at each point of 1m from the surfaces of the packaging with GM survey meters. Confirm that no measurement exceeds 2mSv/h and 0.1mSv/h respectively, and record the measurement results.

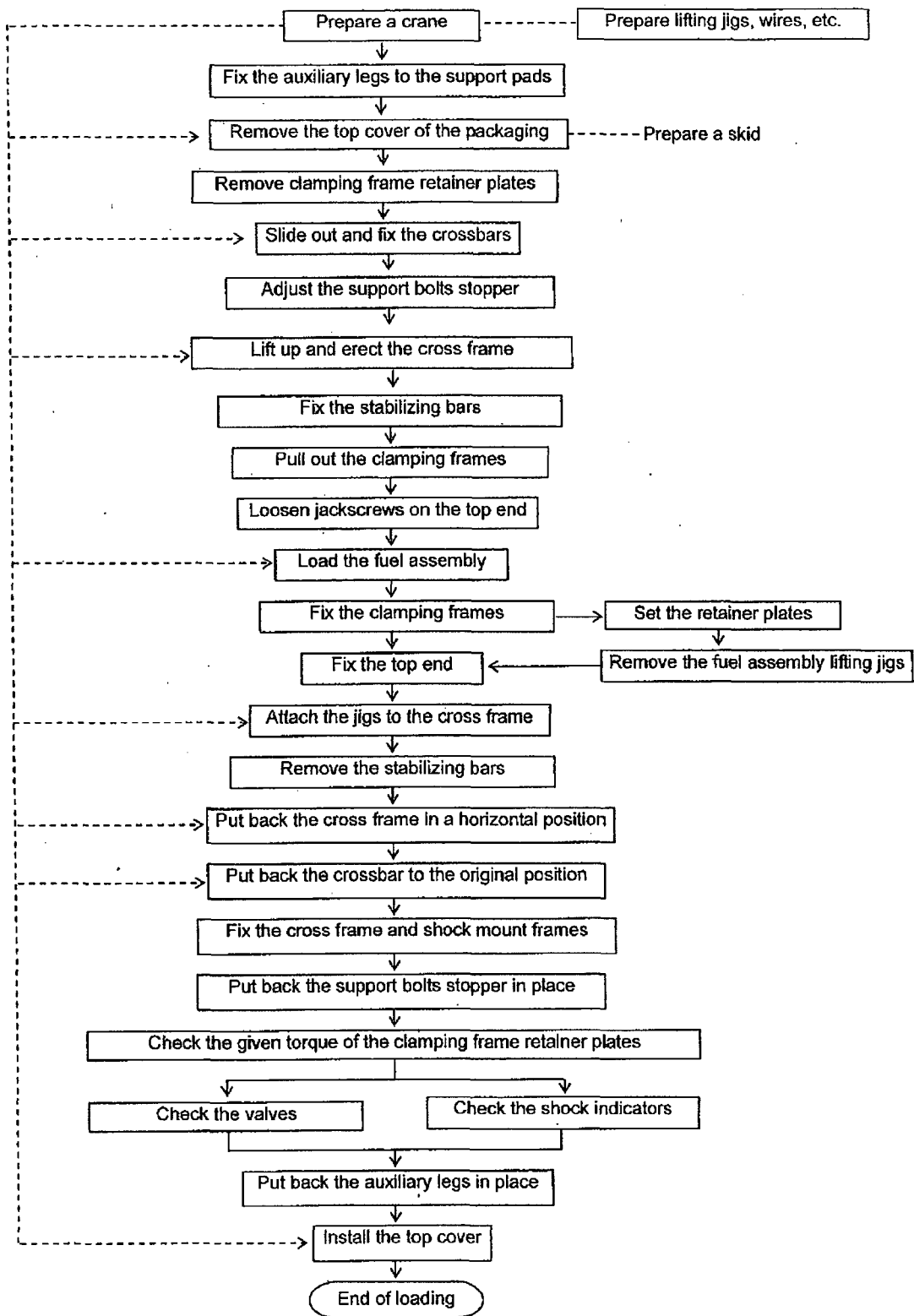


Fig. IV-A. 2 Fuel Assembly Loading Flow

Proprietary Information on Pages IV-A-6 through IV-A-13 Withheld Pursuant to 10 CFR 2.390

IV-A-6

(10) Shipment

Load or unload a package with enough care not to damage its safety using a crane or a folk lift that can sufficiently withstand the total weight of the package.

A.2 Inspection before Shipment of Package

Procedures for tests/inspections which are conducted prior to each shipment of packages are shown in Table IV-A. 1.

Proprietary Information Withheld Pursuant to 10 CFR 2.390

A.3 Unloading Procedures

The procedures from opening of the top cover of the packaging to unloading of fuel assemblies are as follows:

- (1) Mounting of the package
 - (a) Unload the package within the controlled area.
 - (b) Place the package on the horizontal floor.
 - (c) Measure radiation dose rates on the packaging surfaces.
 - (d) Conduct visual inspection on damage of the package during transport before unpacking it.
- (2) Unpacking of the package
 - (a) Check and remove the sealing of the package.
 - (b) Open the air valves and make the internal and external pressure of the packaging to be equal.
 - (c) Fix the auxiliary legs (the same as the above A.1.2 (1))
 - (d) Unscrew the tightening bolts, and lift and remove the top cover not to contact with the fuel assembly and vibration absorbing structure.
- (3) Erection of the cross frame
 - (a) Fix the bottom of the cradle assembly.
 - (b) Erect and fix the cross frame. (See Fig. IV-A. 10)
 - (c) Fix the stabilizing bars in place. (See Fig. IV-A. 10)
- (4) Attachment of the fuel assembly jigs
 - (a) Attach fuel assembly jigs to the crane, and fix them on the top nozzle. Lift it up and stretch the lifting wire a little tight.
- (5) Unloading of the fuel assembly
 - (a) Pull out the clamping frames from the bottom end toward the top end not to loosen the support grid pads. (See Fig. IV-A. 10)
 - (b) Check that all the clamping frames are pulled out and the support grid pads do not disturb the unloading of the fuel assembly.
 - (c) Lift up the fuel assembly around 30 to 40cm and unload it without contacting the lower container flanges of the packaging.
 - (d) Mount the fuel assembly on the interim storage stand, remove the cardboards temporarily, and conduct visual inspection whether the fuel assembly was damaged during transport.
 - (e) Keep the fuel assembly surrounded by the cardboards again on the storage stand after the inspection.
 - (f) Repeat the above operations (5) (a) through (e) for the other fuel assembly.

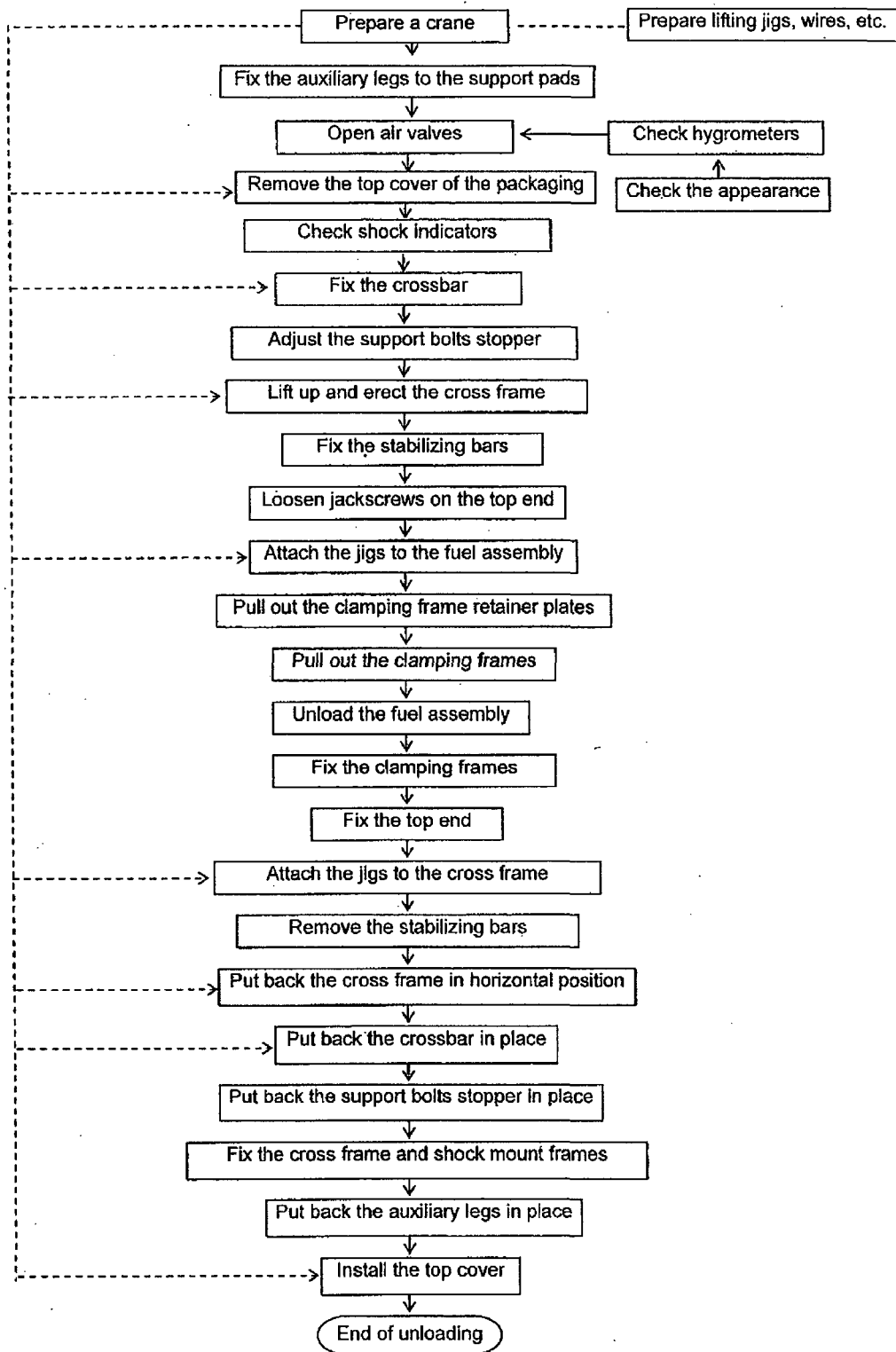


Fig. IV-A. 11 Fuel Assembly Unloading Flow

A.4 Preparation of Empty Packaging

Quality Assurance section shall inspect the following items on an empty packaging after loading and unloading of the contents (fuel assemblies).

A.4.1 Visual Inspection

- (1) Check marks outside of the container, peeling of coating, skid cracks and gap between a skid and the floor surface.
- (2) Check distortion and bending of flanges in the contact area between the top cover and the lower container, and abrasion and cracks of O-rings.
- (3) Check the tightening bolts for abrasion and failure.
- (4) Check the shock mounts for marks, stretch and loose.
- (5) Check the shock indicators for break and bending.

A.4.2 Operating Tests

- (1) Check operating and condition during use of the auxiliary legs.
- (2) Check operation of the clamping frames.
- (3) Check the mobility of the support grid pads.
- (4) Check operation of the cross frame fixing bolts and ball-locking pins.
- (5) Check operation of the crossbars.
- (6) Check erection operation and fixing condition of the cross frame.
- (7) Check operation of the support bolts stopper.
- (8) Check operation of air valves.

IV-B MAINTENANCE CONDITIONS

Proprietary Information on Pages IV-B-1 through IV-B-3
Withheld Pursuant to 10 CFR 2.390

**V PARTICULAR ITEMS ON SAFETY DESIGN
AND SAFE TRANSPORT**

V Particular Items on Safety Design and Safe Transport

There is no particular item to be applied.

APPENDIX

III MANUFACTURING OF PACKAGING

III -A MANUFACTURING PROCEDURES OF PACKAGING

Proprietary Information on Pages 1 through 53 Withheld
Pursuant to 10 CFR 2.390